Universitat de Lleida

Vegetation drives greenhouse gas exchange, and carbon and nitrogen cycling in grassland ecosystems

Mercedes Ibañez Raffaele

http://hdl.handle.net/10803/669268

ADVERTIMENT. L'accés als continguts d'aquesta tesi doctoral i la seva utilització ha de respectar els drets de la persona autora. Pot ser utilitzada per a consulta o estudi personal, així com en activitats o materials d'investigació i docència en els termes establerts a l'art. 32 del Text Refós de la Llei de Propietat Intel·lectual (RDL 1/1996). Per altres utilitzacions es requereix l'autorització prèvia i expressa de la persona autora. En qualsevol cas, en la utilització dels seus continguts caldrà indicar de forma clara el nom i cognoms de la persona autora i el títol de la tesi doctoral. No s'autoritza la seva reproducció o altres formes d'explotació efectuades amb finalitats de lucre ni la seva comunicació pública des d'un lloc aliè al servei TDX. Tampoc s'autoritza la presentació del seu contingut en una finestra o marc aliè a TDX (framing). Aquesta reserva de drets afecta tant als continguts de la tesi com als seus resums i índexs.

ADVERTENCIA. El acceso a los contenidos de esta tesis doctoral y su utilización debe respetar los derechos de la persona autora. Puede ser utilizada para consulta o estudio personal, así como en actividades o materiales de investigación y docencia en los términos establecidos en el art. 32 del Texto Refundido de la Ley de Propiedad Intelectual (RDL 1/1996). Para otros usos se requiere la autorización previa y expresa de la persona autora. En cualquier caso, en la utilización de sus contenidos se deberá indicar de forma clara el nombre y apellidos de la persona autora y el título de la tesis doctoral. No se autoriza su reproducción u otras formas de explotación efectuadas con fines lucrativos ni su comunicación pública desde un sitio ajeno al servicio TDR. Tampoco se autoriza la presentación de su contenido en una ventana o marco ajeno a TDR (framing). Esta reserva de derechos afecta tanto al contenido de la tesis como a sus resúmenes e índices.

WARNING. Access to the contents of this doctoral thesis and its use must respect the rights of the author. It can be used for reference or private study, as well as research and learning activities or materials in the terms established by the 32nd article of the Spanish Consolidated Copyright Act (RDL 1/1996). Express and previous authorization of the author is required for any other uses. In any case, when using its content, full name of the author and title of the thesis must be clearly indicated. Reproduction or other forms of for profit use or public communication from outside TDX service is not allowed. Presentation of its content in a window or frame external to TDX (framing) is not authorized either. These rights affect both the content of the thesis and its abstracts and indexes.

Universitat de Lleida

TESI DOCTORAL

Vegetation drives greenhouse gas exchange, and carbon and nitrogen cycling in grassland ecosystems

Mercedes Ibañez Raffaele

Memòria presentada per optar al grau de Doctor per la Universitat de Lleida

Programa de Doctorat en Gestió Forestal i del Medi Natural

Directora

Maria Teresa Sebastià

Co-directora

Àngela Ribas

2019

Acknowledgements

I would like to very thank my supervisor Dr. Maria Teresa Sebastià for giving me the opportunity to pursue this PhD and for her enthusiasm and good guidance during the process. I would also like to very thank my co-supervisor Dr. Àngela Ribas for her continuous supervision and good suggestions. I would like to thank the Spanish Science Foundation for the FPI fellowship (BES-2014-069243) through the project BIOGEI (CGL2013-49142-C2-1-R), which provided the funding to pursue my doctoral research at University of Lleida, which I would also like to thank.

I am very thankful to Dr. Jaleh Gashghaie, from the Université Paris Sud, where I stayed two months learning about isotopic analysis and to Dr. Werner Eugster, from the ETH-Zurich, where I stayed two months more learning about eddy covariance. Both provided me a very valuable opportunity to expand the horizons of this thesis.

I would also like to very thank Dr. Maria José Leiva, Dr. Cristina Chocarro, Dr. Salvador Aljazairi and Dr. Núria Altimir for their support and revisions of this thesis and potential research papers.

I would like to very thank Núria Llop and Sandra Cervelló for their technical and administrative support whenever was needed.

I would also like to thank all the colleagues and good friends who provided their friendship and good advices during the development of this thesis: Antonio Rodriguez, Haifa Debouk, Teresa Mari, Esther Íñiguez, Christian Mestre, Pepe Manjón and in general all the members of the GAMES research group. I would like to very thank all the colleagues that provided support during field and laboratory tasks: Miquel Sala, Leticia San Emeterio, Gianluca Segalina… and very especially to Helena Sarri and David Estany for their continuous hard work and efficiency.

Finally, I would like to thank all the good friends that I made at the University of Lleida.

Thanks to all of you.

Summary

Grasslands are the most widespread habitat in the world, and can play a crucial role in climate change mitigation. However, predictions about greenhouse gas (GHG) fluxes, and carbon (C) and nitrogen (N) cycling, are still marked by great uncertainty, which in good part lies on soil – vegetation interactions. Accordingly, this thesis investigates the role of vegetation, in terms of phenology, structure, composition and diversity, as a driver of GHG exchange, C and N cycling. We selected grasslands along a climatic gradient (from alpine semi-natural grasslands in the Pyrenees to dehesa ecosystems in the southwest of the Iberian Peninsula), which in addition provided information about interactions between climate and vegetation. GHG recording was done combining continuous (eddy covariance) and discrete chamber based measurements. C and N cycling was assessed using C and N content, and ^{13}C and ^{15}N isotope ratios as a proxy. Our results showed that vegetation influenced GHG fluxes and C and N cycling along the climatic gradient and management regimes. In mountain environments, phenology determined interactions between CO_2 exchange, vegetation and environmental variables, depending on the elevation belt. In dehesa ecosystems, the tree – open grassland structure drove CO_2 and N_2O fluxes, with some differences among tree species. Under the canopy, C and N content, and discrimination against ^{13}C and ^{15}N increased compared to the open grassland. The tree – open grassland structure influenced the plant functional type composition, which presented marked differences in their C and N acquisition and use strategies. Moreover, vegetation composition influenced GHG exchange. Legume identity effects enhanced net CO_2 uptake and N_2O emissions; species composition drove ecosystem respiration and N_2O exchange. Cereal – legume interactions enhanced net CO_2 uptake compared to cereal monocultures, as result of higher gross CO_2 uptake, while respiratory fluxes did not increase. Overall, the inclusion of vegetation structure, composition and diversity terms improved the understanding of mechanisms affecting GHG exchange, as well as C and N cycling.

Resumen

Los pastos son el hábitat más extenso del mundo, siendo fundamentales para la mitigación del cambio climático. Sin embrago, las predicciones sobre emisiones de gases de efecto invernadero (GEI), ciclo del carbono (C) y del nitrógeno (N), todavía están marcadas por una alta incertidumbre, la cual subyace en gran medida en las interacciones entre suelo y vegetación. La presente tesis investiga cómo la vegetación influye sobre el intercambio de GEI y la dinámica del C y el N, en términos de fenología, estructura, composición y diversidad. Para este fin, se han seleccionado pastos a lo largo de un gradiente climático (desde pastos alpinos del Pirineo hasta dehesas en el suroeste de la Península Ibérica). El intercambio de GEI se determinó combinado medidas continuas (eddy covariance) y discretas (cámaras de suelo). La dinámica del C y el N, se aproximó mediante el contenido de C y N, y el ratio isotópico de ^{13}C y ^{15}N. Los resultados mostraron que la vegetación influyó sobre el intercambio de GEI y la dinámica del C y N a lo largo del gradiente climático y de gestión. En ambientes de montaña la fenología condicionó las interacciones entre intercambio de CO_2 y vegetación, en función del estrato altitudinal. En dehesas, la estructura compuesta por árboles y pasto, condicionó las emisiones de CO_2 y N_2O, siendo importante la especie de árbol. El contenido de C y N, y la discriminación contra ^{13}C y ^{15}N incrementó bajo copa en comparación con el pasto abierto. Dicha estructura determinó la composición de grupos funcionales de plantas, éstos presentando particularidades en la adquisición y uso de C y N. Así mismo, la composición de la vegetación influyó sobre el intercambio de GEI. Las legumbres incrementaron la asimilación neta de CO_2 y las emisiones de N_2O; la composición de especies influyo sobre la respiración y el intercambio de N_2O. La interacción entre cereales y legumbres incrementó la asimilación neta de CO_2 en comparación con monocultivos de cereal, como resultado de una mayor asimilación bruta pero no mayor respiración. La inclusión de la vegetación mejoró la comprensión sobre los mecanismos que afectan al intercambio de GEI y la dinámica del C y el N.

Resum

Les pastures són l'hàbitat més extens del món, essent fonamentals per a la mitigació del canvi climàtic. Tot i així, les prediccions respecte a les emissions de gasos d'efecte hivernacle (GEH) i cicle del carboni (C) i del nitrogen (N), estan encara marcades per una gran incertesa, la qual recau en bona part en les interaccions entre el sòl i la vegetació. Aquesta tesi investiga com la vegetació influeix sobre el intercanvi de GEH i la dinàmica del C i el N, en termes de fenologia, estructura, composició i diversitat. Per a aquesta finalitat, es van seleccionar pastures al llarg d'un gradient climàtic (des de prats alpins del Pirineu fins a deveses al sud-oest de la Península Ibèrica). El intercanvi de GEH es va determinar mitjançant mesures continues (eddy covariance) i discretes (cambres de sòl). La dinàmica del C i el N, es va aproximar mitjançant el contingut de C i N, i el rati isotòpic de ^{13}C i ^{15}N. Els resultats mostraren que la vegetació va influir sobre el intercanvi de GEH i la dinàmica del C i N al llarg del gradient climàtic i de gestió. En ambients de muntanya la fenologia va condicionar les interacciones entre el intercanvi de CO_2 i la vegetació, en funció del estrat altitudinal. A les deveses l'estructura composta per arbres i pastures, va condicionar les emissions de CO_2 i N_2O, essent important l'espècie d'arbre. El contingut de C i N, i la discriminació contra ^{13}C i ^{15}N va incrementar sota copa en comparació amb la pastura oberta. Aquesta estructura va determinar la composició de grups funcionals de plantes, els quals presentaren particularitats en l'adquisició i ús de C i N. Així mateix, la composició de la vegetació influí sobre el intercanvi de GEH. Les lleguminoses incrementaren l'assimilació neta de CO_2 i las emissions de N_2O; la composició d'espècies va influir sobre la respiració i el intercanvi de N_2O. La interacció entre cereals i lleguminoses incrementà l'assimilació neta de CO_2 en comparació amb monocultius de cereal, com a resultat d'una major assimilació bruta però no major respiració. En general, la inclusió de la vegetació va millorar la comprensió sobre els mecanismes que afecten al intercanvi de GEH i la dinàmica del C i el N.

Contents

Acknowledgements 1

Summary 3

Resumen 4

Resum 5

Contents 7

Index of tables 11

Index of figures 16

Chapter 1 General introduction and objectives 23

1.1 Climate change and the role of grassland ecosystems 23

1.2 The role of vegetation as driver of greenhouse gas exchange and carbon and nitrogen cycling 25

1.2.1 Vegetation structure and phenology 26

1.2.2 Vegetation diversity and composition 27

1.3 Major objectives 29

1.4 Study sites overview 32

Chapter 2 Phenology and plant functional type dominance drive CO_2 exchange in semi-natural grasslands in the Pyrenees 37

2.2 Abstract 38

2.2 Introduction 39

2.3 Material and methods 41

2.3.1 Study sites 41

2.3.2 Sampling design 43

2.3.3 CO_2 exchange flux calculations 46

2.3.4 Data analysis 47

2.4 Results 49

2.4.1 Seasonal CO_2 flux dynamics in montane and subalpine grasslands 49

2.4.2 Plant functional type dominance on NEE light response 53

2.5 Discussion 56

2.5.1 Differential contributions of phenology and environmental variables on CO_2 seasonal dynamics between elevation belts 56
2.5.2 Plant functional type dominance on NEE light response 59
2.6 Conclusions 61
2.7 Supplementary material 63

Chapter 3 Forage species drive CO_2 exchange responses in a sown grassland of the eastern Pyrenees 65

3.1 Abstract 66
3.2 Introduction 67
3.3 Material and methods 70
3.3.1 Study site and experimental design 70
3.3.2 Eddy covariance measurements 72
3.3.3 CO_2 exchange modelling 75
3.4 Results 80
3.4.1 Cereal monocultures *vs.* cereal-legume mixtures: CO_2 exchange dynamics and budgets 80
3.4.2 Grassland species interaction effects on seasonal NEE 83
3.4.3 Grassland species influence on NEE_{day} light response 84
3.4.4 Grassland species influence on $R_{eco,night}$ response to temperature and soil water content 87
3.5 Discussion 90
3.5.1 Management associated with grassland species: influence on NEE dynamics and NBP 91
3.5.2 Grassland species influence on gross CO_2 uptake and respiration 92
3.6 Conclusions 94
3.7 Supplementary material 96

Chapter 4 Tree – open grassland structure drives carbon and nitrogen cycling in dehesa ecosystems of the Iberian Peninsula 99

4.1 Abstract 100
4.2 Introduction 101
4.3 Material and methods 104
4.3.1 Study sites and sampling design 104

4.3.2 Aboveground biomass sampling 107
4.3.3 Belowground biomass, soil and faeces sampling 107
4.3.4 C and N content and isotopic ratio determination 107
4.3.5 Intrinsic water use efficiency calculation 108
4.3.6 Data analysis 109
4.4 Results 110
4.4.1 Carbon content 110
4.4.2 ^{13}Carbon isotopic ratio 112
4.4.3 Intrinsic water use efficiency 115
4.4.4 Nitrogen content 117
4.4.5 ^{15}Nitrogen isotopic ratio 119
4.4.6 Carbon and nitrogen relationships 122
4.5 Discussion 123
4.5.1 Tree – open grassland structure influence on carbon dynamics 123
4.5.2 Tree – open grassland structure influence on nitrogen dynamics 127
4.6 Conclusions 129
4.7 Supplementary material 131

Chapter 5 Tree – open grassland structure drives greenhouse gas exchange mediated by the herbaceous layer in dehesa ecosystems of the Iberian Peninsula 135

5.1 Abstract 136
5.2 Introduction 137
5.3 Material and methods 140
5.3.1 Study sites and sampling design 140
5.3.2 Greenhouse gas exchange measurements 140
5.3.3 Vegetation sampling 143
5.3.4 Belowground biomass sampling and soil water content determination 143
5.3.5 Data analysis 143
5.4 Results 147
5.4.1 Microclimatic conditions 147
5.4.2 Structure and composition of the herbaceous layer 148
5.4.3 Greenhouse gas exchange 154
5.5 Discussion 162

5.5.1 Plot and canopy as drivers of the structure and composition of the herbaceous layer 162
5.5.2 Plot, canopy and herbaceous layer interactions as drivers of greenhouse gas exchange 165
5.6 Conclusions 171
5.7 Supplementary material 173
Chapter 6 General discussion 177
6.1 Vegetation contribution to the understanding of greenhouse gas exchange and carbon and nitrogen cycling 177
6.1.1 Vegetation structure and phenology 177
6.1.2 Vegetation composition: identity effects 179
6.1.3 Vegetation composition: diversity interaction effects 180
6.2 Forage mixtures: management opportunities 181
6.3 Implications of our research 182
Chapter 7 General conclusions 185
Bibliography 189

Index of tables

Table 2.1. CO_2 exchange linear model results: net ecosystem exchange (NEE), gross primary production (GPP) and ecosystem respiration (R_{eco}), as function of aboveground living biomass (AGLB), standing dead biomass (SDB), litter, air temperature (T_a), soil water content (SWC) and site. Site with BERT as reference level. Estimates of the explanatory variables (Est.), standard error (SE), t and p-value. 52

Table 2.2. Nonlinear mixed-effects models results, by the logistic sigmoid light response function (Equation 2.3). Net ecosystem exchange (NEE) as a function of photosynthetically active radiation (PAR): (1) NEE ~ PAR per grassland ground area (NEE, µmol CO_2 m^{-2} s^{-1}) and (2) NEE normalized by living biomass (NEE_{AGLB}, µmol CO_2 g^{-1} s^{-1}). Model 1.1 and 2.1 (null models), parameters as fixed effects: quantum yield (α), asymptotic gross primary production (GPP_{sat}) and daytime ecosystem respiration ($R_{eco,day}$). Models 1.2 and 2.2 plant functional type (PFT) dominance as covariates. PFT dominance with legumes dominated (L-dominated) as reference level. Estimates (Est.), standard error (SE), t and p-value, R^2 and ANOVAs comparing models. 55

Table 3.1. Management events: grassland type, grassland species, fertilizer type (NPK 9-23-30: nitrogen 9%, phosphorus 23%, potassium 30 %; urea; and NAC 27: calcium ammonium nitrate 27% nitrogen) and rate, sowing date and rate, harvesting date, yield and C exported through yield. 71

Table 3.2. Diversity-interaction model results. Net ecosystem exchange (NEE) as function of air temperature (T_a), net radiation (R_{net}), vapour pressure deficit (VPD), and species proportions: barley, triticale, wheat, oat and vetch (see grassland species proportions in Figure 3.2). Model performed on weekly averaged values of all the variables. Estimates (Est.) of the explanatory variables, standard error (SE), t and p-value. 84

Table 3.3. $R_{eco,night}$ soil temperature and soil water content response parameters by the equations proposed by Reichstein et al. (2002, Equations 3.5 – 3.7): reference ecosystem respiration ($R_{eco,ref}$); soil water content below which R_{eco} ceases (SWC_0); soil water content at which maximal $R_{eco,night}$ halves ($SWC_{1/2}$); and *a* and *b* parameters of the activation energy linear function ($E_0 = a + b \cdot SWC$). Model performed on weekly averaged values of all the variables. Estimates (Est.) and standard error (SE) of the parameters. Estimates in bold are significantly different from zero ($p < 0.05$)..... 89

Table 4.1. Soil characteristics per plot and depth. Soil analysis performed at the Agronomy Service of the Seville University (https://etsia.us.es/), according to standard methods: pH (Porta Casanellas et al., 1986), organic C (Walkley and Black, 1934), total N (Elemental analyser CNS-Trumac, LECO Corporation, MI, USA) and texture (Gee and Bauder, 1986). 105

Table 4.2. Linear model results. C content in belowground biomass (BGB) and soil, as function of plot and canopy. Plot with SM-ilex as reference level, and canopy with open grassland (OG) as reference level. Estimates of the explanatory variables (Est.), standard error (SE), t and p-value. 112

Table 4.3. Linear model results. $\delta^{13}C$ in forbs, grasses and legumes, as function of plot and canopy. Plot with SM-ilex as reference level, and canopy with open grassland (OG) as reference level. Estimates of the explanatory variables (Est.), standard error (SE), t and p-value. 114

Table 4.4. Linear model results. N content in forbs, legumes and soil as function of plot and canopy. Plot with SM-ilex as reference level, and canopy with open grassland (OG) as reference level. Estimates of the explanatory variables (Est.), standard error (SE), t and p-value. 119

Table 5.1. Linear model results. Aboveground biomass (AGB), litter and plant functional type (PFT) biomass: forbs, grasses and legumes, as function of season, plot and canopy.

Season with spring as reference level, plot with SM-ilex as reference level, and canopy with open grassland (OG) as reference level. Estimates of the explanatory variables (Est.), standard error (SE), t and p-value. 150

Table 5.2. Linear model results. Species evenness and species richness (SR) as function of season, plot and canopy. Season with spring as reference level, plot with SM-ilex as reference level, and canopy with open grassland (OG) as reference level Estimates of the explanatory variables (Est.), standard error (SE), t and p-value..... 152

Table 5.3. Diversity-interaction model PFT-oriented results. Net ecosystem exchange (NEE), ecosystem respiration (R_{eco}) and soil respiration (R_{soil}) as function of season, plot, canopy, photosynthetically active radiation (PAR), air temperature (T_a), aboveground biomass (AGB), belowground biomass (BGB) and plant functional type (forbs, grasses and legumes) proportions. Season with spring as reference level, and canopy with open grassland (OG) as reference level. Estimates of the explanatory variables (Est.), standard error (SE), t and p-value..... 157

Table 5.4. Diversity-interaction model species-oriented results. Net ecosystem exchange (NEE), ecosystem respiration (R_{eco}) and soil respiration (R_{soil}) as function of season, plot, canopy, photosynthetically active radiation (PAR), air temperature (T_a), aboveground biomass (AGB), belowground biomass (BGB), species richness (SR) and canonical correspondence analysis axes 1-3 (CCA1-CCA3). Season with spring as reference level, plot with SM-ilex as reference level, and canopy with open grassland (OG) as reference level. Estimates of the explanatory variables (Est.), standard error (SE), t and p-value..... 158

Table 5.5. Diversity-interaction model PFT-oriented results. CH_4 and N_2O exchange as function of as function of season, plot, canopy, soil temperature (T_s), soil water content (SWC), litter, belowground biomass (BGB) and plant functional type (forbs, grasses and legumes) proportions. Season with spring as reference level and canopy with open

grassland (OG) as reference level. Estimates of the explanatory variables (Est.), standard error (SE), t and p-value. 160

Table 5.6. Diversity-interaction model species-oriented results. CH_4 and N_2O exchange as function of season, plot, canopy, photosynthetically active radiation (PAR), soil temperature (T_s), aboveground biomass (AGB), belowground biomass (BGB), species richness (SR) and canonical correspondence analysis axes 1-2 (CCA1-CCA2). Season with spring as reference level, plot with SM-ilex as reference level, and canopy with open grassland (OG) as reference level. Estimates of the explanatory variables (Est.), standard error (SE), t and p-value. 161

Supplementary material tables

Table S3.1. Forage quality indicators (mass-% of dry weight). Analysis performed in the Department of Animal and Food Science, Universitat Autònoma de Barcelona (https://www.uab.cat/department/animal-food-science) according to standard methods: Carbon (C) and nitrogen (N) content (Elemental Analyser EA1108, Carlo-Instruments, Germany); crude protein (CP, according to Kjeldahl method N x 6.25, on a KjeltecTM 8400 analyser, FOSS, Denmark); neutral detergent fibre (NDF, Van Soest et al., 1991); acid detergent fibre (ADF) and acid detergent lignin (ADL) according to Goering and Soest (1970) on an ANKOM analyser (Ankom Thechnology, 2005). Mean ± standard error (SE). Not available (NA) data when there was not enough sample to perform the corresponding analysis or there was only one sample. 96

Table S3.2. CO_2 fluxes data coverage and data retained. Estimated over total potential data (1 value every 30 minutes). 96

Table S3.3. Light response parameters (Equation 3.4): apparent initial quantum yield (α); asymptotic gross primary production (GPP_{sat},); and average daytime ecosystem respiration ($R_{eco,day}$) ANOVAs as function of forage type and period. Forage type with cereal monoculture as reference level, and period with growth as reference level. 97

Table S4.1. Cross section at breast height of the trees of the under the canopy (UC) treatment, per plot and tree species. Number of trees (N), mean and standard error (SE). 131

Table S4.2. Linear model results. $\delta^{13}C$ in grassland species as function of plot, species and canopy. Explanatory variables selected by a stepwise analysis. Plot with SM-ilex as reference level, species with *B. hordeaceu*s as reference level, and canopy with open grassland (OG) as reference level. Estimates of the explanatory variables, standard error (SE), t and p-value. 131

Table S4.3. Linear model results. $\delta^{15}N$ in grassland species as function of plot, species and canopy. Explanatory variables selected by a stepwise analysis. Plot with SM-ilex as reference level, species with *B. hordeaceus* as reference level, and canopy with open grassland (OG) as reference level. Estimates of the explanatory variables, standard error (SE), t and p-value. 132

Table S5.1. Linear model results. Photosynthetically active radiation (PAR), soil temperature (T_s) and soil water content (SWC) as function of season, plot and canopy. Explanatory variables selected by a stepwise procedure. Plot with SM-ilex as reference level, season with spring as reference level, and canopy with open grassland (OG) as reference level. Estimates of the explanatory variables (Est.), standard error (SE), t and p-value. 173

Table S5.2. Soil C content, N content, $\delta^{15}N$ and C/N ratio per plot and canopy: open grassland (OG) and under the canopy (UC). Mean and standard error (SE). Summarized from Section 4.4. 174

Index of figures

Figure 1.1 Graphical abstract: Chapter number, main objectives of each chapter, altitude and management regime of the study sites. 29

Figure 2.1. Climatic and environmental variables of the study sites: Bertolina (BERT) and Castellar (CAST). (A) Mean climatic (1970–2000) monthly air temperature (T_a, solid symbols and line) and monthly precipitation (bars), source: WorldClim (Fick and Hijmans, 2017); (B) 2012 meteorological data: T_a (grey line), and soil water content at 5 cm depth (SWC, black line), lines fitted using generalized additive models with integrated smoothness estimation (gam), mgcv package (Wood, 2004), source: eddy covariance flux stations; (C) 2012 normalized difference vegetation index (NDVI, black line) and its 0.95 confidence interval (grey band), line fitted using local polynomial regression fitting (loess), source: eddy covariance flux stations. Vertical black dashed lines indicate the beginning and the end of the study period. 42

Figure 2.2. Map of the study sites, Bertolina (BERT) and Castellar (CAST), and scheme of the seasonal sampling design. White blocks: sampling points, black blocks: eddy covariance stations. Every sampling day new sampling points were selected. Contour line interval 10 m. 44

Figure 2.3. Scheme of the gas-exchange measurement system set-up. (1) metal collars (height = 8 cm, inner diameter = 25 cm), hammered into the soil around three weeks before to let the system recover from the disturbance; (2) methacrylate chamber (height = 38.5 cm, inner diameter = 25 cm), rubber joint at its base to provide sealing at the chamber-ring junction; (3) multi-logger thermometer (TMD-56, Amprove, USA); (4) vent to avoid underpressure inside the chamber (Davidson et al. 2002); (5) fan to homogenize the air in the headspace; (6) batteries; (7) polyethylene liner with ethyl vinyl acetate shell tube (Bev a Line IV, longitude = 15.3 m, inner diameter = 3.175 mm); (8) air filter (pore size = 0.1 µm); (9) infrared gas analyser (LI-840, LI-COR, USA); (10) laptop and (11) air pump, output flow set at $1.67 \cdot 10^{-5}$ $m^3 s^{-1}$, which is 1 L min^{-1}. 46

Figure 2.4. Seasonal dynamics (DOY: day of year): (A) Mean daytime CO_2 exchange fluxes: net ecosystem exchange (NEE), gross primary production (GPP) and ecosystem respiration (R_{eco}) ± standard error; (B) 30 min. averaged air temperature (T_a) and volumetric soil water content (SWC) at 5 cm depth, source: eddy covariance stations. A system failure of the eddy covariance flux station at CAST caused missing meteorological data from DOY 219 up to the end of the study period; (C) mean litter, standing dead biomass (SDB) and aboveground living biomass (AGLB). Grey dashed vertical lines indicate the beginning and end of the grazing period. 50

Figure 2.5. Relative importance of the explicative variables according to the linear models (Table 2.1). 52

Figure 2.6. Observed NEE (points) vs. predicted NEE (line) by the logistic sigmoid light response function (Equation 2.3) per site and per plant functional type (PFT) dominance — forbs dominated (F-dominated), grasses dominated (G-dominated), and legumes dominated (L-dominated) — based on (A) NEE per unit of grassland ground area (NEE, µmol CO_2 m^{-2} s^{-1}) and (B) NEE per unit of aboveground living biomass (NEE_{AGLB}, µmol CO_2 g^{-1} s^{-1}) 53

Figure 3.1. (A) Ortho-image of the study site (date: May 2013, source: Institut Cartogràfic i Geològic de Catalunya, https://www.icgc.cat/es) and contour plot example of the footprint, based in by the Kljun model (Kljun et al., 2004). Contours show the 10% to 90% flux contribution areas at 10% intervals. (B) Situation of the study site on the Iberian Peninsula 70

Figure 3.2. Grassland rotation timeline, species proportions and management events: black dashed lines indicate harvesting and solid black lines indicate sowing. Top black bands indicate fallow periods in which there was grazing. 72

Figure 3.3. Daily averaged (A) CO_2 fluxes: net ecosystem exchange (NEE), gross primary production (GPP) and ecosystem respiration (R_{eco}); (B) air temperature (T_a); (C)

volumetric soil water content (SWC); and (D) normalized difference vegetation index (NDVI). Titles in the top panel indicate grassland species. Black dashed lines indicate harvest events and solid black lines indicate sowing events. Top black bands indicate fallow periods in which there was grazing. 80

Figure 3.4. Net ecosystem exchange (NEE), gross primary production (GPP) and ecosystem respiration (R_{eco}) budgets after gap-filling per: (A) grassland season, defined as the time from sowing to next sowing; (B) growth period, defined as the time from sowing to harvest; and (C) fallow period, defined as the time from harvest to next sowing. Solid diagonal line indicates NEE = 0 g C m^{-2}, dashed diagonal lines indicate ± 200 g C m^{-2} NEE intervals. Open symbols indicate cereal monocultures and solid symbols cereal-legume mixtures. 81

Figure 3.5. Net biome production (NBP), net ecosystem exchange (NEE) and yield during the grassland growth period, defined as the time from sowing to harvest. Solid diagonal line indicates NBP = 0 g C m^{-2}, dashed diagonal lines indicate ± 100 g C m^{-2} NBP intervals. Open symbols indicate cereal monocultures and solid symbols cereal-legume mixtures. 82

Figure 3.6. Seasonal dynamics of NEE_{day} light response parameters (Equation 3.4): (A) apparent initial quantum yield (α); (B) asymptotic gross primary production (GPP_{sat}); and (C) daytime ecosystem respiration ($R_{eco,day}$). Weekly averaged values and corresponding standard error bars. Top titles in the top panels indicate grassland species. Black dashed lines indicate harvesting events. Top black bands indicate fallow periods in which there was grazing. Gaps are due to missing data or not significant estimates ($p \geq 0.05$), which have been discarded 85

Figure 3.7. Light response parameters (Equation 3.4): (A) apparent initial quantum yield (*α*); (B) asymptotic gross primary production (GPP_{sat}); and (C) average daytime ecosystem respiration ($R_{eco,day}$) mean ± standard error, and Tukey post-hoc test per forage type (C: cereal monoculture, CL: cereal-legume mixture) and period (crop and

fallow). Letters indicate significant differences among groups ($p < 0.05$). See ANOVAs results in Table S3.3. 86

Figure 3.8. $R_{eco,night}$ trend surface as a function of soil temperature (T_s) and soil water content (SWC), by the equations proposed by Reichstein et al. (2002, Equations 3.5 – 3.7). Model performed on weekly averaged data of all the variables. The grid shows the trend surface and dots are observed data. 88

Figure 4.1. (A) C content, (B) $\delta^{13}C$, (C) N content, and (D) $\delta^{15}N$, per ecosystem compartments, including tree leaves; forbs, F; grasses, G; legumes, L; litter; faeces; belowground biomass, BGB; and soil. Mean ± standard error, and Tukey post-hoc test among ecosystem compartments. Letters indicate significant differences among groups ($p < 0.05$). 110

Figure 4.2. C content per ecosystem compartment, plot and canopy: open grassland (OG) and under the canopy (UC) on: (A) tree leaves; (B) litter; (C) forbs; (D) grasses; (E) legumes; (F) belowground biomass, BGB; and (G) soil. Mean ± standard error. 111

Figure 4.3. $\delta^{13}C$ per ecosystem compartment, plot and canopy: open grassland (OG) and under the canopy (UC) on: (A) tree leaves; (B) litter; (C) forbs; (D) grasses; (E) legumes; (F) belowground biomass, BGB; and (G) soil. Mean ± standard error. 113

Figure 4.4. $\delta^{13}C$ of dominant plant species of each plant functional type: grasses (*B. hordeaceus*), forbs (*C. arvensis*, *C. mixtum*, *C. capillaris*, *E. moschatum*, *G. molle*), and legumes (*O. sativus*, *T. subterraneum*), per plot and canopy: open grassland (OG) and under the canopy (UC). Mean ± standard error. 115

Figure 4.5. Intrinsic water use efficiency (iWUE) = $\Delta^{13}C \sim Ci/Ca$ per (A) ecosystem compartment (■ forbs, ● grasses, ▲legumes and▼ tree leaves), and canopy (open dots indicate open grassland, and solid dots indicate under the canopy); and per (B) ecosystem compartment, plot and canopy. Mean ± standard error. 116

Figure 4.6 (A) Grasses N content ~ forbs N content relationship, and (B) grasses $\delta^{15}N$ ~ forbs $\delta^{15}N$ relationship, per plot (● SM-ilex, ■ DN-mixed, ▼ DN-suber, ▲DN-pinea) and canopy (open dots indicate open grassland, and solid dots indicate under the canopy). Mean ± standard error. Diagonal line indicates the 1:1 relationship. 118

Figure 4.7. N content per ecosystem compartment, plot and canopy: open grassland (OG) and under the canopy (UC) in: (A) tree leaves; (B) forbs; (C) grasses; (D) legumes; (E) belowground biomass, BGB; and (F) soil. Mean ± standard error. 118

Figure 4.8. $\delta^{15}N$ per ecosystem compartment, plot and canopy: open grassland (OG) and under the canopy (UC) in: (A) tree leaves; (B) forbs; (C) grasses; (D) legumes; (E) belowground biomass, BGB; and (F) soil. Mean ± standard error. 120

Figure 4.9. $\delta^{15}N$ of dominant plant species of each plant functional type: grasses (*B. hordeaceus*), forbs (*C. arvensis*, *C. mixtum*, *C. capillaris*, *E. moschatum*, *G. molle*), and legumes (*O. sativus*, *T. subterraneum*), per plot and canopy: open grassland (OG) and under the canopy (UC). Mean ± standard error. 121

Figure 4.10. (A) Soil C ~ soil N relationship, (B) belowground biomass (BGB) C content ~ soil N content relationship, and (C) BGB $\delta^{15}N$ ~ soil N content relationship, per plot (● SM-ilex, ■ DN-mixed, ▼ DN-suber, ▲DN-pinea) and canopy (open dots indicate open grassland, solid dots indicate under the canopy). Mean ± standard error. 122

Figure 5.1. Microclimatic sampling conditions per season, plot and canopy: open grassland (OG) and under the canopy (UC). (A) Photosynthetically active radiation (PAR); (B) soil temperature (T_s) and; (C) soil water content (SWC). Boxplot's midline indicates the median; upper and lower limits of the box indicate the third and first quartile; whiskers extend up to 1.5 times the interquartile range from the top/bottom of the respective box, and points represent data beyond the whiskers. 147

Figure 5.2. Mean biomass of forbs, grasses, legumes, litter and belowground biomass (BGB) per season, plot and canopy: open grassland (OG) and under the canopy (UC). The sum of all plant functional types biomass equates aboveground biomass. 149

Figure 5.3. (A) Species evenness and (B) species richness (SR) per season, plot and canopy: open grassland (OG) and under the canopy (UC). Boxplot's midline indicates the median; upper and lower limits of the box indicate the third and first quartile; whiskers extend up to 1.5 times the interquartile range from the top/bottom of the respective box, and points represent data beyond the whiskers. 151

Figure 5.4. Canonical correspondence analysis (CCA): (A) axis 1 (CCA1) vs. axis 2 (CCA2) per season (black: spring, grey: autumn) and plot (● SM-ilex, ■ DN-mixed, ▼ DN-suber, ▲DN-pinea); and (B) CCA1 vs. axis 3 (CCA3) per season and canopy (OG: open grassland, UC: under the canopy). Mean values ± standard error. 153

Figure 5.5. Greenhouse gas exchange per season, plot and canopy: open grassland (OG) and under the canopy (UC). (A) Net ecosystem CO_2 exchange (NEE), ecosystem respiration (R_{eco}) and soil respiration (R_{soil}); (B) CH_4 and (C) N_2O exchange. Mean ± standard error. 154

Figure 5.6. Predicted net ecosystem exchange (NEE, μmol CO_2 m^{-2} s^{-1}) according to the diversity-interaction model PFT-oriented (Table 5.3, environmental conditions set as the mean of the given treatment level). *F* indicates forbs, *G* grasses and *L* legumes. Negative NEE values indicate net CO_2 uptake, and positive values indicate emissions. 156

Figure 5.7. Predicted N_2O exchange (nmol m^{-2} s^{-1}) according to the diversity-interaction model PFT-oriented (Table 5.5, environmental conditions and litter set as the mean of the given treatment level). *F* indicates forbs, *G* grasses and *L* legumes. Negative values indicate N_2O uptake, and positive values indicate emissions. 159

Supplementary material figures

Figure S2.1. Plant functional type (PFT) dominance groups — forbs dominated (F-dominated), grasses dominated (G-dominated), and legumes dominated (L-dominated) — after clustering (Ward's method), based in the proportion of each PFT and the evenness index (Kirwan et al., 2007). The position in the ternary plot indicates the proportion of the corresponding PFT and the size of the point corresponds to the evenness index. 63

Figure S2.2. Aboveground living biomass (AGLB) per site and per plan functional type (PFT) dominance group: forbs dominated (F-dominated), grasses dominated (G-dominated) and legumes dominated (L-dominated). 63

Figure S3.1. Example (April of 2012) of observed net ecosystem exchange (NEE) data (black dots) and their theoretically predicted NEE data by gap-filling (grey line), by the sMDSGapFill function (Reichstein et al., 2005). 98

Figure S3.2. Boxplot of nigh time (PAR < 5 µmol photons m^{-2} s^{-1}) ecosystem respiration ($R_{eco,night}$) as a function of soil temperature (T_s). 98

Figure S4.1. Plant functional type (forbs, grasses and legumes) proportions per plot (SM-ilex, DN-mixed, DN-suber, DN-pinea) and canopy, open grassland (OG) and under the canopy (UC). Adapted from Section 5.4.2. 133

Figure S5.1. Soil respiration (R_{soil}) ~ ecosystem respiration (R_{eco}) relationship, mean ± standard error per season, plot and canopy. 175

Chapter 1 General introduction and objectives

1.1 Climate change and the role of grassland ecosystems

Climate change is mainly driven by an increase in the atmosphere of greenhouse gas (GHG) from anthropogenic sources, including CO_2, CH_4 and N_2O. Such increase in the atmospheric concentrations of GHG produces an excess of the warming effect, which has already increased global temperature ≈ 1 ºC from pre-industrial times (1880), and temperature is projected to keep increasing during the incoming years (≈ 0.1 per decade following the current tendency). In addition, changes in the precipitation regime and in the frequency of extreme meteorological events are already ongoing, and are projected to increase in the future. Such climatic changes are predicted to deeply impact carbon (C) and nitrogen (N) cycles, which may create feedback effects, aggravating the climatic situation (Hartmann et al., 2013).

In addition, some world regions are especially vulnerable to climate change. Mediterranean climatic regions, and especially mountain areas in the Mediterranean basin, are susceptible to increase their temperatures above the average, and suffer frequent severe droughts (García-Ruiz et al., 2011).

In this context, the challenge is to keep the global temperature at 1.5 – 2 ºC above pre-industrial times, but important mitigation efforts would be needed to reach that goal (Allen et al., 2018). In this regard, grasslands may play a crucial role in global change mitigation, especially in terms of C sequestration (O'Mara, 2012). Grasslands provide crucial goods and services for human population, and are the most widespread habitat in the world, including from grazed lands covered with herbaceous plants (< 10 % of tree or shrub cover) to wooded grasslands or silvo-pastoral systems (10 – 40 % tree and shrub cover, FAO 2005). In addition, the term grassland includes a wide variety of species and managements, from semi-natural grasslands to intensively managed grasslands (Allen et al., 2011).

Accordingly, each type of grassland will have a specific GHG budget and dynamics, providing different GHG mitigation possibilities. Generally, extensively managed grasslands tend to be small CO_2 sinks, while the CO_2 uptake capacity of the system tends to increase in more intensively managed grasslands (Hörtnagl et al., 2018; Soussana et al., 2007). However, extensively managed grasslands are less productive, and the amount of exported C through grazing is lower; while intensively managed grasslands tend to be more productive, and C exported through grazing and/or harvesting is higher.

In addition, it is crucial to quantify the net biome production (NBP) of the system, considering all C inputs (fertilizer, sowing) and exports (harvesting, grazing), to fully account the C that remains in the system, beyond the exchanged CO_2. Indeed, many grasslands and forage crops may be acting as CO_2 sinks when only assessing the net ecosystem CO_2 exchange (NEE), but they become CO_2 sources when accounting for the oxidation of total exported biomass (Ceschia et al., 2010; Kutsch et al., 2010; Moors et al., 2010).

On the other hand, grasslands can emit and uptake CH_4 and N_2O. CH_4 and N_2O are emitted at relatively low magnitudes in grasslands, although emissions tend to increase with fertilizer applications (Hörtnagl et al., 2018; Soussana et al., 2004, 2010). Yet, CH_4 and N_2O fluxes are very variable throughout time and space, and emissions can offset the C sink capacity of the system due to their enormous warming potential (Schulze et al., 2009; Soussana et al., 2004). Moreover, CH_4 and N_2O emission patterns and mechanisms are poorly understood, and there is an important lack of empirical data, especially from the Mediterranean basin and from the high elevations, where GHG datasets are very scare (Oertel et al., 2016).

Thus, the GHG budget of a given grassland will depend on the interaction of many abiotic, biotic and management factors, and although the role of main abiotic drivers, such as temperature and soil moisture, on CO_2 (Albergel et al., 2010; Davidson and

Janssens, 2006; Yvon-Durocher et al., 2012), CH_4 and N_2O fluxes (Luo et al., 2013) have been described to some extent, predicting and modelling GHG fluxes still is marked by a great uncertainty, which in good part lies in soil – vegetation interactions and how these influence GHG exchange, and finally C and N cycling (Heimann and Reichstein, 2008). In addition, vegetation structure and composition may suffer modifications under global change (Debouk et al., 2015; Sebastià, 2007; Sebastià et al., 2008), increasing the complexity of GHG exchange predictions.

To this regard, disentangling the vegetation influence on GHG exchange, as well as on C and N cycling, may provide some insight into the underling mechanisms, and the possibility to perform better GHG predictions under climate change. Such knowledge can guide management strategies to mitigate GHG emissions and increase C and N stocks, while optimizing grasslands productivity and quality.

1.2 The role of vegetation as driver of greenhouse gas exchange and carbon and nitrogen cycling

Vegetation is the interface between the soil and the atmosphere, and may strongly influence GHG exchange, and C and N cycling at different levels. Vegetation ecophysiological characteristics directly influence productivity and gross CO_2 uptake and release, as well as organic matter flows. In addition, vegetation influences soil physical and microbiological conditions, which in turn regulate GHG fluxes, and there is a continuum C and N turnover between soil and vegetation (De Deyn et al., 2008; Metcalfe et al., 2011; Oelmann et al., 2007).

Regarding CO_2 exchange, vegetation may determine both NEE components: gross primary production (GPP) and ecosystem respiration (R_{eco}) separately (Chen et al., 2017; Heimann and Reichstein, 2008; Niu et al., 2013). For instance, Chen et al. (2017), reported that changes in the aboveground biomass and species composition drove a

GPP increase, while it did not enhance R_{eco}, resulting in a higher net CO_2 uptake, under warming induced conditions (Chen et al., 2017).

On the other hand, vegetation can indirectly influence CH_4 (Praeg et al., 2017) and N_2O (Baggs et al., 2000; Lin et al., 2013; Shaaban et al., 2016) fluxes, via modifying soil conditions. For instance, Praeg et al. (2017) described changes in the soil microbial community under different plant species, which could drive differences in CH_4 fluxes. In addition, the direct role of vegetation as CH_4 driver still remains controversial, since some authors have described that vegetation may act as CH_4 conduit (Dorodnikov et al., 2011; Gogoi et al., 2005; Nisbet et al., 2009) and/or source (Butenhoff and Khan Khalil, 2007; Carmichael et al., 2014; Keppler et al., 2008, 2006; Nisbet et al., 2009; Praeg et al., 2017; Vigano et al., 2008), even at aerobic conditions.

In any case, it is key to disentangle the mechanisms behind the vegetation influence on GHG exchange, since such effect may be exerted from different perspectives: (1) vegetation structure and phenology, and (2) vegetation diversity and composition.

1.2.1 Vegetation structure and phenology

Grassland vegetation is highly dynamic, with a phenology constantly changing, driving important changes in the proportion of live and dead biomass. Indices of phenological development related to plant productivity, such as total green biomass, normalized difference vegetation index, or leaf area index have already been used to estimate CO_2 gross uptake (Filippa et al., 2015), release (Reichstein et al., 2003; Ryan and Law, 2005), and CH_4 and N_2O exchange fluxes (Imer et al., 2013). However, when assessing grasslands under altitudinal and climatic gradients there are differences in phenological cycles between elevation belts (Debouk et al., 2015), which may result in more complex vegetation - GHG interactions than expected.

Also, the combination of trees and open grassland in silvo-pastoral systems, will modify soil and vegetation conditions, and these in turn GHG exchange and C and N cycling.

Trees increase soil C and N content under the canopy (Andivia et al., 2015; Gómez-Rey et al., 2013; Howlett et al., 2011; Pulido-Fernández et al., 2013), and change grassland vegetation structure (Gea-Izquierdo et al., 2009; Hussain et al., 2009; Moreno et al., 2007) and composition (Lopez-Carrasco et al., 2015; Marañón et al., 2009; Rossetti et al., 2015). However, few studies have assessed the canopy influence on GHG exchange, and those that did found divergent results. Some authors reported an increase of CO_2 emissions under the canopy, mainly driven by higher soil C content (Tang and Baldocchi, 2005; Uribe et al., 2015); while others reported higher CO_2 emissions in the open grassland, manly driven by increased temperatures (Hussain et al., 2009).

On the other hand, the few studies that have focused on the influence of the tree – open grassland structure on CH_4 and N_2O fluxes (Shvaleva et al., 2015, 2014), have related those fluxes to soil water content but dependent on the canopy presence. Yet, how all the ecosystem compartments interact, including above and belowground biomass and soil to drive GHG fluxes and C and N cycling still remains unclear.

1.2.2 Vegetation diversity and composition

Vegetation diversity and composition effects on GHG exchange, C and N cycling (or any other ecosystem function) may be addressed from a species or a functional perspective. Both approximations are complementary (Zhou et al., 2017), providing the first information about the species *per se*, while the latter provides a mechanistic link between vegetation and the given ecosystem function (Petchey and Gaston, 2006).

Whether assessing the vegetation influence from a species or a functional perspective, disentangling diversity (species richness, evenness or functional diversity), from compositional (species/plant functional type identity and interactions) effects, is key to understand the role of vegetation, since diversity and composition may affect complementarily ecosystem functioning (De Deyn et al., 2009; Kahmen et al., 2005; Orwin et al., 2014; Ribas et al., 2015; Schultz et al., 2011). For instance De Deyn et al. (2009) reported that diversity indexes and composition were both

important, since NEE increased with species richness but species identity was also significant. Similarly, Ribas et al. (2015), reported that evenness decreased N_2O and increased CO_2 emissions, while species identity and interaction effects had also significant effects on both fluxes.

To this effect, different methodologies have been proposed to unravel those diversity and compositional effects, as for instance to: (a) test the effect of the dominant species or plant functional type (PFT) on a given ecosystem function; (b) disaggregate compositional (identity and interactions) from diversity effects (evenness), using the diversity-interaction model proposed by Kirwan et al. (2009); and (c) reduce the dimensionality of the species composition matrix using ordination methods (Kahmen et al., 2005; Legendre and Legendre, 1998; Sandau et al., 2014), which allow to synthesise species composition effects, this especially indicated when assessing the effect of a wide number of species.

Ultimately, understanding the mechanisms through which the vegetation influences GHG fluxes and C and N cycling can significantly improve management strategies to mitigate climate change, while optimizing productivity and forage quality in grassland ecosystems.

1.3 Major objectives

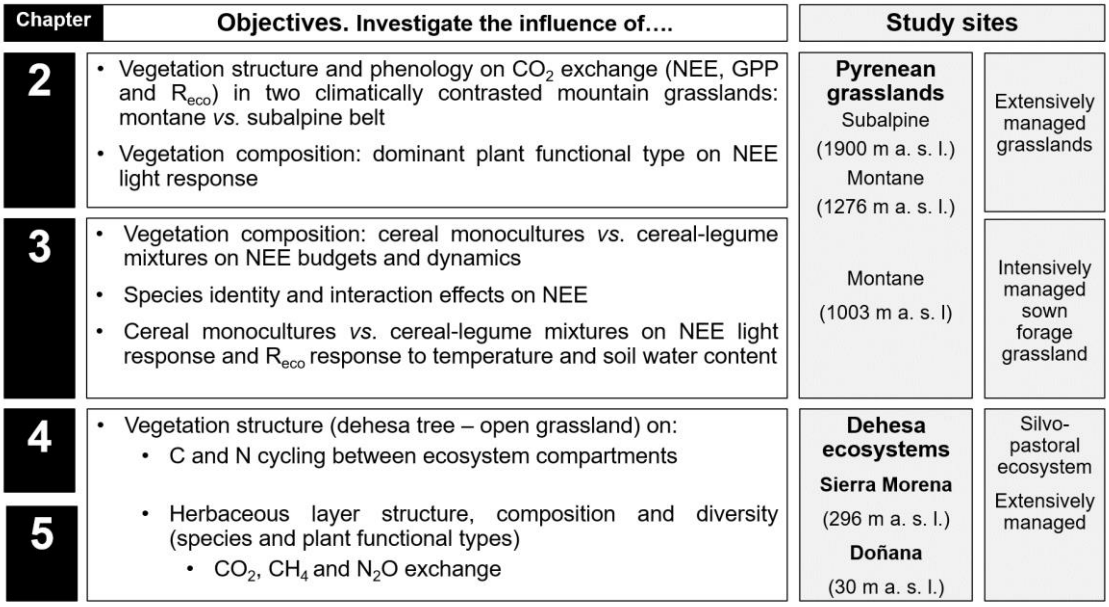

Figure 1.1 Graphical abstract: Chapter number, main objectives of each chapter, altitude and management regime of the study sites.

The major objective of this thesis is to increase the understanding about the relationship among vegetation, GHG exchange and C and N cycling. For that purpose, we selected grasslands along an altitudinal and climatic gradient, from alpine grasslands in the Pyrenees to silvo-pastoral ecosystems (dehesas) in the Southwest of the Iberian Peninsula (see study sites pictures in Section 1.4). These grasslands were in addition subjected to different management regimes, including extensively managed mountain grasslands, intensively managed sown forage grasslands, and extensively manged silvo-pastoral ecosystems (Figure 1.1). The selection of the study sites allowed us to investigate interactions between climate, vegetation and the given ecosystem function (GHG exchange and C and N cycling), as well as to validate our results under different management regimes.

The first chapter introduces the *state-of-the-art of* such vegetation - GHG exchange and C and N cycling relationships, from different perspectives: vegetation structure, diversity

and compositional effects. The following chapters (2-6) address main research aspects posed in the general introduction of this thesis (Figure 1.1). Chapter 6 provides an overall discussion about the results, and Chapter 7 summarizes the main conclusions of this thesis.

Chapter 2

Chapter 2 investigates the influence of the vegetation structure and phenology on CO_2 exchange. The research was conducted in two climatically contrasted mountain grasslands along an altitudinal gradient (montane *vs.* subalpine belt). This climatic gradient allowed us to assess whether the phenology influence on CO_2 exchange was climate - belt dependent. Moreover, we investigated the influence of vegetation composition, in terms of the dominant PFT on NEE light response.

Chapter 3

Chapter 3 investigates the influence of the vegetation composition on CO_2 exchange fluxes, from a perspective of species identity and diversity interaction effects. First, we assessed differences in the NEE budget between cereal monocultures *vs*. cereal-legume mixtures. Second, we investigated species identity and diversity interaction effects on seasonal NEE. Finally, we compared cereal monocultures *vs*. cereal-legume mixtures in their NEE light response and R_{eco} response to temperature and soil water content. The study was conducted in an intensively managed sown forage grassland, which in addition provided the opportunity to assess the influence of management practices associated to each forage type (cereal monocultures *vs*. cereal-legume mixtures) on NEE dynamics and budgets.

Chapter 4

Chapter 4 investigates the influence of the vegetation structure on C and N cycling between ecosystem compartments. The research was conducted in silvo-pastoral ecosystems (dehesas), which are characterized by matrix of trees and open grassland.

Thus, we investigated how the tree – open grassland structure, drove C and N cycling among above and belowground biomass and soil, and how this ecosystem compartments interacted. We paid special attention to the vegetation of the herbaceous layer, assessing separately main PFT (forbs, grasses and legumes). For that purpose C and N content, and isotopic ratios (^{13}C and ^{15}N) were used as a proxy of C and N acquisition and processing.

Chapter 5

Chapter 5 combines all the research questions posed in this thesis. The research was conducted in the same dehesa ecosystems of the fourth chapter. First, we assessed how the tree – open grassland structure and the different tree species influenced on the structure, diversity and composition (in terms of species and PFT) of the herbaceous layer. Second, we assessed the combined influence of: dehesa structure (tree – open grassland) and herbaceous layer structure, diversity and composition on GHG exchange (CO_2, CH_4 and N_2O). We addressed vegetation diversity and compositional effects on GHG exchange separately from a species and a functional perspective.

1.4 Study sites overview

Alpine grasslands in the Pyrenees

La Bertolina (BERT)

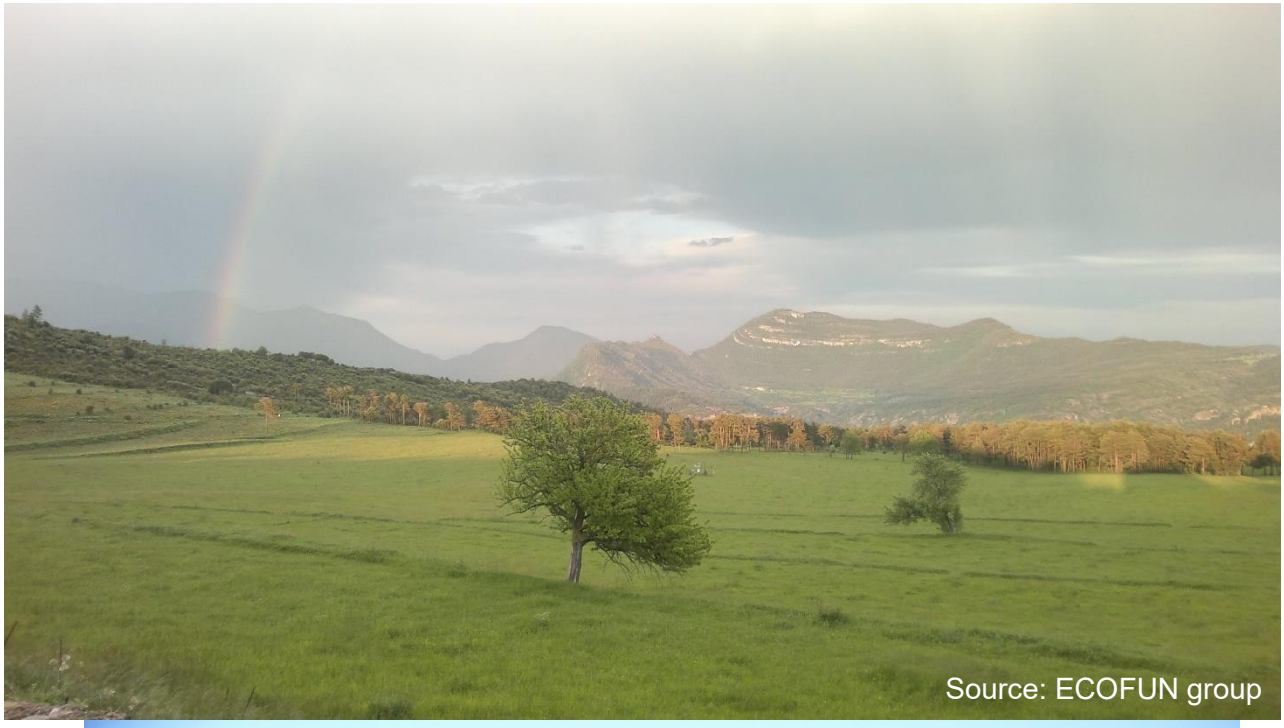

Source: ECOFUN group

Source: ECOFUN group

Castellar de n'Hug (CAST)

Pla de Riart


Source: ECOFUN group


Source: ECOFUN group

Silvo-pastoral ecosystems (dehesas)

Doñana (DN)

Sierra Morena (SM)

Chapter 2 Phenology and plant functional type dominance drive CO_2 exchange in semi-natural grasslands in the Pyrenees

CO_2 exchange in mountain grasslands

Mercedes Ibañez[1]*, Núria Altimir[2a], Àngela Ribas[3,4], Werner Eugster[5], Maria Teresa Sebastià[1,2]

[1]GAMES group & Dept. HBJ, ETSEA, University of Lleida (UdL), Lleida, Spain.

[2]Laboratory of Functional Ecology and Global Change, Forest Sciences Centre of Catalonia (CTFC), Solsona, Spain.

[3]Universitat Autònoma de Barcelona, Bellaterra, Spain.

[4]Centre for Ecological Research and Forestry Applications (CREAF), Bellaterra, Spain.

[5]ETH Zürich, Institute of Agricultural Sciences, Zürich, Switzerland.

[a]Current address: Institute for Atmospheric and Earth System Research (INAR), University of Helsinki, Helsinki, Finland.

MI performed research, analysed data and wrote the paper; NA conceived and designed the study, performed research and revised the paper; AR conceived and designed the study, performed research and revised the paper; WE has been involved in drafting the manuscript and revised the paper; MTS conceived and designed the study and revised the paper.

*Corresponding author; e-mail: mercedes.ibanez@hbj.udl.cat; phone: +34 973702623.

2.2 Abstract

A better understanding of the mechanisms underlying net ecosystem CO_2 exchange (NEE) in mountain grasslands is important to quantify their relevance in the global carbon budget. However, complex interactions between environmental variables and vegetation on CO_2 exchange remain unclear. In addition, there is lack of empirical data, especially from the highest elevations and the Mediterranean region. To investigate CO_2 exchange drivers, we carried out a chamber-based survey of CO_2 exchange measurements in two climatically contrasted grasslands (montane *vs.* subalpine) in the south-eastern Pyrenees during the whole growing season. We assessed the relative contribution of phenology and environmental variables on CO_2 exchange at seasonal scale, and the influence of plant functional type dominance (PFT: grasses, forbs and legumes) on NEE, via PFT-specific light responses. Our results show that phenology plays a crucial role as CO_2 exchange driver, suggesting a differential behaviour of the vegetation community depending on the environment. The subalpine grassland had a more delayed phenology compared to the montane, being more temperature than water constrained. However, temperature increased net CO_2 uptake at a higher rate in the subalpine than in the montane grassland, and during the peak biomass, productivity (+74%) and net CO_2 uptake (NEE +48%) were higher in the subalpine grassland than in the montane grassland. The delayed phenology at the subalpine grassland also reduced vegetation's sensitivity to summer dryness, and CO_2 exchange fluxes were less constrained by the low soil water content. The assessment of PFT-specific light response suggested that legume dominated plots had higher net CO_2 uptake per unit of biomass than grasses. Our study shows that detailed information on phenology and vegetation composition is essential to understand elevation and climatic differences on CO_2 exchange.

Key words: Ecosystem respiration (R_{eco}), grasses, gross primary production (GPP), net ecosystem exchange (NEE), light response, legumes.

2.2 Introduction

Grasslands are among the most widespread habitats in the world (FAO, 2005) and they provide important ecosystem services, including climate regulation and carbon cycling (Hooper et al., 2005). Extensively managed mountain grasslands in particular, are some of the most species-rich ecosystems (Wilson et al., 2012), store about 100 t ha^{-1} of soil carbon (Sjögersten et al., 2011), and their net ecosystem exchange (NEE, Woodwell and Whittaker 1968) is mostly dominated by assimilation (Berninger et al., 2015; Gilmanov et al., 2007; Soussana et al., 2007).

However, there is still a lack of empirical data, mainly from the highest elevations and from some regions, including the Mediterranean basin, in which climate change impacts are projected to be very severe (García-Ruiz et al., 2011). In the particular case of the Pyrenees, despite the few corresponding studies (Berninger et al., 2015; Sjögersten et al., 2012; Wohlfahrt et al., 2008a), NEE datasets are very limited, and knowing the particularities of these systems may provide some guidelines to adapt and mitigate climate change effects in this region.

Moreover, mountain grasslands are especially vulnerable to climate and land use changes (European Commission 2008) and mid- to long-term effects on the carbon budget still remain controversial (Wu et al., 2011), partly due to complex interactions between environmental variables and vegetation. Indeed, although the role of main environmental CO_2 exchange drivers, such as photosynthetically active radiation (Wohlfahrt et al., 2008b), temperature and soil moisture (Albergel et al., 2010; Davidson and Janssens, 2006; Yvon-Durocher et al., 2012) has been widely assessed, how they interact with the vegetation still needs deeper understanding.

Vegetation in mountain grasslands is highly dynamic, changing its structure and composition over time and space (Faurie et al., 1996; Giunta et al., 2009; Mitchell and Bakker, 2016), resulting in a variable patchy configuration of species (Schwinning and

Parsons, 1996), and generating differences in biogeochemical cycles and CO_2 exchange (Reich et al., 1997). While it is known that the aboveground living biomass directly takes-up (Nakano and Shinoda, 2014; Wohlfahrt et al., 2008b) and releases CO_2 (Kardol et al., 2010; Thakur and Eisenhauer, 2015), phenology and vegetation structure may be also determinant for the NEE. Indices of phenological development related to plant productivity, including total green biomass and normalized difference vegetation index (Gao et al., 2016; Zhou et al., 2016) have already been used to estimate gross primary production (GPP, Filippa et al., 2015) and ecosystem respiration (R_{eco}, Reichstein et al., 2003; Ryan and Law, 2005).

However, when assessing mountain grasslands there are differences in phenological cycles between elevation belts, and this may result in more complex vegetation-CO_2 exchange interactions than expected. In addition, there are other vegetation fractions, such as standing dead biomass (dead biomass attached to the plant) and litter (dead plant material, detached from the plant and laying on the soil surface), which are present in considerable amounts in grasslands, and whose specific role as CO_2 exchange drivers has been barely considered.

On the other hand, vegetation composition has also been reported to drive CO_2 exchange fluxes (De Deyn et al., 2009; Metcalfe et al., 2011; Ribas et al., 2015). A common approximation to assess this vegetation-CO_2 exchange relationship is to separate plant species into plant functional types (PFT) that share a common response to an environmental factor, “response traits”, and/or a common effect on ecosystem processes, “effect traits” (Lavorel and Garnier, 2002). In the specific case of grasslands, species are often classified in grasses, non-legume forbs (hereafter “forbs”) and legume forbs (hereafter “legumes”), classification that is based on nitrogen and light (and therefore CO_2) acquisition and use (Tilman 1997; Symstad 2000; Díaz et al., 2007; defined as "guilds" in Sebastià 2007). Thus, legumes have the capacity to fix symbiotic nitrogen, while grasses have some advantages when competing for light as they are

usually taller than legumes and forbs, and have erect high-density leaves that ensure good light penetration (Craine et al., 2001). However, there is still some uncertainty about how these PFT can differentially influence CO_2 exchange at plot scale and under field conditions.

Accordingly, in the present study we investigate the interaction between environmental variables and vegetation on CO_2 exchange fluxes, and more specifically we aim to: (1) compare the contribution of vegetation phenology and environmental variables in two climatically contrasted mountain grasslands in the Pyrenees; and (2) assess the influence of vegetation composition, in terms of the dominant PFT (forbs, grasses and legumes), on light response and therefore on NEE. For that purpose, we performed a survey of CO_2 exchange measurements with a non-steady state chamber, aboveground biomass sampling and environmental variables recording in two extensively managed mountain grasslands in the Pyrenees, located in the montane and subalpine elevation belts, respectively.

2.3 Material and methods

2.3.1 Study sites

The study sites were two grazed mountain grasslands in the south-eastern Pyrenees: La Bertolina (BERT), located in Pla de Busa (42° 05' 56.2" N, 1° 39' 41.5" E, 1276 m a. s. l.), and Castellar de n'Hug (CAST) in Plans del Ginebrar (42° 18' 18" N, 2° 02' 01" E, 1900 m a. s. l.). Both sites are characterized by a Mediterranean climate regime, with spring and autumn precipitations and relatively high summer temperatures (Figure 2.1.A). However, each grassland has its own specific climatic characteristics and phenological particularities, respective to the given elevation belt.

BERT is a typical montane grassland, with mean annual temperature of 9 ºC and mean annual precipitation of 870 mm (Figure 2.1.A). In BERT, vegetation starts to grow

(Figure 2.1.C) as soon as soil water content (SWC, Figure 2.1.B) starts to increase, and senescence starts (Figure 2.1.C) as soon as SWC drops and summer temperatures become high (Figure 2.1.B). On the other hand, CAST is a subalpine grassland, with mean annual temperature of 5.1 ºC and mean annual precipitation of 1189 mm (Figure 2.1.A). CAST is more temperature limited, and vegetation does not start to grow (Figure 2.1.C) until temperatures start to increase, irrespective of the highest spring SWC, which coincides with the snowmelt period and cold temperatures ($T_a \leq 5$ ºC, Figure 2.1.B). Senescence starts later at CAST than at BERT, and progresses more slowly (Figure 2.1.C), despite the low-mid summer SWC (Figure 2.1.B).

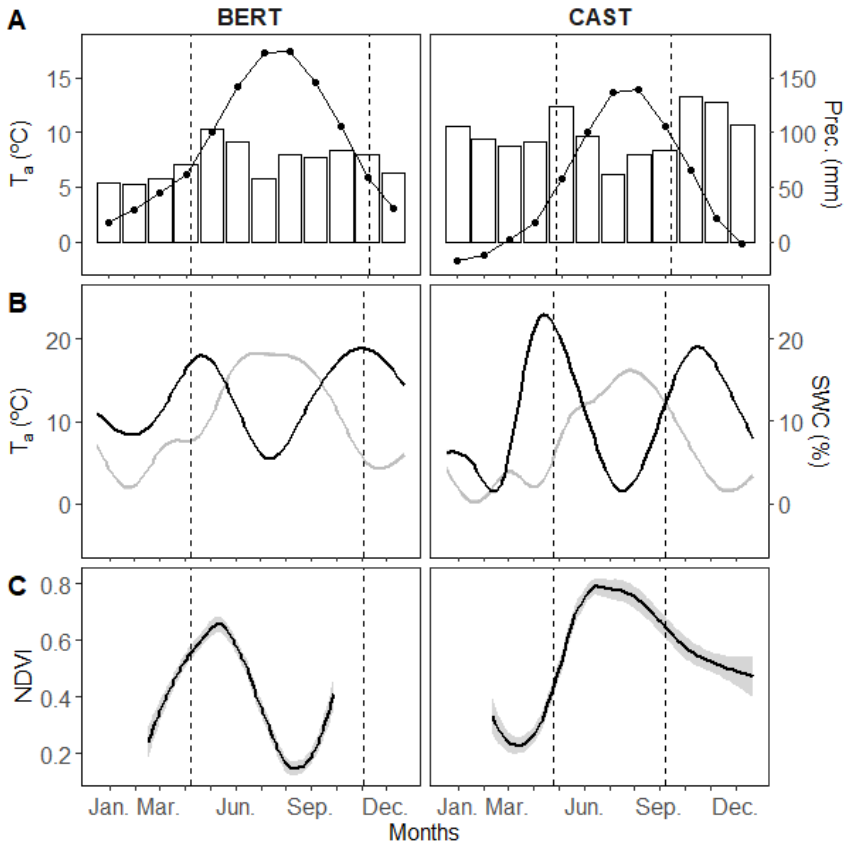

Figure 2.1. Climatic and environmental variables of the study sites: Bertolina (BERT) and Castellar (CAST). (A) Mean climatic (1970–2000) monthly air temperature (T_a, solid symbols and line) and monthly precipitation (bars), source: WorldClim (Fick and Hijmans, 2017); (B) 2012 meteorological data: T_a (grey line), and soil water content at 5 cm depth (SWC, black line), lines fitted using generalized additive models with integrated smoothness estimation (gam), mgcv package (Wood, 2004), source: eddy covariance flux stations; (C) 2012 normalized difference vegetation index (NDVI, black line) and its 0.95 confidence interval (grey band), line fitted using local polynomial regression fitting (loess), source: eddy covariance flux stations. Vertical black dashed lines indicate the beginning and the end of the study period.

Vegetation composition at BERT is characteristic of a montane meso-xerophytic grassland, dominated by grasses (*Festuca arundinacea* Schreb., *Poa bulbosa* L., *Dactylis glomerata* L.) and other species commonly found that include forbs (*Plantago lanceolata* L., *Plantago media* L., *Ranunculus bulbosus* L.) and legumes (*Trifolium pratense* L., *Trifolium repens* L., *Medicago lupulina* L.). CAST is a mesic subalpine grassland, also dominated by grasses (*Festuca nigrescens* Lam., *Agrostis rupestris* All., *Koeleria pyramidata* Lam.), and with the presence of forbs (*Endressia pyrenaica* (Gay ex DC.) J.Gay, *Cirsium acaule* Scop., *Galium verum* L., *Ranunculus* species), legumes (*Trifolium pratense* L., *Trifolium montanum* L., *Astragalus australis* (L.) Lam, *Astragalus sempervirens* Lam.), and some sedges (genus *Carex* L. and *Luzula* DC.). Also is possible to find occasional dwarf-shrubs in both sites.

Both sites are extensively grazed, by cattle at BERT (0.44 livestock units (LSU) ha^{-1}) from May to November, and by cattle and sheep at CAST (0.74 LSU ha^{-1}), from late June to November. The montane grassland (BERT) can only sustain a lower livestock density, although during a longer time period (~3.1 LSU month ha^{-1} yr^{-1}). On the contrary, the subalpine grassland (CAST) is highly productive during the summer and can sustain a higher livestock density, but during a shorter time (~4.4 LSU month ha^{-1} yr^{-1}). Farmers' expectation of the carrying capacity is ~44% higher at CAST than at BERT. Grazing calendar and stocking rates were provided by the farmers and later confirmed during sampling visits. Soil at BERT is udic calciustept and at CAST is lithic udorthent (FAO, 1998).

2.3.2 Sampling design

We established two sampling designs to achieve the aims of this paper: a seasonal and a diel sampling. In the seasonal sampling, we aimed to record temporal CO_2 variability over the growing season and its relationship with environmental variables and vegetation phenology. The seasonal sampling was carried out from April to December of 2012, at three-weekly intervals. Every sampling day sampling points of grassland patches (n = 10

at BERT and n = 8 at CAST) were systematically placed within the footprint of the respective eddy covariance flux stations previously installed at each site (Figure 2.2), which provided ancillary meteorological variables (Section 2.3.3).

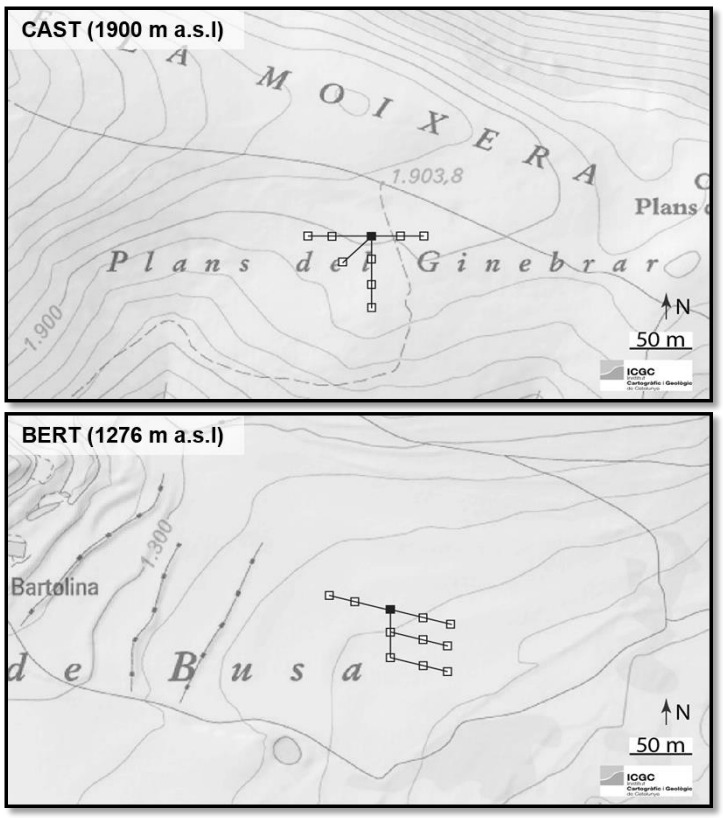

Figure 2.2. Map of the study sites, Bertolina (BERT) and Castellar (CAST), and scheme of the seasonal sampling design. White blocks: sampling points, black blocks: eddy covariance stations. Every sampling day new sampling points were selected. Contour line interval 10 m.

At each sampling point, we recorded complete CO_2 exchange measurements (NEE and ecosystem respiration, R_{eco}, Section 2.3.3), twice during daytime (08:00-16:30 UTC). After CO_2 exchange measurement were done, we harvested total aboveground biomass at ground level. To characterize vegetation phenological changes we separated total biomass into the different vegetation fractions: aboveground living biomass (AGLB), standing dead biomass (SDB, dead biomass attached to the plant) and litter (dead plant material, detached from the plant and on the soil surface). Afterwards, we determined the dry weight (DW, g m^{-2}) of all vegetation fractions, after oven drying at 60 ºC until constant weight.

With the diel sampling, we aimed to assess the effect of the dominant PFT on NEE, via PFT-specific light response. For this purpose, we carried out a campaign of intensive CO_2 exchange measurements at each site, coinciding with the peak biomass (end of May at BERT, DOY 150-152, and end of June at CAST, DOY 172-173), in order to reduce the variability related to different phenological stages and/or environmental conditions, and focusing on the effect of the PFT dominance. Sampling points were selected to ensure the presence of patches with dominance of forbs (F-dominated), grasses (G-dominated) and legumes (L-dominated), selecting three replicates for each PFT (n = 9 in both sites). CO_2 exchange complete measurements (NEE and R_{eco}) were done intensively during 48 h at BERT and 24 h at CAST, resulting in 75 complete CO_2 exchange measurements in BERT and 46 at CAST.

As in the seasonal sampling, we harvested total aboveground biomass after CO_2 exchange measurements, and we processed the vegetation samples in the same way. Moreover, to verify that the PFT dominance classification (F-dominated, G-dominated, L-dominated) given in the field was correct, we separated the AGLB of each sample into PFT (forbs, grasses and legumes) to determine the fraction of each PFT, after oven drying at 60 ºC until constant weight.

Afterwards, we calculated the evenness index according to Kirwan et al., (2007), which has been defined as a measure of the distribution of the relative abundance of each PFT or species, and lies between 0, for mono-specific plots, and 1 when all species or PFT are equally represented (Kirwan et al., 2007). Eventually, we performed a cluster analysis (Ward's method) based on the PFT proportions and the evenness index, confirming the PFT dominance classification given in the field. Generally, plots G-dominated had very low evenness and very high grass proportion, while F-dominated and L-dominated plots had higher values of evenness and the proportion of forbs and legumes, respectively, was not so high (Figure S2.1).

2.3.3 CO_2 exchange flux calculations

CO_2 exchange measurements were carried out using a self-made non-steady state chamber, connected to an infrared gas analyser (LI-840, LI-COR, USA). Resulting CO_2 mixing ratios (ppm) were recorded at five seconds intervals by a laptop computer connected to the gas analyser (Figure 2.3).

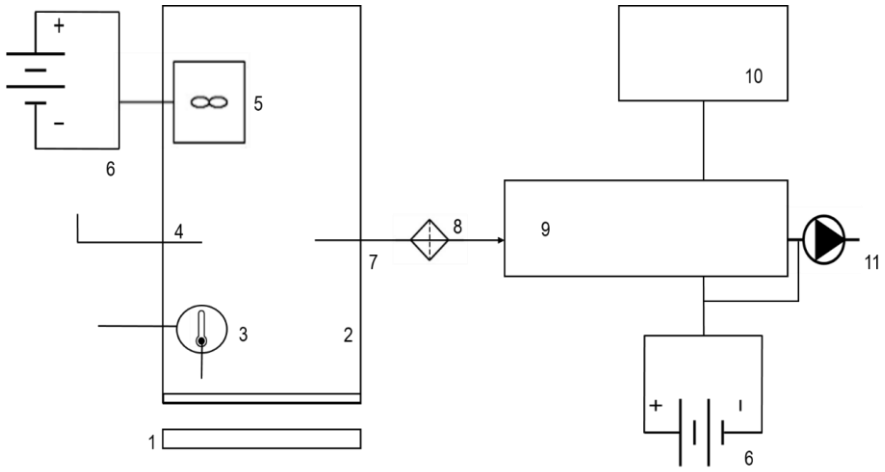

Figure 2.3. Scheme of the gas-exchange measurement system set-up. (1) metal collars (height = 8 cm, inner diameter = 25 cm), hammered into the soil around three weeks before to let the system recover from the disturbance; (2) methacrylate chamber (height = 38.5 cm, inner diameter = 25 cm), rubber joint at its base to provide sealing at the chamber-ring junction; (3) multi-logger thermometer (TMD-56, Amprove, USA); (4) vent to avoid underpressure inside the chamber (Davidson et al. 2002); (5) fan to homogenize the air in the headspace; (6) batteries; (7) polyethylene liner with ethyl vinyl acetate shell tube (Bev a Line IV, longitude = 15.3 m, inner diameter = 3.175 mm); (8) air filter (pore size = 0.1 µm); (9) infrared gas analyser (LI-840, LI-COR, USA); (10) laptop and (11) air pump, output flow set at $1.67 \cdot 10^{-5}$ $m^3 s^{-1}$, which is 1 L min^{-1}.

CO_2 exchange measurements were performed closing the chamber during 30 seconds in light conditions (NEE), and shading the chamber to create dark conditions (R_{eco}). Gross primary production (GPP) was estimated as the sum of both fluxes. Prior to flux calculation, mixing ratios were converted to molar densities (in mol m^{-3}, termed as concentration in what follows) using the ideal gas law. Afterwards, we calculated CO_2 fluxes (µmol CO_2 m^{-2} s^{-1}) based on the concentration change, following the mass balance equation (Equation 2.1, Altimir et al., 2002):

$$CO_2\ flux = q\ \frac{Ct - Ca}{A} + \frac{V\ dC}{A\ dt}$$

(Equation 2.1)

Here q is the air flow rate (1.67 10^{-5} $m^3\ s^{-1}$, which is 1 L min^{-1}), C_a the atmospheric CO_2 concentration, C_t the CO_2 concentration inside the chamber at time t (s), V the chamber volume (0.019 m^3), A the sampling surface (0.049 m^2) and (dC/dt) the first derivative of the CO_2 concentration in relation to time (mol $m^{-3}\ s^{-1}$). Fluxes from the atmosphere to the biosphere are considered negative, and from the biosphere to the atmosphere are positive, according the micrometeorological sign convention (Aubinet et al., 2012b).

Finally, we checked data quality based on the flux detection limit, calculated from the standard deviation of the ambient concentration observed over the measuring time, and on linearity (R^2) of the concentration change during the chamber closure. Fluxes with an adjusted $R^2 < 0.8$ and/or below the detection limit were excluded from further analysis (Debouk et al., 2018).

In addition, the eddy covariance flux stations previously installed at each site provided 30 min averaged meteorological data used in the site description (Section 2.3.1) and CO_2 exchange modelling (Section 2.3.4): air temperature (T_a, HMP45C, Vaisala Inc, Helsinki, Finland); volumetric soil water content at 5 cm depth (SWC, CS616, Campbell Scientific, Logan UT, USA); photosynthetically active radiation (PAR, SKP215, Skye Instruments Ltd, Powys, UK); and normalized difference vegetation index, calculated as NDVI = (NIR – Red) / (NIR + Red), where “Red” and “NIR” are the spectral reflectance measurements acquired in the red and near-infrared regions, respectively.

2.3.4 Data analysis

2.3.4.1 Seasonal CO_2 dynamics

All data analyses were performed using the R software (R core Team, 2015). To describe seasonal CO_2 dynamics, we calculated average daytime CO_2 exchange fluxes using

data obtained between 8:00 and 16:30 UTM. Moreover, to investigate the influence of phenology and environmental variables on CO_2 exchange fluxes in the two climatically contrasted mountain grasslands of study, we ran a linear models with the given CO_2 flux (NEE, GPP, R_{eco}, μmol CO_2 m^{-2} s^{-1}), as function of vegetation fractions as a proxy of phenological changes (AGLB, SDB and litter, g DW m^{-2}); and abiotic variables: T_a (ºC), SWC (fraction) and PAR (μmol photons m^{-2} s^{-1}); in interaction with site (Equation 2.2).

$$CO_2\ flux = Site \cdot (\beta_{AGLB}AGLB + \beta_{SDB}SDB + \beta_{litter}Litter + \beta_{Ta}T_a + \beta_{SWC}SWC) + \varepsilon$$

(Equation 2.2)

Collinearity among variables was tested by the variance inflation factors (VIF) tests, using the vif function, car package (Fox and Weisberg, 2011). Collinearities between variables were found to be not relevant (VIF < 5, Zuur et al., 2007). Final models were selected by a stepwise procedure based on the Akaike information criterion (AIC) using the stepAIC function, MASS package (Venables and Ripley 2002). The relative importance of each predictive variable was determined by the calc.relimp function, relaimpo package (Groemping, 2006).

2.3.4.2 Plant functional type dominance on NEE light response

To assess the influence of PFT dominance on NEE, we first fitted NEE *vs.* PAR using a logistic sigmoid light response function (Equation 2.3, Moffat 2012).

$$NEE = -2 \cdot GPP_{sat} \cdot \left(-0.5 + \frac{1}{1+e^{\frac{-2\cdot\alpha\cdot PAR}{GPP_{sat}}}}\right) + R_{eco,day}$$

(Equation 2.3)

Here GPP_{sat} is the asymptotic gross primary production, *α* is the apparent initial quantum yield, defined as the initial slope of the light-response curve, and $R_{eco,day}$ the average daytime ecosystem respiration (Equation 2.3). Two variants of NEE *vs.* PAR relationships were fitted to our data: (1) using flux densities per grassland ground area

(NEE, μmol CO_2 m^{-2} s^{-1}) and (2) using NEE normalized by aboveground living biomass (NEE_{AGLB}, μmol CO_2 g^{-1} s^{-1}).

Afterwards, we tested the PFT dominance effect on light response parameters in both cases, using nonlinear mixed-effects models (Pinheiro and Bates, 2000), by the nlme function of the nlme package (Pinheiro et al., 2015). For that purpose, we performed corresponding null models in each case (NEE ~ PAR, Model 1.1, and NEE_{AGLB} ~ PAR, Model 2.1), with site as random factor and light response parameters (Equation 2.3: α, GPP_{sat} and $R_{eco,day}$) as fixed effects. Afterwards, corresponding models with PFT dominance as covariates of the parameters, α, GPP_{sat} and $R_{eco,day}$ (Model 1.2 and Model 2.2) were also run. Null models and models including PFT dominance as covariates were compared by an analysis of variance (ANOVA).

2.4 Results

2.4.1 Seasonal CO_2 flux dynamics in montane and subalpine grasslands

Mean daytime NEE was mostly dominated by assimilation at both sites, ranging from −2 ± 1 to −10 ± 2 μmol CO_2 m^{-2} s^{-1} at BERT, and from 2 ± 1 to −20 ± 3 μmol CO_2 m^{-2} s^{-1} at CAST. Mean daytime GPP showed the strongest seasonal pattern and the highest differences between sites, ranging from −5 ± 1 to −20 ± 2 μmol CO_2 m^{-2} s^{-1} at BERT and form −6 ± 1 to −32 ± 2 μmol CO_2 m^{-2} s^{-1} at CAST. Finally, mean daytime R_{eco} ranged from 3.0 ± 0.4 to 10 ± 1 μmol CO_2 m^{-2} s^{-1} at BERT and from 3.1 ± 0.5 to 15 ± 5 μmol CO_2 m^{-2} s^{-1} at CAST (Figure 2.4.A).

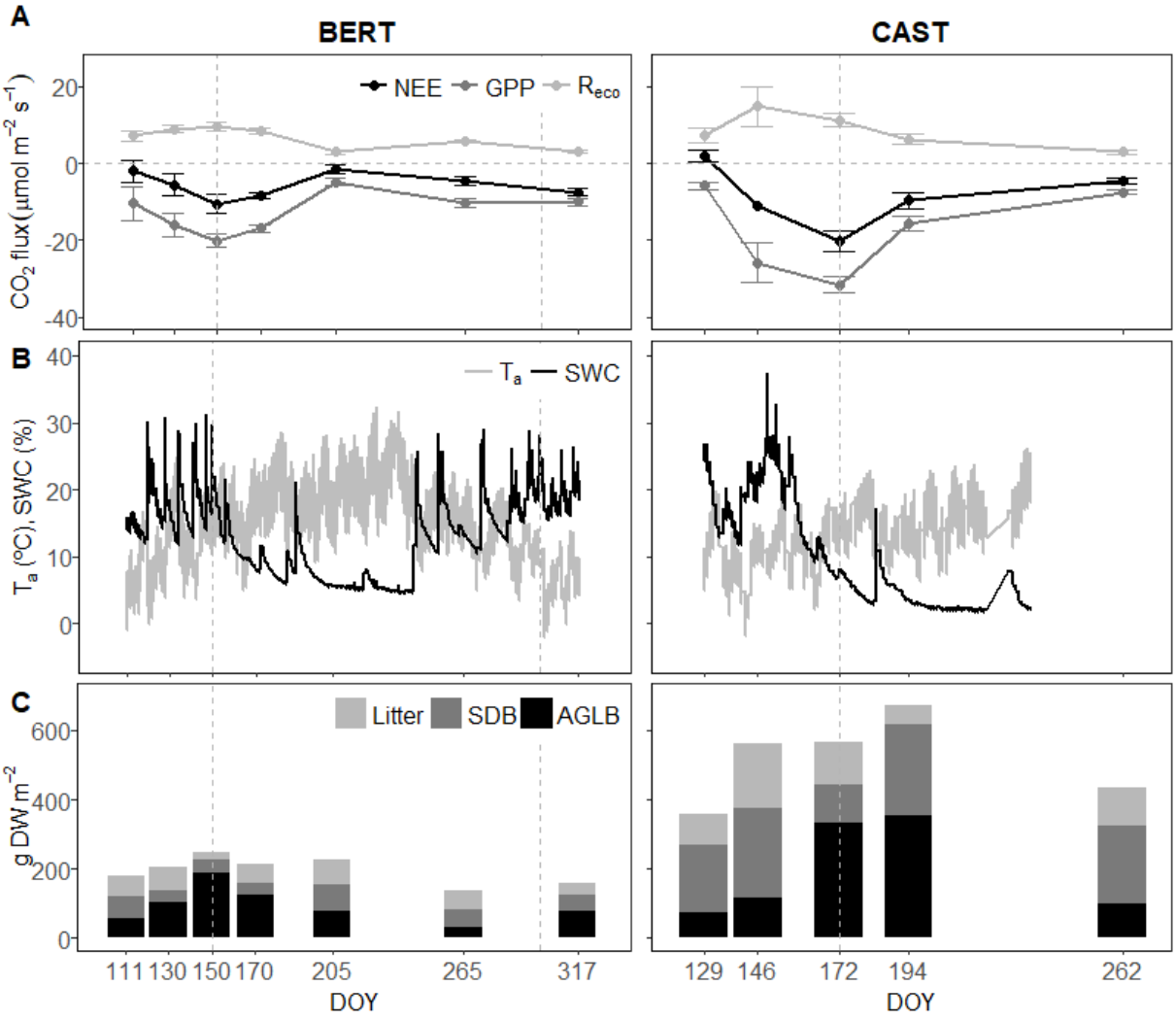

Figure 2.4. Seasonal dynamics (DOY: day of year): (A) Mean daytime CO_2 exchange fluxes: net ecosystem exchange (NEE), gross primary production (GPP) and ecosystem respiration (R_{eco}) ± standard error; (B) 30 min. averaged air temperature (T_a) and volumetric soil water content (SWC) at 5 cm depth, source: eddy covariance stations. A system failure of the eddy covariance flux station at CAST caused missing meteorological data from DOY 219 up to the end of the study period; (C) mean litter, standing dead biomass (SDB) and aboveground living biomass (AGLB). Grey dashed vertical lines indicate the beginning and end of the grazing period.

CO_2 exchange seasonal patterns (Figure 2.4.A), evolved according to environmental conditions (Figure 2.4.B) and phenology (Figure 2.4.C), with some differences between sites (Table 2.1 and Figure 2.5). The modelling showed that NEE was mainly driven by AGLB (Figure 2.5), NEE taking more negative values — increasing net CO_2 uptake — with increasing AGLB (AGLB effect, $t = -4.70$, $p < 0.001$, Table 2.1); while NEE took more positive values — CO_2 emissions — with increasing SDB (SDB effect, $t = 2.16$,

p = 0.03, Table 2.1) and litter (litter effect, t = 2.30, p = 0.02, Table 2.1). Moreover, NEE was a priori less negative in CAST than at BERT, lower net CO_2 uptake (site effect, t = 3.23, p = 0.002, Table 2.1), but net CO_2 uptake increased with temperature at a higher rate at CAST than at BERT (site x T_a effect, t = −2.81, p = 0.006, Table 2.1). Also, NEE became more negative with increasing litter at CAST (site x litter effect, t = −3.08, p = 0.003, Table 2.1), and the net CO_2 uptake capacity of the AGLB was lower in CAST than at BERT (site x AGLB effect, t = 1.83, p = 0.07, Table 2.1).

GPP behaved similarly to NEE. GPP was mainly driven by AGLB (Figure 2.5), taking more negative values with increasing AGLB (AGLB effect, t = −5.39, p < 0.001, Table 2.1), and less negative values with SDB (SDB effect, t = 1.88, p = 0.06, Table 2.1). GPP was in addition more negative with increasing temperature (T_a effect, t = −1.82, p = 0.06, Table 2.1) and SWC (SWC effect, t = −2.08, p = 0.04). GPP presented the same interactions between site, environmental variables and vegetation as NEE did (Table 2.1).

Finally, R_{eco} was also mainly driven by AGLB (Figure 2.5), increasing emissions with AGLB (AGLB effect, t = 4.37, p < 0.001, Table 2.1), followed by temperature (T_a effect, t = 5.76, p < 0.001, Table 2.1), and SWC (SWC effect, t = 5.77, p < 0.001, Table 2.1).

Table 2.1. CO_2 exchange linear model results: net ecosystem exchange (NEE), gross primary production (GPP) and ecosystem respiration (R_{eco}), as function of aboveground living biomass (AGLB), standing dead biomass (SDB), litter, air temperature (T_a), soil water content (SWC) and site. Site with BERT as reference level. Estimates of the explanatory variables (Est.), standard error (SE), t and p-value.

	CO_2 flux (µmol m^{-2} s^{-1})											
	NEE				GPP				R_{eco}			
	Est.	SE	t	p	Est.	SE	t	p	Est.	SE	t	p
Intercept	−7	3	−2.46	0.02	4	6	0.60	0.6	−10	2	−4.01	< 0.001
AGLB (g DW m^{-2})	−0.05	0.01	−4.70	< 0.001	−0.06	0.01	−5.39	< 0.001	0.015	0.004	4.37	< 0.001
SDB (g DW m^{-2})	0.019	0.009	2.16	0.03	0.018	0.010	1.88	0.06				
Litter (g DW m^{-2})	0.05	0.02	2.30	0.02	0.04	0.02	1.63	0.1				
T_a (ºC)	0.2	0.2	0.95	0.3	−0.5	0.3	−1.92	0.06	0.6	0.1	5.76	< 0.001
SWC (fraction)					−36	17	−2.08	0.04	34	6	5.77	< 0.001
Site	27	8	3.23	0.002	29	10	2.92	0.005	1.5	0.9	1.75	0.08
Site x AGLB	0.03	0.02	1.83	0.07	0.04	0.02	2.01	0.05				
Site x litter	−0.08	0.03	−3.08	0.003	−0.07	0.03	−2.43	0.02				
Site x T_a	−1.7	0.6	−2.81	0.006	−2.1	0.7	−2.97	0.004				
R^2_{Adj}	0.53			< 0.001	0.65			< 0.001	0.50			< 0.001

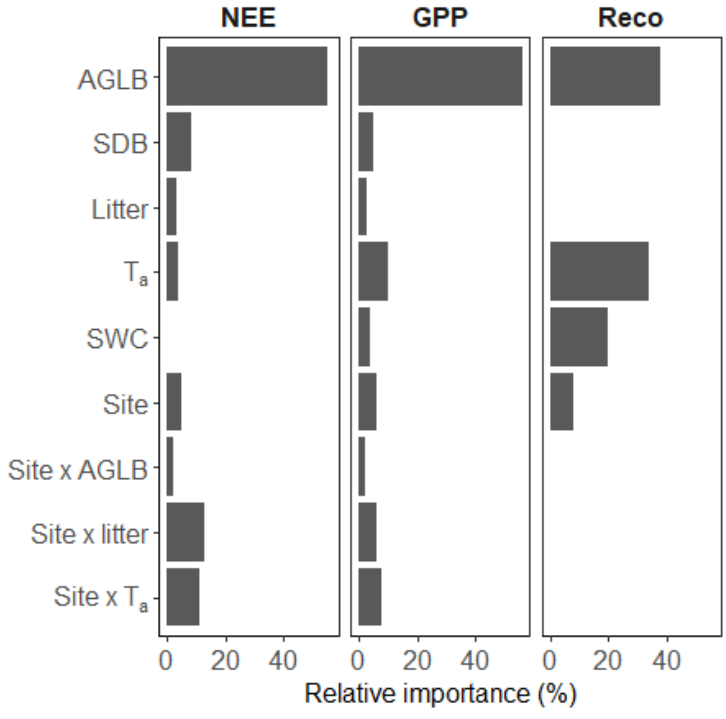

Figure 2.5. Relative importance of the explicative variables according to the linear models (Table 2.1).

2.4.2 Plant functional type dominance on NEE light response

CO_2 exchange fluxes recorded during the intensive diel campaign confirmed that NEE was mainly driven by PAR at a diel timescale (Figure 2.6). The logistic sigmoid light response function (Equation 2.3) explained 69% of the variability, when assessing NEE per grassland ground area (Model 1.1, Table 2.2).

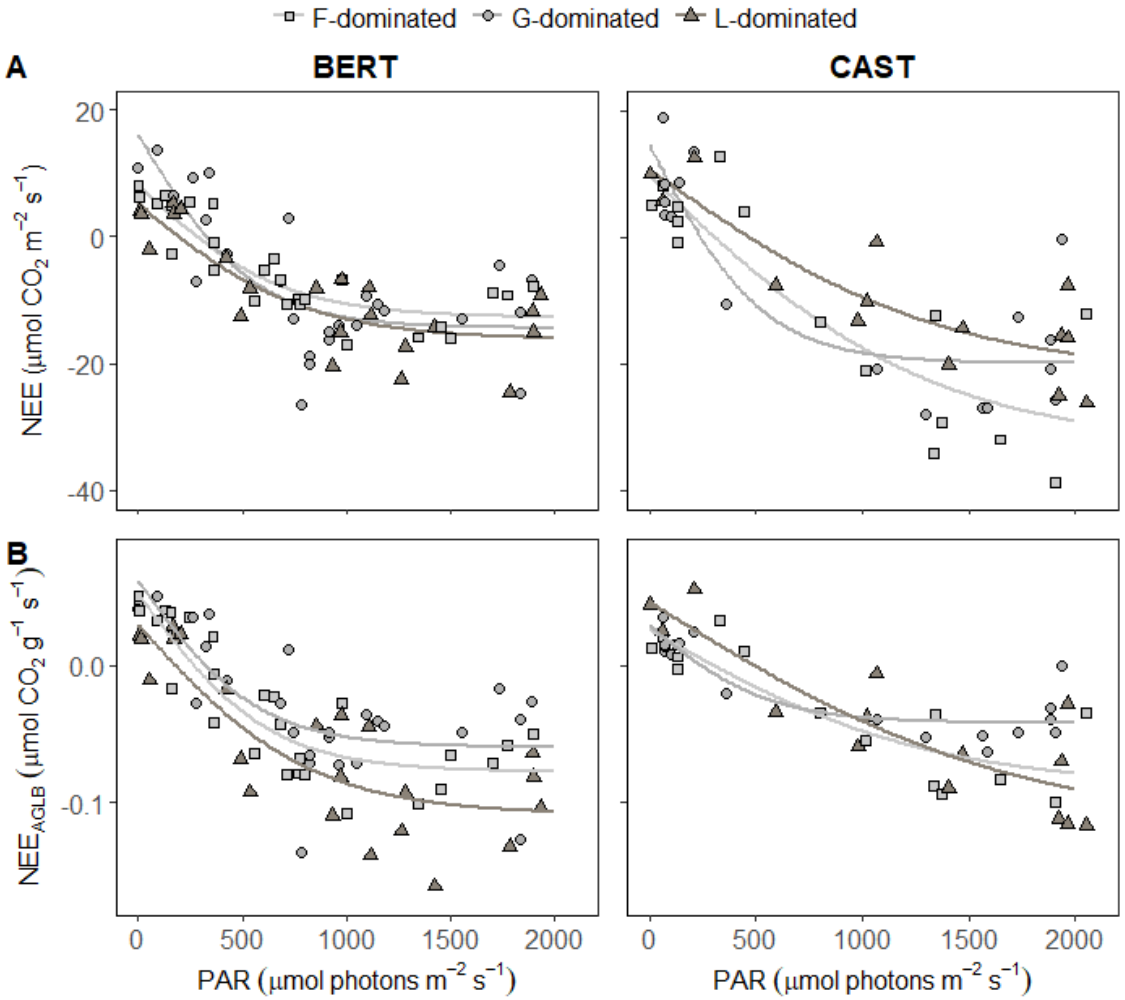

Figure 2.6. Observed NEE (points) vs. predicted NEE (line) by the logistic sigmoid light response function (Equation 2.3) per site and per plant functional type (PFT) dominance — forbs dominated (F-dominated), grasses dominated (G-dominated), and legumes dominated (L-dominated) — based on (A) NEE per unit of grassland ground area (NEE, µmol CO_2 m^{-2} s^{-1}) and (B) NEE per unit of aboveground living biomass (NEE_{AGLB}, µmol CO_2 g^{-1} s^{-1}).

The inclusion of PFT dominance as covariates of the light response function parameters (α, GPP_{sat} and $R_{eco,day}$), was not significant when assessing NEE per grassland ground area (Model 1.2, Table 2.2). However, the logistic sigmoid adjustment per site and per PFT dominance suggested that there were differences between PFT when assessing the NEE per unit of AGLB (NEE_{AGLB}, Figure 2.6.B). Accordingly, when assessing the NEE_{AGLB} ~ PAR relationship, there were significant differences between the null model and the model that included PFT dominance as covariate of the parameters (ANOVA Model 2.1 *vs*. Model 2.2, $p = 0.001$, Table 2.2), which also increased the explained variability, from 66% to 72% (R^2 Model 2.1 *vs*. Model 2.2, Table 2.2). Differences among PFT in the NEE_{AGLB} were mainly driven by differences in the GPP_{sat}, G-dominated plots having significantly lower GPP_{sat} than L-dominated plots ($t = -2.29$, $p = 0.02$, Model 2.2, Table 2.2).

Table 2.2. Nonlinear mixed-effects models results, by the logistic sigmoid light response function (Equation 2.3). Net ecosystem exchange (NEE) as a function of photosynthetically active radiation (PAR): (1) NEE ~ PAR per grassland ground area (NEE, μmol CO_2 m^{-2} s^{-1}) and (2) NEE normalized by living biomass (NEE_{AGLB}, μmol CO_2 g^{-1} s^{-1}). Model 1.1 and 2.1 (null models), parameters as fixed effects: quantum yield (α), asymptotic gross primary production (GPP_{sat}) and daytime ecosystem respiration ($R_{eco,day}$). Models 1.2 and 2.2 plant functional type (PFT) dominance as covariates. PFT dominance with legumes dominated (L-dominated) as reference level. Estimates (Est.), standard error (SE), t and p-value, R^2 and ANOVAs comparing models.

Model	Parameter		Est.	SE	t	p	R^2
Model 1.1 NEE ~ PAR	**α**	Intercept	0.035	0.006	5.83	< 0.001	0.69
	GPP_{sat}	Intercept	28	4	7.92	< 0.001	
	$R_{eco,day}$	Intercept	10	2	6.12	< 0.001	
Model 1.2 NEE ~ PAR + PFT	**α**	Intercept	0.025	0.008	3.00	0.003	0.68
		F-dominated	0.00	0.01	0.20	0.8	
		G-dominated	0.02	0.02	1.44	0.2	
	GPP_{sat}	Intercept	25	4	6.76	< 0.001	
		F-dominated	6	6	1.03	0.3	
		G-dominated	6	5	1.31	0.2	
	$R_{eco.day}$	Intercept	7	3	2.45	0.02	
		F-dominated	1	4	0.41	0.7	
		G-dominated	7	4	1.73	0.1	
ANOVA model 1.1 vs. 1.2						0.97	
Model 2.1 NEE_{AGLB} ~ PAR	**α**	Intercept	0.00013	0.00004	3.47	0.0007	0.66
	GPP_{sat}	Intercept	0.12	0.01	10.26	< 0.001	
	$R_{eco,day}$	Intercept	0.037	0.009	4.34	< 0.001	
Model 2.2 NEE_{AGLB} ~ PAR + PFT	**α**	Intercept	0.00012	0.00004	2.97	0.004	0.72
		F-dominated	0.00003	0.00004	0.64	0.5	
		G-dominated	0.00002	0.00007	0.35	0.7	
	GPP_{sat}	Intercept	0.14	0.02	7.43	< 0.001	
		F-dominated	−0.02	0.02	−1.10	0.3	
		G-dominated	−0.05	0.02	−2.29	0.02	
	$R_{eco.day}$	Intercept	0.03	0.01	2.58	0.01	
		F-dominated	0.01	0.01	0.68	0.5	
		G-dominated	0.01	0.02	0.64	0.5	
ANOVA model 2.1 vs. 2.2						0.001	

2.5 Discussion

2.5.1 Differential contributions of phenology and environmental variables on CO_2 seasonal dynamics between elevation belts

Contextualizing our CO_2 exchange fluxes (Figure 2.4.A), these were higher than in other semi-natural grasslands in the Pyrenees previously reported (Gilmanov et al., 2010, 2007; Sjögersten et al., 2012; Wohlfahrt et al., 2008a). For instance, Gilmanov et al. (2007) reported in Alinyà, a montane grassland (1770 m a.s.l) that might be climatically comparable to BERT, daily aggregated GPP maximum values of −25.7 g CO_2 m^{-2} d^{-1}. Whereas in BERT, considering the light response function (Equation 2.3), the estimates of the parameters subtracted from the NEE_{AGLB} ~ PAR relationship (Table 2.2, Model 2.1), and the AGLB sampled during the peak biomass (190 ± 21 g DW m^{-2}, DOY 150, Figure 2.4.C), we can estimate daily aggregated GPP ≈ −31 g CO_2 m^{-2} d^{-1} during the peak biomass. Such difference may well be because there are important vegetation differences between both sites, with a maximum productivity at Alinyà around 131 ± 12 g DW m^{-2} (unpublished data), while at BERT it is roughly a 45% higher (190 ± 21 g DW m^{-2}), although other factors, as for instance soil differences — soil at Alinyà is a lithic cryrendoll (Gilmanov et al., 2007), while the soil at BERT is a udic calciustept — may also be influencing.

Another example is the CO_2 exchange fluxes reported by Sjögersten et al. (2012) in a subalpine grassland of the southeaster Pyrenees, very close to our subalpine site CAST. They reported maximum NEE values of −0.7 ± 0.8 μmol CO_2 m^{-2} s^{-1} in June, while our NEE in a similar date (DOY 172, −20 ± 3 μmol CO_2 $m^{-2}s^{-1}$, Figure 2.4.A) amply exceed this value. Such a huge difference is only realistic if it is the result of a large difference in AGLB between both grasslands, possibly in combination with different phenological development stages and grazing pressure. Sjögersten et al. (2012) reported in June an AGLB of 107 ± 15 g DW m^{-2}, while in our site CAST we had 330 ± 40 g DW m^{-2} in late June (+210%, DOY 172, Figure 2.4.C), reaching the peak biomass around that date.

Indeed, the AGLB reported by Sjögersten et al. (2012) in June is more similar to our value in late May (DOY 146, 116 ± 33 g DW m^{-2}, Figure 2.4.C). These differences reveal how dynamic those grasslands are, and exemplify the need for a better understanding of CO_2 drivers in mountain ecosystems to perform accurate predictions and upscaling.

In line with this dynamism, our results emphasize the role that phenology plays as an important factor influencing CO_2 exchange fluxes (Table 2.1). The well-known effect of AGLB as CO_2 exchange driver was clear (Table 2.1 and Figure 2.5), but our results also highlighted the relevance of other vegetation fractions, including SDB and litter, which lowered the gross and net CO_2 uptake capacity of the ecosystem (see SDB and litter effects on NEE and GPP, Table 2.1 and Figure 2.5).

Moreover, there were interesting interactions between site, phenology and environmental variables (Table 2.1). On one hand, the AGLB at the subalpine grassland, CAST, was proportionally taking-up CO_2 (site x AGLB effect on GPP, Table 2.1) at lower rates than at the montane grassland BERT; resulting in proportionally lower rates of NEE per unit of AGLB (site x AGLB effect on NEE, Table 2.1). This suggests that environmental conditions were more constraining in CAST than at BERT, and vegetation at CAST could proportionally photosynthesize at lower rates than at BERT. However, although CAST was probably more temperature limited, the gross and net CO_2 uptake capacity increased more markedly in CAST than at BERT as soon as temperatures increased (site x T_a effect on NEE and GPP, Table 2.1).

Accordingly, some ecosystem functions, including biomass production and CO_2 exchange, in high elevation mountain grasslands have been reported to be more temperature-limited than water-limited (Sebastià, 2007), being mostly constrained to the warm months. Thus, the pronounced gross and net CO_2 uptake (Figure 2.4.A) with vegetation development at CAST (Figure 2.4.C), is in line with the fact that in the Mediterranean region high-elevation grasslands are generally highly productive during

the summer, while montane grasslands have a longer growing season but less productive (García-González, 2008).

On the other hand, our data suggested important site differences in the way that SWC drove GPP and R_{eco} (Figure 2.4), partly related to phenological differences between both elevations and vegetation development strategies. SWC enhanced both gross CO_2 uptake (SWC effect on GPP, Table 2.1) and release fluxes (SWC effect on R_{eco}, Table 2.1), in agreement with earlier works (Bahn et al., 2008; Davidson and Janssens, 2006; Flanagan and Johnson, 2005; Imer et al., 2013; Law et al., 2002). However, when the SWC dropped (Figure 2.4.B), CO_2 exchange fluxes diminished especially at BERT, while that diminishment at CAST was not so pronounced (Figure 2.4.A). Hence, although the SWC during the peak-biomass was clearly lower at CAST than at BERT (Figure 2.4.B, SWC below 10% indicates a dry period), the low SWC did not cause an immediate decrease of the CO_2 exchange fluxes at CAST (Figure 2.4.A).

This may well be because CAST had high SWC during the spring (Figure 2.4.B), which allowed the development of the vegetation (Figure 2.4.C), once the temperature increased (Figure 2.4.B). The well-developed AGLB (Figure 2.4.C) was able to cope with the SWC deficit during the summer drought (Figure 2.4.B), and GPP and R_{eco} did not decrease at CAST as much as at BERT (Figures 4.A). This suggests that BERT was probably more water-limited than CAST, in agreement with some studies that have highlighted that summer drought effects on productivity (Gilgen and Buchmann, 2009) and CO_2 assimilation (Bollig and Feller, 2014) may be more intense at sites with lower annual precipitation, as is the case of BERT in comparison to CAST.

Accordingly, vegetation may be adopting different development strategies between sites. Plants at CAST may be taking a “water spending strategy” (Leitinger et al., 2015), meaning that in no water-limited environments, some of the typical grassland species may not regulate the stomatal conductance until the SWC approaches the wilting point under occasional droughts (Brilli et al., 2011). However, it must be considered that long

term changes in water availability would finally lead to shifts in vegetation composition towards more opportunistic species in perennial alpine and subalpine grasslands (Debouk et al., 2015; Sebastià, 2007).

Also, CAST has a less stony soil, which allows the development of a more complex radicular system (mean belowground biomass in the first 20 cm at the peak biomass stage in 2012: BERT, 730 and CAST, 3158 g DW m^{-2}, unpublished data), which could be offsetting superficial SWC deficit.

Ultimately, the inclusion of site could be acting as a proxy of the intrinsic characteristics of each altitudinal belt (montane *vs.* subalpine), including information of complex interactions between biotic and abiotic variables, as well as current and past management practices (Leifeld et al., 2015).

Finally, AGLB was also an important driver of R_{eco} (Table 2.1 and Figure 2.5), indicating that CO_2 release was most likely dominated by the autotrophic than by the heterotrophic component of R_{eco}. In agreement, it has been reported that the magnitude of R_{eco} components changes considerably over the year in grassland ecosystems, and the autotrophic respiration reaches its maximum during the growing season (Gomez-Casanovas et al., 2012).

2.5.2 Plant functional type dominance on NEE light response

Our results suggested that PFT dominance influenced on light response parameters, when accounting for NEE per unit of biomass (Model 2.2, Table 2.2). Grass dominated (G-dominated) plots had lower asymptotic gross primary production than plots dominated by legumes (GPP_{sat}, Model 2.2, Table 2.2). This is in agreement with previous studies that have reported that legumes yield higher CO_2 exchange rates than forbs and grasses, per unit of biomass (Reich et al., 2003). Such differences in CO_2 exchange rates between PFT dominance groups are most likely related to identity effects regarding the ecophysiological characteristics of each PFT. Legumes have the ability to fix atmospheric

nitrogen (e.g. Reich et al., 2003, 1997) and have higher leaf nitrogen content, which results in higher photosynthetic capacity and CO_2 uptake (Busch et al., 2018; Lee et al., 2003; Reich et al., 1998, 1997). In addition, legumes have higher specific leaf area than grasses, a trait that has been related to increased photosynthesis rates (Reich et al., 1998).

However, L-dominated plots tended to have lower AGLB than G-dominated and F-dominated plots (Figure S2.2), and although G-dominated plots had lower GPP_{sat}, resulting in lower NEE_{AGLB} than L-dominated plots (Figure 2.6.B), their higher biomass (Figure S2.2) offset this difference at grassland ground scale (Model 1.2, Table 2.2). In this regard, previous studies showed that different PFT have different strategies to produce and maintain their biomass and access resources (Craine et al., 2002). Legumes access nitrogen to avoid nutrient limitation and produce high-nitrogen biomass, while grasses and forbs produce low-nitrogen biomass. Low-nitrogen species, especially grasses, have lower rates of physiological activity but generate dense and long-lived tissues that result in more biomass in the long term compared to high-nitrogen species, as is the case of legumes (Craine et al., 2002). Moreover, symbiotic fixation of atmospheric nitrogen by legumes requires additional energy in comparison to nitrogen acquisition from the soil (Minchin and Witty, 2005; Postgate, 1998), causing more investment of photosynthates in the nitrogen fixation processes.

In addition, apart from the effects referable to the identity effects of each PFT, we must consider possible interactions between PFT. L-dominated plots had higher evenness than G-dominated plots (Figure S2.1), meaning that L-dominated plots had higher functional diversity. Hence, functional diversity and PFT interactions may be producing an enhancement of the CO_2 exchange per unit of biomass in addition to the rates of each single PFT. This would be in agreement with the “complementarity hypothesis”, which postulates that trait dissimilarity among species or PFT maximizes resource use strategies and ecosystem functioning (Tilman et al., 1997). Several studies have

reported diversity and compositional effects, mainly due to grasses-legumes interactions on several ecosystem functions, including CO_2 exchange, yield and/or nitrogen availability (Finn et al., 2013; Nyfeler et al., 2011, 2009; Ribas et al., 2015). For instance, Ribas et al. (2015) found the highest CO_2 respiration rates in plots dominated by legumes with a certain proportion of grasses, and a positive effect of evenness on respiration, verifying and disaggregating a coupled effect of the dominant PFT from PFT interaction (evenness) effects.

In our study case we cannot disentangle dominance from interaction effects, but certainly our results show that PFT composition was influencing NEE per unit of aboveground living biomass (Model 2.2, Table 2.2), via PFT-specific light response differences, in semi-natural mountain grasslands.

2.6 Conclusions

Our study shows that phenology plays an important role as CO_2 exchange driver at seasonal scale, driving differences between elevation belts (montane *vs.* subalpine). Although the subalpine grassland (CAST) had a later vegetation development, CAST was clearly more productive (AGLB ~ +74%) than the montane grassland (BERT) during the peak biomass stage, and yielded higher NEE values (NEE ~ +48%). Thus, at least in mountain environments, detailed information on phenology is key to understand the *a priori* counterintuitive finding that a high-elevation grassland (CAST) is more productive than a comparable grassland at the montane elevation (BERT), with a longer growing season and warmer summer temperature. Our results also suggest that there are site differences in the way that environmental variables and phenology mediate CO_2 exchange fluxes. Although CAST was more temperature constrained, temperature enhanced gross and net CO_2 uptake at higher rates at CAST than at BERT. Also, both grasslands experienced a pronounced summer dry period, which substantially reduced productivity at the lower elevation, from which only a minor recovery could be observed

in autumn. However, the delayed phenology at the subalpine grassland reduced vegetation's sensitivity to summer dryness, which did not experience a reduction in CO_2 exchange, even though the low SWC.

Moreover, our results showed that vegetation composition, in terms of PFT, influenced on the CO_2 exchange. Legume dominated plots presented higher NEE rates than grass dominated plots per unit of aboveground living biomass; grass dominated plots having lower asymptotic gross primary production (GPP_{sat}) than legume dominated plots. Overall, a deeper knowledge of phenology and vegetation ecophysiological responses under different climatic conditions is key to upscale CO_2 exchange fluxes in a seasonal and inter-annual scale in semi-natural mountain grasslands.

Acknowledgements

Thanks to all the colleagues who collaborated in laboratory and fieldwork tasks: Helena Sarri, Haifa Debouk, Cristina Rota, Fabrice Gouriveau, Carla Bellera and Dafne Padrós. This study was developed within the project CAPACITI supported by a Marie Curie Intra European Fellowship within the 7th European Community Framework for Núria Altimir (PIEF-GA-2010-275855) and the project BIOGEI (CGL2013-49142-C2-1-R) supported by a FPI fellowship for Mercedes Ibañez (BES-2014-069243) funded by the Spanish Science Foundation (FECYT).

2.7 Supplementary material

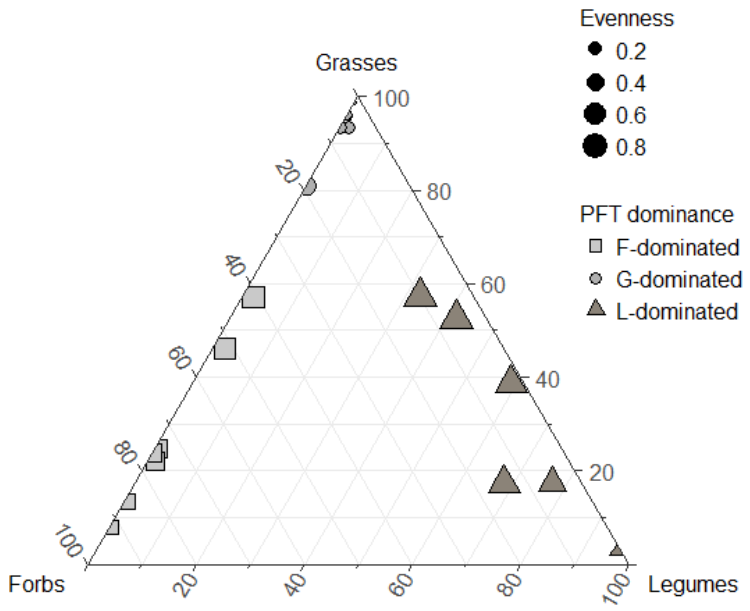

Figure S2.1. Plant functional type (PFT) dominance groups — forbs dominated (F-dominated), grasses dominated (G-dominated), and legumes dominated (L-dominated) — after clustering (Ward's method), based in the proportion of each PFT and the evenness index (Kirwan et al., 2007). The position in the ternary plot indicates the proportion of the corresponding PFT and the size of the point corresponds to the evenness index.

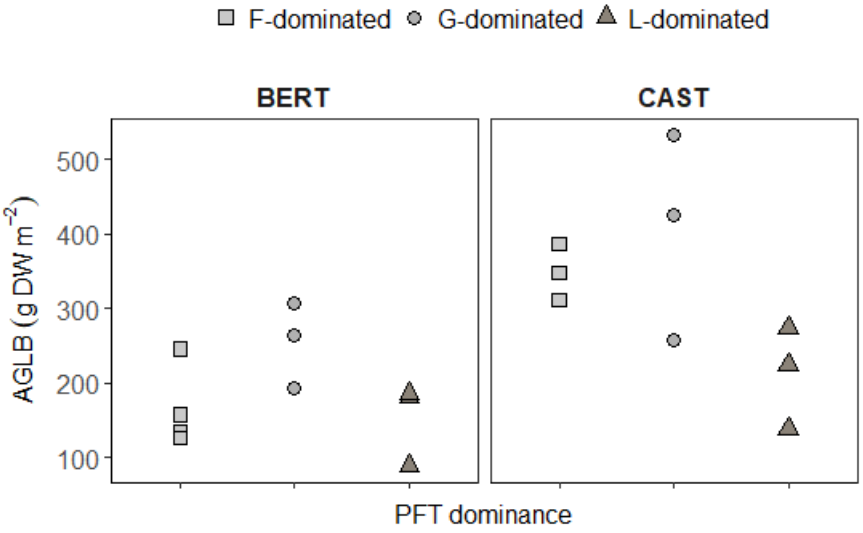

Figure S2.2. Aboveground living biomass (AGLB) per site and per plan functional type (PFT) dominance group: forbs dominated (F-dominated), grasses dominated (G-dominated) and legumes dominated (L-dominated).

Chapter 3 Forage species drive CO_2 exchange responses in a sown grassland of the eastern Pyrenees

Mercedes Ibañez[1]*, Núria Altimir[2a], Àngela Ribas[3,4], Werner Eugster[5], Maria Teresa Sebastià[1,2]

[1]GAMES group & Dept. HBJ, ETSEA, University of Lleida (UdL), Lleida, Spain

[2]Laboratory of Functional Ecology and Global Change, Forest Sciences Centre of Catalonia (CTFC), Solsona, Spain

[3]Universitat Autònoma de Barcelona, Bellaterra, Spain

[4]Centre for Ecological Research and Forestry Applications (CREAF), Bellaterra, Spain

[5]ETH Zürich, Institute of Agricultural Sciences, Zürich, Switzerland

[a]Current address: Institute for Atmospheric and Earth System Research (INAR), University of Helsinki, Finland

MI performed research, analysed data and wrote the paper; NA conceived and designed the study, performed research and revised the paper; AR conceived and designed the study and revised the paper; WE analysed data and revised the paper; MTS conceived and designed the study and revised the paper.

*Corresponding author; e-mail: mercedes.ibanez@hbj.udl.cat; phone: +34 973702623.

3.1 Abstract

Intensively managed sown forage grasslands provide essential resources for animal feeding. Assessing the influence of grassland species on the net ecosystem CO_2 exchange (NEE) is key to develop management strategies that can help mitigate climate change, while at the same time optimizing productivity of these systems. However, little is known about the effect of grassland species on CO_2 exchange fluxes and the net biome production (NBP); considering separately growth and fallow periods, and taking into account the management associated with the given species, and species ecophysiological responses. Our study assesses the influence of cereal monocultures *vs.* cereal-legume mixtures on CO_2 gross and net uptake, and ecosystem respiration, during the growth and fallow periods; NBP during the grassland growth period; and potential sensitivities of CO_2 exchange related to light, temperature and soil water content in a sown forage grassland of the Pyrenees. In addition, our study presents the first long term (seven years) NEE dataset of a sown forage grassland in the Pyrenees. Results provide strong evidence that cereal-legume mixtures lead to higher net CO_2 uptake than cereal monocultures. All cereal-legume mixtures and some cereal monocultures had a negative NBP (net gain of C) during the grassland growth period, indicating C input to the system, besides the yield. Management associated with cereal-legume mixtures favoured vegetation voluntary regrowth during the fallow period, which was decisive for the cumulative net CO_2 uptake of the entire grassland season. In addition, increased net CO_2 uptake in cereal-legume mixtures resulted from higher gross CO_2 uptake, while respiratory fluxes did not significantly increase. Overall, cereal-legume mixtures enhanced the net CO_2 sink capacity of sown forage grasslands, while ensuring productivity and forage quality.

Key words: Diversity-interaction models, ecosystem respiration (R_{eco}), gross primary production (GPP), legumes, light response, management, net ecosystem exchange (NEE).

3.2 Introduction

Forage systems represent 26% of the world's surface and provide crucial goods and services for human population (FAOSTAT 2019). Assessing the influence of forage species on the carbon (C) balance of these systems is essential to develop management strategies that can mitigate climate change, while optimizing productivity. In this regard, sown forage grasslands are cropped plant systems used for grazing, hay or silage, ploughed and harvested/grazed every one to five years (Allen et al., 2011; Huyghe et al., 2014), combining thus characteristics of both grasslands and croplands.

Sown forage grasslands provide a good opportunity to assess the influence of different management practices on C dynamics. They combine an alternation of forage species, including cereals, legumes, or a combination of both; with extensively grazing during the fallow, the latter especially carried out in Mediterranean mountain regions (Sebastià et al., 2011). These practices have been traditionally conducted to increase productivity and keep soil fertility (Sánchez et al., 2013); but only recently research has started to focus on the effect that those management practices may have on C dynamics, paying special attention to grassland species selection.

To this regard, cereal-legume mixtures have been generally related to a higher productivity (De Deyn et al., 2009; Finn et al., 2013; Hector et al., 1999), resulting from the higher leaf nitrogen of legumes, which means higher photosynthetic capacity (Busch et al., 2018; Lee et al., 2003; Reich et al., 1998) and gross primary production (GPP). In addition, legumes can also increase the resource use efficiency of the overall community, including water (Chapagain and Riseman, 2015; Liu et al., 2016), nitrogen and light (Hofer et al., 2017; Milcu et al., 2014), enhancing productivity. Accordingly, grassland species can drive several ecosystem functions via species identity effects, but also via species interactions, evenness and complementarity effects (Kirwan et al., 2007; Orwin et al., 2014; Wolfgang et al., 2017).

However, the NEE is the budget between GPP, and ecosystem respiration (R_{eco}), and although an increase in productivity has been described to some extent under cereal-legume mixtures compared to mono-specific stands, how grassland species influence GPP, R_{eco}, and finally the NEE budget still is not well understood. In addition, R_{eco} is the sum of autotrophic and heterotrophic respiration, and grassland species are expected to influence these components in different ways, increasing the complexity. Therefore, there is a need for a deeper understanding of the role of grassland species and species interactions on NEE and its components — GPP and R_{eco} — to assess the overall C cycle during the grassland growth, but also during the fallow period.

On the other hand, it is also crucial to understand the role of grassland species on net biome production (NBP), accounting for all C inputs and exports (NBP = NEE – C_{input} + C_{export}), to assess the final C budget, beyond the NEE. Many grasslands and forage crops may be acting as net CO_2 sinks when only assessing NEE, but they become net CO_2 sources when accounting for the oxidation (via digestion by animals) of total exported biomass (Ceschia et al., 2010; Kutsch et al., 2010; Moors et al., 2010). However, species richness, and especially cereal-legume mixtures, have been reported to increase NBP via increasing soil C storage (Fornara and Tilman, 2008; Wolfgang et al., 2017), among other mechanisms.

Finally, the interaction among grassland species, local conditions and management practices result in high CO_2 exchange variability (Moors et al., 2010; Oertel et al., 2016). While information on CO_2 exchange in grasslands (Berninger et al., 2015; Imer et al., 2013; Schaufler et al., 2010) and forage crops (Ceschia et al., 2010; Kutsch et al., 2010; Vuichard et al., 2016) of central and northern Europe is rather abundant, in the Mediterranean basin such information is very scarce, despite the fact that sown forage grasslands are crucial for animal feeding in this region. Grassland productivity in Mediterranean areas is among the lowest in Europe (Smit et al., 2008), due to important water constraints (Porqueddu et al., 2016); and while direct grazing from permanent

grasslands fulfils an important part of livestock requirements in north-central Europe, sown forage grasslands are more important in Mediterranean areas (Smit et al., 2008). Thus, more information is needed from the Mediterranean region, and especially from Mediterranean mountain areas, to establish management practices that may enhance C sequestration, ensuring productivity in this area highly vulnerable to climate change (FAO, 2010).

Our study presents the first long-term (seven years) dataset of NEE measurements of a sown forage grassland in the Pyrenees; which in addition has been in a crop rotation system of three different cereal species grown in monocultures and two different combinations of cereal-legume mixtures. Accordingly, we assess differences between cereals grown in monoculture and forage cereal-legume mixtures in (1) NEE, considering gross CO_2 uptake (GPP) and respiration fluxes (R_{eco}) separately for the two periods of (a) grassland growth and (b) fallow; (2) NBP during the grassland growth period; and (3) potential sensitivities of CO_2 exchange related to short-term variations in light, temperature and soil water content. We hypothesize that cereal-legume mixtures in comparison to cereal monocultures: (1) show more negative NEE (more net CO_2 uptake); (2) show more negative NBP during the grassland growth period; and (3) lead to more negative NEE due to increased GPP in combination with not increased R_{eco}.

For that purpose, we have been monitoring management events, recording ecosystem-scale CO_2 fluxes, and micrometeorological data with an eddy covariance flux station, from 2011 to 2017, in a sown forage grassland in the Eastern Pyrenees.

3.3 Material and methods

3.3.1 Study site and experimental design

The study site is a sown forage grassland located in the montane elevation belt of the Eastern Pyrenees, in Pla de Riart (42° 03' 48" N, 1° 30' 48" E, Figure 3.1), at 1003 m a.s.l. Climate is sub-Mediterranean (Peel et al., 2007), typical in mountain areas with Mediterranean influences, with a mean annual precipitation of 750 mm and mean annual temperature of 11 ºC (Ninyerola et al., 2000), including the summer drought period. The soil is a petrocalcic calcixerept (Badía-Villas and del Moral, 2016).

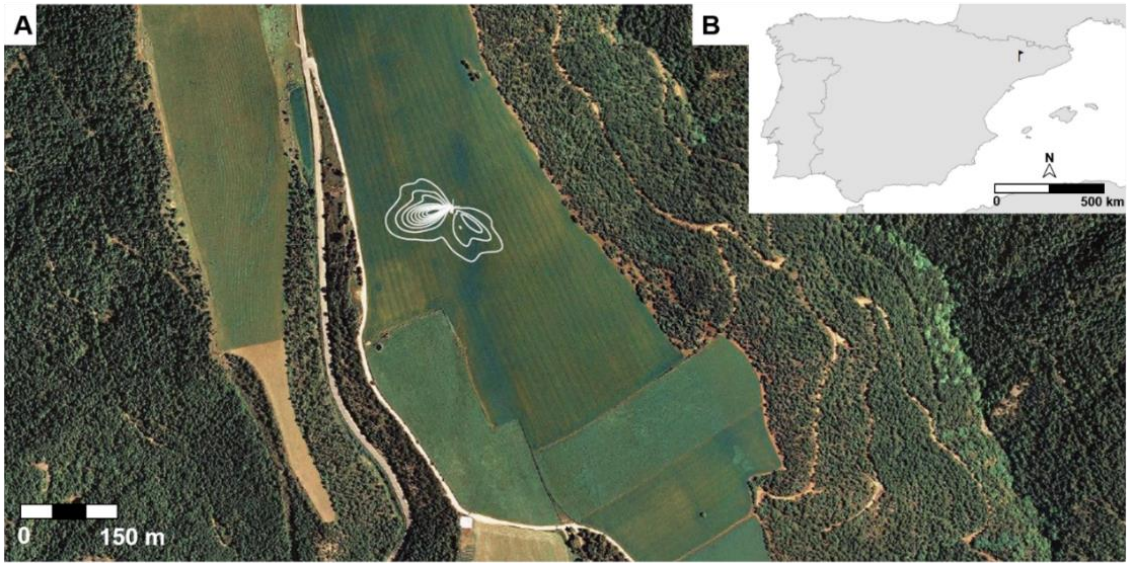

Figure 3.1. (A) Ortho-image of the study site (date: May 2013, source: Institut Cartogràfic i Geològic de Catalunya, https://www.icgc.cat/es) and contour plot example of the footprint, based in by the Kljun model (Kljun et al., 2004). Contours show the 10% to 90% flux contribution areas at 10% intervals. (B) Situation of the study site on the Iberian Peninsula

All management events, including fertilizing, sowing and harvesting (Table 3.1) were reported by the manager of the site and validated by in-situ visits.

Table 3.1. Management events: grassland type, grassland species, fertilizer type (NPK 9-23-30: nitrogen 9%, phosphorus 23%, potassium 30 %; urea; and NAC 27: calcium ammonium nitrate 27% nitrogen) and rate, sowing date and rate, harvesting date, yield and C exported through yield.

Grassland type	Grassland species	Fertilizer (kg ha^{-1})	Sowing date	Sowing rate (kg ha^{-1})	Harvesting date	Yield (dry weight)	
						(kg ha^{-1})	(g C m^{-2})
Cereal monoculture	Barley	NPK 9-23-30, 250	01/11/2010	221	07/07/2011	3000	138
Cereal monoculture	Triticale	Urea, 140	01/11/2011	221	01/07/2012	13133	607
Cereal-legume mixture	Triticale, oat, vetch	Not applied	01/11/2012	225	19/06/2013	7500	339
Cereal-legume mixture	Oat, vetch	Urea, 130	01/11/2013	239	01/07/2014	6720	304
Cereal monoculture	Wheat	NPK 9-23-30, 250 Urea, 120	01/11/2014	212	01/08/2015	2580	118
Cereal monoculture	Barley	NAC 27, 100	01/11/2015	221	01/09/2016	4500	208
Cereal-legume mixture	Oat, vetch	Not applied	01/11/2016	235	01/06/2017	7200	326

The site was managed by a rotation of cereals grown in monoculture and cereal-legume mixtures (Figure 3.2). Every year the yield was harvested, and during the fallow (from harvest to next sowing), the voluntary regrowth of the vegetation was extensively grazed by around 30 cattle (≈ 0.91 livestock units (LSU) ha^{-1}) from late August to late October. Harvesting practices differed between cereal monocultures and cereal-legume mixtures. When the grassland was a cereal monoculture, the yield was harvested in July or early August, while cereal-legume mixtures were harvested when the yield was still fresh for silage, in late May or early June. Sowing was done in October or early November (Figure 3.2), after ploughing, which was done in September-October.

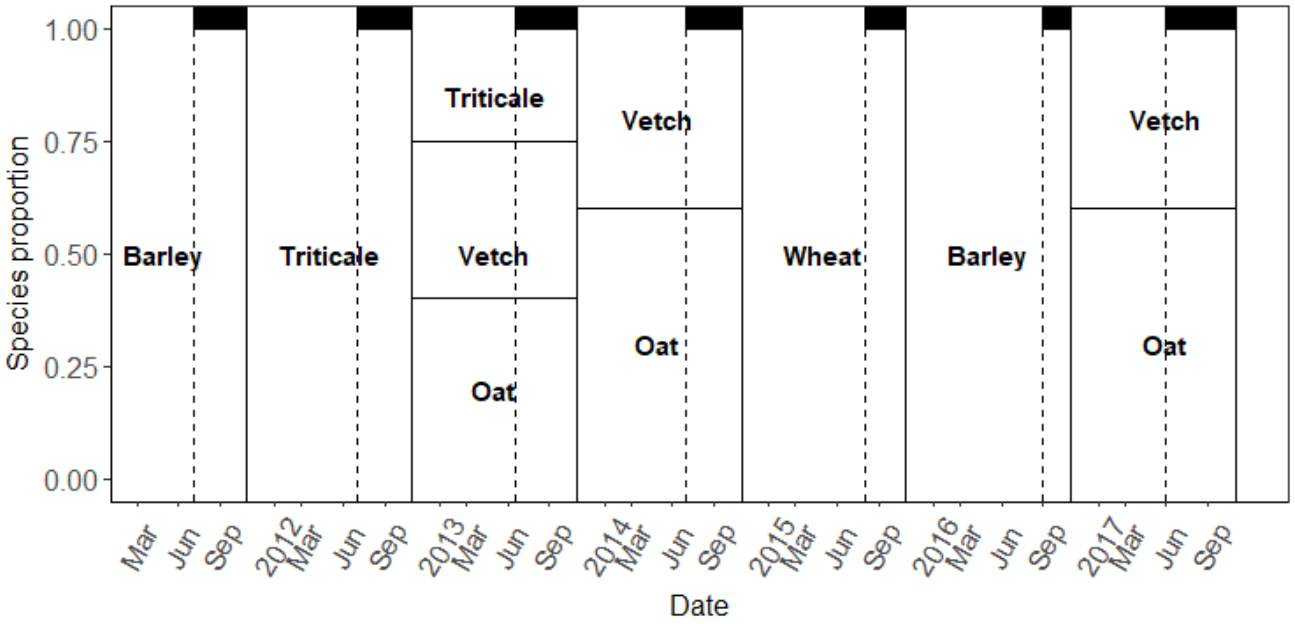

Figure 3.2. Grassland rotation timeline, species proportions and management events: black dashed lines indicate harvesting and solid black lines indicate sowing. Top black bands indicate fallow periods in which there was grazing.

Yield was estimated (Table 3.1) considering the productivity reported by the manager and *in situ* samplings after oven drying plant material at 60 ºC until constant weight. In addition, plant material sampled during *in situ* visits was analysed to determine C content and forage quality indicators (Table S3.1). Analysis were performed by the Department of Animal and Food Science, Universitat Autònoma de Barcelona (https://www.uab.cat/department/animal-food-science) according to standard methods (Table S3.1). Afterwards, C exported through yield (Table 3.1) was estimated, considering the yield, species proportions (Figure 3.2), and species C content (Table S3.1). C exported through yield was used to account for the NBP (Section 3.3.2).

3.3.2 Eddy covariance measurements

The site is equipped with an eddy covariance flux station, running since August 2010, and our study period included data from sowing of the first studied grassland season (barley, sown 01/11/2010) until the end of the fallow period of the last studied grassland season (oat and vetch mixture, sown 01/11/2017, Figure 3.2). The eddy covariance flux

station continuously measured the concentration of CO_2 (mmol m^{-3}) and H_2O (mmol m^{-3}) using an open-path CO_2 and H_2O gas analyser (LI-7500, LI-COR Inc., Lincoln, NE, USA), and turbulent flux components, including wind direction and speed using a 3D sonic anemometer (CSAT-3, Campbell Scientific Inc, Logan, UT, USA) to calculate CO_2, H_2O, and energy exchange at the ecosystem level.

In addition, the station recorded ancillary meteorological variables, including incoming and outgoing shortwave and longwave radiation (NR01, Hukseflux, Delft, the Netherlands); air temperature (T_a, CS215, Campbell Scientific Inc, Logan, UT, USA); average soil temperature 1-20 cm (T_s, TCAV, Campbell Scientific Inc, Logan, UT, USA); volumetric soil water content (SWC, CS616, Campbell Scientific Inc, Logan, UT, USA); photosynthetically active radiation (PAR, SKP215, Skye Instruments Ltd, Powys, UK); and normalized difference vegetation index, calculated as NDVI = (NIR – Red) / (NIR + Red), where “Red” and “NIR” are the spectral reflectance measurements acquired in the red and near-infrared regions, respectively.

Raw data provided by the sensors were processed and CO_2 fluxes were calculated as 30 minutes averages using the EddyPro software (LI-COR Inc, Lincoln, NE, USA). The sign convention used here uses negative values if the flux was from the atmosphere to the biosphere and positive values if the flux was from the biosphere to the atmosphere (micrometeorological sign convention).

Frequency response corrections (Moncrieff et al., 2004, 1997), density fluctuation corrections (Webb et al., 1980), and determination of data quality using the Foken et al. (2004) approach were applied. The Foken et al. (2004) approach suggests a quality scale ranging from 1 (highest data quality) to 9 (poorest data quality). Records with quality 7 or higher were excluded (Papale, 2012). Also, CO_2 fluxes outside a physically realistic range (± 50 μmol m^{-2} s^{-1}) were rejected.

Night-time (PAR < 5 μmol photons m^{-2} s^{-1}) CO_2 fluxes were inspected, as they are susceptible to be underestimated under low turbulence (Aubinet et al., 2012a), conditions that can be frequent at night. We inspected the possibility of a low turbulence effect assessing the existence of an u_* threshold at all recorded T_s classes (Reichstein et al., 2005), ranging from –3 to 34 ºC in 1 ºC intervals. Relevant u_* thresholds were not detected. In addition, we inspected night-time CO_2 fluxes in order to detect possible outliers and calculated the 0.025, 0.25, 0.5, 0.75 and 0.975 quantiles for each T_s class. Data below the lowest (0.025) or the highest quantile (0.975) were excluded from further analysis.

Data were filtered according to the footprint, based on the Kljun model (Kljun et al., 2004), including all the fluxes in which more than 80% of the contribution came from the study field (Göckede et al., 2008). After all data cleaning and filtering, retained data for further analysis were a 65% of all the available data, ranging between 81% and 53% depending on year (Table S3.2).

Afterwards, NEE data were gap-filled using the sMDSGapFill function (Reichstein et al., 2005) of the REddyProc package (Wutzler et al., 2018) for R software (R core Team, 2017), which combines the mean diel variation method and lookup tables when meteorological data are available. The goodness of the gap-filling was also inspected comparing observed NEE data with their theoretically predicted data by gap-filling (see an example in Figure S3.1).

To assess NEE, GPP and R_{eco} seasonal patterns, gap-filled NEE data were also partitioned into GPP and R_{eco}, using the night-time based partitioning approximation, SMRFLuxPartition equation (Reichstein et al., 2005), also of the REddyProc package (Wutzler et al., 2018). Afterwards, we performed NEE, GPP and R_{eco} budgets (expressed in g C m^{-2}) for each: (a) grassland season, defined as the time from sowing to next sowing; (b) grassland growth period, defined as the time from sowing to harvest; and (c) fallow period, defined as the time from harvesting to next sowing. In 2014 systematic

data gaps occurred due to energy supply problems, for which NEE, GPP and R_{eco} budgets could not be calculated. However, 2014 gap-filled data were used to describe CO_2 exchange dynamics, and real recorded data were included in all the modelling.

Finally, NBP during the growth period was estimated. NBP can be estimated knowing the NEE; C exports, including harvest/grazing and other gas emissions such as methane or volatile organic compounds; and C imports, including organic C fertilizers and sowing. In our study, C exports through methane were expected to be not very significant, because methane effluxes require water saturated soils, typically with standing water (Oertel et al., 2016), which was never the case; and volatile organic compounds were expected to be negligible (Soussana et al., 2010). C inputs through sowing and fertilizers (mostly inorganic nitrogen fertilizers) could also be neglected as they only represent a very small C amount (Table 3.1). Therefore, NBP during the grassland growth was estimated as the sum of the NEE budget of that period and C exported through the yield (Equation 3.1).

$$NBP = NEE + Yield$$

(Equation 3.1)

3.3.3 CO_2 exchange modelling

3.3.3.1 Grassland species influence on NEE: diversity-interaction model

To assess the influence of grassland species on NEE, we modelled observed NEE data as a function of grassland species composition, main environmental variables and time, based on a diversity-interaction model (Kirwan et al., 2009, 2007). The modelling compares a null model, in which a change in the diversity has no effect on the response variable, to models that address the diversity influence at different levels. In our study we compared the null model (Equation 3.2), in which NEE (μmol CO_2 m^{-2} s^{-1}) depended only on environmental variables, including T_a (ºC), net radiation (R_{net}, W m^{-2}), SWC (fraction), vapour pressure deficit (VPD, hPa), and time — considering time as grassland season —

to a diversity-interaction model, which included species identity and species interaction effects (Equation 3.3).

$$NEE = \beta_{T_a} T_a + \beta_{R_{net}} R_{net} + \beta_{SWC} SWC + \beta_{VPD} VPD + \beta_{time} time + \varepsilon$$

(Equation 3.2. Null model)

$$NEE = Null\ model + \beta_B P_B + \beta_T P_T + \beta_W P_W + \beta_{OV} P_{OV} + \beta_{TOV} P_{TOV} + \varepsilon$$

(Equation 3.3. Diversity-interaction model)

Here *P* indicates species proportions and the sub-index *B* indicates barley, *T* triticale, *W* wheat, *O* oat and *V* vetch respectively. The models were run without intercept in order to test the effect of all the species proportions at the same time.

A preliminary modelling showed that SWC and time could be excluded from the null model (Equation 3.2), since the inclusion of these variables did not provide a better fitting. Then, the null model (Equation 3.2) and the diversity-interaction model (Equation 3.3) were compared by an analysis of variance (ANOVA). The diversity-interaction model was significantly different from the null model ($F = 7.65$, $p < 0.001$). Accordingly, the final model was the diversity-interaction model, which included the proportion of each grassland species and its interactions, in addition to environmental variables (T_a, R_{net}, VPD).

The modelling was run on all observed data (30 minute averages); on daily averaged data; and on weekly averaged data. The model performed the best fitting (best adjusted R^2) when using weekly averaged data, probably due to a considerable day-to-day variability of the environmental variables and CO_2 fluxes. Also, considering that the main goal of this modelling was to assess the influence of grassland species on NEE, whose influence is probably more noticeable at a seasonal scale, we present the model run on the weekly averaged data, as it was able to reduce noise and extract the influence of grassland species with greater reliability. Finally, we explored differences between cereal monocultures and cereal-legume mixtures from a mechanistic

perspective, modelling by separately light response of observed CO_2 fluxes during daytime (termed as NEE_{day} in what follows), and T_s and SWC response of night time fluxes (termed as $R_{eco,night}$ in what follows) as explained below.

3.3.3.2 Grassland species influence on NEE_{day} light response

In order to assess differential ecophysiological responses between cereal monocultures and cereal-legume mixtures on the NEE_{day} (PAR > 5 µmol photons m^{-2} s^{-1}) light response, we used the logistic sigmoid model (Moffat, 2012), which models NEE_{day} (µmol CO_2 m^{-2} s^{-1}) as function of PAR (Equation 3.4).

$$NEE_{day} = -2 \cdot GPP_{sat} \cdot \left(-0.5 + \frac{1}{1+e^{\frac{-2 \cdot \alpha \cdot PAR}{GPP_{sat}}}}\right) + R_{eco,day}$$

(Equation 3.4)

Here GPP_{sat} (µmol CO_2 m^{-2} s^{-1}) is the asymptotic gross primary production, α (dimensionless) is the apparent initial quantum yield, defined as the initial slope of the light-response curve, and $R_{eco,day}$ (µmol CO_2 m^{-2} s^{-1}) the average daytime ecosystem respiration. Light response parameters (GPP_{sat}, α and $R_{eco,day}$) were calculated for each day and grassland season, using the nlsList function of the nlme package (Pinheiro et al., 2015). Parameters whose estimates were not significantly different from zero ($p \geq 0.05$) were discarded from further analysis.

Afterwards, we described light response dynamics and assessed differences on the light response parameters between cereal monocultures and cereal-legume mixtures. For that purpose we run anovas ANOVAs and tukey post-hoc tests, using the HSD.test function of the agricolae package (Mendiburu, 2017), with the given parameter (GPP_{sat}, α and $R_{eco,day}$) as a function of forage type (cereal monoculture and cereal-legume mixture) and period (growth and fallow).

3.3.3.3 Grassland species influence on $R_{eco,night}$ response to temperature and soil water content

A preliminary overview of $R_{eco,night}$ (PAR < 5 µmol photons m^{-2} s^{-1}) suggested that $R_{eco,night}$ increased with T_s at T_s < 20°C, but decreased above this threshold (Figure S3.2). Therefore, we modelled $R_{eco,night}$ (µmol CO_2 m^{-2} s^{-1}) as a function of T_s (ºC) and SWC (fraction) using the equations proposed by Reichstein et al. (2002), which consider changes in the temperature sensitivity depending on soil moisture (Equations 3.5 – 3.7).

$$R_{eco,night} = R_{eco,ref} \cdot f(T_s, SWC) \cdot g(SWC)$$

(Equation 3.5)

$$f(T_s, SWC) = e^{E_0(SWC)\cdot\left(\frac{1}{T_{ref}-T_0}-\frac{1}{T_s-T_0}\right)}$$

(Equation 3.6)

$$g(SWC) = \frac{SWC - SWC_0}{\left(SWC_{1/2} - SWC_0\right) + (SWC - SWC_0)}$$

(Equation 3.7)

Here the activation energy, E_0 ($ºC^{-1}$), is a linear function of SWC (E_0 = a+b·SWC); T_{ref} is the reference temperature, set as the mean temperature of a given period, here set as the mean T_s of the entire measuring period (T_{ref} = 12.12 ºC); T_0 the lower limit for $R_{eco,night}$, here set at –46.02 ºC, as in the original model by Lloyd and Taylor (1994); SWC_0 (fraction) the soil water content below which $R_{eco,night}$ vanishes; $SWC_{1/2}$ (fraction) the soil water content at which maximal $R_{eco,night}$ halves; and $R_{eco,ref}$ (µmol CO_2 m^{-2} s^{-1}) the reference ecosystem respiration at standard conditions (T_{ref}) and non-limiting SWC (Reichstein et al., 2002). $R_{eco,night}$ response parameters ($R_{eco,ref}$, E_0, SWC_0 , $SWC_{1/2}$) were calculated for each grassland season, using the nlsList function.

Similarly as in the diversity-interaction model (Section 3.3.3.1), we performed the $R_{eco,night}$ modelling on all observed data (30 minutes averaged), on daily averaged data and on

weekly averaged data. Afterwards, we calculated R^2 as the linear relationship between modelled and measured observations. The modelling performed the best R^2 when using weekly averaged data, probably due to the high day-to-day variability of $R_{eco,night}$ and T_s. The model based on weekly averaged data is presented and discussed.

3.4 Results

3.4.1 Cereal monocultures *vs.* cereal-legume mixtures: CO_2 exchange dynamics and budgets

Seasonal CO_2 flux dynamics in the studied sown forage grassland evolved according to environmental conditions, grassland growing and management events (Figure 3.3). CO_2 exchange capacity of the system decreased with harvesting (Figure 3.3.A), also showed by the drastic decrease of the NDVI (Figure 3.3.D). Maximum net CO_2 uptake was achieved during spring, when temperatures were mild, SWC increased, and grassland development reached its peak biomass (Figure 3.3).

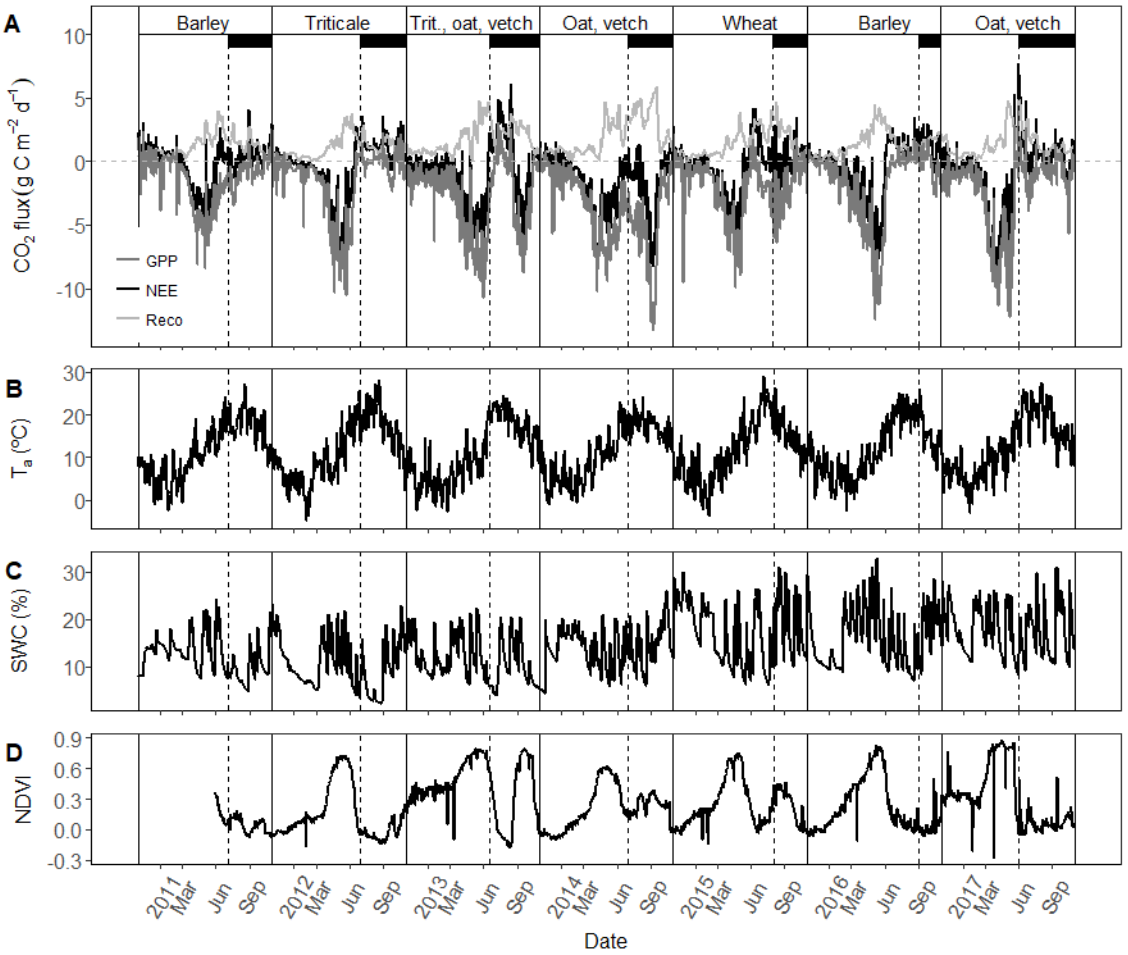

Figure 3.3. Daily averaged (A) CO_2 fluxes: net ecosystem exchange (NEE), gross primary production (GPP) and ecosystem respiration (R_{eco}); (B) air temperature (T_a); (C) volumetric soil water content (SWC); and (D) normalized difference vegetation index (NDVI). Titles in the top panel indicate grassland species. Black dashed lines indicate harvest events and solid black lines indicate sowing events. Top black bands indicate fallow periods in which there was grazing.

The field acted as a net CO_2 sink throughout all the studied grassland seasons (negative NEE, Figure 3.4.A). NEE of cereal-legume mixtures was more negative and less variable (−363 g C m^{-2}, year 2013, and −383 g C m^{-2} year 2017, Figure 3.4.A) than that of cereal monocultures (ranging from −70 to −226 g C m^{-2}, Figure 3.4.A).

The system acted as a net sink during the grassland growth (negative NEE, Figure 3.4.B) and as a small net source during the fallow period (positive NEE, Figure 3.4.C). Cereal-legume mixtures showed the highest net CO_2 uptake during grassland growth, with a NEE of –359 and −429 g C m^{-2}, in 2013 and 2017 respectively. On the other hand, cereal monocultures had a NEE that ranged from –128 to −348 g C m^{-2} (Figure 3.4.B), with triticale being the cereal monoculture with the highest net uptake (−348 g C m^{-2}, Figure 3.4.B).

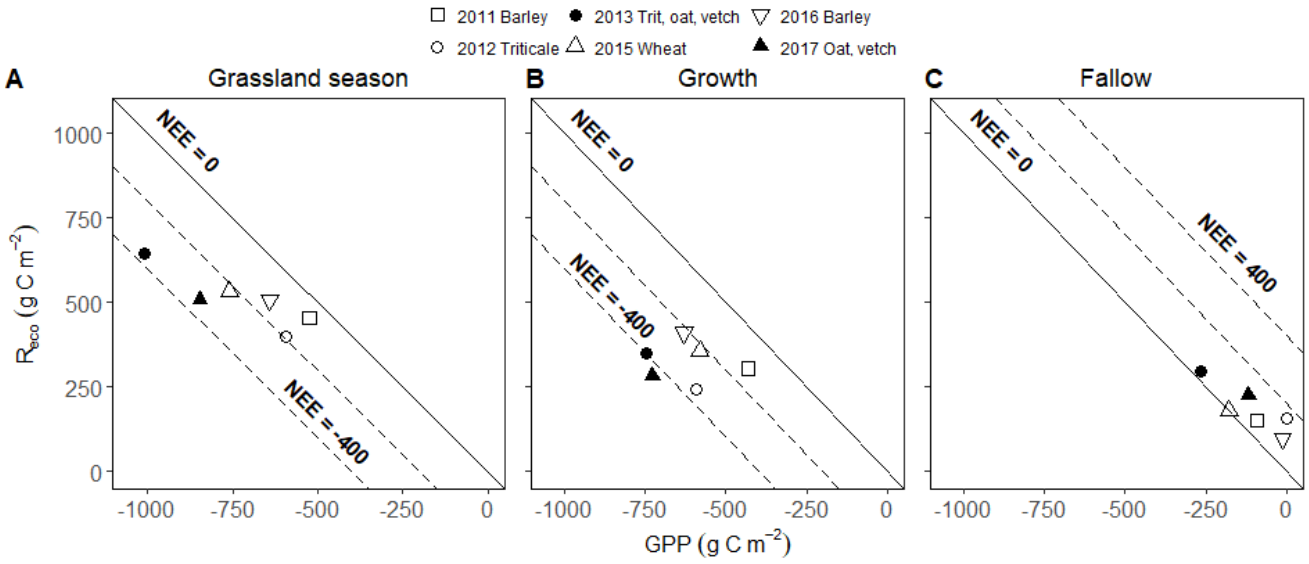

Figure 3.4. Net ecosystem exchange (NEE), gross primary production (GPP) and ecosystem respiration (R_{eco}) budgets after gap-filling per: (A) grassland season, defined as the time from sowing to next sowing; (B) growth period, defined as the time from sowing to harvest; and (C) fallow period, defined as the time from harvest to next sowing. Solid diagonal line indicates NEE = 0 g C m^{-2}, dashed diagonal lines indicate ± 200 g C m^{-2} NEE intervals. Open symbols indicate cereal monocultures and solid symbols cereal-legume mixtures.

Moreover, NBP during the grassland growth showed net C input into the system (negative NBP), except during the cereal monocultures of triticale (year 2012), and barley (year 2011, Figure 3.5). The most negative NBP was achieved during the wheat monoculture in 2015 (NBP ≈ −108 g C m^{-2}, Figure 3.5), followed by the oat and vetch mixture in 2017 (NBP ≈ −67 g C m^{-2}, Figure 3.5).

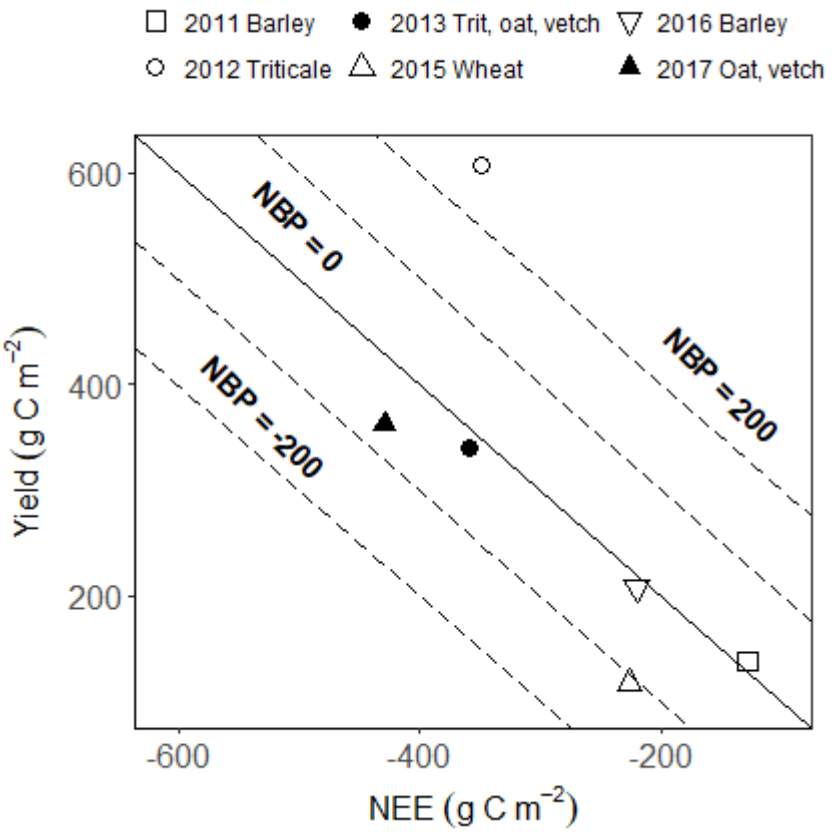

Figure 3.5. Net biome production (NBP), net ecosystem exchange (NEE) and yield during the grassland growth period, defined as the time from sowing to harvest. Solid diagonal line indicates NBP = 0 g C m^{-2}, dashed diagonal lines indicate ± 100 g C m^{-2} NBP intervals. Open symbols indicate cereal monocultures and solid symbols cereal-legume mixtures.

Finally, R_{eco} was the dominant flux during the fallow period in all cases (Figure 3.4.C), although there were some differences in the CO_2 exchange dynamics between cereal monocultures and cereal-legume mixtures during that period (Figure 3.3.A). During the fallow of grass-legume mixtures there was a more marked voluntary regrowth of the vegetation (Figure 3.3.D) that promoted a period of net CO_2 uptake after the harvest,

which was especially strong in the triticale, oat and vetch mixture (year 2013), and the oat and vetch mixture (year 2014, Figure 3.3.A). Note that although gap-filled 2014 data were not used to account for CO_2 exchange budgets (Figure 3.4) due to systematic gaps; 2014 gap-filled data could be used to describe CO_2 exchange dynamics and was possible to identify this rebound in the net CO_2 uptake during the fallow period of that year.

On the contrary, when the grassland was a cereal monoculture there was no voluntary regrowth during the fallow period (Figure 3.3.D), and gross and net CO_2 uptake capacity of the system decreased drastically (Figure 3.3.A). The exception was the wheat monoculture in 2015, when there was vegetation voluntary regrowth after the harvest that resulted in net CO_2 uptake during the fallow period.

3.4.2 Grassland species interaction effects on seasonal NEE

The diversity-interaction model (Table 3.2) confirmed the influence of grassland species on NEE already detected through the analysis of CO_2 exchange dynamics and budgets (Section 3.4.1). The model estimates indicated less net CO_2 uptake in cereal monocultures than in cereal-legume mixtures (Table 3.2, negative sign in the estimate means uptake), again with a high variability within cereal monocultures. Barley was the cereal monoculture with the lowest net uptake (-1.0 ± 0.3 μmol CO_2 m^{-2} s^{-1}, $t = -3.39$, $p < 0.001$, Table 3.2) and triticale was the cereal monoculture with the highest net uptake among the monocultures (-1.6 ± 0.4 μmol CO_2 m^{-2} s^{-1}, $t = -4.40$, $p < 0.001$, Table 3.2). Cereal-legume mixtures, however, showed significantly higher net CO_2 uptake rates (oat x vetch -2.0 ± 0.3 μmol CO_2 m^{-2} s^{-1}, $t = -7.44$, $p < 0.001$, Table 3.2) than all cereal species in monoculture. The addition of triticale in the mixture did not have a significant effect on NEE (Table 3.2).

Table 3.2. Diversity-interaction model results. Net ecosystem exchange (NEE) as function of air temperature (T_a), net radiation (R_{net}), vapour pressure deficit (VPD), and species proportions: barley, triticale, wheat, oat and vetch (see grassland species proportions in Figure 3.2). Model performed on weekly averaged values of all the variables. Estimates (Est.) of the explanatory variables, standard error (SE), t and p-value.

	NEE (μmol CO_2 m^{-2} s^{-1})			
	Est.	**SE**	**t**	**p**
T_a (ºC)	0.19	0.04	5.06	< 0.001
R_{net} (W m^{-2})	−0.030	0.002	−12.61	< 0.001
VPD (hPa)	0.17	0.05	3.56	< 0.001
Barley (fraction)	−1.0	0.3	−3.39	< 0.001
Triticale (fraction)	−1.6	0.4	−4.40	< 0.001
Wheat (fraction)	−1.5	0.3	−4.42	< 0.001
Oat x vetch (fraction)	−2.0	0.3	−7.44	< 0.001
Triticale x oat x vetch (fraction)	1	2	0.58	0.6
R^2_{Adj}	0.45			< 0.001

3.4.3 Grassland species influence on NEE_{day} light response

All three light response parameters exhibited pronounced seasonality (Figure 3.6), as result of phenological changes and management events. In addition, GPP_{sat} exhibited slightly higher values during the growth of cereal-legume mixtures than of cereal monocultures (Figure 3.7). Moreover, α and GPP_{sat} showed a different pattern between cereal monocultures and cereal-legume mixtures (Figure 3.6 and Figure 3.7), resulting from the different voluntary regrowth dynamics during the fallow, as described in Section 3.4.1. Thus, GPP_{sat} and α achieved the highest values previous to the harvest, but when the grassland was a cereal-legume mixture both parameters significantly increased again during the fallow period (Figure 3.7), due to the voluntary regrowth of the vegetation (Figure 3.3.D).On the contrary, cereal monocultures did not show this α or GPP_{sat} increment during the fallow period (Figure 3.7), except during the fallow of the wheat monoculture in year 2015 (Figure 3.6), in which there was vegetation voluntary regrowth after the harvest (Figure 3.3.D).

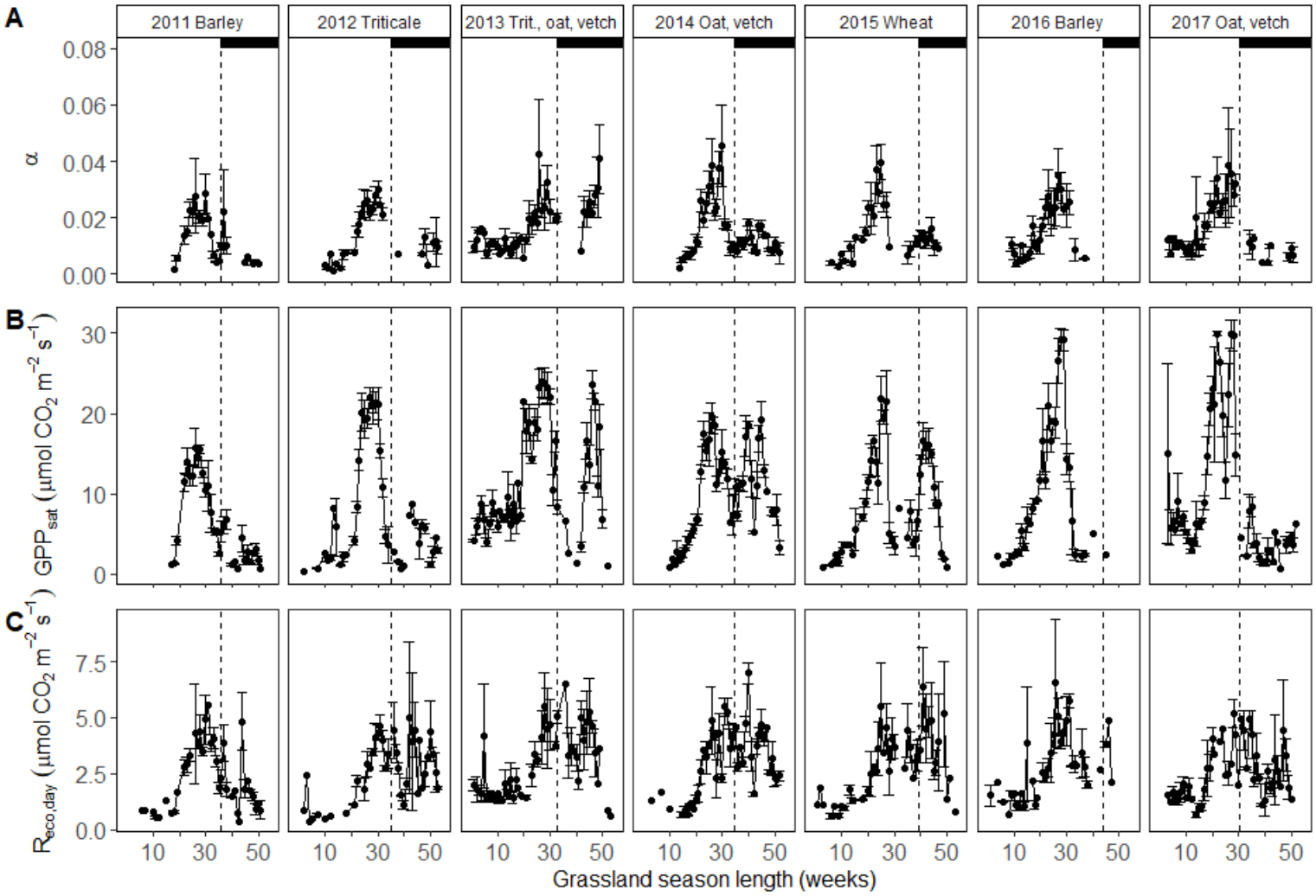

Figure 3.6. Seasonal dynamics of NEE_{day} light response parameters (Equation 3.4): (A) apparent initial quantum yield (α); (B) asymptotic gross primary production (GPP_{sat}); and (C) daytime ecosystem respiration ($R_{eco,day}$). Weekly averaged values and corresponding standard error bars. Top titles in the top panels indicate grassland species. Black dashed lines indicate harvesting events. Top black bands indicate fallow periods in which there was grazing. Gaps are due to missing data or not significant estimates ($p \geq 0.05$), which have been discarded

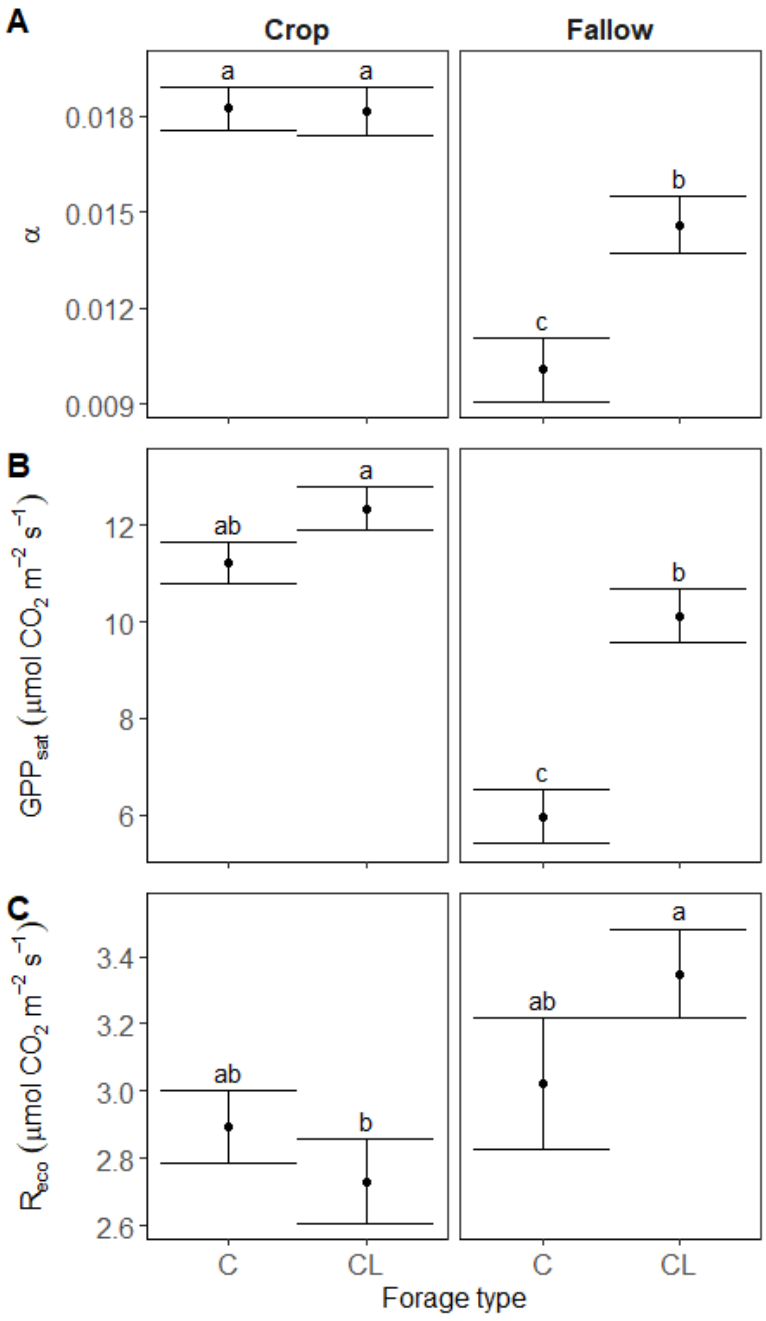

Figure 3.7. Light response parameters (Equation 3.4): (A) apparent initial quantum yield (*α*); (B) asymptotic gross primary production (GPP_{sat}); and (C) average daytime ecosystem respiration ($R_{eco,day}$) mean ± standard error, and Tukey post-hoc test per forage type (C: cereal monoculture, CL: cereal-legume mixture) and period (crop and fallow). Letters indicate significant differences among groups ($p < 0.05$). See ANOVAs results in Table S3.3.

3.4.4 Grassland species influence on $R_{eco,night}$ response to temperature and soil water content

$R_{eco,night}$ modelling according to the equations proposed by Reichstein et al. (2002, our Equations 3.5 – 3.7) presented a satisfactory fitting, with a R^2 that ranged from 0.19 to 0.75 between grassland seasons (Table 3.3). Moreover, $R_{eco,night}$ was considerably driven by T_s and SWC when assessing all grassland seasons together (Figure 3.8). The activation energy (E_0) was significantly dependent on SWC (E_0~a+b·SWC, a = 76 ± 40 and b = 483 ± 259 $ºC^{-1}$, Table 3.3), indicating that temperature sensitivity was dependent on SWC (Equation 3.6). Also, soil water content at which maximal $R_{eco,night}$ halves ($SWC_{1/2}$) was significant (0.06 ± 0.01, Table 3.3), indicating that $R_{eco,night}$ decreased to half-maximum or lower at a SWC ≤ 6 ±1 %.

However, some estimates of the $R_{eco,night}$ response parameters were not significantly different from zero ($p \geq 0.05$, see significant estimates in bold, Table 3.3); and when assessing differences between forage types, nonsignificant estimates were not considered for comparison. Yet, E_0 of barley, in year 2011 (b = 3668 ± 1645 $ºC^{-1}$, Table 3.3), and of wheat, in year 2015 (b = 850 ± 627 $ºC^{-1}$, Table 3.3), were significantly dependent on SWC, both values being much higher than the average of all grassland seasons (b = 483 ± 259 $ºC^{-1}$, Table 3.3).

Also, the reference ecosystem respiration ($R_{eco,ref}$) of triticale in year 2012, was also significantly different from zero (4 ± 2 µmol CO_2 m^{-2} s^{-1}, Table 3.3), exceeding $R_{eco,ref}$ of all grassland seasons (2.8 ± 0.3 µmol CO_2 m^{-2} s^{-1}, Table 3.3). Finally, soil water content below which $R_{eco,night}$ vanishes (SWC_0) and $SWC_{1/2}$ had a significant influence on R_{eco} in the triticale, oat and vetch mixture (year 2013), the oat and vetch mixture (year 2014), and in the wheat monoculture (year 2015, Table 3.3). Both cereal-legume mixtures (year 2013 and 2014), had a $SWC_{1/2}$ that was very close to SWC_0 , indicating that SWC could reach very low values before $R_{eco,ref}$ halved, although this SWC value was already very

close to the limit at which $R_{eco,ref}$ vanishes (SWC_0). On the contrary, during the wheat monoculture of 2015, $SWC_{1/2}$ (0.08 ± 0.03, Table 3.3) doubled SWC_0 (0.04 ± 0.03, Table 3.3).

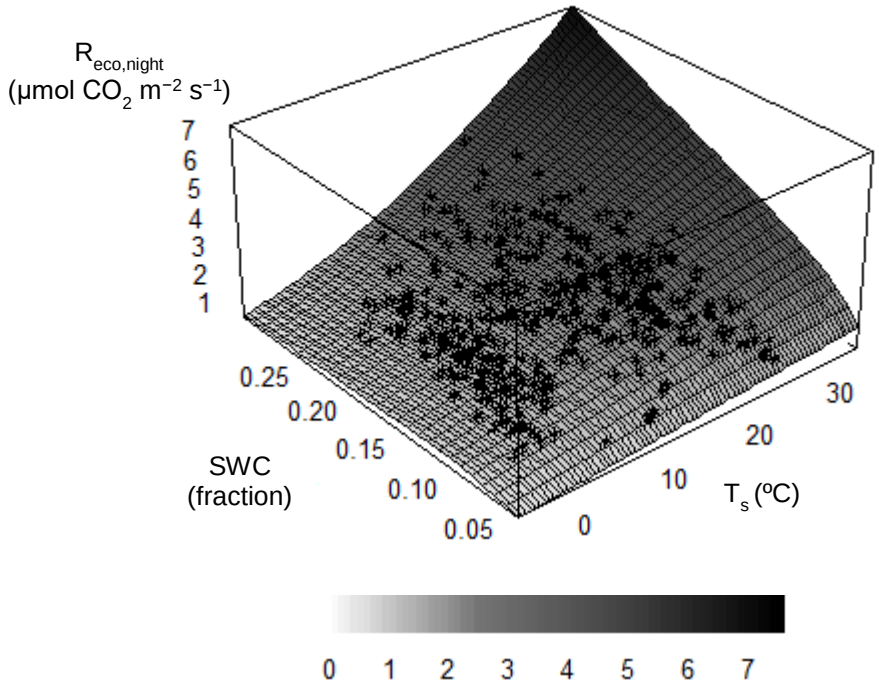

Figure 3.8. $R_{eco,night}$ trend surface as a function of soil temperature (T_s) and soil water content (SWC), by the equations proposed by Reichstein et al. (2002, Equations 3.5 – 3.7). Model performed on weekly averaged data of all the variables. The grid shows the trend surface and dots are observed data.

Table 3.3. $R_{eco,night}$ soil temperature and soil water content response parameters by the equations proposed by Reichstein et al. (2002, Equations 3.5 – 3.7): reference ecosystem respiration ($R_{eco,ref}$); soil water content below which R_{eco} ceases (SWC_0); soil water content at which maximal $R_{eco,night}$ halves ($SWC_{1/2}$); and *a* and *b* parameters of the activation energy linear function ($E_0 = a + b \cdot SWC$). Model performed on weekly averaged values of all the variables. Estimates (Est.) and standard error (SE) of the parameters. Estimates in bold are significantly different from zero ($p < 0.05$).

Parameters	2011 Barley		2012 Triticale		2013 Triticale, oat, vetch		2014 Oat, vetch		2015 Wheat		2016 Barley		2017 Oat, vetch		All grassland seasons	
	Est.	**SE**	**Est.**	**SE**	**Est.**	**SE**	**Est.**	**SE**	**Est.**	**SE**	**Est.**	**SE**	**Est.**	**SE**	**Est.**	**SE**
$R_{eco,ref}$ (µmol CO_2 m^{-2} s^{-1})	1	2	**4**	**2**	**2.9**	**0.3**	**2.3**	**0.2**	**2.7**	**0.6**	9	15	3	2	**2.8**	**0.3**
SWC_0 (fraction)	0.3	0.6	0.01	0.02	**0.048**	**0.005**	**0.05**	**0.002**	**0.04**	**0.03**	0.03	0.06	0	0.2	0.01	0.01
$SWC_{1/2}$ (fraction)	0.4	0.9	0.1	0.1	**0.054**	**0.003**	**0.052**	**0.002**	**0.08**	**0.03**	0	1	0.1	0.07	**0.06**	**0.01**
a ($^oC^{-1}$)	–263	221	136	135	**215**	**94**	162	138	64	118	83	140	18	126	**76**	**40**
b ($^oC^{-1}$)	**3688**	**1645**	596	1251	–603	744	547	987	**850**	**627**	-37	833	451	694	**483**	**259**
R^2	0.59		0.61		0.49		0.69		0.75		0.36		0.19		0.35	

3.5 Discussion

Forage species drove CO_2 exchange responses consistently along the assessed years and different environmental conditions in the studied sown grassland of the Eastern Pyrenees. Cereal-legume mixtures had more negative NEE, during the whole grassland season (Figure 3.4.A) and during the grassland growth (Figure 3.4.B) than cereal monocultures. Also, cereal-legume mixtures had lower NEE inter-annual variability (−363 g C m^{-2}, year 2013, and −383 g C m^{-2} year 2017, Section 3.4.1) than cereal monocultures (ranging from −70 to −226 g C m^{-2}, Section 3.4.1), suggesting a consistent diversity effect on NEE along different grassland mixtures and proportions of species in the mixtures.

Moreover, the diversity-interaction model (Table 3.2) confirmed the capacity of cereal-legume mixtures to take up more CO_2, oat and vetch being the mixture with the highest net CO_2 uptake (Table 3.2). The inclusion of legumes was key for promoting this diversity effect, since the oat and vetch mixture had a significant effect on NEE, while the triticale addition in the mixture did not significantly increase the net CO_2 uptake (Table 3.2).

These results were in agreement with our first hypothesis: cereal-legume mixtures enhancing the net CO_2 uptake in comparison to the studied cereal monocultures (barley, wheat and triticale). Those differences on CO_2 fluxes between cereal-legume mixtures and cereal monocultures could be explained by complementary and simultaneous mechanisms related to management (Section 3.5.1); and ecophysiological responses, including CO_2 uptake light response, and CO_2 respiration response to temperature and soil water content (Section 3.5.2).

3.5.1 Management associated with grassland species: influence on NEE dynamics and NBP

Differences in harvesting time between cereal monocultures and cereal-legume mixtures resulted in differences in vegetation voluntary regrowth and CO_2 dynamics. Cereal monocultures were harvested once the yield was sufficiently dry, while cereal-legume mixtures were harvested when the vegetation was still fresh for silage; the latter being a conventional practice to improve forage nutritional value.

The earlier harvesting in cereal-legume mixtures favoured a higher voluntary regrowth of vegetation during the fallow (Figure 3.3.D), which was decisive for the cumulative net CO_2 uptake of the whole grassland season (Figure 3.3.A). Accordingly, the vegetation could still regrow after a harvest in May or early June because the vegetation still is in an earlier stage of phenological development. During that time of the season, environmental conditions are also favourable for voluntary regrowth. On the contrary, cereal monocultures remained in the field until they were sufficiently dry and had completed their development cycle. This usually left no room for voluntary regrowth after harvest (Figure 3.3.D) and hence no net CO_2 uptake during the fallow period (Figure 3.3.A). Also, seeds that remain in the field after the harvest do not encounter the environmental conditions required to germinate, since temperatures are too high and SWC is too low (Figure 3.3).

On the other hand, all cereal-legume mixtures had a NBP that was negative during the grassland growth (Figure 3.5), indicating that there was C input into the system during that period. In this regard, it is worth estimating the optimum amount of biomass that can be harvested and left in the field, in order to achieve the maximum NBP of the system, without compromising the yield. Yet, our second hypothesis had to be rejected: cereal-legume mixtures did not clearly increase NBP as compared to cereal monocultures during the grassland growth, since some cereal monocultures (wheat, year

2015, and barley, year 2016) had a similar NBP during the grassland growing (Figure 3.5). However, we still are convinced that cereal-legume mixtures could have shown an increase in NBP magnitude (more negative NBP) compared to cereal monocultures, but if we had assessed the entire grassland season. The especially pronounced voluntary regrowth of the vegetation during the fallow period during cereal-legume mixture years (Figure 3.3.D), provided a profitable resource for livestock, besides providing an important litter input into the system. This combined with a low grazing intensity (≈ 0.91 LSU ha^{-1}) left an important part of the vegetation in the field, thereby increasing NBP, and partly offsetting C losses due to the harvest. Thus, for future studies we recommend to estimate C exports through grazing during the fallow period (in addition to determining soil C content), to more accurately estimate C inputs and exports, and consequently NBP during the whole grassland season in the studied sown forage grassland.

Finally, legumes present in cereal-legume mixtures had higher crude protein, lower neutral detergent fibre, and higher nitrogen content than all cereals (Table S3.1). Accordingly, vegetation remaining in the field during the growing of cereal-legume mixtures could also be increasing soil nitrogen. Soil nitrogen determination would also be recommendable in further studies to fully assess the effect of grassland species on soil fertility.

3.5.2 Grassland species influence on gross CO_2 uptake and respiration

From a mechanistic perspective cereal-legume mixtures had higher light use efficiency than cereal monocultures, as indicated the higher values of GPP_{sat} achieved during grassland growth, and the α and GPP_{sat} rebound during the fallow (Figure 3.7). Cereal-legume mixtures have been reported to increase CO_2 uptake, not only via the increased photosynthesis of legumes (e.g. Reich et al., 2003, 1997), but also increasing photosynthesis of the overall community via nitrogen transfer from the legume to the cereal in the mixture (Kirwan et al., 2009; Mulder et al., 2002; Pirhofer-Walzl et al., 2012).

On the other hand, $R_{eco,night}$ was clearly driven by T_s and SWC (Albergel et al., 2010; Davidson and Janssens, 2006; Yvon-Durocher et al., 2012), although it was limited at the highest T_s and lowest SWC (Figure 3.8). In agreement, some authors have identified a temperature threshold at which temperature sensitivity changes, decreasing respiration (Carey et al., 2016; Hernandez and Picon-Cochard, 2016; Reichstein et al., 2002). This change in respiration-temperature sensitivity has been explained by (a) changes in microbial activity (Balser and Wixon, 2009), decreasing the heterotrophic component of R_{eco}; and (b) by an indirect effect through limitations on GPP, resulting in limitations on the autotrophic component of R_{eco}; this particularly affected by the combination of high temperatures with low SWC (Niu et al., 2012; Reichstein et al., 2002).

In our study, we did not partition R_{eco} into autotrophic and heterotrophic respiration, but this shift on the respiration-temperature at the highest temperatures and the lowest SWC mostly happened after harvest (Figure 3.3), which irretrievably decreased GPP and photosynthesis, and most likely lowered the autotrophic component of R_{eco} (Larsen et al., 2007).

Moreover, $R_{eco,night}$ responded similarly to T_s and SWC in both cereal monocultures and cereal-legumes mixtures, since differences in CO_2 respiration response to T_s and/or SWC were not detected (inconsistent differences between response parameters: $R_{eco,ref}$, SWC_0 , $SWC_{1/2}$ and E_0; see Table 3.3). This may well be because although generally legumes have higher autotrophic respiration rates, with both higher leaf (Li et al., 2016) and root respiration rates (Warembourg et al., 2003) than cereals, and there is a strong nitrogen content – respiration relationship (Reich et al., 2008); this increase in respiration is largely driven by higher GPP and photosynthetic activity (Larsen et al., 2007). Thus, although there had been differences in the autotrophic respiration resulting from differences in photosynthetic rates, this does not necessarily mean that night-time fluxes ($R_{eco,night}$) of cereal-legume mixtures had higher temperature and/or SWC sensitivity than cereal monocultures. In addition, even if there had been differences between legume

and cereal species in their $R_{eco,night}$ sensitivity to T_s and SWC, this differences were not noticeable at the community scale (Table 3.3).

Interestingly, this suggests that the increase in the CO_2 input favoured by the presence of legumes in the community overcompensated CO_2 respiration losses. This is in agreement with our third hypothesis, cereal-legume mixtures having more negative NEE (Table 3.2) due to higher photosynthetic rates, but not higher respiration rates. Chen et al. (2017) found a similar result, with legumes increasing gross CO_2 uptake (higher GPP), but not enhancing CO_2 release, resulting in more negative NEE. Most likely, increased total nitrogen availability, mediated by legumes, increased photosynthetic activity of the overall community at a higher rate than respiration losses (Chen et al., 2017).

3.6 Conclusions

Based on the findings of seven years of continuous NEE measurements in a sown forage grassland in the Pyrenees, we found strong evidence that cereal-legume mixtures increased net CO_2 uptake compared to cereal monocultures. Management practices associated with cereal-legume mixtures, particularly an earlier harvesting time, allowed higher voluntary regrowth of the vegetation during the fallow period. This provided additional feed for the livestock, and enhanced net CO_2 uptake during that period. Thus, legumes mixed with a cereal were decisive for the net CO_2 budget of the whole grassland season. Our results also highlighted the capability of cereal-legume mixtures to enhance photosynthetic activity and gross CO_2 uptake, but without significantly increasing respiration. This resulted in higher net CO_2 uptake of cereal-legume mixtures. Cereal-legume mixtures provide important advantages to increase net CO_2 uptake capacity of forage systems compared to cereal monocultures, while ensuring productivity and forage quality.

Acknowledgments

We would like to thank F. Gouriveau, E. Ceschia and J. Elbers for their critical contribution to the installation of the eddy covariance tower and to data analysis, and D. Estany and H. Sarri for field assistance. The flux tower was installed during the FLUXPYR project (INTERREG IV-A POCTEFA, financed by EU-ERDF, Generalitat de Catalunya and Conseil Régional Midi-Pyrénées; http://ecofun.ctfc.cat/fluxpyr/eng/). The following additional projects also contributed with funding to this work: CAPACITI (FP7/2007-2013 grant agreement n° 275855), AGEC 2012 (Generalitat de Catalunya), CAPAS (Spanish Science Foundation, CGL2010-22378-C03-01), BIOGEI (Spanish Science Foundation, CGL2013-49142-C2-1-R, supported by a FPI fellowship for Mercedes Ibañez, BES-2014-069243) and IMAGINE (Spanish Science Foundation, CGL2017-85490-R). The authors acknowledge CTFC (www.ctfc.cat) for support with study site maintenance.

3.7 Supplementary material

Table S3.1. Forage quality indicators (mass-% of dry weight). Analysis performed in the Department of Animal and Food Science, Universitat Autònoma de Barcelona (https://www.uab.cat/department/animal-food-science) according to standard methods: Carbon (C) and nitrogen (N) content (Elemental Analyser EA1108, Carlo-Instruments, Germany); crude protein (CP, according to Kjeldahl method N x 6.25, on a KjeltecTM 8400 analyser, FOSS, Denmark); neutral detergent fibre (NDF, Van Soest et al., 1991); acid detergent fibre (ADF) and acid detergent lignin (ADL) according to Goering and Soest (1970) on an ANKOM analyser (Ankom Thechnology, 2005). Mean ± standard error (SE). Not available (NA) data when there was not enough sample to perform the corresponding analysis or there was only one sample.

Species	Sampling date	C		N		CP		NDF		ADF		ADL	
		Mean	SE	Mean	SE	Mean	SE	Mean	SE	Mean	SE	Mean	SE
Barley	01/07/2011	46.10	0.02	0.815	0.007	5.10	0.05	56.9	NA	32.5	NA	4.2	NA
Triticale	26/04/2012	45.5	0.5	2.46	0.01	15.41	0.09	37.2	0.4	19.3	0.4	1.6	0.1
Oat		45.3	0.2	1.64	0.04	10.2	0.2	NA	NA	NA	NA	NA	NA
Triticale	07/05/2013	45.0	0.1	1.40	0.05	8.7	0.3	48.8	NA	26.0	NA	1.8	NA
Vetch		45.2	0.2	3.18	0.06	19.9	0.4	35.1	0.2	25.2	0.2	5.40	0.02
Triticale and oat	11/06/2013	45.6	0.1	0.97	0.02	6.1	0.1	53	1	29.9	0.8	2.6	0.1
Vetch		45.3	0.2	2.63	0.07	16.5	0.4	34.4	0.3	25.7	0.2	5.6	0.3
Barley	20/05/2016	46.2	0.4	1.200	0.003	7.50	0.02	46.6	NA	24.9	NA	2.0	NA
Barley	16/06/2016	45.79	0.07	1.061	0.002	6.63	0.01	46.1	NA	24.3	NA	2.4	NA

Table S3.2. CO_2 fluxes data coverage and data retained. Estimated over total potential data (1 value every 30 minutes).

Year	% Data coverage	% Data retained
2011	0.80	0.69
2012	0.93	0.81
2013	0.77	0.67
2014	0.64	0.56
2015	0.68	0.57
2016	0.62	0.53
2017	0.85	0.72
Average	0.76	0.65

Table S3.3. Light response parameters (Equation 3.4): apparent initial quantum yield (α); asymptotic gross primary production ($GPP_{sat,}$); and average daytime ecosystem respiration ($R_{eco,day}$) ANOVAs as function of forage type and period. Forage type with cereal monoculture as reference level, and period with growth as reference level.

	α (dimenssionless)		**GPP_{sat} (μmol CO_2 m^{-2} s^{-1})**		**$R_{eco,day}$ (μmol CO_2 m^{-2} s^{-1})**	
	F	**p**	**F**	**p**	**F**	**p**
Forage type	0.13	0.7	9.41	0.002	0.28	0.6
Period	26.60	< 0.001	38.60	< 0.001	7.78	0.005
Forage type x period	4.78	0.03	7.13	0.008	3.15	0.08

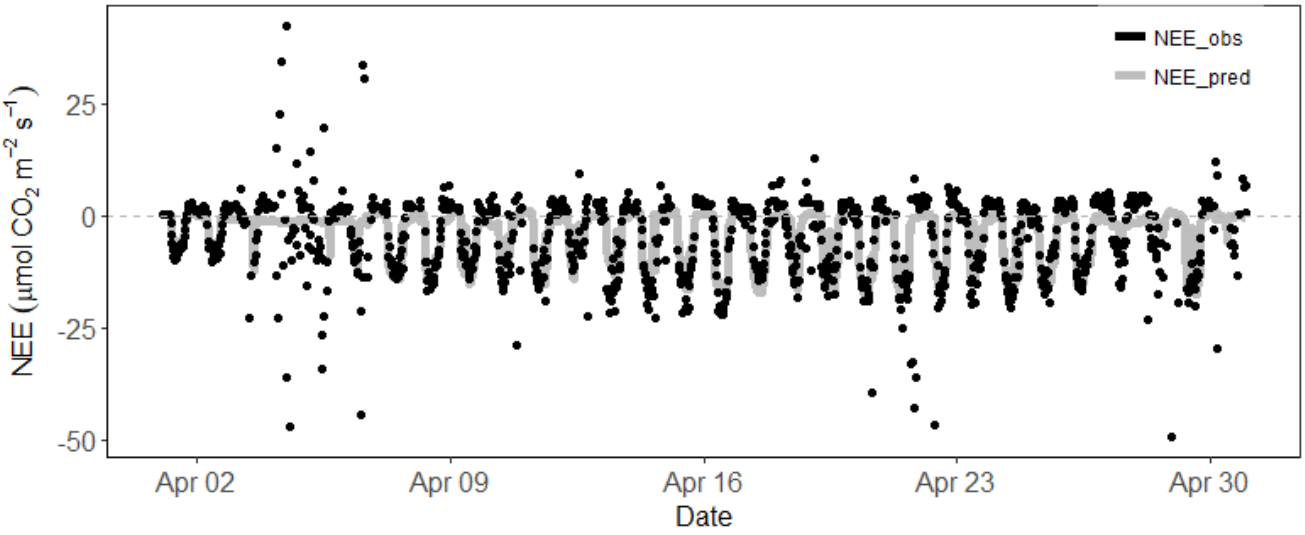

Figure S3.1. Example (April of 2012) of observed net ecosystem exchange (NEE) data (black dots) and their theoretically predicted NEE data by gap-filling (grey line), by the sMDSGapFill function (Reichstein et al., 2005).

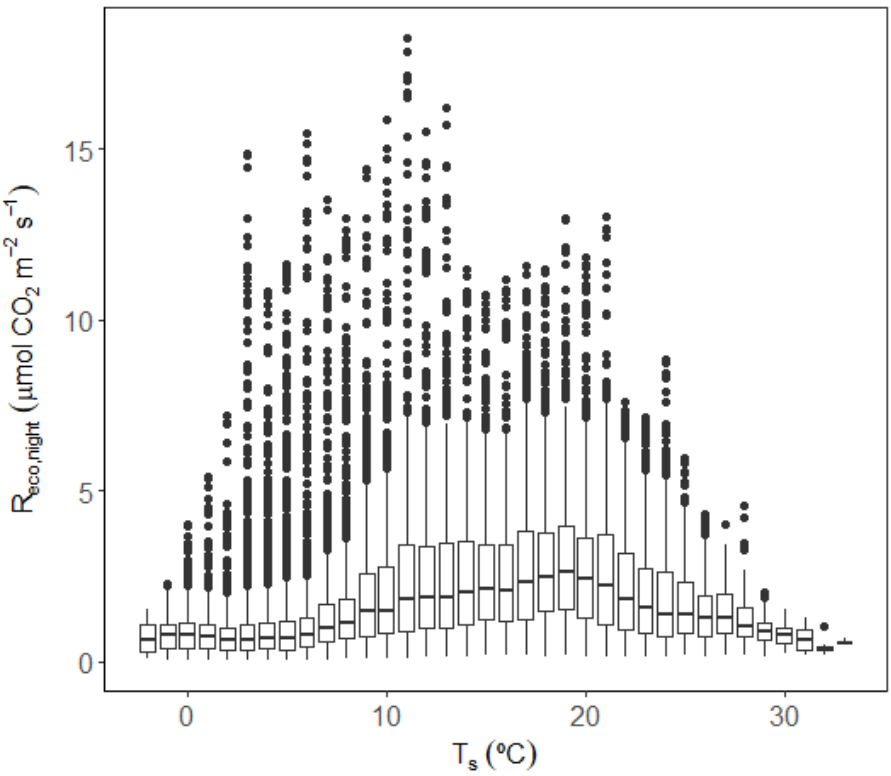

Figure S3.2. Boxplot of nigh time (PAR < 5 µmol photons m^{-2} s^{-1}) ecosystem respiration ($R_{eco,night}$) as a function of soil temperature (T_s).

Chapter 4 Tree – open grassland structure drives carbon and nitrogen cycling in dehesa ecosystems of the Iberian Peninsula

Mercedes Ibañez[1]*, Salvador Aljazairi[1], Maria Teresa Sebastià[1,2]

[1]GAMES group & Dept. HBJ, ETSEA, University of Lleida (UdL), Lleida, Spain.

[2]Laboratory of Functional Ecology and Global Change, Forest Sciences Centre of Catalonia (CTFC), Solsona, Spain.

MI performed research, analysed data and wrote the paper; SA performed research and revised the paper; MTS revised the paper.

*Corresponding author; e-mail: mercedes.ibanez@hbj.udl.cat; phone: +34 973702623.

4.1 Abstract

Dehesas, also called holm oak meadows or oak savannahs, are the largest agroforestry system in Europe, providing important goods and services. Traditional uses have shaped dehesas into a matrix of trees and open grassland, driving carbon (C) and (N) cycling among ecosystem compartments. However, little is known about how this tree – open grassland structure may influence C and N dynamics, considering interactions between soil, belowground biomass and plant functional types (PFT: forbs, grasses and legumes) of the herbaceous layer, under different environments. Our study provides insight to this regard, using C and N content and ^{13}C and ^{15}N isotope ratios as a proxy. Results show that changes in the tree – open grassland structure of dehesas will imply deep changes in C and N storage and cycling. Soil C and N content were higher under the canopy than in the open grassland. The higher soil N under the canopy, increased N content in shoots and favoured discrimination against ^{15}N by roots. Generally, stomatal conductance and discrimination against ^{13}C also increased under the canopy compared to the open grassland, especially in forbs. Each PFT presented specific ecophysiological characteristics, which interacted with the tree – open grassland structure shaping C and N cycling and storage. The C content in the belowground biomass was higher under the canopy than in the open grassland, which could be related with the PFT composition of the herbaceous layer. Grasses had higher N content than forbs and lower $\delta^{15}N$, suggesting that grasses may be more efficient taking-up N, and/or exploiting symbiotic N sources, fact that could represent an important competitive advantage. Differences between under the canopy and the open grassland on C and N storage and cycling were generally more pronounced with increasing environmental constrains, highlighting the relevance of trees as drivers of ecosystem fertility, and C and N relationships, especially in more constrained environments.

Key words: $\delta^{13}C$, $\delta^{15}N$, canopy, forbs, grasses, legumes.

4.2 Introduction

Dehesas, also called holm oak meadows or oak savannahs, are semi-natural savanna-like systems that result from the thinning of the Mediterranean forest, in which an herbaceous layer and an arboreal canopy (mostly *Quercus* species) coexist. Dehesas are one of the largest agroforestry systems in Europe (Eichhorn et al., 2006), covering 3.5 – 4 million ha, mostly along the South West of the Iberian Peninsula (Olea et al., 2005), and are also present in other world regions with Mediterranean climate, mainly in California (Gaman and Firman, 2006; Huntsinger et al., 2013; Marañón et al., 2009). Also, Mediterranean savannas, with trees belonging to different taxonomic groups can be found in South Africa, south-western Australia and central Chile (Marañón et al., 2009).

Dehesas have traditionally provided a wide variety of goods and services, including production of forage, acorns, timber and cork; being ecosystems of high cultural and economic value. Such traditional uses have shaped dehesas into a matrix of trees and open grassland, driving carbon (C) and (N) cycling, among ecosystem compartments. However, tree coverage in dehesas is changing. Traditional uses are declining towards intensive farming; plantations of fast-growing trees, mostly *Eucalyptus* and *Pinus* species; shrub encroachment due to land abandonment; and there is a worrying lack of tree regeneration (Costa et al., 2011; Costa Pérez et al., 2006), with the consequent implications that this may have on ecosystem functioning.

Yet, little is known about how the tree – open grassland structure of dehesas may influence C and N storage and cycling between different ecosystem compartments, considering interactions among soil, above and belowground biomass. Besides, the fact that the vegetation of the herbaceous layer of dehesas is highly diverse (Marañon, 1985) increases the complexity in assessing C and N cycling. Indeed, most common plant functional types (PFT) in grasslands, including grasses, non-legume forbs (hereafter “forbs”) and legume forbs (hereafter “legumes”), have different N and light (and therefore

CO_2) use and acquisition strategies (Tilman 1997; Symstad 2000; Díaz et al., 2007; Sebastià 2007), which may result in different responses to tree canopies in their C and N content and cycling.

To this regard, ^{13}C and ^{15}N isotope ratios ($\delta^{13}C$ and $\delta^{15}N$) can be used as a proxy to assess C and N cycling, providing information about resource acquisition and processing (Dawson et al., 2002; Ferrio et al., 2005; Kahmen and Buchmann, 2007). On one hand, photosynthesis, net assimilation and stomatal conductance are directly linked to discrimination against ^{13}C in C_3 plants, increasing discrimination against ^{13}C with increasing stomatal conductance (Farquhar et al., 1989). Variations in $\delta^{13}C$ are then controlled by physiological and environmental factors (Farquhar et al., 1989, 1982) and $\delta^{13}C$ has been identified as a useful tool to assess CO_2 and water exchange relationships (Ehleringer et al., 1990). Inter-species isotopic variability will be mainly genetically and physiologically driven (Yang et al., 2015), while environmental factors, including soil moisture (Korol et al., 1999), irradiance (Zimmerman and Ehleringer, 1990), temperature (Welker et al., 1993) and atmospheric CO_2 concentration (Williams et al., 2001), among others, will influence mainly intra-species isotopic variability.

Tree canopies influence directly light availability, and this in turn controls photosynthetic activity and C cycling (Bonafini et al., 2013). Light reduction below the canopy increases stomatal conductance, making possible more discrimination against ^{13}C and generating organic matter ^{13}C depleted (more negative $\delta^{13}C$ values). Several authors have reported variations in the $\delta^{13}C$ of leaves related to their position in the canopy, being leaves in the lower parts of the canopy or in the understory more ^{13}C depleted than in the upper parts (Bonafini et al., 2013; Buchmann et al., 1997; Della Coletta et al., 2009; van der Merwe and Medina, 1991).

In addition, $\delta^{13}C$ provides also the opportunity to assess carbon-water relationships using intrinsic water use efficiency (iWUE) as indicator. iWUE is defined as the ratio of C assimilated per water transpired over a period of time, and can be approximated as the

relationship between ^{13}C isotope discrimination ($\Delta^{13}C$) during photosynthesis and atmospheric and sub-stomatal CO_2 partial pressures ratio (*Ci/Ca*, Farquhar and Richards 1984). Accordingly, iWUE differences, resulting from differences in the C use, between trees and PFT (forbs, grasses and legumes), and between under the canopy *vs.* the open grassland, are also expected.

On the other hand, $\delta^{15}N$ in the above and belowground biomass will depend mostly on the type and amount of N sources and N cycling steps (Dawson et al., 2002; Robinson, 2001). At high N availability, denitrification and leaching of inorganic N forms will usually discriminate against ^{15}N, and the remaining source will be more ^{15}N enriched, while the biomass exploiting the N source will be ^{15}N depleted (Yoneyama et al., 2001). On the contrary, at limiting N conditions, there will be very low ^{15}N discrimination and the exploiting biomass will have a $\delta^{15}N$ similar to the source (Evans et al., 1996). Also, at low N availability, plants will be more dependent on symbiotic N fixed from atmospheric N_2 by bacteria (Evans, 2001; Santi et al., 2013).

To this regard, legumes naturally form symbiotic N_2-fixing associations, and therefore legume tissues have a $\delta^{15}N$ close to atmospheric N_2 (atmospheric N_2 has by definition a $\delta^{15}N$ of 0‰, Evans 2001; Robinson 2001). Neighbouring non-legume plants that are exploiting symbiotic N will be more ^{15}N depleted than plants exploiting a non-symbiotic N source (Pirhofer-Walzl et al., 2012). Such N transfer from legumes to neighbouring non-legume species has been explained through several mechanisms, including decomposition of legume root tissues, exudation of soluble N compounds, and transfer of N mediated by plant-associated mycorrhizae (Thilakarathna et al., 2016).

Accordingly, in dehesa ecosystems the environment generated by trees, with specific conditions of light and water, will modify CO_2 and water exchange fluxes, affecting ^{13}C discrimination processes and iWUE. Also, trees will regulate nutrient availability and cycling, influencing N sources, and affecting ^{15}N discrimination processes. However, there are no studies conducted in dehesas assessing specifically how this tree – open

grassland structure may influence C and N cycling among the different ecosystem compartments, using C and N content, and $\delta^{13}C$ and $\delta^{15}N$ as a proxy. Moreover, little is known about the effect of different environmental conditions and tree species on those variables. For these reasons, in the present study we aim to: (1) assess differences among ecosystem compartments in the C and N content and cycling, considering separately tree leaves, PFT of the herbaceous layer (forbs, grasses and legumes), litter, faeces, belowground biomass (BGB) and soil; and (2) assess the influence of plots under (a) different environmental conditions and (b) dominated by different tree canopies (*Quercus ilex* L.*, Quercus suber* L. and *Pinus pinea* L. or by a combination of *Q. ilex* and *Q. suber*) on the C and N content and cycling of those ecosystem compartments.

4.3 Material and methods

4.3.1 Study sites and sampling design

Field work was carried out in the spring (05/04/2016 – 10/04/2016), coinciding with the most productive moment of the system. The study sites were distributed in two locations in the South West of the Iberian Peninsula: Doñana Natural Park (37° 15' 34" N, 6° 19' 55" W) and Sierra Morena mountains (37° 39' 50" N, 5° 56' 20" W). The location of Doñana (DN) is at 30 m a. s. l. and is grazed by goat and cattle, with a livestock density of 0.40 livestock units (LSU) ha^{-1}. The Sierra Morena (SM) location is situated at 296 m a. s. l., and is grazed by cattle, at a livestock density of 0.36 LSU ha^{-1}, and by Iberian pigs, whose livestock density varies depending on the acorns production of the year, but with a maximum density of 1.25 pigs ha^{-1}. Although grazer animals were different between locations, grazing intensity was very similar (DN 0.40 and SM 0.36 LSU ha^{-1}), and both can be considered as extensive farming.

Both locations have a Mediterranean climate regime with warm, dry summers, and mild winters (Peel et al., 2007). Mean annual temperature in DN is 18.1 ºC and in SM 16.8 ºC,

and mean annual precipitation in DN is 543 mm and in SM is 648 mm; being SM slightly fresher and wetter than DN.

Grassland in both locations is dominated by herbaceous annual species, including grasses (*Bromus hordeaceus* L., *Lolium perenne* L.), forbs (*Erodium moschatum* L., *Chamamelum mixtum* L.) and legumes (*Trifolium subterraneum* L., *Ornithopus sativus* Brot. *Medicago doliata* Car.), among others.

Study plots were selected according to their tree composition, with representative canopy types of Iberian dehesas (Costa Pérez et al., 2006): one plot in the SM location, pure *Q. ilex* stand (SM-ilex); and three plots in the DN location, one pure *Q. suber* stand (DN-suber); one *Q. ilex* and *Q. suber* mixed stand (DN-mixed); and one pure *P. pinea* stand (DN-pinea), the latter being a common tree plantation replacing traditional stands. To characterize soil properties of the study plots, soil samples were taken and analysed by the agronomy service of the Seville University (https://etsia.us.es/), according to standard methods (Table 4.1).

Table 4.1. Soil characteristics per plot and depth. Soil analysis performed at the Agronomy Service of the Seville University (https://etsia.us.es/), according to standard methods: pH (Porta Casanellas et al., 1986), organic C (Walkley and Black, 1934), total N (Elemental analyser CNS-Trumac, LECO Corporation, MI, USA) and texture (Gee and Bauder, 1986).

Plot	**SM-ilex**		**DN-mixed**		**DN-suber**		**DN-pinea**	
Depth (cm)	**0 – 40**	**40 – 80**	**0 – 30**	**30 – 60**	**0 – 30**	**30 – 60**	**0 – 30**	**30 – 60**
pH	6.7	7.2	7.9	7.8	7.5	7.8	7.0	7.4
Organic C (%)	0.80	0.30	0.32	0.34	0.60	0.02	1.52	0.51
Total N (%)	0.85	0.60	0.15	0.04	0.06	0.05	0.20	0.11
Clay (%)	18	30	10	11	13	4	16	16
Silt (%)	29	28	25	15	18	9	22	21
Sand (%)	54	42	65	74	69	87	62	63

Texture in the SM-ilex plot varied from sandy clay loam (0 – 40 cm depth) to clay (40 – 80 cm depth). All DN soils had a sandy clay loam texture, except the 30 – 60 cm layer of the DN-suber plot, which was sandy loam. The SM-ilex plot had a slightly acid pH and DN plots had a neutral-basic pH. Organic C was very low in all the plots, although the value in the first 30 cm of the DN-pinea plot doubled the average. Finally, total N was in general quite low, except in the SM-ilex plot (Table 4.1).

Study treatments were therefore established according to: plot (SM-ilex, DN-mixed, DN-suber and DN-pinea) and canopy (open grassland, OG, and under the canopy, UC). Trees of the UC treatment were selected with a similar size (see average cross section at breast height of selected trees, Table S4.1). Also, sampling points of the UC treatment were always placed at 1 m distance from the selected tree trunk and sampling points of the OG treatment were placed at a minimal distance of 3 m from the selected tree, clearly outside the canopy influence. Sampling points were systematically placed following the north orientation respect to the tree trunks.

At each treatment level we sampled 4 replicates, resulting in 40 sampling points. In the DN-mixed plot we discriminated between both *Quercus* species (*Q. suber* and *Q. ilex*) to stablish sampling points. However, we performed preliminary comparative analysis in the DN-mixed plot on environmental and vegetation characteristics under the canopy of both *Quercus* species and relevant differences between *Quercus* species were not found. DN-mixed results are then always presented combining both tree species. At each sampling point we sampled aboveground biomass (Section 4.3.2), belowground biomass and soil (Section 4.3.3). In addition, microclimatic sampling conditions (photosynthetically active radiation and soil water content) per plot and under the canopy *vs.* the open grassland were extracted from Section 5.4.1, and used to interpret and discuss our results.

4.3.2 Aboveground biomass sampling

At each sampling point we sampled tree leaves, litter (dead leaves detached from the plant and on the soil surface), and main species of each PFT, including forbs: *Calendula arvensis* L., *Chamamelum mixtum* L, *Crepis capillaris* L., *Erodium moschatum* L., *Geranium molle* L.; grasses: *Bromus hordeaceus* L. and legumes: *Ornithopus sativus* Brot. and *Trifolium subterraneum* L. In addition, to characterize the herbaceous layer composition, in terms of PFT proportions, we extracted this information from Section 5.4.2 (summarized in Figure S4.1), and used it to interpret and discuss our results.

4.3.3 Belowground biomass, soil and faeces sampling

Two soil cores of 9 cm^2 surface and 0 – 10 cm depth were extracted at each sampling point. In the laboratory, one of the cores was washed and filtered with a 0.2 mm pore size strainer to obtain belowground biomass (BGB). The second core was used for soil analysis. In addition, we collected 2 samples of faeces in the SM location and 3 samples of faeces in the DN location, mainly in order to characterize N sources.

4.3.4 C and N content and isotopic ratio determination

All collected samples (tree leaves, PFT of the herbaceous layer — forbs, grasses and legumes —, litter, faeces, BGB and soil) were oven dried at 60ºC until constant weigh. Tree leaves, litter, and main species of each PFT (Section 4.3.2) were pooled in one sample per treatment (4 replicates each), only using leaves. Afterwards, all collected samples were powdered and tin capsuled.

For determining C content and $\delta^{13}C$ in all our samples, except in the soil, we used glutamic acid and acetanilide as standards, both calibrated using glutamic acid from IAEA, USGS40. For determining the percentage of N and $\delta^{15}N$ an additional standard was also used (N_1), calibrated using IAEA-N_1. Samples were prepared in the Institut de Biologie des Plantes (http://www.ips2.u-psud.fr). Afterwards, samples were analysed in

the Isolab of the Grassland Sciences group at ETH Zurich (http://www.gl.ethz.ch/), with a Flash EA 1112 Series elemental analyser (Finnigan MAT, Bremen, Germany), coupled to a DeltaplusXP isotope ratio mass spectrometer (Finnigan MAT, Bremen, Germany) via a 6-port valve (Brooks et al., 2003) and a ConFlo III interface (Werner et al., 1999).

For determining C content and $\delta^{13}C$ in the soil, we used acetanilide and caffeine as standards, both calibrated using glutamic acid from IAEA, USGS40, and NBS-22. In determining the percentage of N and $\delta^{15}N$ tyrosine was also used as standard, this calibrated using IAEA-N_1. Soil samples were prepared and analysed in the Isolab of the Grassland Sciences group at ETH Zurich, as described before.

Isotopic ratios ($\delta^{13}C$ and $\delta^{15}N$) were both calculated as deviation of the corresponding isotope ratio (R = $^{13}C/^{12}C$ or R = $^{15}N/^{14}N$) from their respective international standard ($\delta = [(R_{sample} / R_{standard}) - 1] \times 1000$), Vienna Pee Dee Belemnite, for $\delta^{13}C$ and air N_2 for $\delta^{15}N$.

4.3.5 Intrinsic water use efficiency calculation

In order to estimate the iWUE of tree leaves and PFT (forbs, grasses and legumes) per plot and under the canopy *vs.* the open grassland, we calculated ^{13}C discrimination (Equation 4.1, $\Delta^{13}C$, Farquhar et al., 1989), which was then used to account for the atmospheric and sub-stomatal CO_2 partial pressures ratio (C_i/C_a), using the simplified model of C_3 photosynthetic isotope discrimination (Equation 4.2, Farquhar et al., 1982).

$$\boldsymbol{\Delta^{13}C} = \frac{(\boldsymbol{\delta^{13}C_a} - \boldsymbol{\delta^{13}C_p})}{\mathbf{1} + (\frac{\boldsymbol{\delta^{13}C_p}}{\mathbf{1000}})}$$

(Equation 4.1)

$$\boldsymbol{\Delta^{13}C} = a + (b - a)\,\frac{\boldsymbol{C_i}}{\boldsymbol{C_a}}$$

(Equation 4.2)

Here $\delta^{13}C_a$ and $\delta^{13}C_p$ (Equation 4.1) are the $\delta^{13}C$ in air CO_2 (−8 ‰) and plant materials, respectively; *a* is the fractionation during binary diffusion in air (4.4 ‰); and *b* is a slightly reduced value of the fractionation during carboxylation in C_3 plants, to account for effect of neglected terms in the simplified model of C_3 photosynthetic isotope discrimination (28 ‰, Brugnoli and Farquhar 2000).The relationship $\Delta^{13}C$ ~ *Ci/Ca* can be used as an indicative of the iWUE (Farquhar and Richards, 1984).

4.3.6 Data analysis

All data analyses were performed using R software (R core Team, 2015). To assess C and N content and isotopic ratios ($\delta^{13}C$, $\delta^{15}N$) differences among ecosystem compartments (tree leaves, forbs, grasses, legumes, litter, faeces, BGB and soil), we performed one way ANOVAs, and tukey post-hoc tests, using the HSD.test function of the agricolae package (Mendiburu, 2017).

Also, we run linear models on C and N content and isotopic ratios ($\delta^{13}C$, $\delta^{15}N$) of each ecosystem compartment as function of plot (SM-ilex, DN-mixed, DN-suber, DN-pinea) and canopy (OG, UC). Final models were selected by a stepwise procedure based on the Akaike information criterion (AIC) using the stepAIC function, MASS package (Venables and Ripley 2002). Only significant models ($p < 0.05$) are presented and discussed, showing the most explicative and parsimonious one. Relationships between C and N dynamics within or between ecosystem compartments are also presented (Section 4.4.6) and discussed when applicable.

4.4 Results

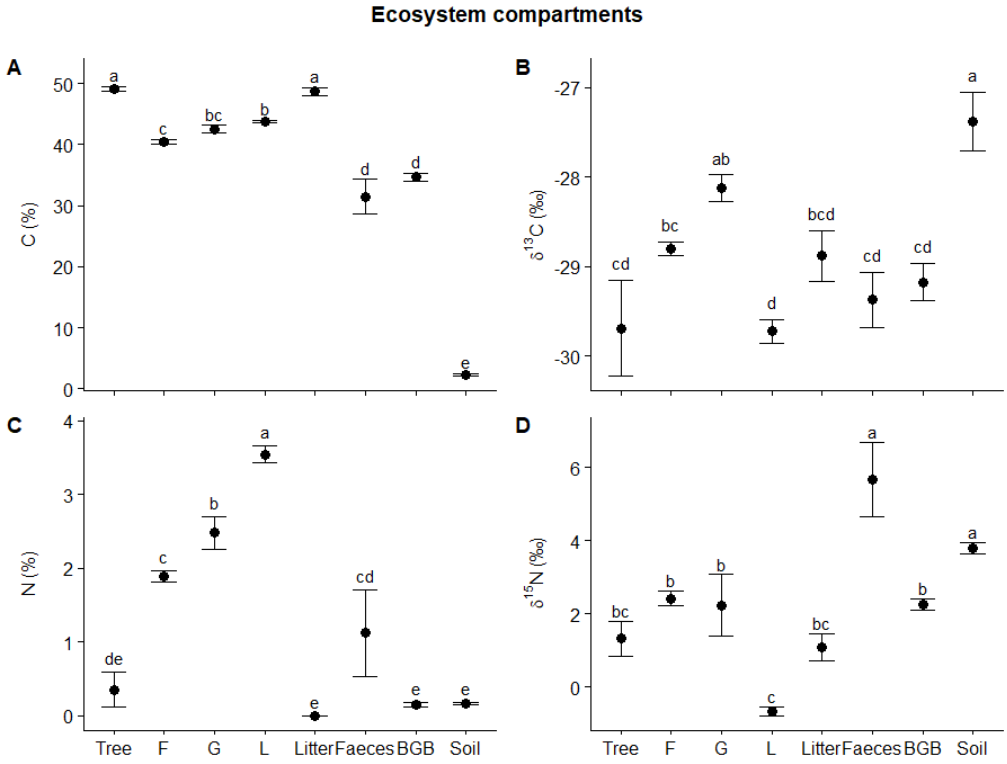

Figure 4.1. (A) C content, (B) $\delta^{13}C$, (C) N content, and (D) $\delta^{15}N$, per ecosystem compartments, including tree leaves; forbs, F; grasses, G; legumes, L; litter; faeces; belowground biomass, BGB; and soil. Mean ± standard error, and Tukey post-hoc test among ecosystem compartments. Letters indicate significant differences among groups ($p < 0.05$).

4.4.1 Carbon content

C content presented important differences among ecosystem compartments (Figure 4.1.A). Tree leaves and litter were the ecosystem compartments with the highest C content and soil the ecosystem compartment with the lowest C content (Figure 4.1.A). Moreover, there was a canopy effect on the C content, dependent on the ecosystem compartment and plot (Figure 4.2). C content in the BGB of all DN plots was higher than in the SM-ilex plot (Figure 4.2.F), especially in the DN-suber (canopy x DN-suber effect, $t = 2.04$, $p = 0.05$, Table 4.2) and DN-pinea (canopy x DN-pinea effect, $t = 4.07$, $p < 0.001$, Table 4.2) plots. On the other hand, C content in the BGB was higher under the canopy than in the open grassland (Figure 4.2.F), except under *P. pinea* canopy

(DN-pinea x canopy effect, t = −2.23, p < 0.003, Table 4.2), in which the C content in the BGB decreased under the canopy compared to the open grassland (Figure 4.2.F).

Soil C content showed differences among plots (Figure 4.2.G). DN-mixed (t = −2.65, p = 0.01, Table 4.2) and DN-pinea (t = −1.73, p = 0.09, Table 4.2) were the plots with the lowest soil C content, especially in the open grassland. In addition, soil C content was consistently higher under the canopy than in the open grassland in all the study plots (canopy effect, t = 6.20, p < 0.001, Table 4.2).

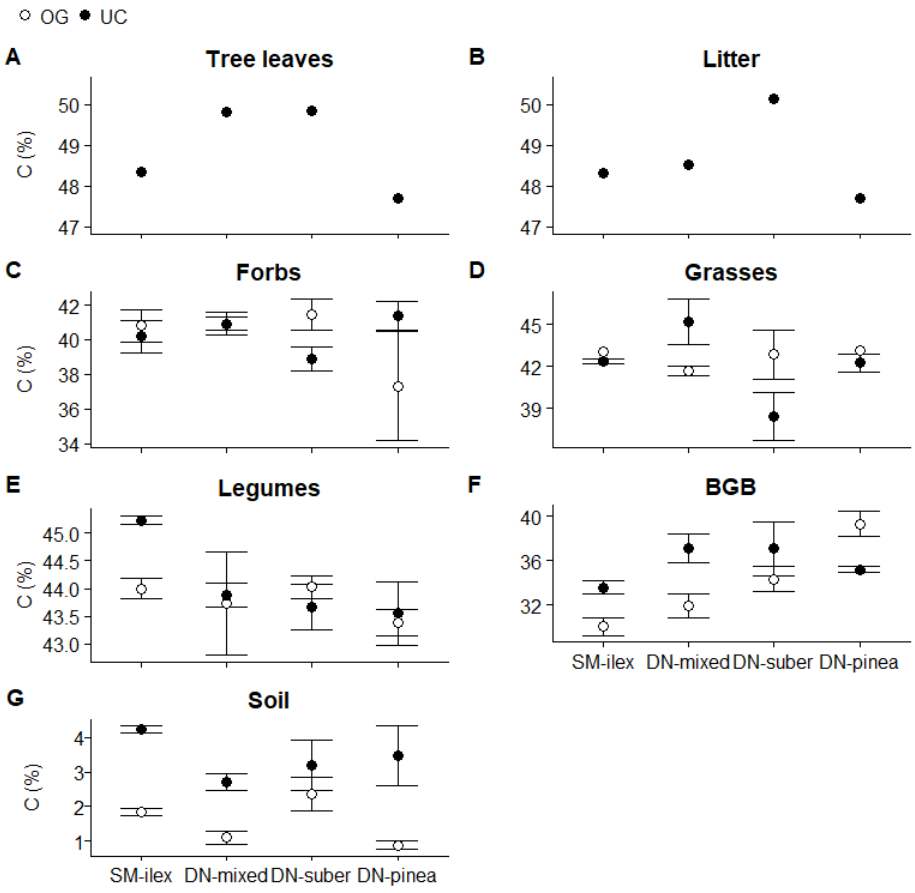

Figure 4.2. C content per ecosystem compartment, plot and canopy: open grassland (OG) and under the canopy (UC) on: (A) tree leaves; (B) litter; (C) forbs; (D) grasses; (E) legumes; (F) belowground biomass, BGB; and (G) soil. Mean ± standard error.

Table 4.2. Linear model results. C content in belowground biomass (BGB) and soil, as function of plot and canopy. Plot with SM-ilex as reference level, and canopy with open grassland (OG) as reference level. Estimates of the explanatory variables (Est.), standard error (SE), t and p-value.

	C content (%)							
	BGB				Soil			
	Est.	SE	t	p	Est.	SE	t	p
(Intercept)	30	1	20.12	< 0.001	2.1	0.4	5.73	< 0.001
Plot (DN-mixed)	2	2	1.03	0.3	−1.1	0.4	−2.65	0.01
Plot (DN-suber)	4	2	2.04	0.05	−0.2	0.5	−0.43	0.7
Plot (DN-pinea)	9	2	4.07	< 0.001	−0.8	0.5	−1.73	0.09
Canopy	4	3	1.37	0.2	1.8	0.3	6.20	< 0.001
Plot (DN-mixed) x canopy	2	3	0.55	0.6				
Plot (DN-suber) x canopy	−1	3	−0.25	0.8				
Plot (DN-pinea) x canopy	−8	3	−2.23	0.03				
$\mathbf{R^2_{Adj}}$	0.41			0.001	0.53			< 0.001

4.4.2 ^{13}Carbon isotopic ratio

$\delta^{13}C$ differed among ecosystem compartments (Figure 4.1.B). Soil was the most ^{13}C enriched ecosystem compartment, and legumes and tree leaves the most ^{13}C depleted (Figure 4.1.B). Also, there was an overall tendency in the herbaceous vegetation to be more ^{13}C depleted under the canopy than in the open grassland (Figure 4.3), but this effect was dependent on the given PFT and plot (Figure 4.3).

Forbs (Figure 4.3.C) were in general more ^{13}C depleted in the DN-mixed plot than in the other plots (DN-mixed effect, t = −2.34, p = 0 0.02, Table 4.3). Moreover, forbs were more ^{13}C depleted under the canopy than in the open grassland (canopy effect, t = −3.72, p < 0.001, Table 4.3), but this canopy effect was especially marked in all DN plots (DN plots effects, Table 4.3), while such effect was not noticeable in the SM-ilex plot (Figure 4.3.C). Grasses (Figure 4.3.D) were also more ^{13}C depleted under the canopy than in the open grassland (canopy effect, t = −3.12, p = 0.01, Table 4.3), except in the DN-mixed plot, where this ^{13}C depleatment under the canopy was not noticeable (DN-mixed x canopy effect, p = 3.40, t = 0.006, Table 4.3).

Finally, legumes (Figure 4.3.E) in general presented the opposite canopy effect than forbs and grasses on $\delta^{13}C$, since legumes tended to be more ^{13}C enriched under the canopy than in the open grassland; this ^{13}C enrichment under the canopy was only significant in the DN-suber plot (DN-suber x canopy effect, t = 2.32, p = 0.03, Table 4.3). The exception were the legumes in the DN-mixed plot, which were more ^{13}C depleted under the canopy than in the open grassland (DN-mixed x canopy, effect t = −2.10, p = 0.04, Table 4.3).

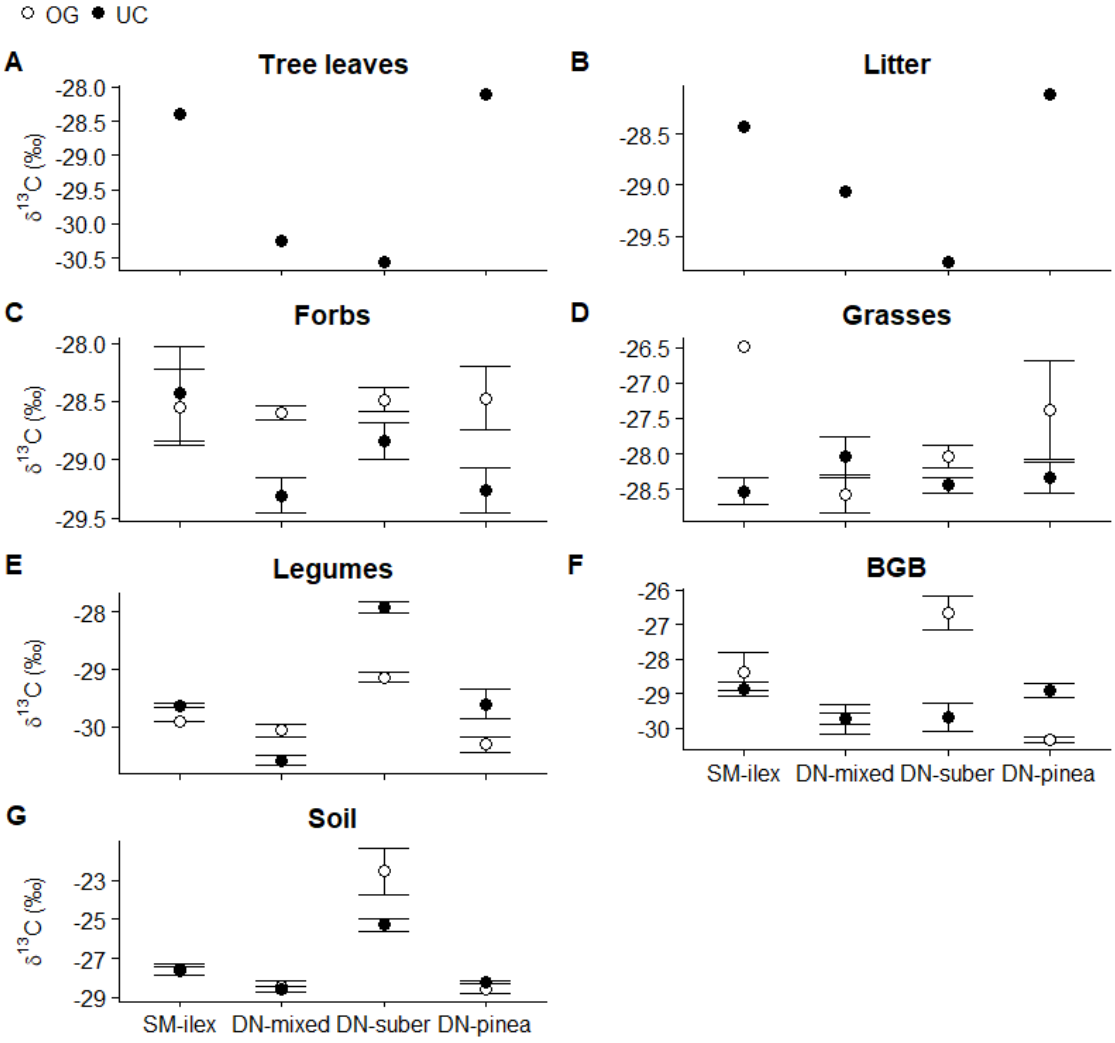

Figure 4.3. $\delta^{13}C$ per ecosystem compartment, plot and canopy: open grassland (OG) and under the canopy (UC) on: (A) tree leaves; (B) litter; (C) forbs; (D) grasses; (E) legumes; (F) belowground biomass, BGB; and (G) soil. Mean ± standard error.

Table 4.3. Linear model results. $\delta^{13}C$ in forbs, grasses and legumes, as function of plot and canopy. Plot with SM-ilex as reference level, and canopy with open grassland (OG) as reference level. Estimates of the explanatory variables (Est.), standard error (SE), t and p-value.

	$\delta^{13}C$ (‰)											
	Forbs				Grasses				Legumes			
	Est.	SE	t	p	Est.	SE	t	p	Est.	SE	t	p
(Intercept)	−28.2	0.2	−154.92	< 0.001	−26.5	0.5	−49.44	< 0.001	−29.9	0.2	−125.36	< 0.001
Plot (DN-mixed)	−0.5	0.2	−2.34	0.02	−2.1	0.6	−3.49	0.005	−0.2	0.3	−0.58	0.6
Plot (DN-suber)	−0.2	0.2	−0.79	0.4	−1.5	0.7	−2.36	0.04	0.8	0.3	2.80	0.009
Plot (DN-pinea)	−0.4	0.2	−1.69	0.09	−0.9	0.7	−1.37	0.2	−0.4	0.3	−1.37	0.2
Canopy	−0.5	0.1	−3.72	< 0.001	−2.0	0.7	−3.12	0.01	0.3	0.3	0.83	0.4
DN-mixed x canopy					2.6	0.8	3.40	0.006	−0.8	0.4	−2.10	0.04
DN-suber x canopy					1.6	0.8	1.94	0.08	0.9	0.4	2.32	0.03
DN-pinea x canopy					1.1	0.8	1.28	0.2	0.4	0.4	1.06	0.3
$\mathbf{R^2_{Adj}}$	0.15			< 0.001	0.39			0.07	0.84			< 0.001

When assessing $\delta^{13}C$ of dominant species of each PFT (Figure 4.4), differences in the $\delta^{13}C$ already detected among forbs, grasses and legumes (Figure 4.1.B) were confirmed. Legume species, including *O. sativus* and *T. subterraneum* and all forbs, including *C. arvensis*, *C. mixtum, E. moschatum, G. molle* and *C. capillaris,* were more ^{13}C depleted than grass species (*B. hordeaceus*, see species estimates on Table S4.2). The canopy effect was confirmed over most of the species (Figure 4.4), species under the canopy being more ^{13}C depleted than in the open grassland (canopy effect, $t = -3.41$, $p < 0.001$, Table S4.2).

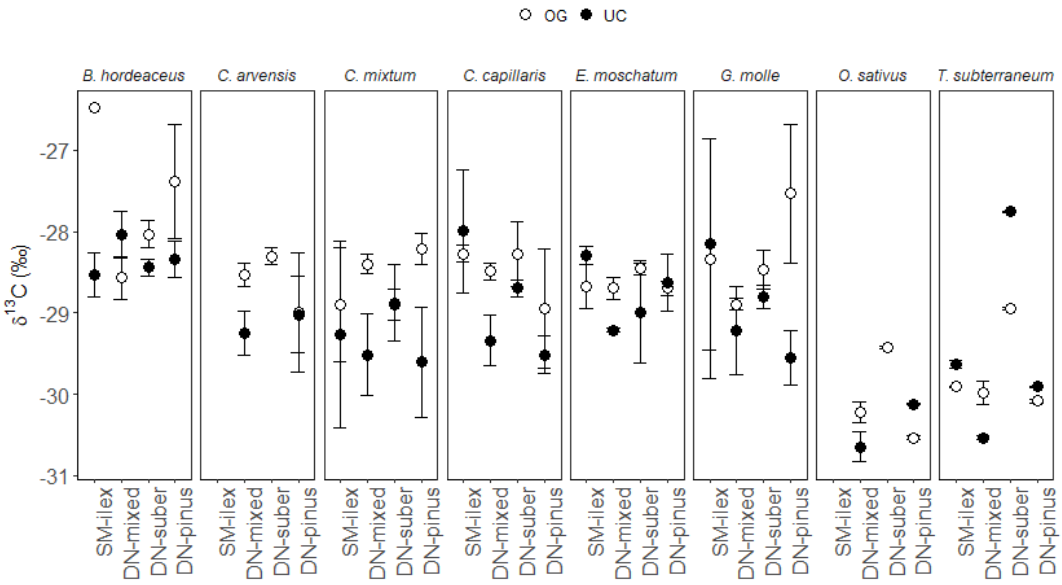

Figure 4.4. $\delta^{13}C$ of dominant plant species of each plant functional type: grasses (*B. hordeaceus*), forbs (*C. arvensis*, *C. mixtum*, *C. capillaris*, *E. moschatum*, *G. molle*), and legumes (*O. sativus*, *T. subterraneum*), per plot and canopy: open grassland (OG) and under the canopy (UC). Mean ± standard error.

4.4.3 Intrinsic water use efficiency

Grasses had the lowest ^{13}C discrimination ($\Delta^{13}C$) and the lowest atmospheric and sub-stomatal CO_2 partial pressures ratio (C_i/C_a), meaning that they had the highest iWUE, followed by forbs, legumes and tree leaves (Figure 4.5.A).

Generally, vegetation under the canopy presented higher $\Delta^{13}C$ and C_i/C_a than in the open grassland, meaning that vegetation under the canopy had lower iWUE than in the open grassland (Figure 4.5.A). However, when assessing each PFT per plot, there were some differences in the way that the canopy influenced the iWUE of each PFT, similarly to what happened with the $\delta^{13}C$. The iWUE of forbs in all DN plots was lower under the canopy than in the open grassland, while forbs in the SM-ilex plot did not show this pattern (Figure 4.5.B). iWUE of grasses in all plots was lower under the canopy than in the open grassland, except in the DN-mixed plot, where grasses under the canopy had higher iWUE than in the open grassland. Finally, legumes generally presented the reverse pattern, with an iWUE under the canopy higher than in the open grassland (Figure 4.5.B).

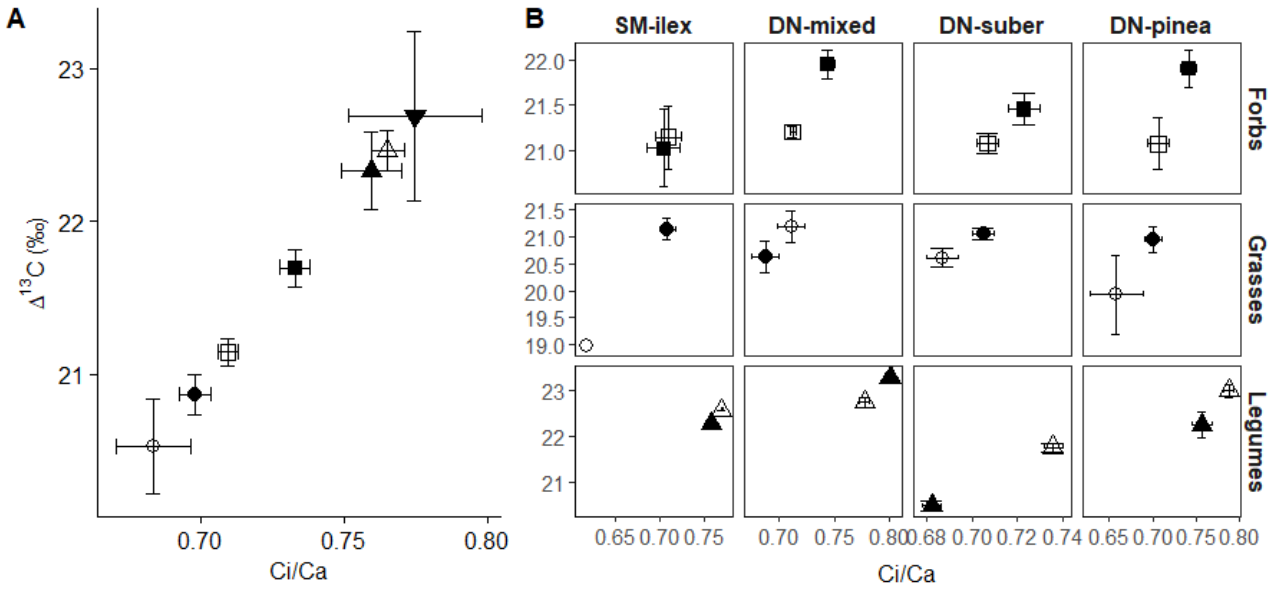

Figure 4.5. Intrinsic water use efficiency (iWUE) = $\Delta^{13}C$ ~ *Ci/Ca* per (A) ecosystem compartment (■ forbs, ● grasses, ▲legumes and▼ tree leaves), and canopy (open dots indicate open grassland, and solid dots indicate under the canopy); and per (B) ecosystem compartment, plot and canopy. Mean ± standard error.

4.4.4 Nitrogen content

N content also strongly differed among ecosystem compartments (Figure 4.1.C). Legumes were the ecosystem compartment with the highest N content, followed by grasses and forbs, grasses always having a higher N content than forbs (Figure 4.6.A). On the contrary, tree leaves, litter, BGB and soil were the ecosystem compartments with the lowest N content (Figure 4.1.C). Note that as the N content in the litter was below detection limit (Figure 4.1.C), plot or canopy effects on N content and $\delta^{15}N$ of litter are not further shown or discussed.

Moreover, the N content was also influenced by the tree canopy, depending on the ecosystem compartment and plot (Figure 4.7). Forbs (Figure 4.7.B) in the open grassland of all DN pots had lower N content than forbs in the SM-ilex plot (see DN plot effects, Table 4.4), but their N content strongly increased under the canopy (see DN plots x canopy effects, Table 4.4). Legumes (Figure 4.7.D) also had generally higher N content under the canopy than in the open grassland (canopy effect, $t = 3.10$, $p = 0.04$, Table 4.4), except in the SM-ilex plot.

N content in BGB showed a tendency to increase under the canopy compared to the open grassland (Figure 4.7.E), although there was not a significant canopy effect. Soil N content (Figure 4.7.F) was consistently higher under the canopy than in the open grassland in all the study plots (canopy effect, $t = 5.39$, $p < 0.001$, Table 4.4).

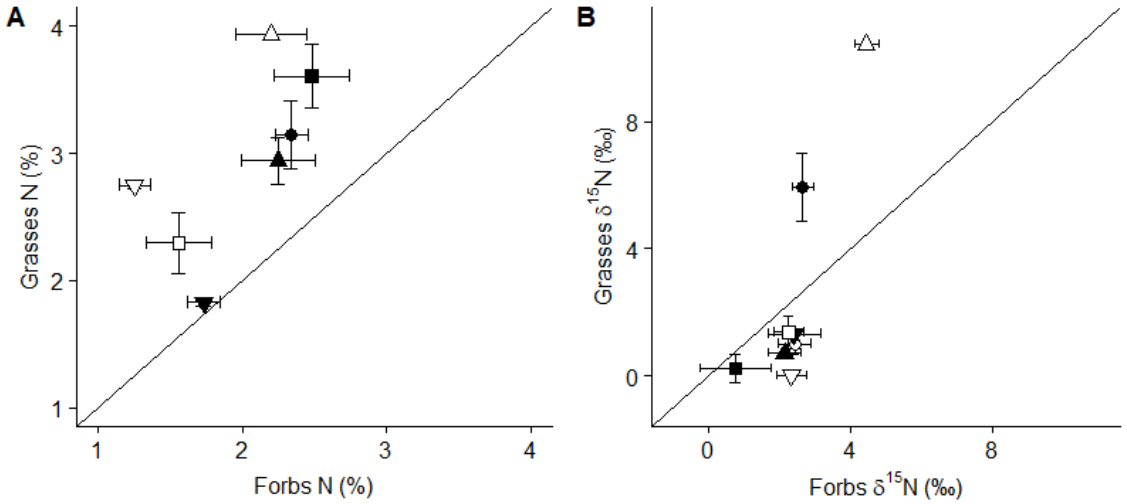

Figure 4.6 (A) Grasses N content ~ forbs N content relationship, and (B) grasses $\delta^{15}N$ ~ forbs $\delta^{15}N$ relationship, per plot (● SM-ilex, ■ DN-mixed, ▼ DN-suber, ▲DN-pinea) and canopy (open dots indicate open grassland, and solid dots indicate under the canopy). Mean ± standard error. Diagonal line indicates the 1:1 relationship.

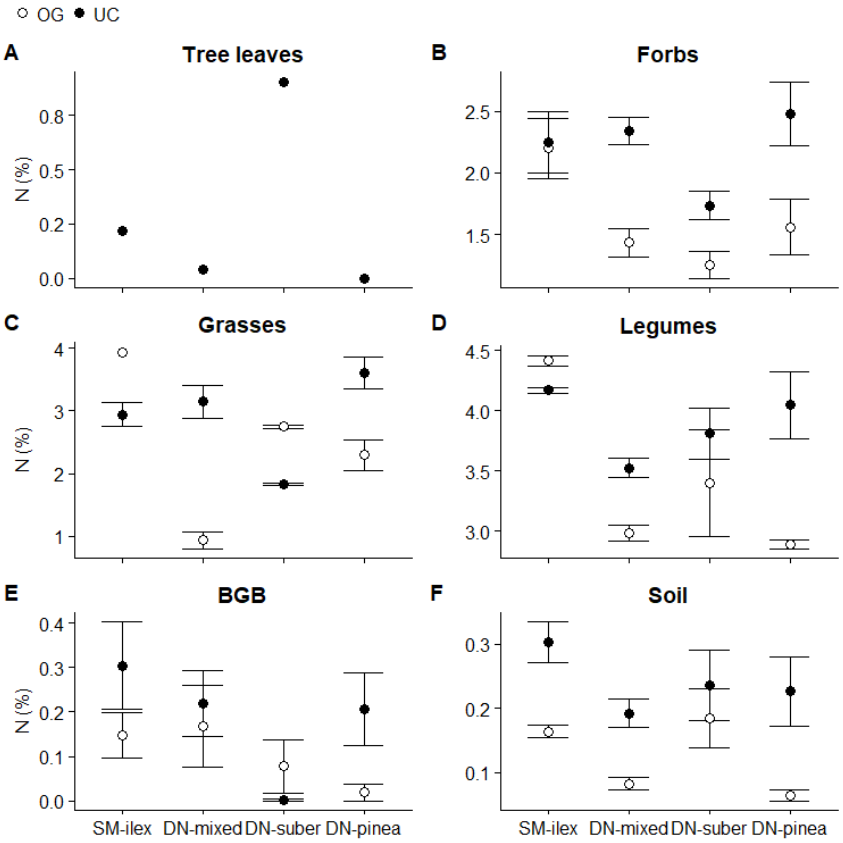

Figure 4.7. N content per ecosystem compartment, plot and canopy: open grassland (OG) and under the canopy (UC) in: (A) tree leaves; (B) forbs; (C) grasses; (D) legumes; (E) belowground biomass, BGB; and (F) soil. Mean ± standard error.

Table 4.4. Linear model results. N content in forbs, legumes and soil as function of plot and canopy. Plot with SM-ilex as reference level, and canopy with open grassland (OG) as reference level. Estimates of the explanatory variables (Est.), standard error (SE), t and p-value.

	N content (%)											
	Forbs				Legumes				Soil			
	Est.	SE	t	P	Est.	SE	t	p	Est.	SE	t	p
(Intercept)	2.2	0.2	10.70	< 0.001	4.0	0.3	13.28	< 0.001	0.18	0.03	6.77	< 0.001
Plot (DN-mixed)	−0.8	0.2	−3.14	0.002	−1.0	0.3	−3.21	0.003	−0.10	0.03	−3.31	0.002
Plot (DN-suber)	−0.9	0.3	−3.43	< 0.001	−0.7	0.3	−1.98	0.06	−0.02	0.03	−0.68	0.5
Plot (DN-pinea)	−0.6	0.3	−2.33	0.02	−0.8	0.3	−2.26	0.03	−0.09	0.03	−2.63	0.01
Canopy	0.0	0.3	0.17	0.9	0.6	0.2	3.10	0.004	0.11	0.02	5.39	< 0.001
Plot (DN-mixed) x canopy	0.9	0.3	2.48	0.01								
Plot (DN-suber) x canopy	0.4	0.4	1.07	0.3								
Plot (DN-pinea) x canopy	0.9	0.4	2.24	0.03								
R^2_{Adj}	0.34			< 0.001	0.29			0.004	0.51			< 0.001

4.4.5 ^{15}Nitrogen isotopic ratio

As expected, an overall assessment of N sources by the $\delta^{15}N$ (Figure 4.1.D), including faeces, confirmed clear differences in the $\delta^{15}N$ among ecosystems compartments, faeces being the ecosystem compartment most ^{15}N enriched, followed by soil. On the contrary, legumes were the ecosystem compartment most ^{15}N depleted (Figure 4.1.D). When comparing $\delta^{15}N$ of forbs and grasses per plot and canopy, grasses were more ^{15}N depleted than forbs, with a $\delta^{15}N$ closer to 0 (except in SM-ilex OG and DN-mixed UC, Figure 4.6.B).

The canopy influence on $\delta^{15}N$ was only clearly consistent on BGB (Figure 4.8.E), as BGB was more ^{15}N depleted under the canopy than in the open grassland (canopy effect = −0.9 ± 0.3, t = −3.26, p = 0.002, R^2_{Adj} = 0.21).

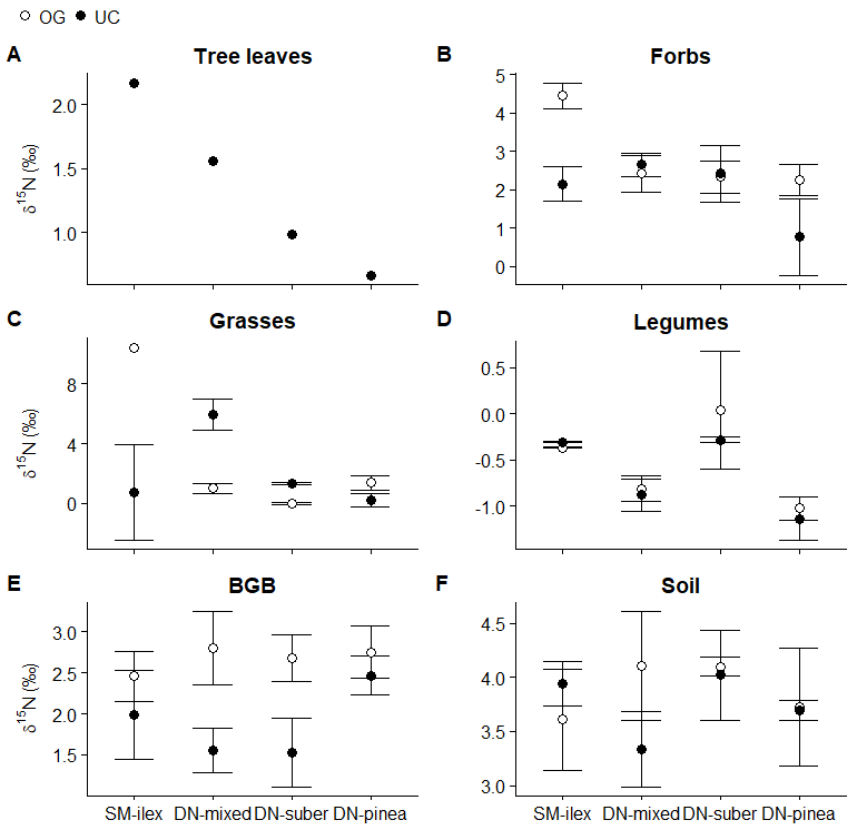

Figure 4.8. $\delta^{15}N$ per ecosystem compartment, plot and canopy: open grassland (OG) and under the canopy (UC) in: (A) tree leaves; (B) forbs; (C) grasses; (D) legumes; (E) belowground biomass, BGB; and (F) soil. Mean ± standard error.

When assessing the $\delta^{15}N$ per species (Figure 4.9), differences in $\delta^{15}N$ already detected among PFT were confirmed. Legume species, *O. sativus* and *T. subterraneum,* were the most ^{15}N depleted, followed by grass species and forbs (see species estimates on Table S4.3). In addition, two forb species were consistently more ^{15}N depleted under the canopy than in the open grassland: *C. arvensis* (*C. arvensis* x canopy effect, $t = -2.98$, $p = 0.003$, Table S4.3) and *C. mixtum* (*C. mixtum* x canopy effect, $t = -4.31$, $p < 0.001$, Table S4.3), but the canopy effect on $\delta^{15}N$ of the other species was plot dependent (Table S4.3).

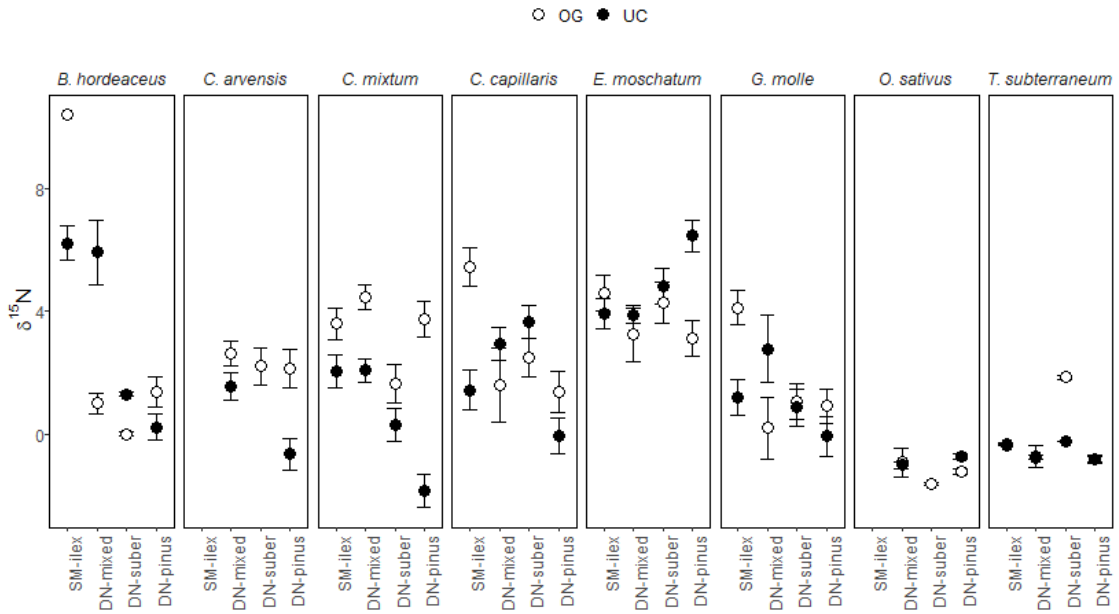

Figure 4.9. $\delta^{15}N$ of dominant plant species of each plant functional type: grasses (*B. hordeaceus*), forbs (*C. arvensis*, *C. mixtum*, *C. capillaris*, *E. moschatum*, *G. molle*), and legumes (*O. sativus*, *T. subterraneum*), per plot and canopy: open grassland (OG) and under the canopy (UC). Mean ± standard error.

4.4.6 Carbon and nitrogen relationships

Soil C was directly related to soil N (Figure 4.10.A). At plot scale, C content in the BGB decreased as soil N content increased (Figure 4.10.B). Also, $\delta^{15}N$ in the BGB decreased with increasing soil N content (Figure 4.10.C).

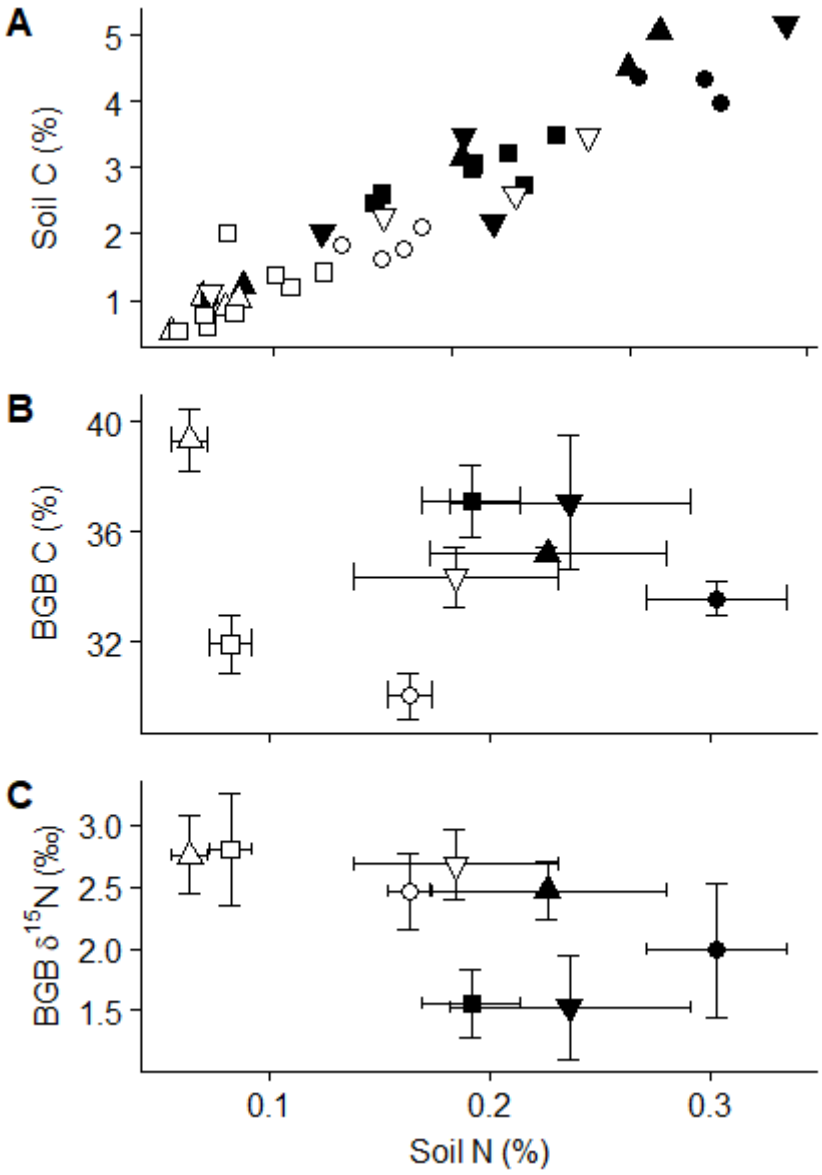

Figure 4.10. (A) Soil C ~ soil N relationship, (B) belowground biomass (BGB) C content ~ soil N content relationship, and (C) BGB $\delta^{15}N$ ~ soil N content relationship, per plot (● SM-ilex, ■ DN-mixed, ▼ DN-suber, ▲DN-pinea) and canopy (open dots indicate open grassland, solid dots indicate under the canopy). Mean ± standard error.

4.5 Discussion

4.5.1 Tree – open grassland structure influence on carbon dynamics

Ecosystem compartments behaved differently in terms of C content and $\delta^{13}C$, indicating differences in the C use and cycling. Tree leaves and litter had the highest C content, and similar C content (Figure 4.1.A) and $\delta^{13}C$ (Figure 4.1.B) values between each other, suggesting that most of the litter sampled under the canopy came effectively from tree leaves. However, litter was on average slightly more ^{13}C-enriched. Microbial respiration tends to discriminate against ^{13}C, emitting CO_2 depleted in ^{13}C, enriching the remaining C source in the process (Santruckova et al., 2000). This fact was also noticeable in the soil, which showed the most enriched ^{13}C values (Figure 4.1.B), most likely as a consequence of such ^{13}C enrichment of the remaining organic matter through microbial respiration (Santruckova et al., 2000).

In addition, litter from the tree species of this study (*Q. ilex, Q. suber, P. pinea*) was probably more recalcitrant than litter from the herbaceous species, resulting in a slower C cycling in the soil under the canopy, increasing soil C stocks (Gómez-Rey et al., 2013). This would explain the higher soil C content under the canopy compared to the open grassland (Figure 4.2.G). Also, the fact that soil C was directly related to soil N (Figure 4.10.A), and the relatively similar $\delta^{13}C$ values of soil and above and belowground biomass (Figure 4.1.B), suggested that soil C came effectively from an organic source, trees probably being main sources of soil C spatial heterogeneity (Andivia et al., 2015; Gómez-Rey et al., 2013; Howlett et al., 2011; Pulido-Fernández et al., 2013).

BGB was naturally a mixture of herb and tree roots, as probably indicated the observed $\delta^{13}C$ (Figure 4.1.B). Thus, $\delta^{13}C$ of BGB was in between the $\delta^{13}C$ of tree leaves and the herbaceous vegetation (forbs, grasses and legumes, Figure 4.1.B), value that could be the result of differences during opposite dark respiration between trees and herbs (Ghashghaie and Badeck, 2014). Leaves tend to be more ^{13}C depleted than roots due

to several discrimination steps, including CO_2 leaf assimilation and respiration, and C distribution and storage in the various plant organs (Aljazairi et al., 2014; Aranjuelo et al., 2009). On the other hand, roots of C_3 herbs (most of the species of our plots) respire enriched CO_2 compared to root's biomass during dark respiration, while C_3 woody species, such as the trees of our study (*Q. ilex*, *Q. suber* and *P. pinea*), respire depleted CO_2 during the same process (Ghashghaie and Badeck, 2014). Hence, dark respiration generates ^{13}C depleted roots of C_3 herbs and ^{13}C enriched roots of C_3 woody species (Ghashghaie and Badeck, 2014), fact that could explain the ^{13}C signal that we observed in our BGB (Figure 4.1.B), a mixture of herb and tree roots.

Moreover, the C content of BGB showed differences among plots, which were probably related to differences in soil fertility, at least in terms of soil N content (Figure 4.10.B). Generally, plants allocate C in shoots and roots to optimize resource acquisition and conservation, and the tendency is to relatively allocate higher C where is needed to get the limiting resource (Ågren and Ingestad, 1987; Gargallo-Garriga et al., 2014). Plants tend to relatively allocate more C to shoots under light constraints (Brouwer, 1983; Hilbert and Reynolds, 1991), and to roots under water or nutrient limitations (Ågren and Franklin, 2003; Aljazairi et al., 2015; Durand et al., 2016; Pausch and Kuzyakov, 2018; Xia et al., 2017). Hence, there was a tendency to decrease the C content in BGB with increasing soil N (Figure 4.10.B), according to this resource acquisition optimization principle.

However, when assessing the intra-plot heterogeneity driven by tree canopies on the C content of BGB, this pattern to optimize resource acquisition was not fulfilled. Under the canopy there were light constrains, higher soil water content (Figure 5.1) and higher soil N content (Figure 4.7.F), conditions that should have promoted relatively lower C content in BGB under the canopy compared to the open grassland, but yet BGB had generally higher C content under the canopy (Figure 4.2.F). The exception was the BGB in the DN-pinea plot, where there was lower C content in BGB under the canopy

compared to the open grassland (Figure 4.2.F); which could be related to the lowest soil N content found in the open grassland of the DN-pinea plot (Figure 4.7.F).

Conversely, the higher C content that we found in the BGB under the canopy compared to the open grassland in the other plots (SM-ilex, DN-mixed and DN-suber, Figure 4.2.E), was probably related to differences in root C allocation between grassland species. Root C allocation varies depending on life forms, PFT and plant species (Warembourg et al., 2003). Annual species tend to lose more C through respiration and exudation, and have lower C use efficiency than perennial species (Warembourg and Estelrich 2001). Moreover, forbs store more C in roots than grasses and legumes, and legumes have higher root respiration rates and lower C storage in roots than forbs and grasses (Warembourg et al., 2003).

In our systems, most of the species were annuals, but certainly there were differences in PFT composition between under the canopy and the open grassland (Figure S4.1). Legumes mostly appeared in the open grassland, while grasses were dominant under the canopy (Figure S4.1). Therefore, BGB in the open grassland could contain a greater amount of legumes' roots in the composition, which could be lowering the overall C content of BGB in the open grassland compared to under the canopy (Figure 4.2.F). Also, although BGB was sampled at a superficial depth (0 - 10 cm), BGB under the canopy could contain a greater amount of fine tree roots than in the open grassland, which could be influencing the overall C content in the BGB.

Regarding the herbaceous vegetation, grasses were the PFT most ^{13}C enriched (Figure 4.1.B), meaning that they had also the highest intrinsic water use efficiency (iWUE, Figure 4.5.A); while legumes were the most ^{13}C depleted (Figure 4.1.B), and had the lowest iWUE (Figure 4.5.A). In agreement, Caldeira et al. (2001) found a similar pattern, legume species having the most negative $\delta^{13}C$, followed by forbs and grasses, grown both in monocultures and in mixtures (Caldeira et al., 2001). Also, Roumet et al.

(2000) found higher stomatal conductance and lower iWUE in legumes compared to grasses (Roumet et al., 2000).

This $\delta^{13}C$ difference among PFT has been related to leaf N content (Li et al., 2016). A higher leaf N content, as is the case of legumes compared to grasses and forbs (Figure 4.1.C), generally implies lower leaf mass/area ratio and lower thicknesses. Those traits mean a shorter internal diffusion pathway from stomata to chloroplasts, generating greater CO_2 conductance and consequently greater CO_2 supply for carboxylation (Li et al., 2016). The greater CO_2 supply leads to enhanced photosynthesis and increased discrimination against ^{13}C. Indeed, this links with the previously discussed root C allocation differences among PFT. Legumes have both higher root respiration (Warembourg et al., 2003) and leaf CO_2 exchange rates (Li et al., 2016), compared to for forbs and grasses; and eventually, higher rates of CO_2 exchange result in more depleted ^{13}C tissues (more negative $\delta^{13}C$).

On the other hand, under the canopy there were lower water constrains and lower light availability (Figure 5.1), conditions that increased the stomatal conductance, resulting in higher discrimination against ^{13}C (Figure 4.3.C), and lower iWUE (Figure 4.5.B) of the herbaceous vegetation, especially on forbs. However, there were some differences between plots in the way that the canopy influenced those parameters. The canopy effect was clear on the $\delta^{13}C$ and iWUE of forbs in all DN plots while this effect was not noticeable in the SM-ilex plot. This suggests that forbs had similar water and CO_2 exchange under the canopy and in the open grassland in the SM-ilex plot, in agreement with the results reported in Section 5.4.3.1 on net ecosystem CO_2 exchange and aboveground biomass from these same plots.

In Section 5.4.3.1 we reported that net ecosystem CO_2 exchange was dominated by net uptake both under the canopy and in the open grassland in the SM-ilex plot, while there was net CO_2 uptake in the open grassland but CO_2 emissions under the canopy in all DN plots. In addition, we reported in Section 5.4.2 that there were no differences in the

aboveground biomass between under the canopy and the open grassland in the SM-ilex plot, while under the canopy the aboveground biomass did decrease in all DN plots. These facts suggest that SM was probably less environmentally constrained than DN, and that the canopy did not influence water and CO_2 exchange so strongly in the SM-ilex plot as in DN plots, where differences between under the canopy and in the open grassland were more pronounced.

4.5.2 Tree – open grassland structure influence on nitrogen dynamics

Differences in N dynamics among ecosystem compartments were clear. Legumes were the PFT with the highest N content (Figure 4.1.C) and the lowest $\delta^{15}N$ (Figure 4.1.D), due to the widely documented capacity of legumes to fix symbiotic N_2 (e.g. Reich et al., 2003, 1997). On the other hand, grasses had higher N content than forbs (Figure 4.6.A) and generally lower $\delta^{15}N$ (Figure 4.6.B), suggesting that grasses may be more efficient taking-up N than forbs, and therefore were able to discriminate more against ^{15}N (Yoneyama et al., 2001), and/or exploiting symbiotic N. Accordingly, N-transfer between legumes (source of symbiotic N) and grasses, maybe more efficient than between legumes and forbs (Pirhofer-Walzl et al., 2012). Grasses usually have fibrous roots (Pirhofer-Walzl et al., 2012; Schenk and Jackson, 2002; Weaver, 1958), trait that may be facilitating higher N absorption from the most superficial soil layers and from symbiotically fixed N sources, while forbs have generally taproots that are not so efficient to this effect (Pirhofer-Walzl et al., 2012).

In addition, besides N symbiotically fixed by legumes, there could be N_2-fixing diazotrophic bacteria, which can develop root associations with different plants, including grasses. Unlike legumes, N_2-fixing bacteria associated to grasses do not form nodules, but can live in close association with the rhizosphere, enhancing the availability of N biologically fixed for the plant, enhancing plant growth and fitness (Bhattacharyya and Jha, 2012; Liu et al., 2017; Santi et al., 2013).

Such differences in the N acquisition and use may provide an important competitive advantage to grasses, probably being one of the causes of their dominance under the canopy (Figure S4.1), where there was higher soil N availability (Figure 4.7.F). Song et al. (2011) found a similar result, with grasses being more competitive than forbs at higher N availability, via increasing their biomass at the expense of forbs (Song et al., 2011). Moreover, this suggests that each PFT (forbs, grasses and legumes) could be exploiting N resources in a particular way under the influence of tree canopies, shaping the structure and composition of the herbaceous layer, and this in turn dehesa N cycling.

Accordingly, N dynamics also differed between under the canopy and the open grassland, with generally higher N content under the canopy in forbs (Figure 4.7.B), legumes (Figure 4.7.D) and soil (Figure 4.7.F) than in the open grassland. The higher litter fall input from tree canopies most likely increased soil N content under the canopy (Andivia et al., 2015; Gallardo, 2003; Gallardo et al., 2000; Moreno et al., 2007), and this in turn, increased N content in the shoot biomass. However, note that such canopy influence on the N content of shoots was again stronger in all DN plots than in the SM-ilex plot. The N content of forbs (Figure 4.7.B) and legumes (Figure 4.7.D) did not differ so much between under the canopy and the open grassland in the SM-ilex plot, while there were important differences in all DN plots. This links with the previously discussed differences regarding the canopy effect on C dynamics between plots; suggesting a coupling between C and N cycling (Aljazairi et al., 2014); and again that the SM-ilex plot was less environmentally constrained than DN plots, also regarding N dynamics. Moreover, this highlights the relevance of trees as drivers of ecosystem fertility (Andivia et al., 2015; Dahlgren et al., 1997; Gómez-Rey et al., 2013; Howlett et al., 2011; Pulido-Fernández et al., 2013), especially in more constrained environments, as is DN *vs.* SM.

Soil N content also influenced ^{15}N discrimination processes, as shows the lower $\delta^{15}N$ in BGB (Figure 4.8.E) under the canopy than in the open grassland, which decreased with increasing soil N content (Figure 4.10.C). Accordingly, at higher N availability, higher

discrimination against ^{15}N is possible (Dawson et al., 2002; Kalcsits et al., 2014), which first occurs during the assimilation of inorganic N (ammonium and nitrate) by roots, and further discrimination steps may occur during N transportation from roots to shoots or to root exudates (Kalcsits et al., 2014).

Finally, lower $\delta^{15}N$ values of BGB under the canopy (Figure 4.7.E) could also be related to the N origin, as biologically fixed N was probably more abundant under the canopy than in the open grassland. The presence of legumes under the canopy was very scarce (Figure S4.1), but N_2-fixing diazotrophic bacteria associated to non-legume species have been described to increase with soil moisture (Oliveira et al., 2004), and therefore they could be more abundant under the canopy, where there was higher soil water content (Figure 5.1.C), increasing the availability of biologically fixed N.

4.6 Conclusions

Dehesa C and N dynamics were strongly modulated by interactions between trees and the herbaceous layer. The higher litter fall from trees increased soil C and N content under the canopy compared to the open grassland. The increased soil N, most likely increased N content in shoots and favoured higher discrimination against ^{15}N by roots. Overall, $\delta^{13}C$ and intrinsic water use efficiency (iWUE) of the herbaceous layer, and especially of forbs, decreased under the canopy, as a result of higher stomatal conductance. Moreover, each plant functional type (PFT, forbs, grasses and legumes) had their own C and N ecophysiological particularities. Legumes had the lowest $\delta^{13}C$ and the lowest iWUE, followed by forbs and grasses. Besides the fact that legumes were the PFT with the highest N content and the most ^{15}N depleted leaves, grasses had higher N content than forbs and generally lower $\delta^{15}N$. This, suggests that grasses may be more efficient taking-up N, and/or exploiting symbiotic N than forbs, which could provide an important competitive advantage to grasses, especially under the canopy, where there

was higher soil N content. Finally, the canopy influence on C and N storage and cycling was generally more noticeable in the DN plots than in the SM-ilex plot, DN being more environmentally constrained than SM. This, highlights the relevance of trees as drivers of ecosystem fertility and C and N relationships, especially in more constrained environments, as is DN *vs.* SM.

Acknowledgements

This work was funded by the Spanish Science Foundation FECYT-MINECO: BIOGEI (GL2013-49142-C2-1-R) and IMAGINE (CGL2017-85490-R) projects, and supported by a FPI fellowship to Mercedes Ibañez (BES-2014-069243). Thanks to all the colleagues who collaborated in laboratory and fieldwork tasks: Antonio Rodríguez, Miquel Sala, Helena Sarri and Gianluca Segalina. Our special thanks to Dehesa de Gato S.L. state and Doñana Research Coordination Office for their support and facilities.

4.7 Supplementary material

Table S4.1. Cross section at breast height of the trees of the under the canopy (UC) treatment, per plot and tree species. Number of trees (N), mean and standard error (SE).

Plot	Tree species	N	Mean (m^2)	SE (m^2)
SM-ilex	*Q. ilex*	4	0.16	0.04
DN-mixed	*Q. ilex*	4	0.14	0.03
	Q. suber	4	0.3	0.1
DN-suber	*Q. suber*	4	0.31	0.04
DN-pinea	*P. pinea*	4	0.31	0.03

Table S4.2. Linear model results. $\delta^{13}C$ in grassland species as function of plot, species and canopy. Explanatory variables selected by a stepwise analysis. Plot with SM-ilex as reference level, species with *B. hordeaceu*s as reference level, and canopy with open grassland (OG) as reference level. Estimates of the explanatory variables, standard error (SE), t and p-value.

	$\delta^{13}C$ (‰)			
	Est.	**SE**	**t**	**p**
(Intercept)	−27.7	0.2	−131.30	< 0.001
Plot (DN-mixed)	−0.5	0.2	−2.86	0.005
Plot (DN-suber)	0.1	0.2	0.28	0.8
Plot (DN-pinea)	−0.3	0.2	−1.72	0.09
Species (*C. arvensis*)	−0.7	0.2	−2.74	0.007
Species (*C. mixtum*)	−0.9	0.2	−4.00	< 0.001
Species (*C. capillaris*)	−0.6	0.2	−2.96	0.004
Species (*E. moschatum*)	−0.7	0.2	−3.05	0.003
Species (*G. molle*)	−0.6	0.2	−2.82	0.005
Species (*O. sativus*)	−2.1	0.2	−8.34	< 0.001
Species (*T. subterraneum*)	−1.6	0.2	−7.57	< 0.001
Canopy	−0.4	0.1	−3.41	< 0.001
R^2_{Adj}	0.47			< 0.001

Table S4.3. Linear model results. $\delta^{15}N$ in grassland species as function of plot, species and canopy. Explanatory variables selected by a stepwise analysis. Plot with SM-ilex as reference level, species with *B. hordeaceus* as reference level, and canopy with open grassland (OG) as reference level. Estimates of the explanatory variables, standard error (SE), t and p-value.

	$\delta^{15}N$ (‰)			
	Est.	**SE**	**t**	**p**
(Intercept)	3.1	0.6	4.86	< 0.001
Plot (DN-mixed)	−1.0	0.4	−2.50	0.01
Plot (DN-suber)	−1.4	0.5	−3.06	0.003
Plot (DN-pinea)	−2.0	0.5	−4.38	< 0.001
Species (*C. arvensis*)	0.6	0.8	0.80	0.4
Species (*C. mixtum*)	1.5	0.8	2.05	0.04
Species (*C. capillaris*)	0.5	0.8	0.63	0.5
Species (*E. moschatum*)	1.7	0.8	2.20	0.03
Species (*G. molle*)	−0.7	0.8	−0.98	0.3
Species (*O. sativus*)	−2.9	0.9	−3.34	0.001
Species (*T. subterraneum*)	−2.2	0.8	−2.91	0.004
Canopy	1.9	0.8	2.50	0.01
Species (*C. arvensis*) x canopy	−3	1	−2.98	0.003
Species (*C. mixtum*) x canopy	−5	1	−4.31	< 0.001
Species (*C. capillaris*) x canopy	−2	1	−2.11	0.04
Species (*E. moschatum*) x canopy	−1	1	−0.93	0.4
Species (*G. molle*) x canopy	−2	1	−1.59	0.1
Species (*O. sativus*) x canopy	−2	1	−1.38	0.2
Species (*T. subterraneum*) x canopy	−2	1	−2.18	0.03
$\mathbf{R^2_{Adj}}$	0.52			< 0.001

Figure S4.1. Plant functional type (forbs, grasses and legumes) proportions per plot (SM-ilex, DN-mixed, DN-suber, DN-pinea) and canopy, open grassland (OG) and under the canopy (UC). Adapted from Section 5.4.2.

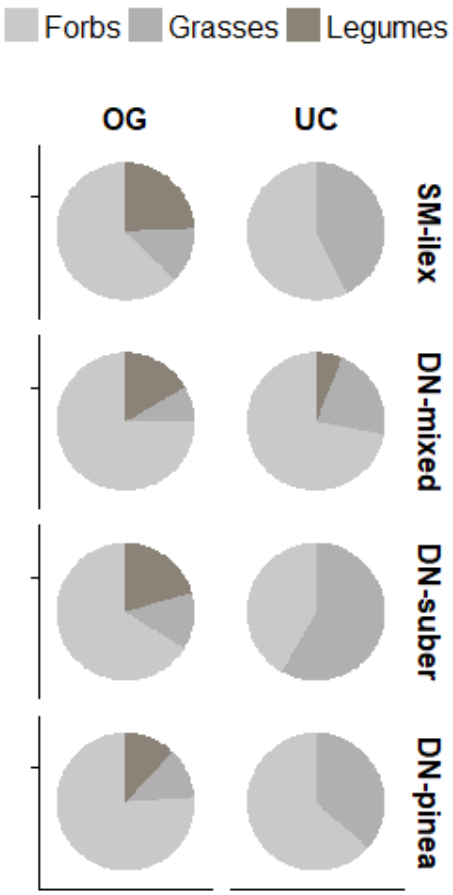

Chapter 5 Tree – open grassland structure drives greenhouse gas exchange mediated by the herbaceous layer in dehesa ecosystems of the Iberian Peninsula

Mercedes Ibañez[1]*, Maria José Leiva[2], Cristina Chocarro[3], Salvador Aljazairi[1], Àngela Ribas[4,5], Maria Teresa Sebastià[1,6]

[1]GAMES group & Dept. HBJ, ETSEA, University of Lleida (UdL), Lleida, Spain.

[2]Plant Biology and Ecology Department, Universidad de Sevilla, Sevilla, Spain.

[3]Department of Crop and Forest Science and Agrotecnio-Center, ETSEA, University of Lleida (UdL), Lleida, Spain.

[4]Universitat Autònoma de Barcelona, Bellaterra, Spain.

[5]Centre for Ecological Research and Forestry Applications (CREAF), Bellaterra, Spain.

[6]Laboratory of Functional Ecology and Global Change, Forest Sciences Centre of Catalonia (CTFC), Solsona, Spain.

MI performed research, analysed data and wrote the paper; MJL conceived and designed the study, performed research and revised the paper; CC performed research and revised the paper; SA performed research and revised the paper; AR revised the paper; MTS conceived and designed the study and revised the paper.

*Corresponding author; e-mail: mercedes.ibanez@hbj.udl.cat; phone: +34 973702623.

5.1 Abstract

Dehesa ecosystems are characterized by a savanna-like structure, which is the result of traditional silvo-pastoral uses. However, traditional uses are declining towards intensive farming and grazing, and there is a worrying lack of tree regeneration. Understanding how the tree – open grassland structure drives ecosystem functioning is essential for dehesas preservation and management. Yet, there are no studies integrating the canopy influence on greenhouse gas (GHG) exchange, including CO_2, CH_4 and N_2O, mediated by the herbaceous layer structure and composition. In addition, little is known about the effect of different tree species (*Quercus ilex*, *Quercus suber* and *Pinus pinea*) on GHG exchange. Our study provides insight into dehesas functioning, showing that the tree – open grassland structure modified the herbaceus layer structure, composition and diversity, both in terms of plant functionalt types (PFT) and species. Moreover, the tree – open grassland structure especially drove CO_2 and N_2O fluxes; emissions under the canopy of *P. pinea* being higher than under *Quercus* species. Composition and diversity of the herbaceus layer (in terms of PFT and species) was also an important GHG driver. Legumes enhanced CO_2 uptake and N_2O emissions; species compositional matrix drove ecosystem respiration and N_2O exchange; and species richness enhanced soil respiration. Interestingly, the inclusion of compositional terms and diversity indexes of the herbaceous layer improved the understanding of mechanisms affecting GHG exchange. Changes in the tree – open grassland structure of dehesas will imply deep changes in the GHG exchange, and that should be taken into account to perform better management strategies.

Key words: Canopy, CH_4, CO_2, diversity-interaction model, N_2O, plant functional types.

5.2 Introduction

Tree coverage in dehesas is changing, with the consequent implications that this may have on ecosystem functioning (Costa et al., 2011; Costa Pérez et al., 2006). Hence, although the canopy influence has been described to some extent on soil (Andivia et al., 2015; Gómez-Rey et al., 2013; Howlett et al., 2011; Pulido-Fernández et al., 2013), vegetation structure (Gea-Izquierdo et al., 2009; Hussain et al., 2009; Moreno et al., 2007) and composition (Lopez-Carrasco et al., 2015; Marañón et al., 2009; Rossetti et al., 2015), there is still a big uncertainty about how the tree – open grassland structure can drive greenhouse gas (GHG) exchange, including CO_2, CH_4 and N_2O, mediated by soil – vegetation interactions.

The only studies about GHG exchange conducted in dehesas have mainly focused on the tree canopy effect on CO_2 fluxes (Casals et al., 2011, 2009; Hussain et al., 2009; Ma et al., 2007; Tang and Baldocchi, 2005; Uribe et al., 2015), although these with divergent results. Some authors have described an enhancement of soil respiration rates under the canopy compared to the open grassland (Tang and Baldocchi, 2005; Uribe et al., 2015), related to a higher soil C and N content, and despite lower soil temperature. While on the contrary, higher CO_2 exchange rates in the open grassland have also been reported, due to higher herbaceous biomass and light availability, as main drivers of CO_2 uptake; and due to higher soil temperature, as main driver of CO_2 release (Hussain et al., 2009).

Furthermore, to our knowledge, the only previous studies addressing CH_4 and N_2O exchange in dehesas, were conducted by Shvaleva et al., (2015, 2014). Shvaleva et al. (2014) related CH_4 and N_2O emissions to soil water content, but the effect of soil water content was dependent on the canopy (Shvaleva et al., 2014): CH_4 uptake increased with soil water content, but the uptake rate was higher in the open grassland than under the canopy; and N_2O uptake increased with soil water content under the canopy, while there were N_2O emissions in the open grassland (Shvaleva et al., 2014).

Accordingly, some of the remaining uncertainty related to the “canopy effect” on GHG exchange may lie in soil – vegetation interactions. Studies conducted in grasslands showed that vegetation structure and composition drove GHG exchange (De Deyn et al., 2009; Praeg et al., 2017; Ribas et al., 2015), via the ecophysiological characteristics of the vegetation and the influence that vegetation exerts on the soil at different levels (Metcalfe et al., 2011). To this regard, there are different approximations to assess vegetation effects on GHG exchange (or any other ecosystem function), including species or functional diversity. Both approximations are complementary (Zhou et al., 2017), providing the first information about the species influence *per se*, while the latter provides a mechanistic link between vegetation and the given ecosystem function (Petchey and Gaston, 2006).

From a functional perspective, it is indicated to account for traits related to C and N acquisition and cycling when assessing GHG exchange. Sorting species into plant functional types (PFT) is an indirect measure of functional diversity, and a commonly used sorting for herbaceous species consists of grasses, non-legume forbs (hereafter “forbs”) and legume forbs (hereafter “legumes”); classification that is mainly based on nitrogen and light (and therefore CO_2) acquisition strategies (Tilman 1997; Symstad 2000; Díaz et al., 2007; defined as "guilds" in Sebastià 2007). Legumes have the capacity to fix symbiotic nitrogen, while grasses have some advantages when competing for light, thanks to erect high-density leaves that ensure good light penetration (Craine et al., 2001).

In any case, disentangling diversity from compositional effects, is key to understand vegetation influence on GHG exchange, since diversity and composition may affect independently ecosystem functioning (Kahmen et al., 2005; Ribas et al., 2015; Schultz et al., 2011). For that purpose, different methodologies have been proposed, which differ in the way that plant composition is included. On one hand, when assessing the effect of species composition in natural ecosystems, the challenge is to include the whole matrix

of species (multivariate) as predictor. Accordingly, one possibility is to reduce the dimensionality of the composition matrix using ordination methods (Kahmen et al., 2005; Legendre and Legendre, 1998; Sandau et al., 2014), allowing to synthesise species composition effects. On the other hand, when assessing a few number of species or PFT, one possible approximation is the diversity-interaction model proposed by Kirwan et al., (2009), which has the advantage to separate identity from interaction effects, in addition to the overall diversity effect (Kirwan et al., 2009).

Yet, there are no studies integrating the influence of all dehesa components on GHG exchange, considering the canopy, but also focussing on the herbaceous layer structure and composition. Knowledge that could be essential to perform better management strategies and keep sustainability of this vast, but vulnerable ecosystem. For these reasons, we selected plots with representative canopy types of Iberian dehesas (Costa Pérez et al., 2006): pure *Quercus ilex* L. and pure *Quercus suber* L. stands, which are the most abundant; followed by *Q. ilex* and *Q. suber* mixed stands; and pure *Pinus pinea* L. stand, the latter being a common tree plantation replacing traditional canopies; and in the present study we aim to: (1) assess the influence of plots dominated by different tree canopies on the structure, diversity and composition (in terms of species and PFT) of the herbaceous layer, and (2) disentangle the influence of these factors on GHG exchange, specially focusing on the role of vegetation, separately from a species and a functional perspective. In addition, although assessing the influence of dehesa structure on soil properties was not a specific aim of this study, soil characteristics were extracted from Chapter 4 (summarized in Table S5.2), and used to interpret and discuss our results.

5.3 Material and methods

5.3.1 Study sites and sampling design

The study sites were same dehesa plots described in Section 4.3.1 and sampling points were systematically placed following the same criteria. However, in order to capture seasonal variability of the studied variables, and effects that may be season dependent, field work was executed in two campaigns: spring (05/04/2016 – 10/04/2016) and autumn (13/12/2016 – 17/12/2016), coinciding with the most productive seasons of the system. Study treatments were therefore established according to: season (spring and autumn); plot (SM-ilex, DN-mixed, DN-suber and DN-pinea); and canopy (open grassland, OG, and under the canopy, UC).

At each treatment level we performed 3-4 replicates, resulting 73 sampling points. At each sampling point we hammered a metal collar (h = 8 cm, diameter = 25 cm), which was necessary for measuring GHG exchange (Section 5.3.2) and that defined the area in which vegetation (Section 5.3.3) and soil (Section 5.3.4) were sampled.

5.3.2 Greenhouse gas exchange measurements

For measuring GHG exchange, including CO_2, CH_4 and N_2O, we used a portable gas-exchange system (see system details in Debouk et al., 2018), consisting of a cylindrical chamber connected to photoacoustic spectroscopy gas analyser (PAS, INNOVA 1412, LumaSense Technologies, Denmark). PAS was calibrated prior to field campaigns by the vendor in the customary way (Moody et al., 2008). Nominal detection limits of the corresponding gases are: 5, 0.03, and 0.24 ppm for CO_2, N_2O, and CH_4, respectively.

At each sampling point, we recorded GHG mixing ratios (in ppm) at 1 minute intervals. Measurements were done closing the chamber over intact vegetation, at light and dark (covering the chamber) conditions. Afterwards, we harvested vegetation inside the metal

collar and performed bare soil measurements at dark conditions. As a result, 219 flux measurements (73 sampling points x 3 different conditions) were recorded.

In the case of CO_2, resulting fluxes measured over vegetation at light conditions can be approximated as net ecosystem CO_2 exchange (NEE); over vegetation at dark conditions can be approximated as ecosystem respiration (R_{eco}); and on bare soil at dark conditions can be approximated as soil respiration (R_{soil}). Closing time of the chamber was always 5 minutes, and previous to each measurement we performed ambient measurements during 4 minutes, to circulate fresh air into the system and to obtain ambient concentration data that was used in further data quality checks.

The analyser was used in the cross-interference and the water-interference modes, to take into account the cross interference between gases and water vapour (Iqbal et al., 2013). However, a preliminary examination of the CH_4 concentration data revealed a remaining water vapour interference at high concentrations (>12 ppb). For correcting that interference, we calculated the slope of the concentration change of CH_4 as a function of water vapour with all the available data. CH_4 concentration values were afterwards lowered by the corresponding factor, proportionally to the change in water vapour since the previous measurement and the CH_4 ~ water vapour slope (Tirol-Padre et al., 2014). CH_4 data that needed to be corrected represented a 37% of total CH_4 data.

Prior to flux calculation, mixing ratios were converted to molar densities (mol m^{-3}) using the ideal gas law. Flux estimation was performed by a linear fitting during the closing time of the chamber (Equation 5.1):

$$F = \frac{V \cdot dC}{A \cdot dt}$$

(Equation 5.1)

Here *F* is the flux in $mols^{-1}m^{-2}$, *V* is the chamber volume in (0.019 m^3), *A* the sampling surface (0.049 m^2) and *dC/dt* is the gas concentration (mol m^{-3}) change versus time (s).

Fluxes from the atmosphere to the biosphere were considered negative, and fluxes from the biosphere to the atmosphere were considered positive, according the micrometeorological sign convention (Aubinet et al., 2012b).

Finally, we checked data quality based on the flux detection limit, calculated from the standard deviation of the ambient concentration observed over the measuring time, and on linearity (R^2) of the concentration change during the chamber closure. Fluxes with an adjusted $R^2 < 0.5$, in the case of the CO_2 and with an adjusted $R^2 < 0.2$ for CH_4 and N_2O and/or below the detection limit were excluded from further analysis (Debouk et al., 2018). However, considering or not fluxes below detection limit remains controversial. While some studies consider fluxes below detection limit unreliable (Langford et al., 2010; Porter et al., 1988), others regard these data as representative of very low fluxes (Croghan and Egeghy, 1990; Helsel, 1990). Since our general goal was to understand mechanisms affecting GHG exchange in dehesas ecosystems, rather than quantifying absolute fluxes, fluxes below detection limit were considered not reliable for this purpose. Retained data after quality filtering represented a 97% in the case of CO_2, a 60% in the case of CH_4 and a 30% in the case of N_2O.

Afterwards, data CO_2 gaps were filled with the average value of the given treatment level and measuring conditions (light or dark and vegetation or soil). CH_4 and N_2O were averaged considering together all measuring conditions (vegetation light and dark and soil dark) and gaps were filled with the mean value of the given treatment level.

Ancillary meteorological variables were recorded to calculate and model GHG fluxes, and to characterize microclimatic sampling conditions, including photosynthetically active radiation (PAR) outside the chamber (AccuPAR model LP-80 PAR/LAI ceptometer, Decagon Devices, Inc. Washington, USA); air temperature (T_a) inside and outside the chamber (multi-logger thermometer, TMD-56, Amprove, Washington, USA); soil temperature (T_s) 1-10 cm; and soil water content (SWC, gravimetric method, Section 5.3.4).

5.3.3 Vegetation sampling

After GHG measurements were done, we harvested biomass at ground level at each sampling point. Thereafter, in the laboratory, we separated aboveground biomass (AGB) from litter (dead plant material detached from the herbaceous vegetation and tree leaves on soil surface). In addition, we separated AGB into plant species and PFT including forbs, grasses and legumes. Vegetation was oven dried at 60ºC until constant weight.

5.3.4 Belowground biomass sampling and soil water content determination

Two soil cores of 9 cm^2 surface and 0-10 cm depth were extracted at each sampling point. In the laboratory one of the cores was washed and filtered with a 0.2 mm pore size strainer to obtain belowground biomass (BGB). The second core was used for SWC determination by gravimetric method, as the difference between fresh and dry soil weight. Both, BGB and soil samples were oven dried at 60ºC until constant weight.

5.3.5 Data analysis

5.3.5.1 Microclimatic sampling conditions

All data analyses were performed using R software (R core Team, 2015). Microclimatic conditions created by the canopy at the sampling moment, considering PAR, T_s and SWC, were compared to the open grassland at each season and plot. To assess the influence of the studied treatments (season, plot and canopy) on each environmental variable (PAR, T_s and SWC) we run linear models with season, plot and canopy as predictors. Final models were selected by a stepwise procedure based on the Akaike information criterion (AIC), using the stepAIC function, MASS package (Venables and Ripley 2002).

5.3.5.2 Structure, composition and diversity of the herbaceous layer

Vegetation of the herbaceous layer was described in terms of structure (AGB, litter and BGB); PFT (forbs, grasses and legumes) composition; and diversity indexes including species richness (SR), defined as the number of species per sample, and evenness (Equation 5.2, Kirwan et al., 2007), per season, plot and canopy. The evenness index has been defined as a measure of the distribution of the relative abundance of species or PFT, and lies between 0, for mono-specific plots, and 1 when all species or PFT are equally represented (Equation 5.2, Kirwan et al., 2007).

$$Evenness = \frac{2S}{S-1}\sum_{i<j} P_i P_j$$

(Equation 5.2)

Here *S* is number of species or PFT in the community matrix and P_iP_j the pairwise interactions between species or PFT. Hence, we calculated the evenness index based on species (species evenness) and based on PFT (PFT evenness). Afterwards, to assess the influence of the studied treatments (season, plot and canopy) on vegetation structure (AGB, litter and BGB), PFT composition (forbs, grasses and legumes), SR and species evenness we modelled each of these variables using season, plot and canopy as predictors. Final models were selected by a stepwise procedure (Venables and Ripley 2002).

On the other hand, to describe the influence of season, plot and canopy on species composition, we performed a canonical correspondence analysis (CCA) to represent the community in a given number of dimensions (Sandau et al., 2014). CCA analysis was performed on species absolute abundance as function of season, plot and canopy, using the cca function of the vegan package (Oksanen et al., 2018). Significance of the CCA terms (season, plot and canopy) and significance of the CCA axes were both tested using the anova.cca function, also of the vegan package (Oksanen et al., 2018). Afterwards, mean values and standard errors of the first three significant ($p < 0.001$) axes were

calculated for each level of the terms included as predictors (season, plot and canopy). Finally, significant CCA axes were included as predictors of GHG exchange, as a proxy of the influence of the species compositional matrix (Section 5.3.5.3).

5.3.5.3 Greenhouse gas exchange modelling

To assess main GHG (CO_2, CH_4 and N_2O) drivers, especially focussing on the role of the dehesa structure (tree – open grassland) and on the influence of the herbaceous layer, in terms of composition and diversity, we used two different approaches: (a) one oriented to PFT, and (b) one oriented to species.

In the first case, we run diversity-interaction models to investigate the influence of PFT (hereafter termed as diversity-interaction model PFT-oriented), following the methodology proposed by Kirwan et al., (2009). The modelling compares a null model, in which the response variable is not affected by diversity and/or composition, to models that address diversity and composition at different levels. In our study, we compared the null model (Equation 5.3), in which the corresponding GHG depended only on: treatment variables, including plot, season and canopy; environmental variables, including PAR (μmol photons m^{-2} s^{-1}), temperature (T, ºC) and SWC (fraction); and structural components of the herbaceous layer, including AGB, litter and BGB (g DW m^{-2}); to models that included PFT composition and diversity in different ways: (1) PFT identity model, which includes PFT identity effects (Equation 5.4); (2) PFT average interaction model, which includes PFT identity effects, plus PFT evenness, as an average interaction term (Equation 5.5); and (3) PFT specific interactions model, which includes specific interactions between PFT in addition to the identity effects (Equation 5.6).

$$GHG = \beta_{Plot}Plot + \beta_{Season}Season * \beta_{Canopy}Canopy + \beta_T T + \beta_{SWC}SWC + \beta_{PAR}PAR + \beta_{AGB}AGB + \beta_{litter}Litter + \beta_{BGB}BGB + \varepsilon$$

(Equation 5.3. Null model)

$$GHG = Null\ model + \beta_F P_F + \beta_G P_G + \beta_L P_L + \varepsilon$$

(Equation 5.4. PFT identity model)

$$GHG = Null\ model + \beta_F P_F + \beta_G P_G + \beta_L P_L + PFT\ evenness + \varepsilon$$

(Equation 5.5. PFT average interaction model)

$$GHG = Null\ model + \beta_F P_F + \beta_G P_G + \beta_L P_L + \beta_{FG} P_F P_G + \beta_{FL} P_F P_L + \beta_{GL} P_G P_L + \beta_{FGL} P_F P_G P_L + \varepsilon$$

(Equation 5.6. PFT specific interaction model)

Here *P* indicates the proportion of the given PFT and the sub-index *F* indicates forbs, *G* grasses and *L* legumes respectively. The models were run without intercept in order to test the effect of all three PFT at the same time.

Analogously, we addressed the influence of species composition on GHG fluxes running linear models (hereafter termed as diversity-interaction model-species oriented) comparing the null model (Equation 5.3) to models that included: (1) the three first significant axes of the CCA as a proxy of species composition effects; and (2) diversity indices, including SR (nº species sample^{-1}) and species evenness (dimensionless). Unlike in the diversity-interaction model PFT-oriented, the diversity-interaction model-species oriented was run with intercept, as it did not include proportions as explicative terms.

Models were compared at each step of modelling by ANOVAs to test significant differences between models in both modelling approaches. The most explicative and parsimonious model of each GHG is shown and discussed.

5.4 Results

5.4.1 Microclimatic conditions

As expected, microclimatic conditions, including PAR, T_s and SWC varied markedly depending on season and canopy (Figure 5.1). PAR (Figure 5.1.A) and T_s were (Figure 5.1.B) lower in autumn than in spring (season effect, Table S5.1) and lower under the canopy than in the open grassland (canopy effect, Table S5.1), being this difference less marked in autumn than in spring (season x canopy effect, Table S5.1). SWC (Figure 5.1.C) showed the lowest values in the DN-pinea plot (plot DN-pinea effect, t = −2.75, p = 0.008, Table S5.1), both in spring and autumn. SWC was also higher under the canopy than in the open grassland (canopy effect, t = 3.15, p = 0.002, Table S5.1).

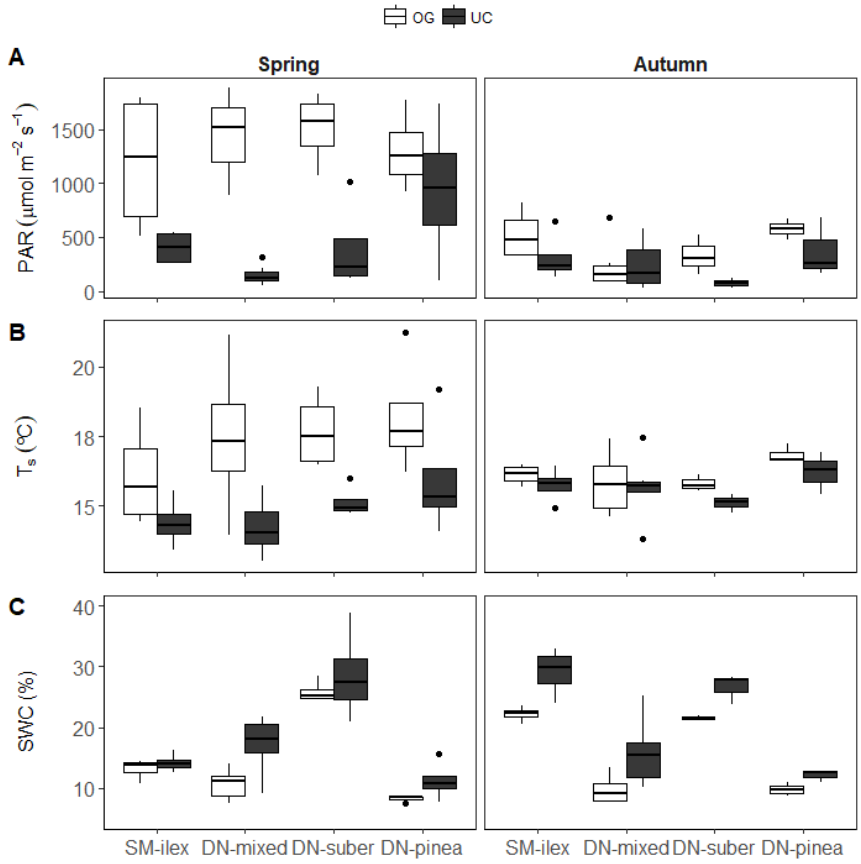

Figure 5.1. Microclimatic sampling conditions per season, plot and canopy: open grassland (OG) and under the canopy (UC). (A) Photosynthetically active radiation (PAR); (B) soil temperature (T_s) and; (C) soil water content (SWC). Boxplot's midline indicates the median; upper and lower limits of the box indicate the third and first quartile; whiskers extend up to 1.5 times the interquartile range from the top/bottom of the respective box, and points represent data beyond the whiskers.

5.4.2 Structure and composition of the herbaceous layer

The vegetation of the herbaceus layer changed among seasons, plots, and canopy (Figure 5.2). AGB decreased in autumn compared to spring (season effect, $t = -10.76$, $p < 0.001$, Table 5.1), and DN plots had less AGB than the SM-ilex plot (plot effects, Table 5.1). Also, AGB was lower under the canopy than in the open grassland (canopy effect, $t = -1.90$, $p = 0.06$, Table 5.1). Litter was markedly higher under the canopy than in the open grassland (canopy effect, $t = 7.98$, $p < 0.001$, Table 2), but this difference between under the canopy and open grassland almost desapeared in autumn (season x canopy effect, $t = -4.99$, $p < 0.001$, Table 5.1). BGB was quite variable among treatments (Figure 5.2), and neither season, plot or canopy explained its variability. Linear modelling on BGB is therefore not shown.

PFT composition also changed among seasons, plots, and canopy (Figure 5.2). Forbs biomass decreased in autumn compared to spring (season effect, $t = -8.73$, $p < 0.001$, Table 5.1), and forbs biomass was lower in all DN plots than in the SM-ilex plot (DN plots effects, Table 5.1). Also, forbs biomass decreased under the canopy compared to the open grassland (canopy effect, $t = -3.19$, $p = 0.002$, Table 5.1). Grasses biomass was also lower in all DN plots compared to the SM-ilex plot (significant DN plots effects, Table 5.1); but unlike forbs, grasses increased under the canopy compared to the open grassland (canopy effect, $t = 4.16$, $p < 0.001$, Table 5.1). The canopy effect on grasses was lower in autumn than in spring (season x canopy effect, $t = -2.33$, $p = 0.02$, Table 5.1), with similar biomass of grasses under the canopy and in the open grassland in autumn (Figure 5.2). Finally, legumes appeared mostly in spring and in the open grassland (season x canopy effect, $t = 3.45$, $p < 0.001$, Table 5.1, and Figure 5.2).

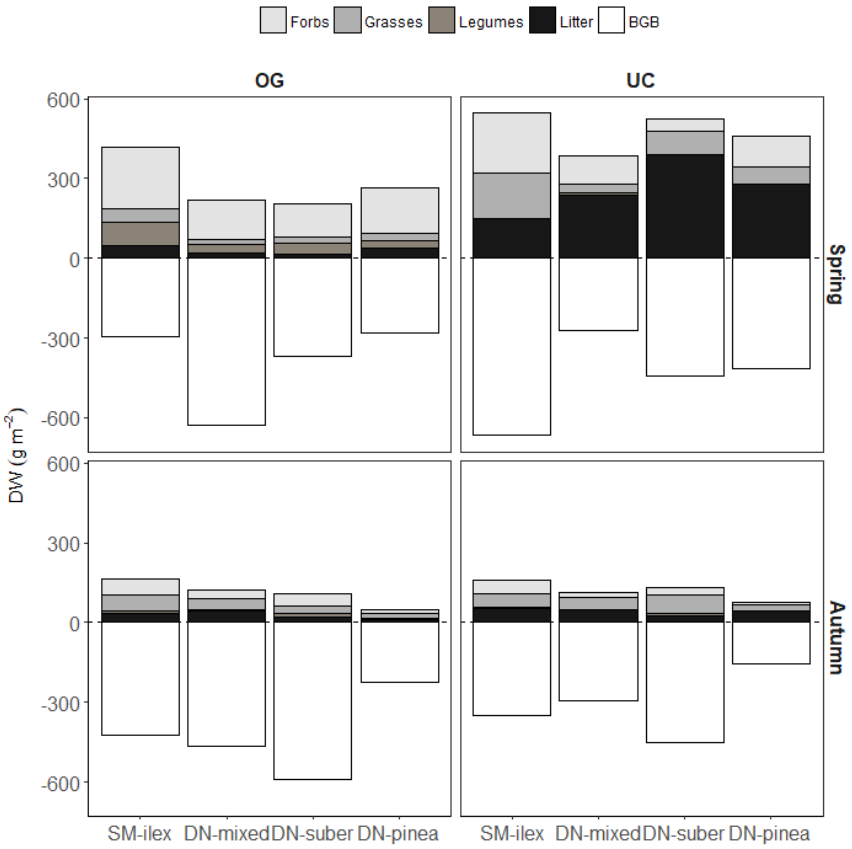

Figure 5.2. Mean biomass of forbs, grasses, legumes, litter and belowground biomass (BGB) per season, plot and canopy: open grassland (OG) and under the canopy (UC). The sum of all plant functional types biomass equates aboveground biomass.

Table 5.1. Linear model results. Aboveground biomass (AGB), litter and plant functional type (PFT) biomass: forbs, grasses and legumes, as function of season, plot and canopy. Season with spring as reference level, plot with SM-ilex as reference level, and canopy with open grassland (OG) as reference level. Estimates of the explanatory variables (Est.), standard error (SE), t and p-value.

	Vegetation structure (g DW m^{-2})								**PFT composition (g DW m^{-2})**											
	AGB				**Litter**				**Forbs**				**Grasses**				**Legumes**			
	Est.	**SE**	**t**	**p**	**Est.**	**SE**	**t**	**p**	**Est.**	**SE**	**t**	**p**	**Est.**	**SE**	**t**	**p**	**Est.**	**SE**	**t**	**p**
(Intercept)	336	17	19.84	< 0.001	28	20	1.41	0.2	224	15	15.36	< 0.001	64	11	5.70	< 0.001	55	7	8.11	< 0.001
Season	−142	13	−10.76	< 0.001	3	30	0.09	0.1	−131	15	−8.73	< 0.001	11	12	0.93	0.4	−36	7	−5.20	< 0.001
Plot DN-mixed	−133	17	−7.62	< 0.001					−68	14	−4.79	< 0.001	−51	11	−4.64	< 0.001	−14	7	−2.06	0.04
Plot DN-suber	−129	21	−6.20	< 0.001					−87	17	−5.12	< 0.001	−36	13	−2.73	0.008	−11	8	−1.36	0.2
Plot DN-pinea	−130	21	−6.28	< 0.001					−66	17	−3.92	< 0.001	−48	13	−3.65	0.0005	−19	8	−2.36	0.02
Canopy	−25	13	−1.90	0.06	232	29	7.98	< 0.001	−46	14	−3.19	0.002	46	11	4.16	< 0.001	−40	7	−5.99	< 0.001
Season x canopy					−218	44	−4.99	< 0.001	34	22	1.59	0.1	−39	17	−2.33	0.02	35	10	3.45	< 0.001
R^2_{Adj}	0.70			< 0.001	0.53			< 0.001	0.66			< 0.001	0.33			< 0.001	0.41			< 0.001

Species evenness (Figure 5.3.A) was only dependent on season, being lower in autumn than in spring (season effect, t = −3.21, p = 0.002, Table 5.2). Species richness (SR, Figure 5.3.B) was lower in autumn than in spring (season effect, t = −3.28, p = 0.002, Table 5.2); DN-pinea plot had the lowest SR (plot DN-pinea effect, t = −2.29, p = 0.02, Table 5.2) and SR was lower under the canopy than in the open grassland (canopy effect, t = −3.26, p = 0.002, Table 5.2). Finally, DN-suber hilighted with the highest SR in the open grassland both in spring and autumn (Figure 5.3.B).

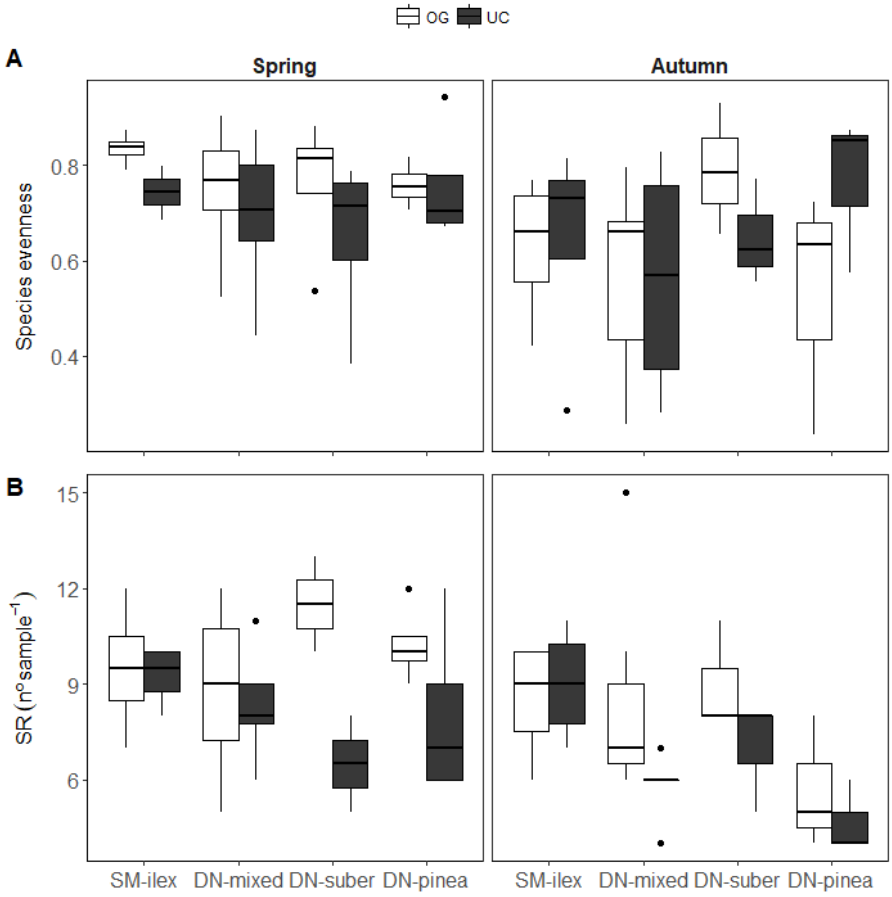

Figure 5.3. (A) Species evenness and (B) species richness (SR) per season, plot and canopy: open grassland (OG) and under the canopy (UC). Boxplot's midline indicates the median; upper and lower limits of the box indicate the third and first quartile; whiskers extend up to 1.5 times the interquartile range from the top/bottom of the respective box, and points represent data beyond the whiskers.

Table 5.2. Linear model results. Species evenness and species richness (SR) as function of season, plot and canopy. Season with spring as reference level, plot with SM-ilex as reference level, and canopy with open grassland (OG) as reference level Estimates of the explanatory variables (Est.), standard error (SE), t and p-value.

	Species evenness (dimensionless)				Species richness (SR, nº species sample^{-1})			
	Est.	**SE**	**t**	**p**	**Est.**	**SE**	**t**	**p**
Intercept	0.74	0.02	30.59	< 0.001	10.6	0.6	17.12	< 0.001
Season	−0.12	0.04	−3.21	0.002	−1.6	0.5	−3.28	0.002
Plot DN-mixed					−1.3	0.6	−1.97	0.05
Plot DN-suber					−0.6	0.8	−0.79	0.4
Plot DN-pinea					−1.7	0.8	−2.29	0.02
Canopy					−1.6	0.5	−3.26	0.002
R^2_{Adj}	0.11			0.002	0.23			< 0.001

CCA of species composition had a constrained inertia of 1.275 over a total of 7.423, representing a 17.2% of explained variance, with season, plot, and canopy as explanatory terms. The anova.cca by terms showed that all the terms included in the CCA (plot, season and canopy) were significant ($p < 0.001$), and the anova.cca by axes showed that the first three axes, out of five, were also significant ($p < 0.001$).

The first CCA axis (CCA1, 35% of total explained variance) captured mainly diffrences in species composition between spring and autumn (CCA1, Figure 5.4.A and Figure 5.4.B). The second axis (CCA2, 26% of total explaiend variance) explained mainy diffrences between plots in their species composition: on one side SM-ilex and DN-suber and on the other side DN-mixed and DN-pinea plots (Figure 5.4.A). Finally, the the third axis (CCA3, 23% of total explaiend variance), captured differences in species composition between under the canopy and the open grassland (CCA3, Figure 5.4.B).

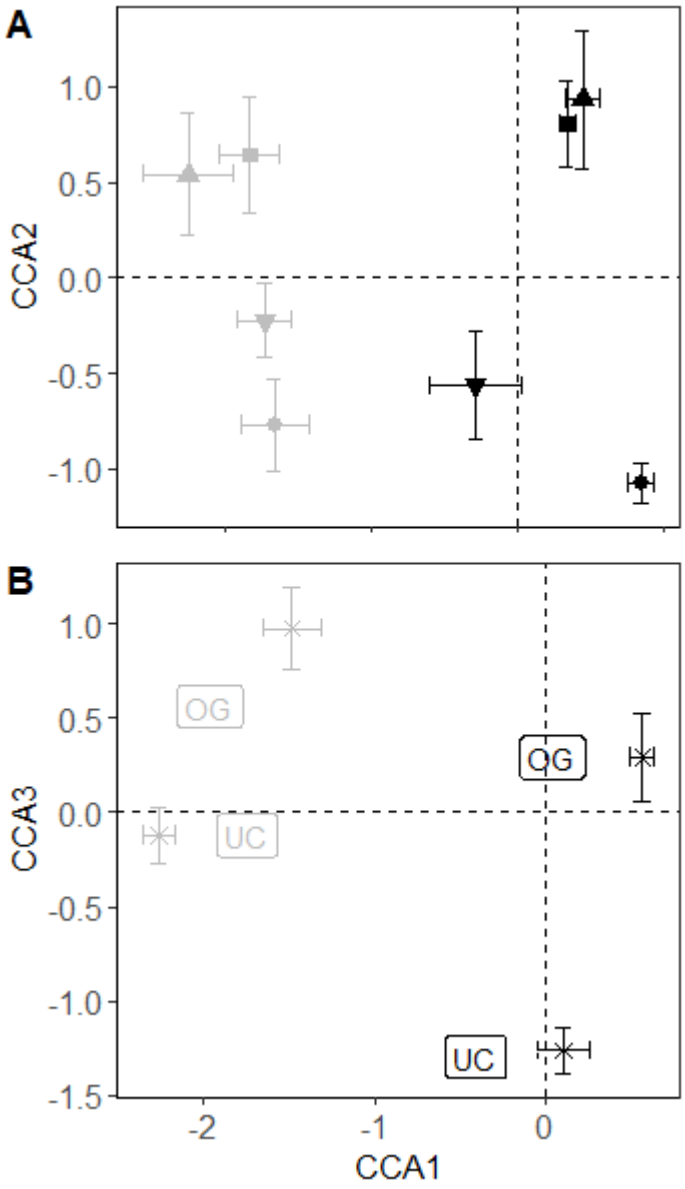

Figure 5.4. Canonical correspondence analysis (CCA): (A) axis 1 (CCA1) vs. axis 2 (CCA2) per season (black: spring, grey: autumn) and plot (● SM-ilex, ■ DN-mixed, ▼ DN-suber, ▲DN-pinea); and (B) CCA1 vs. axis 3 (CCA3) per season and canopy (OG: open grassland, UC: under the canopy). Mean values ± standard error.

5.4.3 Greenhouse gas exchange

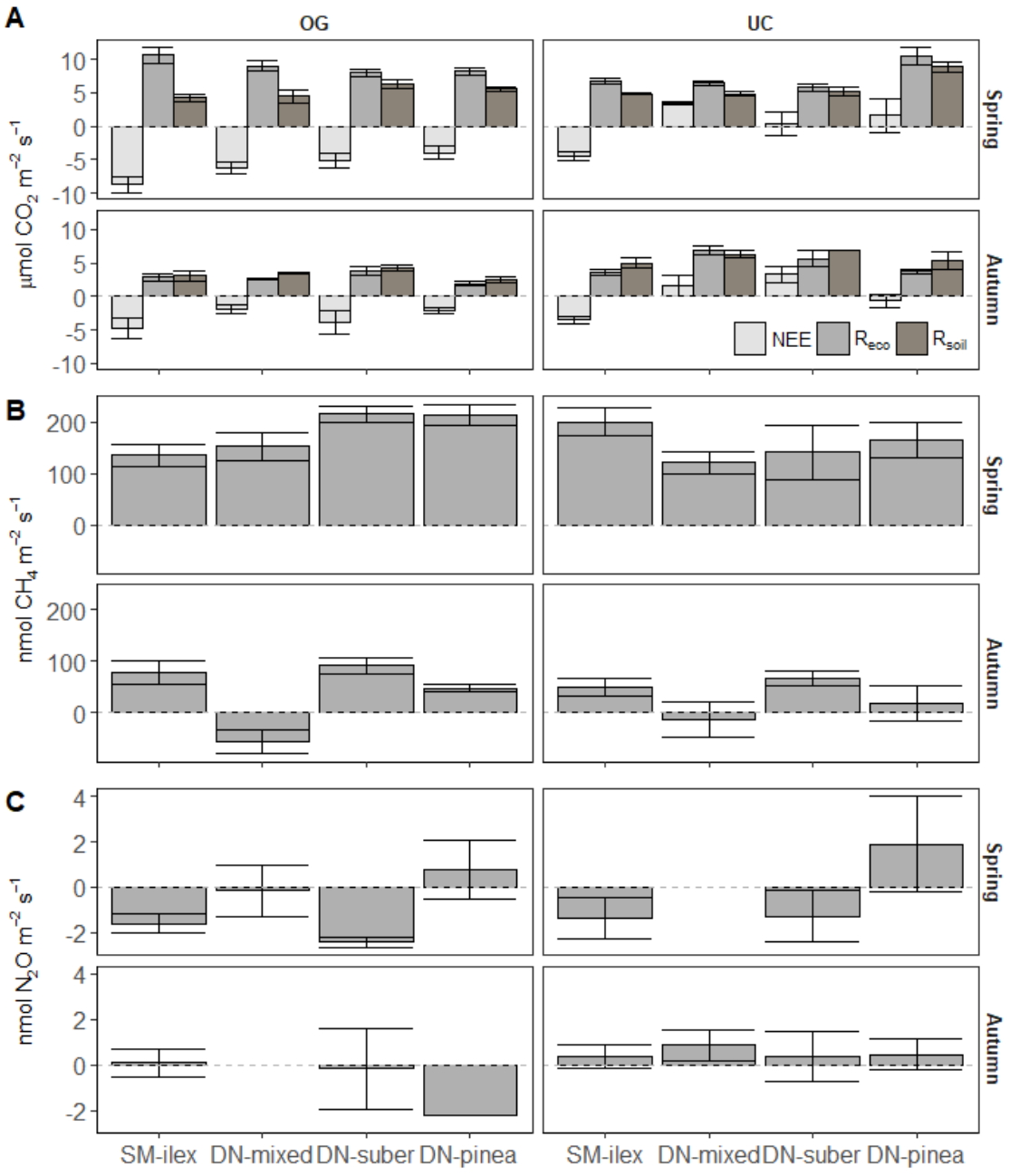

Figure 5.5. Greenhouse gas exchange per season, plot and canopy: open grassland (OG) and under the canopy (UC). (A) Net ecosystem CO_2 exchange (NEE), ecosystem respiration (R_{eco}) and soil respiration (R_{soil}); (B) CH_4 and (C) N_2O exchange. Mean ± standard error.

5.4.3.1 CO_2 exchange

CO_2 uptake was similar in spring and autumn (NEE, Figure 5.5.A), while CO_2 emissions (R_{eco} and R_{soil}, Figure 5.5.A) were lower in autumn compared to spring (season effect, Table 5.3 - Table 5.4). The open grassland of the SM-ilex plot showed the highest net CO_2 uptake rates (NEE, Figure 5.5.A) and the highest R_{eco} rates (Figure 5.5.A), while under the canopy, DN-pinea was the plot with the highest CO_2 emissions (R_{eco} and R_{soil}, Figure 5.5.A).

Thus, canopy itself had a strong influence over CO_2 fluxes. NEE under the canopy was generally dominated by CO_2 emissions (canopy effect, Table 5.3 - Table 5.4), NEE being strongly driven by PAR (PAR effect, Table 5.3 - Table 5.4). The exception was the SM-ilex plot, where there was CO_2 uptake under the canopy, instead of emissions (NEE, Figure 5.5.A). On the other hand, under the canopy decreased R_{eco} rates in spring (canopy effect, Table 5.3 - Table 5.4) compared to the open grassland, but R_{eco} increased under the canopy in autumn (season x canopy effect, Table 5.3 - Table 5.4). Finally, canopy enhanced R_{soil} (canopy effect, Table 5.3 - Table 5.4), especially in autumn (season x canopy effect, Table 5.3 - Table 5.4), R_{soil} being also enhanced by T_a (T_a, effect, Table 5.3 - Table 5.4).

PFT composition also drove CO_2 fluxes. The diversity-interaction modelling PFT-oriented (Table 5.3) showed that the most explicative and parsimonious model was a PFT specific interaction model (Equation 5.6), with legumes enhancing net CO_2 uptake rates (legumes effect, $t = -3.97$, $p < 0.001$, Table 5.3 and Figure 5.6), and slightly lower net uptake rates with the addition of forbs (forbs x legumes effect, $t = 3.84$, $p < 0.001$, Table 5.3) and grasses (grasses x legumes effect, $t = 4.07$, $p < 0.001$, Table 5.3) in the mixture. Note that predicted NEE (Figure 5.6) was modelled with a maximum proportion of legumes of 50%, according to the legumes proportion observed in the field (Figure 5.2). A higher proportion of legumes would not be realistic in the studied dehesas.

In addition, the diversity-interaction model-species oriented (Table 5.4) showed that R_{eco} was influenced by vegetation structure, BGB increasing R_{eco} (BGB effect, t = 2.63, p = 0.01, Table 5.4), and by species composition, with a significant effect of the second and the third CCA axis (CCA2 and CCA3 effects, Table 5.4). Finally, R_{soil} was also enhanced by BGB (BGB effect, t = 2.77, p = 0.007, Table 5.4) and by species richness (SR effect, t = 2.97, p = 0.004, Table 5.4).

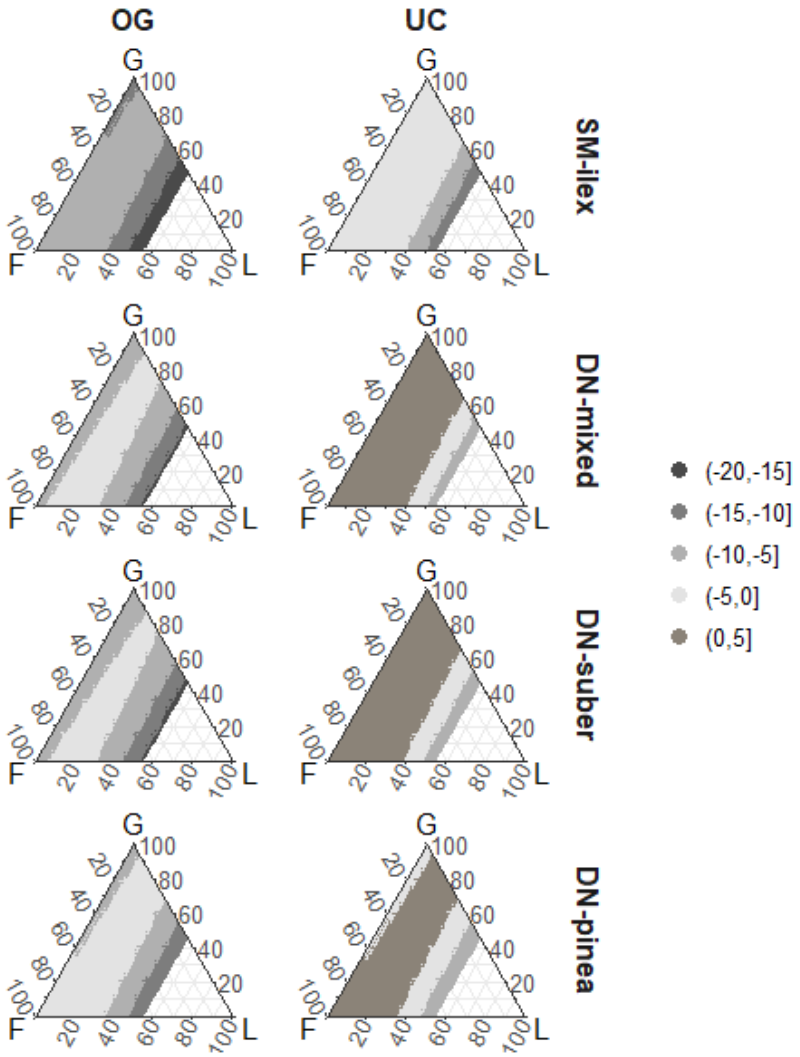

Figure 5.6. Predicted net ecosystem exchange (NEE, μmol CO_2 m^{-2} s^{-1}) according to the diversity-interaction model PFT-oriented (Table 5.3, environmental conditions set as the mean of the given treatment level). *F* indicates forbs, *G* grasses and *L* legumes. Negative NEE values indicate net CO_2 uptake, and positive values indicate emissions.

Table 5.3. Diversity-interaction model PFT-oriented results. Net ecosystem exchange (NEE), ecosystem respiration (R_{eco}) and soil respiration (R_{soil}) as function of season, plot, canopy, photosynthetically active radiation (PAR), air temperature (T_a), aboveground biomass (AGB), belowground biomass (BGB) and plant functional type (forbs, grasses and legumes) proportions. Season with spring as reference level, and canopy with open grassland (OG) as reference level. Estimates of the explanatory variables (Est.), standard error (SE), t and p-value.

Diversity-interaction model PFT-oriented												
CO_2 flux (µmol m^{-2} s^{-1})												
	NEE				R_{eco}				R_{soil}			
	Est.	SE	t	p	Est.	SE	t	p	Est.	SE	t	p
Season					−6.2	0.6	−9.88	< 0.001	−1.3	0.5	−2.56	0.01
Plot SM-ilex	−6	3	−1.81	0.07	8.9	0.6	14.60	< 0.001	0	1	0.35	0.7
Plot DN-mixed	−2	3	−0.54	0.6	9.0	0.5	18.82	< 0.001	1	1	0.55	0.6
Plot DN-suber	−2	3	−0.57	0.6	8.6	0.6	13.74	< 0.001	2	1	1.33	0.2
Plot DN-pinea	−1	3	−0.38	0.7	9.2	0.6	14.69	< 0.001	1	1	0.65	0.5
Canopy	4	0.7	5.58	< 0.001	−1.8	0.6	−2.98	0.004	1.1	0.5	2.10	0.04
Season x canopy					4.3	0.9	4.73	< 0.001	1.8	0.7	2.40	0.02
PAR (µmol photons m^{-2} s^{-1})	−0.003	0.001	−4.58	< 0.001								
T_a (ºC)									0.15	0.05	3.06	0.003
BGB (g DW m^{-2})									0.0015	0.0007	2.21	0.03
Forbs (fraction)	0	3	0.15	0.9								
Grasses (fraction)	−1	3	−0.22	< 0.001								
Legumes (fraction)	−67	17	−3.97	< 0.001								
Forbs x legumes (fraction)	97	25	3.84	< 0.001								
Grasses x legumes (fraction)	96	24	4.07	< 0.001								

Table 5.4. Diversity-interaction model species-oriented results. Net ecosystem exchange (NEE), ecosystem respiration (R_{eco}) and soil respiration (R_{soil}) as function of season, plot, canopy, photosynthetically active radiation (PAR), air temperature (T_a), aboveground biomass (AGB), belowground biomass (BGB), species richness (SR) and canonical correspondence analysis axes 1-3 (CCA1-CCA3). Season with spring as reference level, plot with SM-ilex as reference level, and canopy with open grassland (OG) as reference level. Estimates of the explanatory variables (Est.), standard error (SE), t and p-value.

Diversity-interaction model species-oriented												
CO_2 flux (µmol m^{-2} s^{-1})												
	NEE				R_{eco}				R_{soil}			
	Est.	SE	t	p	Est.	SE	t	p	Est.	SE	t	p
Intercept	−5.3	0.9	−6.06	< 0.001	3	2	1.81	0.08	−2	1	−1.57	0.1
Season					−5	1	−4.61	< 0.001	−0.9	0.5	−1.75	0.09
Plot DN-mixed	4.2	0.8	5.54	< 0.001	2.0	0.9	2.31	0.02	0.6	0.5	1.24	0.2
Plot DN-suber	3.9	0.9	4.31	< 0.001	0.5	0.8	0.65	0.5	1.4	0.6	2.44	0.02
Plot DN-pinea	4.8	0.9	5.20	< 0.001	2.2	1.0	2.27	0.03	1.2	0.7	1.70	0.09
Canopy	3.5	0.7	5.23	< 0.001	−0.6	0.9	−0.65	0.5	1.5	0.5	2.98	0.004
Season x canopy					3.9	0.9	4.47	< 0.001	1.8	0.7	2.51	0.01
PAR (µmol photons m^{-2} s^{-1})	−0.003	0.001	−5.11	< 0.001								
T_a (ºC)					0.14	0.07	1.99	0.05	0.14	0.05	2.89	0.005
BGB (g DW m^{-2})					0.0022	0.0008	2.63	0.01	0.0018	0.0007	2.77	0.007
SR (nº species sample $^{-1}$)									0.26	0.09	2.97	0.004
CCA1					0.8	0.5	1.68	0.10				
CCA2					−0.7	0.3	−2.11	0.04				
CCA3					0.6	0.3	2.13	0.04				
R^2_{Adj}	0.66			< 0.001	0.63			< 0.001	0.43			< 0.001

5.4.3.2 CH_4 and N_2O exchange

CH_4 emissions were mainly enhanced by T_s (T_s effect, Table 5.5 - Table 5.6), being lower in autumn than in spring (season effect, Table 5.5 - Table 5.6). In addition, CH_4 emissions decreased with the presence of litter (litter effect, Table 5.5 - Table 5.6).

N_2O showed an overall tendency to uptake, except under the canopy in autumn (canopy x season effect, t = 2.25, p = 0.03, Table 5.6) and under *P. pinea* canopy in spring, where there were N_2O emissions (Figure 5.5). Moreover, vegetation composition and structure influenced N_2O exchange. The diversity-interaction model PFT-oriented (Table 5.5) showed that the most explicative and parsimonious model was a PFT identity model (Equation 5.4), with legumes enhancing N_2O emissions (legumes effect, t = 2.49, p = 0.02, Table 5.5 and Figure 5.7). Species composition influenced over N_2O exchange, with a significant effect of the first and the second CCA axis (CCA1 and CCA2 effects, Table 5.6). Finally, litter and BGB (Table 5.5 - Table 5.6) also enhanced N_2O emissions.

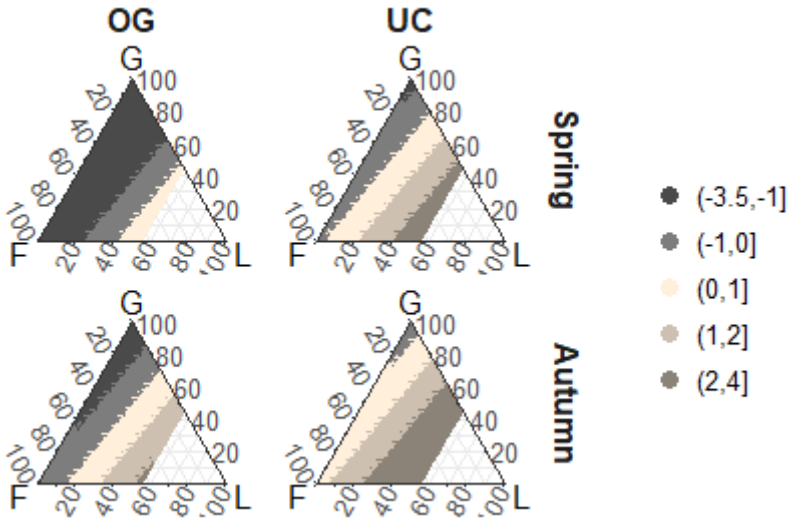

Figure 5.7. Predicted N_2O exchange (nmol m^{-2} s^{-1}) according to the diversity-interaction model PFT-oriented (Table 5.5, environmental conditions and litter set as the mean of the given treatment level). *F* indicates forbs, *G* grasses and *L* legumes. Negative values indicate N_2O uptake, and positive values indicate emissions.

Table 5.5. Diversity-interaction model PFT-oriented results. CH_4 and N_2O exchange as function of as function of season, plot, canopy, soil temperature (T_s), soil water content (SWC), litter, belowground biomass (BGB) and plant functional type (forbs, grasses and legumes) proportions. Season with spring as reference level and canopy with open grassland (OG) as reference level. Estimates of the explanatory variables (Est.), standard error (SE), t and p-value.

	Diversity-interaction model PFT-oriented							
	CH_4 (nmol m^{-2} s^{-1})				**N_2O (nmol m^{-2} s^{-1})**			
	Est.	**SE**	**t**	**p**	**Est.**	**SE**	**t**	**p**
Season spring					−13	5	−2.73	0.008
Season autumn	−150	15	−9.68	< 0.001	−11	5	−2.30	0.03
Plot SM-ilex	−24	81	−0.30	0.8				
Plot DN-mixed	−83	81	−1.03	0.3				
Plot DN-suber	−22	85	−0.26	0.8				
Plot DN-pinea	−28	85	−0.33	0.7				
Canopy					2.1	0.8	2.68	0.010
T_s (ºC)	13	5	2.72	0.008	0.4	0.2	2.44	0.02
SWC (fraction)	1.4	0.8	1.83	0.07	−0.05	0.03	−2.00	0.05
Litter (g DW m^{-2})	−0.1	0.1	−1.89	0.06	0.007	0.003	2.84	0.006
BGB (g DW m^{-2})					0.002	0.001	1.75	0.09
Forbs (fraction)					3	3	1.02	0.3
Grasses (fraction)					2	3	0.47	0.6
Legumes (fraction)					10	4	2.49	0.02

Table 5.6. Diversity-interaction model species-oriented results. CH_4 and N_2O exchange as function of season, plot, canopy, photosynthetically active radiation (PAR), soil temperature (T_s), aboveground biomass (AGB), belowground biomass (BGB), species richness (SR) and canonical correspondence analysis axes 1-2 (CCA1-CCA2). Season with spring as reference level, plot with SM-ilex as reference level, and canopy with open grassland (OG) as reference level. Estimates of the explanatory variables (Est.), standard error (SE), t and p-value.

	Diversity-interaction models species-oriented							
	CH_4 (nmol m^{-2} s^{-1})				**N_2O (nmol m^{-2} s^{-1})**			
	Est.	**SE**	**t**	**p**	**Est.**	**SE**	**t**	**p**
(Intercept)	35	85	0.41	0.7	−9	4	−2.52	0.01
Season	−160	16	−9.86	< 0.001	3	2	2.22	0.03
Plot DN-mixed	−65	19	−3.46	< 0.001				
Plot DN-suber	2	22	0.08	0.9				
Plot DN-pinea	−6	23	−0.25	0.8				
Canopy					0	1	−0.02	1.0
Season x canopy					3	1	2.25	0.03
T_s (ºC)	13	5	2.89	0.005	0.3	0.2	1.70	0.09
SWC (fraction)	1.3	0.7	1.73	0.09				
Litter (g DW m^{-2})	−0.12	0.06	−2.08	0.04	0.011	0.003	3.30	0.002
BGB (g DW m^{-2})					0.002	0.001	2.34	0.02
SR (nº species sample $^{-1}$)	−85	45	−1.87	0.07				
CCA1					1.3	0.6	2.39	0.02
CCA2					0.6	0.3	2.15	0.04
R^2_{Adj}	0.65			< 0.001	0.24			0.002

5.5 Discussion

Our main goal was to assess the influence of dehesa structure (tree – open grassland), and different tree canopies on the structure and composition of the herbaceous layer, and these in turn on GHG exchange. Therefore, although seasonality was an important driver of vegetation and GHG dynamics, in the following discussion we focus on our main goals, without losing sight on seasonality and its interactions.

5.5.1 Plot and canopy as drivers of the structure and composition of the herbaceous layer

Tree canopies were important drivers of vegetation spatial heterogeneity, both in terms of structure and composition. Overall, AGB tended to decrease under the canopy compared to the open grassland (canopy effect, Table 5.1), especially in spring (Figure 5.2).This AGB reduction could be partly caused by lower light availability under the canopy compared to the open grassland (UC PAR ~−340% in spring and −150% in autumn, Figure 5.1.A), in agreement with similar light constrains on biomass production reported under the canopy in dehesas (Hussain et al., 2009; Seddaiu et al., 2018).

However, several studies have described that although under the canopy there is less light available, usually the canopy in dehesas creates a favourable environment, with increased soil moisture (Holmgren et al., 1997), higher nutrient availability (Gallardo, 2003; Gallardo et al., 2000) and amelioration of extreme temperatures (Marañón et al., 2009), which may result in higher productivity of the herbal layer (Gea-Izquierdo et al., 2009; Moreno et al., 2007). In our study case, under the canopy there was higher SWC (Figure 5.1.C), lower T_s (Figure 5.1.B), and higher soil C and N (Table S5.2); but yet, AGB tended to be lower under the canopy compared to the open grassland (canopy effect, Table 5.1).This fact suggests that light was really a limiting resource under the canopy, but also that some other limiting factors could be influencing.

First, a main limiting factor for AGB production could be the presence of litter, which was considerably higher under the canopy than in the open grassland, essentially in spring (Figure 5.2). Although certainly litter can increase soil organic matter and fertility in long term, increasing productivity; litter accumulation under the canopy was probably limiting AGB production via mulching the soil and/or having an allellopatic effect on some species growth (Marañón et al., 2009).

In addition, the combination of light limitations and litter accumulation could be causing changes in species and PFT composition, especially in spring, with forbs being dominant in the open grassland; grasses being dominant under the canopy, and legumes moslty apearing in the open grassland (Table 5.1). Accordingly, previous studies have also described dominance of grasses under the canopy (Gea-Izquierdo et al., 2009; Olsvig-Whittaker et al., 1992), while the presence of forbs and legumes is limited under the canopy (Gea-Izquierdo et al., 2009; Lopez-Carrasco et al., 2015; Marañón et al., 2009). Species of high light demand are limited in their growth under the canopy, affected by light constrains, litter accumulation, and competition with species tolerant to these conditions (Marañón, 1986; Marañón et al., 2009). Therefore, accumulated litter may influence in different ways on the growth of the different life forms, negatively affecting forbs and legumes — dicotyledons — while not having a negative impact on the growth of grasses — monocotyledons — with dense erect leaves (Barrantes Díaz, 1986; Roldán Ruiz, 1993).

On the other hand, the higher litter input under the canopy most likely increased soil N content (Table S5.2), which could be favouring the growth of grasses. Song et al. (2011) found a similar result, with grasses increasing their biomass at high N availability at the expense of forbs (Song et al., 2011). Moreover, results reported in Section 4.4.4 and 4.4.5 from the same study plots, suggested that there could be differences in N acquisition and use strategies between grasses and forbs. Grasses had generally higher N content and lower $\delta^{15}N$ than forbs (Figure 4.6), especially under the canopy,

suggesting that grasses were able to uptake more N, and therefore discriminate more against ^{15}N than forbs (Robinson, 2001; Yoneyama et al., 2001), and/or uptake a greater amount of symbiotically fixed N. As already discussed in Section 4.5.2, grasses usually have fibrous roots (Pirhofer-Walzl et al., 2012; Schenk and Jackson, 2002; Weaver, 1958), trait that may be facilitating N absorption from the most superficial soil layers and from symbiotically fixed N sources (Pirhofer-Walzl et al., 2012). These differences in the N acquisition and use could represent an important competitive advantage for grasses, displacing other species under the canopy, fact that also agrees with the lower species richness (SR) observed under the canopy in comparison to the open grassland (canopy effect, Table 5.2).

Competition for water resources between species of the herbaceous layer and trees could be also influencing grassland structure and composition, especially in the most arid dehesas (Gea-Izquierdo et al., 2009; Moreno, 2008). In our case, the DN location was drier than SM (higher temperatures, lower precipitation and more sandy soils, Section 4.3.1), and although the SWC under the canopy was always higher than in the open grassland (Figure 5.1.C), competition for water resources could be limiting in the DN location. In fact, AGB decreased under the canopy in all DN plots, while the canopy had a neutral effect on the AGB of SM-ilex plot (Figure 5.2). In agreement, Gea-Izquierdo et al., (2009) found that plants could only profit from the increase in soil fertility mediated by the canopy without water stress, the canopy effect being dependent on water availability (Gea-Izquierdo et al., 2009).

Species diversity and composition was also mediated by the tree – open grassland structure. Species richness (SR) decreased under the canopy compared to the open grassland (canopy effect, Table 5.2), in agreement with pervious SR inventories in dehesa ecosystems (Lopez-Carrasco et al., 2015; Marañón et al., 2009; Olsvig-Whittaker et al., 1992; Rossetti et al., 2015). Same conditions that were decreasing AGB production under the canopy, including lower light availability, higher litter input and

competition between species, could also be lowering SR (Marañón, 1986; Marañón et al., 2009; Marañon and Bartolomé, 1993). In addition, the higher SWC (Figure 5.1.C) and higher soil N content (Table S5.2) under the canopy, could be enhancing the growing of some dominant species (mostly grasses) at the expense of less competitive species (Rice and Nagy, 2000). This agrees with the observed tendency of species evenness to be lower under the canopy than in the open grassland in spring (Figure 5.3.A), suggesting a more homogeneous composition of species.

Finnally, the CCA showed that plot and canopy drove species composition, in addition to the varaibility associated to the seasonality (CCA1, Figure 5.1). Species composition diffreed between plots (CCA2, Figure 5.4.A), with the SM-ilex and DN-suber plots having similar species composition, probably due to similar microclimatic conditions, since DN-suber was the fresher plot among all DN plots (Figure 5.1). On the other hand, species composition differed between under the canopy and the open grassland (CCA3, Figure 5.4.B), showing that the tree – open grassland structure allowed the growing of a wide variety of species, incerasing SR at the ecosystem scale.

5.5.2 Plot, canopy and herbaceous layer interactions as drivers of greenhouse gas exchange

5.5.2.1 CO_2 exchange

CO_2 exchange was closely driven by the dehesa tree – open grassland structure, with tree canopies driving microclimatic conditions, soil characteristics and the structure and composition of the herbaceous layer vegetation, and those in turn driving CO_2 fluxes. Net ecosystem CO_2 exchange (NEE) in the open grassland was uptake dominated in all the study plots, SM-ilex being the plot with the highest up-take rates and DN-pinea the plot with the lowest uptake rates (Figure 5.5.A). On the contrary, NEE under the canopy was emissions dominated in all DN plots, while in the SM-ilex plot there was net CO_2 uptake (Figure 5.5.A).These results support the well-known effect of light as CO_2 uptake

driver (Hussain et al., 2009; Wohlfahrt et al., 2008b), but also suggest interactions between the environment created by the canopy and local conditions. Thus, although light reduction under the canopy in the SM-ilex plot was in the same range of magnitude than in the DN plots (Figure 5.1.A), the vegetation kept taking-up CO_2. This links with the previously discussed neutral canopy effect on AGB in the SM-ilex plot, since the canopy did not have a noticeable impact on biomass production, which was able to photosynthesise at similar rates under the canopy and in the open grassland. This suggests again that the SM-ilex plot was less environmentally constrained than all DN plots, and that the environment created under the canopy did not differ so much to the open grassland, in opposition to the strong differences found in all DN plots.

Moreover, the inclusion of PFT composition improved NEE explained variability, and highlighted the relevance of PFT identity and interaction effects (Table 5.3 and Figure 5.6). Indeed, specific interactions among PFT were even more explicative than AGB and evenness, the latter being considered as an average interaction term. Legumes were key NEE drivers, enhancing net CO_2 uptake (Table 5.3 and Figure 5.6), in agreement with previous studies that reported higher photosynthetic capacity of legumes compared to grasses and forbs (Busch et al., 2018; Lee et al., 2003; Reich et al., 1998, 1997). Also, legumes transfer symbiotic N to other species, increasing photosynthesis of the overall community (Mulder et al., 2002; Pirhofer-Walzl et al., 2012); and acquisition of symbiotic N by legumes can be at the same time stimulated by the presence of grasses (Nyfeler et al., 2011). Accordingly, symbiotic N fixed by legumes could provide an important advantage for photosynthesis, especially in N limited systems, as is the case in our plots, which have a very low soil N content, and also a $\delta^{15}N$ quite low (Table S5.2), suggesting that symbiotic N may be an important N source in these systems.

On the other hand, ecosystem respiration (R_{eco}, Figure 5.5.A) was influenced by interactions between season and canopy, with lower R_{eco} under the canopy in spring (canopy effect, Table 5.3 - Table 5.4), but higher R_{eco} under the canopy in autumn (season

x canopy effect, Table 5.3 - Table 5.4), suggesting a differential magnitude of R_{eco} components ($R_{eco} = R_{autotrophic} + R_{heterotrophic}$) and its biotic and abiotic drivers depending on the season. First, higher R_{eco} rates in spring and in the open grassland (Figure 5.5.A) were most likely linked to higher soil temperature (T_s effect, Table 5.1), which is known to be an important R_{eco} driver (Hussain et al., 2009), especially enhancing the heterotrophic component of R_{eco} (Davidson and Janssens, 2006).

Second, higher R_{eco} rates in the open grassland could be indirectly related to higher CO_2 uptake rates (NEE, Figure 5.5.A). Respiration is one of the most important C release pathways of recently fixed C photo-assimilated by plants (Aljazairi et al., 2015), and autotrophic respiration is directly linked to photosynthetic activity (Larsen et al., 2007). The magnitude of the autotrophic component of R_{eco} in spring was clear when the AGB was removed, and the remaining respiratory flux (R_{soil}) clearly decreased compared to R_{eco} (Figure S5.1). On the contrary, R_{eco} and R_{soil}, equalized in autumn, R_{soil} even exceeding R_{eco} in some cases (Figure S5.1), suggesting that respiration derived from photosynthetic activity was really very low in autumn.

However, note that although the tendency in spring was to lower R_{eco} under the canopy compared to the open grassland (canopy effect, Table 5.2), our data also suggested that R_{eco} (and also R_{soil}) tended to increase under *P. pinea* canopy (Figure 5.5.A, spring). This might be because the *P. pinea* canopy was more open than *Quercus* canopies, as reflects the lower PAR differences between under the canopy and the open grassland (Figure 5.1.A), increasing temperatures under the canopy (T_s, Figure 5.1.B), conditions that could have enhanced respiration rates. In addition, litter of *P. pinea* has been reported to be more recalcitrant than litter of *Quercus* species (Fioretto et al., 2008; Sheffer et al., 2015), and this could be increasing soil organic C at the plot level (Table 4.1) and C/N ratio in the soil under the canopy (Table S5.2). In agreement, soil organic C and C/N ratio have been positively linked to the heterotrophic component of

R_{eco}, since soil microorganisms respire more C in absolute terms and per unit of microbial biomass when decomposing C-rich and/or N-poor substrates (Spohn, 2015).

On the other hand, the increase in R_{eco} (as well as R_{soil}) under the canopy in autumn compared to the open grassland (canopy x season, Table 5.2), was probably related to litter decomposition processes. The big amount of litter that was present under the canopy in spring was no longer present in autumn (Figure 5.2), suggesting that litter was already incorporated into the soil, and that was probably on mineralization process, increasing the heterotrophic component of R_{eco}.

Respiratory fluxes, R_{eco} and R_{soil}, were also influenced by the structure and species composition of the herbaceous layer. R_{eco} and R_{soil} were both enhanced by belowground biomass (BGB effect, Table 5.3 and Table 5.4), which has been linked to auto and heterotrophic respiration (Wang et al., 2017; Zhu et al., 2016). Previous studies have explained this increase in respiration rates related to BGB via an increase in species richness (Corrêa Dias et al., 2010). Howerver, our results suggested that species composition and richness explained some extra variabity of respiratory fluxes beyond BGB. Part of R_{eco} variability was explained by the CCA axes (CCA2 and CCA3 effects, Table 5.4), which represent a reduction of the dimensionality of the whole matrix of species, and R_{soil} was enhanced by SR (Table 5.4).

5.5.2.2 CH_4 and N_2O exchange

CH_4 and N_2O assessments from Mediterranean grasslands or meadows are very scarce (Oertel et al., 2016); and although quantifying absolute fluxes was not our goal, but to understand mechanisms affecting GHG exchange in dehesas ecosystems, we considered appropriate to contextualize our CH_4 and N_2O fluxes in the literature. Accordingly, our CH_4 (Figure 5.5.B) and N_2O (Figure 5.5.C) fluxes were much higher than previously reported fluxes from dehesa ecosystems (maximum CH_4 emissions $\cong$ 20 μg C m^{-2} h^{-1} $\cong$ 0.46 nmol CH_4 m^{-2} s^{-1}, and N_2O exchange

range ≅ −10 – 10 μg N m^{-2} s^{-1} ≅ 0.10 nmol N_2O m^{-2} s^{-1}, Shvaleva et al., 2014); although other studies carried out in grasslands have reported CH_4 and N_2O exchange rates in the same magnitude (Debouk et al., 2018; Dengel et al., 2011; Merbold et al., 2014). Yet, it must be taken into account that we did not consider fluxes below detection limit (Section 5.3.2), fact that could be increasing the average.

CH_4 emissions were more driven by a strong seasonality than by differences between under the canopy and the open grassland. CH_4 shifted from high emissions in spring, to low emissions or uptake in autumn (Figure 5.5.B), probably as result of several factors occurring simultaneously. First, high CH_4 emissions in spring were enhanced by high temperatures (T_s effect, Table 5.5 - Table 5.6), which could be favouring methanogenic activity and methane diffusion (Oertel et al., 2016). Second, SWC enhanced CH_4 emissions (although marginally significant, Table 5.5 - Table 5.6), and drying-rewetting cycles, typical in spring, could also be enhancing CH_4 soil emissions (Jugold et al., 2012). Finally, some studies have suggested that vegetation may have a role as CH_4 driver, as conduit (Dorodnikov et al., 2011; Gogoi et al., 2005) and/or as source, even at aerobic conditions (Butenhoff and Khan Khalil, 2007; Carmichael et al., 2014; Keppler et al., 2006; Praeg et al., 2017; Vigano et al., 2008). Thus, despite such role of vegetation as CH_4 source is still controversial, it has been suggested that CH_4 emissions from plants may be driven by ester methyl groups of pectin that can serve as CH_4 precursors (Keppler et al., 2008); UV radiation that may promote vegetation cellular breakdown emitting CH_4 (Nisbet et al., 2009; Vigano et al., 2008); and/or plants can transpire methane already dissolved in soil water (Nisbet et al., 2009). In our study we did not find a significant effect of AGB on CH_4 exchange, but certainly AGB was much higher in spring than in autumn (season effect, Table 5.1), which could be creating favourable conditions for CH_4 emissions.

Regarding N_2O exchange, there was an overall tendency to N_2O uptake in spring, except under *P. pinea*, where there were N_2O emissions (Figure 5.5.C, spring). Note that again

the DN-pinea plot had a differential GHG exchange behaviour than plots dominated by *Quercus* species*,* probably due to litter characteristics of *P. pinea,* influencing N dynamics*.* On the contrary, in autumn all study plots were small N_2O sources (Figure 5.5.C), especially under the canopy (canopy x season effect, Table 5.6), which could be driven by the higher soil N content (Table S5.2) and nitrification and denitrification processes (Luo et al., 2013; Oertel et al., 2016; Senapati et al., 2016).

Moreover, N_2O exchange was also influenced by the structure and composition of the herbaceous layer, increasing N_2O emissions with litter, BGB and the presence of legumes in the community (Table 5.5 - Table 5.6). The influence of litter and BGB on N_2O exchange at field conditions is not well understood, but there are some experiments assessing the effect of cover crops on N_2O exchange that may provide some understanding (Baggs et al., 2000; Lin et al., 2013; Maris et al., 2018; Shaaban et al., 2016). For instance, an experimental study by Shaaban et al., (2016), reported increasing N_2O emissions with the addition of litter onto soil surface, and specially with the addition of nodulated roots into the soil. The authors related the input of organic matter to stimulated microbial activity and denitrification, resulting in N_2O production (Shaaban et al., 2016). Also, N_2O emissions were negatively correlated to the C/N ratio of the substrate (Shaaban et al., 2016).

This agrees with our results of legumes enhancing N_2O emissions (Table 5.5 and Figure 5.7). Legumes increase N availability and decrease C/N ratio of the substrate, leading to an increase in N_2O emissions (Shaaban et al., 2016; Stehfest and Bouwman, 2006). On the other hand, species composition also influenced N_2O exchange (CCA1 and CCA2 effects, Table 5.6), in agreement with previous studies that have identified species composition as a key component underlying N_2O exchange (Abalos et al., 2014; Dijkstra et al., 2010).

Eventually, the inclusion of vegetation composition and diversity indexes, both in terms of species and PFT, improved the understanding of mechanisms affecting GHG (CO_2 and N_2O) in dehesa ecosystems.

5.6 Conclusions

Our study provides insight into dehesa ecosystems functioning, showing that the typical tree – open grassland structure modifies the structure and compostion (both in terms of speices and PFT) of the herbaceus layer. Morover the tree – open grassland structure and the herbaceus layer interacted to drive GHG fluxes. Tree canopies especially drove CO_2 and N_2O fluxes, increasing emissions under *P. pinea* canopy compared to *Quercus* species. GHG fluxes were also driven by PFT and species composition. Legume identity effects enhanced net CO_2 uptake and N_2O emissions; species richness increased R_{soil}; and species compositional matrix drove R_{eco} and N_2O exchange. The inclusion of vegetation composition and diversity indexes improved the understanding of mechanisms affecting GHG fluxes in dehesa ecosystems. Changes in the tree species and the tree coverage, mediated by changes in the composition of the herbaceous layer, will imply deep changes in the GHG exchange of dehesas. Facts that should be taken into account to perform better management strategies of this vast but vulnerable ecosystem.

Acknowledgements

This work was funded by the Spanish Science Foundation FECYT-MINECO: BIOGEI (GL2013-49142-C2-1-R) and IMAGINE (CGL2017-85490-R) projects, and supported by a FPI fellowship to Mercedes Ibañez (BES-2014-069243). Thanks to all the colleagues who collaborated in laboratory and fieldwork tasks: Antonio Rodríguez, Miquel Sala, Helena Sarri and Gianluca Segalina. Our special thanks to Dehesa de Gato S.L. state and Doñana Research Coordination Office for their support and facilities.

5.7 Supplementary material

Table S5.1. Linear model results. Photosynthetically active radiation (PAR), soil temperature (T_s) and soil water content (SWC) as function of season, plot and canopy. Explanatory variables selected by a stepwise procedure. Plot with SM-ilex as reference level, season with spring as reference level, and canopy with open grassland (OG) as reference level. Estimates of the explanatory variables (Est.), standard error (SE), t and p-value.

	PAR (µmol photons m^{-2} s^{-1})				T_s (ºC)				SWC (%)			
	Est.	**SE**	**t**	**p**	**Est.**	**SE**	**t**	**p**	**Est.**	**SE**	**t**	**p**
(Intercept)	1385	107	12.90	< 0.001	17.0	0.4	39.54	< 0.001	16	3	6.37	< 0.001
Season	−1001	110	−9.06	< 0.001	−1.3	0.4	−3.04	0.003				
Plot DN-mixed	−92	105	−0.88	0.4	0.2	0.4	0.54	0.6	−4	3	−1.39	0.2
Plot DN-suber	−16	125	−0.13	0.9	0.4	0.5	0.81	0.4	6	3	1.84	0.07
Plot DN-pinea	195	125	1.56	0.1	1.2	0.5	2.49	0.02	−9	3	−2.75	0.008
Canopy	−977	106	−9.25	< 0.001	−2.7	0.4	−6.26	< 0.001	7	2	3.15	0.002
Season x canopy	847	159	5.33	< 0.001	2.3	0.6	3.57	< 0.001				
R^2_{Adj}	0.66			< 0.001	0.36			< 0.001	0.28			< 0.001

Table S5.2. Soil C content, N content, $\delta^{15}N$ and C/N ratio per plot and canopy: open grassland (OG) and under the canopy (UC). Mean and standard error (SE). Summarized from Section 4.4.

Variables	SM-ilex				DN-mixed			
	OG		UC		OG		UC	
	Mean	SE	Mean	SE	Mean	SE	Mean	SE
C (%)	1.8	0.1	4.2	0.1	1.1	0.2	2.7	0.3
N (%)	0.164	0.010	0.30	0.03	0.082	0.010	0.19	0.02
$\delta^{15}N$ (‰)	3.6	0.5	3.9	0.2	4.1	0.5	3.3	0.3
C/N (fraction)	11.2	0.1	14.0	0.1	13.3	0.3	14.1	0.2
	DN-suber				DN-pinea			
	OG		UC		OG		UC	
	Mean	SE	Mean	SE	Mean	SE	Mean	SE
C (%)	2.4	0.5	3.2	0.7	0.9	0.1	3.5	0.9
N (%)	0.18	0.05	0.24	0.05	0.064	0.008	0.23	0.05
$\delta^{15}N$ (‰)	4.10	0.09	4.0	0.4	3.7	0.5	3.69	0.09
C/N (fraction)	12.8	0.5	13.6	0.5	13.6	0.3	15.4	0.5

	Average all plots			
	OG		UC	
	Mean	SE	Mean	SE
C (%)	1.4	0.2	3.2	0.3
N (%)	0.12	0.01	0.23	0.02
$\delta^{15}N$ (‰)	3.9	0.2	3.7	0.2
C/N (fraction)	12.6	0.2	14.0	0.2

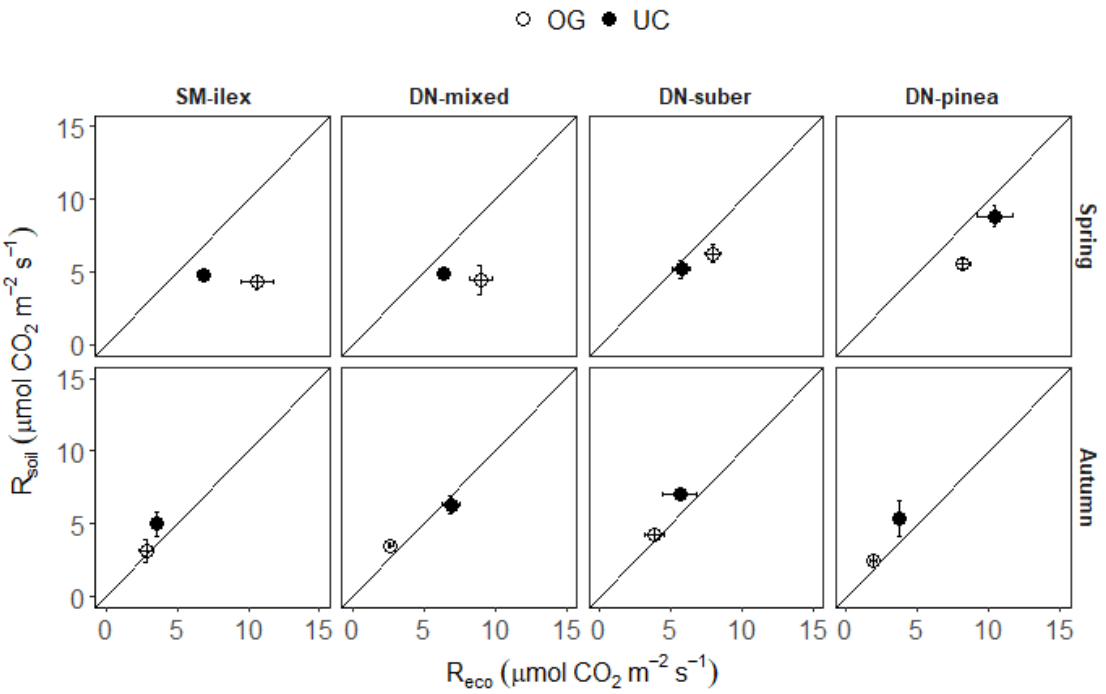

Figure S5.1. Soil respiration (R_{soil}) ~ ecosystem respiration (R_{eco}) relationship, mean ± standard error per season, plot and canopy.

Chapter 6 General discussion

6.1 Vegetation contribution to the understanding of greenhouse gas exchange and carbon and nitrogen cycling

Our results showed that vegetation was an important driver of greenhouse gas (GHG) exchange and carbon (C) and nitrogen (N) cycling along the assessed climatic gradient and management regimes. Such vegetation influence was exerted from a perspective of phenology, structure and composition as detailed below.

6.1.1 Vegetation structure and phenology

The influence of vegetation structure and phenology on GHG fluxes and C and N cycling was consistent on both alpine grasslands and dehesa ecosystems. Regarding GHG exchange, we showed in Chapter 2 that CO_2 exchange fluxes in mountain grasslands were dependent on phenology and climatic belt characteristics. Temperature and soil water content influenced on different ways on the two altitudinal belts. The subalpine grassland (CAST) was more temperature constrained than water constrained then the montane grassland (BERT), and vegetation did not start to grow until temperatures increased (Figure 2.4). However, temperature increased CO_2 exchange in a higher magnitude in the subalpine grassland, being highly productive during summer. In addition, the well-developed vegetation kept exchanging CO_2, even though the summer drought; while drought effects were stronger in the montane grassland (BERT, Figure 2.4).

This suggests that vegetation may have different resource use and acquisition strategies depending on the environment (Brilli et al., 2011; Leitinger et al., 2015), and highlights the need of detailed information on phenology, in order to accurately upscale CO_2 exchange fluxes. Moreover, this illustrates potential changes that CO_2 fluxes may suffer, mediated by vegetation, under an increase of global temperatures.

On the other hand, the tree – open grassland structure in dehesa ecosystems also drove GHG fluxes (Chapter 5). An example is the lower net CO_2 uptake that we found under the canopy compared to the open grassland (Figure 5.5). Interestingly, GHG fluxes were affected differently between tree species (*Q. ilex, Q. suber and P. pinea*). Generally, emissions under the canopy of *P. pinea* differed from *Quercus* species, with higher CO_2 (soil and ecosystem respiration) and N_2O emissions under the canopy of *P. pinea* than under the canopy of *Q. ilex* and *Q. suber* (Figure 5.5). These facts evidence that changes in the tree cover, and in the tree species composition may imply profound changes in GHG exchange. This should be taken into account when assessing the impacts of land use changes, and of plantations that are replacing traditional *Quercus* species stands (Costa et al., 2011; Costa Pérez et al., 2006).

In addition, the tree – open grassland structure also influenced C and N cycling and storage between ecosystem compartments (Chapter 4). Overall, under the canopy there was higher C (Figure 4.2) and N (Figure 4.7) content in the soil and the above and belowground biomass, and there was higher discrimination against ^{13}C (Figure 4.3) and ^{15}N (Figure 4.8) than in the open grassland.

Interestingly, the canopy influence was generally stronger in all Doñana (DN) plots than in the Sierra Morena plot (SM-ilex), where the canopy effect tended to be neutral. An example of this difference on the canopy effect would be the $\delta^{13}C$ of forbs, which had lower $\delta^{13}C$ (higher discrimination against ^{13}C) under the canopy than in the open grassland in all DN plots, while this effect was not noticeable in the SM-ilex plot (Figure 4.3.C). This may well be because DN is more environmentally constrained than SM, which is slightly fresher and wetter, and the canopy really generates an environment that is markedly different from the open grassland in DN. Moreover, this highlights the relevance of trees as drivers of ecosystem fertility and C and N relationships, especially in more constrained environments, and the fact that the optimum tree coverage may differ depending on the given ecosystem function and environmental conditions.

Finally, the tree – open grassland structure of dehesas also drove the composition of the herbaceous layer, both in terms of species and plant functional types (PFT, Section 5.4.2). Thus, since each PFT has its own C and N acquisition and use strategies (Chapter 4), PFT also acted as drivers of GHG exchange and C and N cycling.

6.1.2 Vegetation composition: identity effects

Indeed, such influence of PFT on GHG exchange, was captured by the diversity-interaction model (Section 5.4.3). Legumes identity effects increased the net CO_2 uptake (NEE, Table 5.3) and N_2O emissions (Table 5.5), most likely due the higher N availability that legumes provided to the system. Species compositional matrix was also explicative of ecosystem respiration (R_{eco}, Table 5.4) and N_2O (Table 5.6), as showed significantly the axes of the canonical correspondence analysis (CCA), which represent a reduction of the dimensionality of the whole matrix of species.

Accordingly, vegetation composition (both in terms of PFT or species) explained an important part of GHG variance, even, in some cases, more than vegetation structural variables, as are above and belowground biomass. For instance, this was observed when modelling the NEE using the diversity-interaction model, in which PFT identity and interaction effects were significant, while above and belowground biomass were not included in the model (Table 5.3). This means that there is a strong relationship between diversity/composition and ecosystem functioning, even beyond the more straightforward relationship between diversity, productivity and GHG (De Deyn et al., 2009; Finn et al., 2013; Hector et al., 1999).

In addition, our results showed that assessing vegetation compositional effects form a species and a PFT approach can be complementary, since some GHG fluxes were explained by vegetation composition in terms of PFT (NEE, Table 5.3), in terms of species (R_{eco}, Table 5.4) or both (N_2O, Table 5.5 - Table 5.6).

However, note that some expected effects may not be noticeable at a given scale, since several PFT ecophysiological characteristics are occurring simultaneously. This is what we observed when assessing the PFT dominance effect on NEE light response in Chapter 2. We observed an effect of the dominant PFT on the NEE per aboveground living biomass (NEE_{AGLB}, μmol CO_2 g^{-1} s^{-1}), but this effect was not noticeable on the NEE per grassland ground area (NEE, μmol CO_2 m^{-2} s^{-1}, Table 2.2). Although legumes have higher photosynthetic capacity, plots dominated by legumes have generally lower biomass than plots dominated by grasses or forbs (Figure S2.2), and the expected higher net CO_2 uptake rates were not noticeable at a grassland ground area scale (Table 2.2). Hence, this highlights the relevance of the scale when assessing composition or diversity effects on a given ecosystem function, since some effects may emerge when using the proper scale.

6.1.3 Vegetation composition: diversity interaction effects

A diversity interaction effect is the performance of a mixed community that differs from the expected combination of individual performances, effects that can be synergistic or antagonistic (Kirwan et al., 2009). To this regard, we reported in Chapter 3 a synergistic effect between cereal and legume species, which experienced an increase in the net CO_2 uptake compared to cereal monocultures (Table 3.2). This probably resulted from a niche complementary effect (Tilman et al., 1997) and an increase in the N availability, which enhanced photosynthesis of the overall community (Kirwan et al., 2009; Mulder et al., 2002; Pirhofer-Walzl et al., 2012). Interestingly, such cereal-legume interaction effects enhanced gross CO_2 uptake, but did not significantly enhance respiration (Sections 3.4.3 - 3.4.4), resulting in higher net CO_2 uptake. This fact raises questions regarding the magnitude of such identity and interaction effects on each NEE component — gross primary production (GPP) and R_{eco} —, as well as on both R_{eco} components, auto and heterotrophic respiration. Further research in this line would be recommendable.

On the other hand, interaction effects can also be antagonistic, and that is what we observed in Chapter 5 when modelling NEE in dehesa ecosystems (Table 5.3). The maximum net CO_2 uptake was achieved with dominance of legumes (legumes identity effect), but net CO_2 uptake decreased with the presence of forbs and grasses in the mixture (Table 5.3). Yet, full dominance of legumes in the studied dehesa ecosystem would not be realistic (Figure 5.2).

Finally, species richness (SR) explained part of R_{soil} (Table 5.4) and CH_4 emissions (SR, marginally significant effect, Table 5.6), but in our study cases generally PFT or species composition were better predictors of GHG exchange than diversity indices, such as SR or evenness. Indeed, the evenness index, which can be considered as an average interaction term, was not included in any of the GHG models, while the inclusion of PFT specific interactions (Table 5.3), and species composition (CCA axes, Table 5.4 and Table 5.6) had significant effects on GHG exchange.

6.2 Forage mixtures: management opportunities

Our results show that species selection can provide interesting management opportunities to mitigate climate change, since legumes (Table 5.3) and cereal-legume mixtures (Table 3.2) increased the net CO_2 uptake. Symbiotic N fixed by legumes provides an important advantage for photosynthesis and CO_2 uptake, especially in N limited systems. In addition, cereal-legume mixtures had higher forage quality (Table S3.1); suggesting the potential of cereal-legume mixtures to increase soil nitrogen content.

On the other hand, each grassland type (cereal monoculture *vs.* cereal-legume mixtures) has associated certain management practices that can simultaneously increase the C uptake of the system. In Chapter 3 we showed that an earlier harvesting of the yield associated to cereal-legume mixtures compared to cereal monocultures, favoured a

second regrowth of the vegetation after the harvest, enhancing the net CO_2 uptake during the fallow period, which was decisive for the cumulative NEE (Section 3.4.1). The voluntary regrowth of the vegetation during the fallow also provided a profitable resource for livestock, besides providing an important litter input into the system, probably increasing the net biome production (NBP), and offsetting partly C losses due to the yield.

These facts evidence the need of a better understanding of phenological cycles, in order to achieve the maximum productivity, maximum net CO_2 uptake (minimizing other GHG emissions), as well as maximum NBP, which will determine the C sink/source behaviour of a given grassland.

However, our results also showed that legumes can increase N_2O emissions (Table 5.5), and further research focusing on the role of vegetation as CH_4 and N_2O driver, would be recommendable to fully assess the C sink potential, minimizing GHG emissions, of forage mixtures.

6.3 Implications of our research

Our research highlights the relevance of vegetation as driver of GHG exchange and C and N cycling in grassland ecosystems, highlighting the enormous potential of grassland ecosystems to mitigate climate change.

Interestingly, the role of vegetation composition was consistent along all the research conducted in this thesis. Vegetation composition (both in terms of PFT or species) explained an important part of GHG variance, even in some cases, more than vegetation structural variables and more aggregated diversity indices (evenness). This an important finding that provides insight into grasslands and agroecosystems functioning, and which can be used to crate management strategies to enhance the C sink potential, minimizing GHG emissions, and enhancing grasslands fertility.

Yet, it is important to consider that any change in the vegetation structure and composition will simultaneously influence several ecosystem functions, and this must be taken into account to optimize the results according to the objective. Moreover, changing plant communities in combination with climate change may lead to complex interactions, significantly affecting GHG exchange and C and N cycles.

To this regard, examine in more detail the mechanisms through which the vegetation influences GHG exchange, especially CH_4 and N_2O, and C and N cycles, would be key to clarify part of the remaining uncertainty. In particular, more research is needed to unravel the role of vegetation on GHG consumption and formation, as well as to unravel vegetation direct from indirect effects.

Chapter 7 General conclusions

Chapter 2

Phenology played an important role as CO_2 exchange driver at seasonal scale, driving differences between elevation belts (montane *vs.* subalpine). The subalpine grassland was more temperature constrained than water constrained, but temperature enhanced gross and net CO_2 uptake at higher rates than in the montane grassland. A delayed phenology at the subalpine grassland reduced vegetation's sensitivity to summer dryness, which did not experience a reduction in CO_2 exchange, even though the low soil water content. During the peak biomass the subalpine grassland was considerably more productive and yielded higher net CO_2 uptake rates than the montane grassland. Accordingly, in mountain environments, detailed information on phenology is key to understand seasonal CO_2 exchange dynamics.

Vegetation composition, in terms of the dominant plant functional type (PFT), influenced net ecosystem exchange (NEE) per unit of aboveground living biomass; grass dominated plots having lower asymptotic gross primary production than legume dominated plots. However, this PFT dominance effect on NEE was not observed on NEE per grassland ground area, highlighting the relevance of the scale when assessing composition or diversity effects on a given ecosystem function, since some effects may emerge when using the proper scale.

Chapter 3

Cereal-legume mixtures increased net CO_2 uptake compared to cereal monocultures. Management practices associated to cereal-legume mixtures, particularly an earlier harvesting time of the yield, favoured the voluntary regrowth of the vegetation during the fallow period, enhancing the net CO_2 uptake during that period, and being decisive for the net CO_2 budget of the whole grassland season. In addition cereal-legume mixtures

enhanced photosynthetic activity and gross CO_2 uptake, while did not significantly increase respiration, resulting in higher net CO_2 uptake. Cereal-legume mixtures provided in this sense important advantages to increase the net CO_2 uptake capacity of forage systems compared to cereal monocultures, while ensuring productivity and forage quality.

Chapter 4

Dehesa carbon (C) and nitrogen (N) dynamics were strongly modulated by interactions between trees and the herbaceous layer. The higher litter fall from trees increased soil C and N content under the canopy compared to the open grassland. The increased soil N, most likely increased N content in shoots and favoured higher discrimination against ^{15}N by roots. Overall, $\delta^{13}C$ and intrinsic water use efficiency (iWUE) of the herbaceous layer, and especially of forbs, decreased under the canopy, as a result of higher stomatal conductance. Moreover, each plant functional type (PFT, forbs, grasses and legumes) had their own C and N ecophysiological particularities. Legumes had the lowest $\delta^{13}C$ and the lowest iWUE, followed by forbs and grasses. Besides the fact that legumes were the PFT with the highest N content and the most ^{15}N depleted leaves, grasses had higher N content than forbs and generally lower $\delta^{15}N$. This, suggests that grasses may be more efficient taking-up N, and/or exploiting symbiotic N than forbs, which could provide an important competitive advantage to grasses, especially under the canopy, where there was higher soil N content. Finally, the canopy influence on C and N storage and cycling was generally more noticeable in the DN plots than in the SM-ilex plot, DN being more environmentally constrained than SM. This, highlights the relevance of trees as drivers of ecosystem fertility and C and N relationships, especially in more constrained environments, as is DN *vs.* SM.

Chapter 5

The tree – open grassland of dehesas also strongly influenced the structure and compostion (both in terms of speices and PFT) of the herbaceus layer, which interacted to drive GHG fluxes. Tree canopies especially drove CO_2 and N_2O fluxes, increasing emissions under *P. pinea* canopy compared to *Quercus* species. GHG fluxes were also driven by PFT and species composition. Legume identity effects enhanced net CO_2 uptake and N_2O emissions; species richness increased R_{soil}; and species compositional matrix drove R_{eco} and N_2O exchange. The inclusion of vegetation composition and diversity indexes improved the understanding of mechanisms affecting GHG fluxes in dehesa ecosystems. Changes in the tree species and the tree coverage, mediated by changes in the composition of the herbaceous layer, will imply deep changes in the GHG exchange of dehesas. Facts that should be taken into account to perform better management strategies of this vast but vulnerable ecosystem.

Bibliography

Abalos, D., De Deyn, G.B., Kuyper, T.W., van Groenigen, J.W., 2014. Plant species identity surpasses species richness as a key driver of N_2O emissions from grassland. Glob. Chang. Biol. 20, 265–275. https://doi.org/10.1111/gcb.12350

Ågren, G.I., Franklin, O., 2003. Root : shoot ratios, optimization and nitrogen productivity. Ann. Bot. 92, 795–800. https://doi.org/10.1093/aob/mcg203

Ågren, G.I., Ingestad, T., 1987. Root : shoot ratio as a balance between nitrogen productivity and photosynthesis. Plant Cell Environ. 10, 579–586. https://doi.org/10.1111/1365-3040.ep11604105

Albergel, C., Calvet, J.-C., Gibelin, A.-L., Lafont, S., Roujean, J.-L., Berne, C., Traullé, O., Fritz, N., 2010. Observed and modelled ecosystem respiration and gross primary production of a grassland in southwestern France. Biogeosciences 7, 1657–1668. https://doi.org/10.5194/bg-7-1657-2010

Aljazairi, S., Arias, C., Nogués, S., 2015. Carbon and nitrogen allocation and partitioning in traditional and modern wheat genotypes under pre-industrial and future CO_2 conditions. Plant Biol. 17, 647–659. https://doi.org/10.1111/plb.12280

Aljazairi, S., Arias, C., Sánchez, E., Lino, G., Nogués, S., 2014. Effects of pre-industrial, current and future [CO_2] in traditional and modern wheat genotypes. J. Plant Physiol. 171, 1654–1663. https://doi.org/10.1016/j.jplph.2014.07.019

Allen, M.R., Dube, O.P., Solecki, W., Aragón-Durand, F., Cramer, W., Humphreys, S., Kainuma, M., Kala, J., Mahowald, N., Mulugetta, Y., Perez, R., Wairiu, M., Zickfeld, K., 2018. Framing and Context, in: Masson-Delmotte, V., Zhai, P., Pörtner, H.-O., Roberts, D., Skea, J., Shukla, P.R., Pirani, A., Moufouma-Okia, W., Péan, C., Pidcock, R., Connors, S., Matthews, J.B.R., Chen, Y., Zhou, X., Gomis, M.I., Lonnoy, E., Maycock, T., Tignor, M., Waterfield, T. (Eds.), Global Warming of 1.5°C. An IPCC Special Report on the Impacts of Global Warming of 1.5°C above Pre-

Industrial Levels and Related Global Greenhouse Gas Emission Pathways, in the Context of Strengthening the Global Response to the Threat of Climate Change,. In Press, pp. 49–91.

Allen, V.G., Batello, C., Berretta, E.J., Hodgson, J., Kothmann, M., Li, X., Mcivor, J., Milne, J., Morris, C., Peeters, A., Sanderson, M., 2011. An international terminology for grazing lands and grazing animals. Grass Forage Sci. 66, 2–28. https://doi.org/10.1111/j.1365-2494.2010.00780.x

Altimir, N., Vesala, T., Keronen, P., Kulmala, M., Hari, P., 2002. Methodology for direct field measurements of ozone flux to foliage with shoot chambers. Atmos. Environ. 36, 19–29. https://doi.org/10.1016/S1352-2310(01)00478-2

Andivia, E., Fernández, M., Alejano, R., Vázquez-piqué, J., 2015. Tree patch distribution drives spatial heterogeneity of soil traits in cork oak woodlands. Ann. For. Sci. 549–559. https://doi.org/10.1007/s13595-015-0475-8

Ankom Thechnology, 2005. Procedures (for NDF, ADF, and in vitro Digestibility) [WWW Document]. URL http://www.ankom.com/09_procedures.shtml

Aranjuelo, I., Irigoyen, J.J., Nogués, S., Sánchez-Díaz, M., 2009. Elevated CO_2 and water-availability effect on gas exchange and nodule development in N_2-fixing alfalfa plants. Environ. Exp. Bot. 65, 18–26. https://doi.org/10.1016/j.envexpbot.2008.06.006

Aubinet, M., Feigenwinter, C., Heinesch, B., Laffineur, Q., Papale, D., Reichstein, M., Rinne, J., Van Gorsel, E., 2012a. Nighttime Flux Correction, in: Aubinet, M., Vesala, T., Papale, D. (Eds.), Eddy Covariance: A Practical Guide to Measurement and Data Analysis. Springer Netherlands, Dordrecht, pp. 133–157. https://doi.org/10.1007/978-94-007-2351-1_5

Aubinet, M., Vesala, T., Papale, D. (Eds.), 2012b. Eddy Covariance. A Practical Guide to Measurement and Data Analysis. Springer Netherlands, London and New York.

https://doi.org/10.1007/978-94-007-2351-1

Badía-Villas, D., del Moral, F., 2016. The Soils of Spain. World Soils Book Series. Springer, Cham. https://doi.org/10.1007/978-3-319-20541-0_4

Baggs, E.M., Rees, R.M., Smith, K.A., Vinten, A.J.A., 2000. Nitrous oxide emission from soils after incorporating crop crop residues. Soil Use Manag. 16, 82–87. https://doi.org/10.1002/9781118676332.ch8

Bahn, M., Rodeghiero, M., Anderson-Dunn, M., Dore, S., Gimeno, C., Drösler, M., Williams, M., Ammann, C., Berninger, F., Flechard, C., Jones, S., Balzarolo, M., Kumar, S., Newesely, C., Priwitzer, T., Raschi, A., Siegwolf, R., Susiluoto, S., Tenhunen, J., Wohlfahrt, G., Cernusca, A., 2008. Soil respiration in European grasslands in relation to climate and assimilate supply. Ecosystems 11, 1352–1367. https://doi.org/10.1007/s10021-008-9198-0

Balser, T.C., Wixon, D.L., 2009. Investigating biological control over soil carbon temperature sensitivity. Glob. Chang. Biol. 15, 2935–2949. https://doi.org/10.1111/j.1365-2486.2009.01946.x

Barrantes Díaz, O., 1986. Influencia de la encina sobre el asto de la Sierra Norte de Sevilla: una aproximación experimental. Ph.D. thesis, Universidad de Sevilla, Sevilla, Spain, 71 pp.

Berninger, F., Susiluoto, S., Gianelle, D., Bahn, M., Wohlfahrt, G., Sutton, M., Garcia-Pausas, J., Gimeno, C., Sanz, M.J., Dore, S., Rogiers, N., Furger, M., Balzarolo, M., Sebastià, M.T., Tenhunen, J., 2015. Management and site effects on carbon balances of European mountain meadows and rangelands. Boreal Environ. Res. 20, 748–760.

Bhattacharyya, P.N., Jha, D.K., 2012. Plant growth-promoting rhizobacteria (PGPR): Emergence in agriculture. World J. Microbiol. Biotechnol. 28, 1327–1350. https://doi.org/10.1007/s11274-011-0979-9

Bollig, C., Feller, U., 2014. Impacts of drought stress on water relations and carbon assimilation in grassland species at different altitudes. Agric. Ecosyst. Environ. 188, 212–220. https://doi.org/10.1016/j.agee.2014.02.034

Bonafini, M., Pellegrini, M., Ditchfield, P., Pollard, A.M., 2013. Investigation of the “canopy effect” in the isotope ecology of temperate woodlands. J. Archaeol. Sci. 40, 3926–3935. https://doi.org/10.1016/j.jas.2013.03.028

Brilli, F., Hörtnagl, L., Hammerle, A., Haslwanter, A., Hansel, A., Loreto, F., Wohlfahrt, G., 2011. Leaf and ecosystem response to soil water availability in mountain grasslands. Agric. For. Meteorol. 151, 1731–1740. https://doi.org/10.1016/j.agrformet.2011.07.007

Brooks, P.D., Geilmann, H., Werner, R.A., Brand, W.A., 2003. Improved precision of coupled $\delta^{13}C$ and $\delta^{15}N$ measurements from single samples using an elemental analyzer/isotope ratio mass spectrometer combination with a post-column six-port valve and selective CO_2 trapping; improved ha. Rapid Commun. Mass Spectrom. 17, 1924–1926. https://doi.org/10.1002/rcm.1134

Brouwer, R., 1983. Functional equilibrium: sense or nonsense? J. Agric. Sci. 153, 335–348.

Brugnoli, E., Farquhar, G.D., 2000. Photosynthetic Fractionation of Carbon Isotopes, in: Leegood, R.C., Sharkey, T.D., Von Caemmerer, S. (Eds.), Photosynthesis: Physiology and Metabolism. Kluwer Academic Publishers, Dordrecht, pp. 399–434. https://doi.org/10.1007/0-306-48137-5_17

Buchmann, N., Kao, W.Y., Ehleringer, J., 1997. Influence of stand structure on carbon-13 of vegetation, soils, and canopy air within deciduous and evergreen forests in Utah, United States. Oecologia 110, 109–119. https://doi.org/10.1007/s004420050139

Busch, F.A., Sage, R.F., Farquhar, G.D., 2018. Plants increase CO_2 uptake by

assimilating nitrogen via the photorespiratory pathway. Nat. Plants 4, 46–54. https://doi.org/10.1038/s41477-017-0065-x

Butenhoff, C.L., Khan Khalil, M.A., 2007. Global Methane Emissions from Terrestrial Plants. Environ. Sci. Technol. 41, 4032–4037. https://doi.org/10.1021/es062404i

Caldeira, M.C., Ryel, J., Lawton, J.H., Pereira, J.S., 2001. Mechanisms of positive biodiversity-production relationships insights provided by $d^{13}C$ analysis in experimental Mediterranean grassland plots. Ecol. Lett. 4, 439–443. https://doi.org/10.1046/j.1461-0248.2001.00238.x

Carey, J.C., Tang, J., Templer, P.H., Kroeger, K.D., Crowther, T.W., Burton, A.J., Dukes, J.S., Emmett, B., Frey, S.D., Heskel, M.A., Jiang, L., Machmuller, M.B., Mohan, J., Panetta, A.M., Reich, P.B., Reinsch, S., Wang, X., Allison, S.D., Bamminger, C., Bridgham, S., Collins, S.L., de Dato, G., Eddy, W.C., Enquist, B.J., Estiarte, M., Harte, J., Henderson, A., Johnson, B.R., Larsen, K.S., Luo, Y., Marhan, S., Melillo, J.M., Peñuelas, J., Pfeifer-Meister, L., Poll, C., Rastetter, E., Reinmann, A.B., Reynolds, L.L., Schmidt, I.K., Shaver, G.R., Strong, A.L., Suseela, V., Tietema, A., 2016. Temperature response of soil respiration largely unaltered with experimental warming. Proc. Natl. Acad. Sci. 113, 13797–13802. https://doi.org/10.1073/pnas.1605365113

Carmichael, M.J., Bernhardt, E.S., Bräuer, S.L., Smith, W.K., 2014. The role of vegetation in methane flux to the atmosphere: should vegetation be included as a distinct category in the global methane budget? Biogeochemistry 119, 1–24. https://doi.org/10.1007/s10533-014-9974-1

Casals, P., Gimeno, C., Carrara, A., Lopez-sangil, L., 2009. Soil CO_2 efflux and extractable organic carbon fractions under simulated precipitation events in a Mediterranean Dehesa. Soil Biol. Biochem. 41, 1915–1922. https://doi.org/10.1016/j.soilbio.2009.06.015

Casals, P., Sangil, L.L., Carrara, A., Gimeno, C., Nogués, S., 2011. Autotrophic and heterotrophic contributions to short-term soil CO_2 efflux following simulated summer precipitation pulses in a Mediterranean dehesa. Global Biogeochem. Cycles 25, 1–12. https://doi.org/10.1029/2010GB003973

Ceschia, E., Béziat, P., Dejoux, J.F., Aubinet, M., Bernhofer, C., Bodson, B., Buchmann, N., Carrara, A., Cellier, P., Di Tommasi, P., Elbers, J.A., Eugster, W., Grünwald, T., Jacobs, C.M.J., Jans, W.W.P., Jones, M., Kutsch, W., Lanigan, G., Magliulo, E., Marloie, O., Moors, E.J., Moureaux, C., Olioso, A., Osborne, B., Sanz, M.J., Saunders, M., Smith, P., Soegaard, H., Wattenbach, M., 2010. Management effects on net ecosystem carbon and GHG budgets at European crop sites. Agric. Ecosyst. Environ. 139, 363–383. https://doi.org/10.1016/j.agee.2010.09.020

Chapagain, T., Riseman, A., 2015. Nitrogen and carbon transformations , water use efficiency and ecosystem productivity in monocultures and wheat-bean intercropping systems. Nutr. Cycl. Agroecosystems 101, 107–121. https://doi.org/10.1007/s10705-014-9647-4

Chen, J., Luo, Y., Xia, J., Wilcox, K.R., Cao, J., Zhou, X., Jiang, L., Niu, S., Estera, K.Y., Huang, R., Wu, F., Hu, T., Liang, J., Shi, Z., Guo, J., Wang, R.W., 2017. Warming Effects on Ecosystem Carbon Fluxes Are Modulated by Plant Functional Types. Ecosystems 20, 515–526. https://doi.org/10.1007/s10021-016-0035-6

Corrêa Dias, A.T., van Ruijven, J., Berendse, F., 2010. Plant species richness regulates soil respiration through changes in productivity. Oecologia 163, 805–813. https://doi.org/10.1007/s00442-010-1569-5

Costa, A., Madeira, M., Lima Santos, J., Oliveira, Â., 2011. Change and dynamics in Mediterranean evergreen oak woodlands landscapes of Southwestern Iberian Peninsula. Landsc. Urban Plan. 102, 164–176. https://doi.org/10.1016/j.landurbplan.2011.04.002

Costa Pérez, J.C., Martín Vicente, Á., Fernández Alés, R., Estirado Oliet, M., Ingeniera de Montes, Consejería de Medio Ambiente, 2006. Dehesas de Andalucía. Caracterización ambiental. Sevilla.

Craine, J.M., Froehle, J., Tilman, D.G., Wedin, D.A., Chapin, F.S., 2001. The relationships among root and leaf traits of 76 grassland species and relative abundance along fertility and disturbance gradients. Oikos 93, 274–285. https://doi.org/10.1034/j.1600-0706.2001.930210.x

Craine, J.M., Tilman, D., Wedin, D., Reich, P., Tjoelker, M., Knops, J., 2002. Functional traits, productivity and effects on nitrogen cycling of 33 grassland species. Funct. Ecol. 16, 563–574. https://doi.org/10.1046/j.1365-2435.2002.00660.x

Croghan, C.W., Egeghy, P.P., 1990. Methods of Dealing with Values Below the Limit of Detection using SAS. Environ. Sci. Technol. 24, 1766–1774. https://doi.org/10.1021/es00082a001

Dahlgren, R.A., Singer, M.J., Huang, X., 1997. Oak tree and grazing impacts on soil properties and nutrients in a california oak woodland. Biogeochemistry 39, 45–64. https://doi.org/10.1023/A:1005812621312

Davidson, E.A., Janssens, I.A., 2006. Temperature sensitivity of soil carbon decomposition and feedbacks to climate change. Nature 440, 165–173. https://doi.org/10.1038/nature04514

Davidson, E.A., Savage, K., Verchot, L. V, Navarro, R., 2002. Minimizing artifacts and biases in chamber-based measurements of soil respiration. Agric. For. Meteorol. 113, 21–37. https://doi.org/10.1016/S0168-1923(02)00100-4

Dawson, T.E., Mambelli, S., Plamboeck, A.H., Templer, P.H., Tu, K.P., 2002. Stable Isotopes in Plant Ecology. Annu. Rev. Ecol. Syst. 33, 507–559. https://doi.org/10.1146/annurev.ecolsys.33.020602.095451

De Deyn, G.B.., Quirk, H., Yi, Z., Oakley, S., Ostle, N.J., Bardgett, R.D., 2009. Vegetation

composition promotes carbon and nitrogen storage in model grassland communities of contrasting soil fertility. J. Ecol. 97, 864–875. https://doi.org/10.1111/j.1365-2745.2009.01536.x

De Deyn, G.B., Cornelissen, J.H.C., Bardgett, R.D., 2008. Plant functional traits and soil carbon sequestration in contrasting biomes. Ecol. Lett. 11, 516–531. https://doi.org/10.1111/j.1461-0248.2008.01164.x

Debouk, H., Altimir, N., Sebastià, M.T., 2018. Maximizing the information obtained from chamber-based greenhouse gas exchange measurements in remote areas. MethodsX 5, 973–983. https://doi.org/10.1016/j.mex.2018.07.021

Debouk, H., De Bello, F., Sebastia, M.T., 2015. Functional trait changes, productivity shifts and vegetation stability in mountain grasslands during a short-term warming. PLoS One 10, 1–17. https://doi.org/10.1371/journal.pone.0141899

Della Coletta, L., Bielefeld Nardoto, G., Ribeiro Latansio-Aidar, S., Ribeiro da Rocha, H., 2009. Isotopic view of vegetation and carbon and nitrogen cycles in a cerrado ecosystem, southeastern Brazil. Sci. Agric. 66, 467–475. https://doi.org/10.1590/S0103-90162009000400006

Dengel, S., Levy, P.E., Grace, J., Jones, S.K., Skiba, U.M., 2011. Methane emissions from sheep pasture, measured with an open-path eddy covariance system. Glob. Chang. Biol. 17, 3524–3533. https://doi.org/10.1111/j.1365-2486.2011.02466.x

Díaz, S., Lavorel, S., McIntyre, S., Falczuk, V., Casanoves, F., Milchunas, D.G., Skarpek, C., Ruschk, G., Sternberg, M., Noy-Meir, I., Landsberg, J., Zhang, W., Clark, H., Campbell, B.D., 2007. Plant trait responses to grazing – a global synthesis. Glob. Chang. Biol. 13, 313–341. https://doi.org/10.1111/j.1365-2486.2006.01288.x

Dijkstra, F.A., Morgan, J.A., LeCain, D.R., Follett, R.F., 2010. Microbially mediated CH_4 consumption and N_2O emission is affected by elevated CO_2, soil water content, and composition of semi-arid grassland species. Plant Soil 329, 269–281.

https://doi.org/10.1007/s11104-009-0152-5

Dorodnikov, M., Knorr, K.H., Kuzyakov, Y., Wilmking, M., 2011. Plant-mediated CH_4 transport and contribution of photosynthates to methanogenesis at a boreal mire: a ^{14}C pulse-labeling study. Biogeosciences 8, 2365–2375. https://doi.org/10.5194/bg-8-2365-2011

Durand, M., Porcheron, B., Hennion, N., Maurousset, L., Lemoine, R., Pourtau, N., 2016. Water deficit enhances C export to the roots in A. thaliana plants with contribution of sucrose transporters in both shoot and roots. Plant Physiol. 170, 1460–1479. https://doi.org/10.1104/pp.15.01926

Ehleringer, J., White, J., Johnson, D.A., Brick, M., 1990. Carbon isotope discrimination, photosynthetic gas exchange, and transpiration efficiency in beans and range grasses. Acta Oecologica 11, 611–625.

Eichhorn, M.P., Paris, P., Herzog, F., Incoll, L.D., Liagre, F., Mantzanas, K., Mayus, M., Moreno, G., Papanastasis, V.P., Pilbeam, D.J., Pisanelli, A., Dupraz, C., 2006. Silvoarable systems in Europe – past , present and future prospects. Agrofor. Syst. 67, 29–50. https://doi.org/10.1007/s10457-005-1111-7

Evans, R.D., 2001. Physiological mechanisms influencing plant nitrogen isotope composition. Trends Plant Sci. 6, 121–126. https://doi.org/10.1016/S1360-1385(01)01889-1

Evans, R.D., Bloom, A.J., Sukrapanna, S.S., Ehleringer, J.R., 1996. Nitrogen isotope composition of tomato (*Lycopersicon esculentum* Mill. cv. T-5) grown under ammonium or nitrate nutrition. Plant, Cell Environ. 19, 1317–1323. https://doi.org/10.1111/j.1365-3040.1996.tb00010.x

FAO, 2010. Challenges and opportunities for carbon sequestration in grassland systems. A technical report on grassland management and climate change mitigation, Integrated Crop Management. https://doi.org/10.3329/jard.v7i1.4430

FAO, 2005. Grasslands of the World. Food and Agriculture Organization of the United Nations (FAO), Rome.

FAO, 1998. World reference base for soil resources. Rome.

Farquhar, G., Richards, A.P., 1984. Isotopic Composition of Plant Carbon Correlates With Water-Use Efficiency of Wheat Genotypes. Aust. J. Plant Physiol. 11, 539–552. https://doi.org/10.1071/PP9840539

Farquhar, G.D., Ehleringer, J.R., Hubick, K.T., 1989. Carbon Isotope Discrimination and Photosynthesis. Annu. Rev. Plant Physiol. Plant Mol. Biol. 40, 503–537. https://doi.org/10.1146/annurev.pp.40.060189.002443

Farquhar, G.D., O'Leary, M.H., Berry, J.A., 1982. On the relationship between carbon isotope discrimination and the intercellular carbon dioxide concentration in leaves. Aust. J. Plant Physiol. 9, 121–137. https://doi.org/10.1071/PP9820121

Faurie, O., Soussana, J.F., Sinoquet, H., 1996. Radiation Interception, Partitioning and Use in Grass-Clover Mixtures. Ann. Bot. 77, 35–45. https://doi.org/10.1006/anbo.1996.0005

Ferrio, P., Resco, V., Williams, D., Serrano, L., Voltas, J., 2005. Stable isotopes in arid and semi-arid forest systems. Investig. Agrar. Sist. y Recur. For. 14, 371–382. https://doi.org/10.5424/srf/2005143-00929

Fick, S.E., Hijmans, R.J., 2017. WorldClim 2: new 1-km spatial resolution climate surfaces for global land areas. Int. J. Climatol. 37, 4302–4315. https://doi.org/10.1002/joc.5086

Filippa, G., Cremonese, E., Galvagno, M., Migliavacca, M., Morra di Cella, U., Petey, M., Siniscalco, C., 2015. Five years of phenological monitoring in a mountain grassland: inter-annual patterns and evaluation of the sampling protocol. Int. J. Biometeorol. 59, 1927–1937. https://doi.org/10.1007/s00484-015-0999-5

Finn, J.A., Kirwan, L., Connolly, J., Sebastià, M.T., Helgadottir, A., Baadshaug, O.H.,

Bélanger, G., Black, A., Brophy, C., Collins, R.P., Čop, J., Dalmannsdóttir, S., Delgado, I., Elgersma, A., Fothergill, M., Frankow-Lindberg, B.E., Ghesquiere, A., Golinska, B., Golinski, P., Grieu, P., Gustavsson, A.-M., Höglind, M., Huguenin-Elie, O., Jørgensen, M., Kadziuliene, Z., Kurki, P., Llurba, R., Lunnan, T., Porqueddu, C., Suter, M., Thumm, U., Lüscher, A., 2013. Ecosystem function enhanced by combining four functional types of plant species in intensively managed grassland mixtures: a 3-year continental-scale field experiment. J. Appl. Ecol. 50, 365–375. https://doi.org/10.1111/1365-2664.12041

Fioretto, A., Papa, S., Pellegrino, A., Fuggi, A., 2008. Leaf litter decomposition dynamics in Mediteranean area, in: Tian-Xiao, L. (Ed.), Soil Ecology Research Developements. Nova Science Publishers, Inc., New York.

Flanagan, L.B., Johnson, B.G., 2005. Interacting effects of temperature, soil moisture and plant biomass production on ecosystem respiration in a northern temperate grassland. Agric. For. Meteorol. 130, 237–253. https://doi.org/10.1016/j.agrformet.2005.04.002

Foken, T., Gockede, M., Mauder, M., Mahrt, L., Amiro, B., Munger, W., 2004. Post-field data quality control, in: Handbook of Mcrometeorology. pp. 181–208. https://doi.org/10.1007/1-4020-2265-4_9

Fornara, D.A., Tilman, D., 2008. Plant functional composition influences rates of soil carbon and nitrogen accumulation. J. Ecol. 96, 314–322. https://doi.org/10.1111/j.1365-2745.2007.01345.x

Fox, J., Weisberg, S., 2011. An R Companion to Applied Regression. Second Edition, Second. ed. Sage, Thousand Oaks, CA.

Gallardo, A., 2003. Effect of tree canopy on the spatial distribution of soil nutrients in a Mediterranean Dehesa. Pedobiologia (Jena). 47, 117–125. https://doi.org/10.1078/0031-4056-00175

Gallardo, A., Rodr, J.J., Covelo, F., Fern, R., 2000. Soil nitrogen heterogeneity in a Dehesa ecosystem. Plant Soil 222, 71–82. https://doi.org/10.1023/A:100472592

Gaman, T., Firman, J., 2006. Oaks 2040. The Status and Future of Oaks in California. Oakland.

Gao, Q., Zhu, W., Schwartz, M.W., Ganjurjav, H., Wan, Y., 2016. Climatic change controls productivity variation in global grasslands. Sci. Rep. 6, 1–10. https://doi.org/10.1038/srep26958

García-González, R., 2008. Management of Natura 2000 habitats. Alpine and subalpine calcareous grasslands 6170, European Commission. https://doi.org/10.2779/61790

García-Ruiz, J.M., López-Moreno, I.I., Vicente-Serrano, S.M., Lasanta-Martínez, T., Beguería, S., 2011. Mediterranean water resources in a global change scenario. Earth-Science Rev. 105, 121–139. https://doi.org/10.1016/j.earscirev.2011.01.006

Gargallo-Garriga, A., Sardans, J., Pérez-Trujillo, M., Rivas-Ubach, A., Oravec, M., Vecerova, K., Urban, O., Jentsch, A., Kreyling, J., Beierkuhnlein, C., Parella, T., Peñuelas, J., 2014. Opposite metabolic responses of shoots and roots to drought. Sci. Rep. 4, 1–7. https://doi.org/10.1038/srep06829

Gea-Izquierdo, G., Montero, G., Cañellas, I., 2009. Changes in limiting resources determine spatio-temporal variability in tree-grass interactions. Agrofor. Syst. 76, 375–387. https://doi.org/10.1007/s10457-009-9211-4

Gee, G.W., Bauder, J.W., 1986. Particle size analysis, in: Klute, A. (Ed.), Methods of Soil Analysis. Part 1. Madison, pp. 383–409.

Ghashghaie, J., Badeck, F.W., 2014. Opposite carbon isotope discrimination during dark respiration in leaves versus roots – a review. New Phytol. 201, 751–769. https://doi.org/10.1111/nph.12563

Gilgen, A.K., Buchmann, N., 2009. Response of temperate grasslands at different altitudes to simulated summer drought differed but scaled with annual precipitation.

Biogeosciences 6, 2525–2539. https://doi.org/10.5194/bg-6-2525-2009

Gilmanov, T.G., Aires, L., Barcza, Z., Baron, V.S., Belelli, L., Beringer, J., Billesbach, D., Bonal, D., Bradford, J., Ceschia, E., Cook, D., Corradi, C., Frank, A., Gianelle, D., Gimeno, C., Gruenwald, T., Guo, H., Hanan, N., Haszpra, L., Heilman, J., Jacobs, A., Jones, M.B., Johnson, D.A., Kiely, G., Li, S., Magliulo, V., Moors, E., Nagy, Z., Nasyrov, M., Owensby, C., Pinter, K., Pio, C., Reichstein, M., Sanz, M.J., Scott, R., Soussana, J.F., Stoy, P.C., Svejcar, T., Tuba, Z., Zhou, G., 2010. Productivity, Respiration, and Light-Response Parameters of World Grassland and Agroecosystems Derived From Flux-Tower Measurements. Rangel. Ecol. Manag. 63, 16–39. https://doi.org/10.2111/REM-D-09-00072.1

Gilmanov, T.G., Soussana, J.F., Aires, L., Allard, V., Ammann, C., Balzarolo, M., Barcza, Z., Bernhofer, C., Campbell, C.L., Cernusca, A., Cescatti, A., Clifton-Brown, J., Dirks, B.O.M., Dore, S., Eugster, W., Fuhrer, J., Gimeno, C., Gruenwald, T., Haszpra, L., Hensen, A., Ibrom, A., Jacobs, A.F.G., Jones, M.B., Lanigan, G., Laurila, T., Lohila, A., Manca, G., Marcolla, B., Nagy, Z., Pilegaard, K., Pinter, K., Pio, C., Raschim, A., Rogiers, N., Sanz, M.J., Stefanim, P., Sutton, M., Tuba, Z., Valentini, R., Williams, M.L., Wohlfahrt, G., 2007. Partitioning European grassland net ecosystem CO_2 exchange into gross primary productivity and ecosystem respiration using light response function analysis. Agric. Ecosyst. Environ. 121, 93–120. https://doi.org/10.1016/j.agee.2006.12.008

Giunta, F., Pruneddu, G., Motzo, R., 2009. Radiation interception and biomass and nitrogen accumulation in different cereal and grain legume species. F. Crop. Res. 110, 76–84. https://doi.org/10.1016/j.fcr.2008.07.003

Göckede, M., Foken, T., Aubinet, M., Aurela, M., Banza, J., Bernhofer, C., Bonnefond, J.M., Brunet, Y., Carrara, A., Clement, R., 2008. Quality control of CarboEurope flux data–Part I: Footprint analyses to evaluate sites in forest ecosystems. Biogeosciences Discuss. 5, 433–450. https://doi.org/10.5194/bg-5-433-2008

Goering, H.K., Soest, P.J. Van, 1970. Forage fiber analyses (Apparatus, Reagents, Procedures, and Some Applications). Agric. Handb. 379, 1–20.

Gogoi, N., Baruah, K.K., Gogoi, B., Gupta, Prabhat, K., 2005. Methane emission characteristics and its relations with plant and soil parameters under irrigated rice ecosystem of northeast India. Chemosphere 59, 1677–1684. https://doi.org/10.1016/j.chemosphere.2004.11.047

Gomez-Casanovas, N., Matamala, R., Cook, D.R., Gonzalez-Meler, M.A., 2012. Net ecosystem exchange modifies the relationship between the autotrophic and heterotrophic components of soil respiration with abiotic factors in prairie grasslands. Glob. Chang. Biol. 18, 2532–2545. https://doi.org/10.1111/j.1365-2486.2012.02721.x

Gómez-Rey, M.X., Madeira, M., Gonzalez-Prieto, S.J., Coutinho, J., 2013. Soil C and N dynamics in a Mediterranean oak woodland with shrub encroachment. Plant Soil 371, 339–354. https://doi.org/10.1007/s11104-013-1695-z

Groemping, U., 2006. Relative Importance for Linear Regression in R: The Package relaimpo. J. Stat. Softw. 17, 1–27. https://doi.org/10.18637/jss.v017.i01

Hartmann, D.L., Klein Tank, A.M.G., Rusticucci, M., Alexander, L.V., Brönnimann, S., Charabi, Y., Dentener, F.J., Dlugokencky, E.J., Easterling, D.R., Kaplan, A., Soden, B.J., Thorne, P.W., Wild, M., Zhai, P.M., 2013. Observations: Atmosphere and Surface, in: Stocker, T.F., Qin, D., Plattner, G.-K., Tignor, M., Allen, S.K., Boschung, J., Nauels, A., Xia, Y., Bex, V., Midgley, P.M. (Eds.), Climate Change 2013: The Physical Science Basis. Contribution of Working Group I to the Fifth Assessment Report of the Intergovernmental Panel on Climate Change. Cambridge University Press, Cambridge and New York, pp. 159–254.

Hector, A., Schmid, B., Beierkuhnlein, C., Caldeira, M.C., Diemer, M., Dimitrakopoulos, P.G., Finn, J.A., Freitas, H., Giller, P.S., Good, J., Harris, R., Ho, P., Leadley, P.W.,

Loreau, M., Minns, A., Mulder, C.P.H., Donovan, G.O., Otway, S.J., Pereira, J.S., Prinz, A., Read, D.J., Schulze, E., Siamantziouras, A.D., Yachi, S., Lawton, J.H., 1999. Plant Diversity and Productivity Experiments in European Grasslands. Science (80-.). 286, 1123–1127. https://doi.org/10.1126/science.286.5442.1123

Heimann, M., Reichstein, M., 2008. Terrestrial ecosystem carbon dynamics and climate feedbacks. Nature 451, 289–292. https://doi.org/10.1038/nature06591

Helsel, D.R., 1990. Less than obvious: Statistical treatment of data below the detection limit. Environ. Sci. Technol. 24, 1766–1774. https://doi.org/10.1021/es00082a001

Hernandez, P., Picon-Cochard, C., 2016. Presence of *Trifolium repens* Promotes Complementarity of Water Use and N Facilitation in Diverse Grass Mixtures. Front. Plant Sci. 7, 1–14. https://doi.org/10.3389/fpls.2016.00538

Hilbert, D.W., Reynolds, J.F., 1991. A Model Allocating Growth Among Leaf Proteins, Shoot Structure, and Root Biomass to Produce Balanced Activity. Ann. Bot. 68, 417–425. https://doi.org/10.1093/oxfordjournals.aob.a088273

Hofer, D., Suter, M., Buchmann, N., Lüscher, A., 2017. Nitrogen status of functionally different forage species explains resistance to severe drought and post-drought overcompensation. Agric. Ecosyst. Environ. 236, 312–322. https://doi.org/10.1016/j.agee.2016.11.022

Holmgren, M., Scheffer, M., Huston, M.A., 1997. The Interplay of Facilitation and Competition in Plant Communities. Ecology 78, 1966–1975. https://doi.org/10.1890/0012-9658(1997)078[1966:TIOFAC]2.0.CO;2

Hooper, D.U., Chapin, F.S., Ewel, J.J., Hector, A., Inchausti, P., Lavorel, S., Lodge, D.M., Loreau, M., Naeem, S., Schmid, B., Setälä, H., Symstad, A.J., Vandermeer, J., Wardle, D.A., 2005. Effects of Biodiversity on Ecosystem Functioning: A Consensus of Current Knowledge. Ecol. Monogr. 75, 3–35. https://doi.org/10.1890/04-0922

Hörtnagl, L., Barthel, M., Buchmann, N., Eugster, W., Butterbach-Bahl, K., Díaz-Pinés,

E., Zeeman, M., Klumpp, K., Kiese, R., Bahn, M., Hammerle, A., Lu, H., Ladreiter-Knauss, T., Burri, S., Merbold, L., 2018. Greenhouse gas fluxes over managed grasslands in Central Europe. Glob. Chang. Biol. 24, 1843–1872. https://doi.org/10.1111/gcb.14079

Howlett, D.S., Moreno, G., Mosquera Losada, M.R., Nair, P.K.R., Nair, V.D., 2011. Soil carbon storage as influenced by tree cover in the Dehesa cork oak silvopasture of central-western Spain. J. Environ. Monit. 13, 1897–1904. https://doi.org/10.1039/c1em10059a

Huntsinger, L., Campos, P., Starrs, P.F., Oviedo, J.L., Díaz, M., Standiford, R.B., Gregorio, M., 2013. Working Landscapes of the Spanish Dehesa and California Oak Woodlands: An Introduction, in: Campos, P., Huntsinger, L., Oviedo, Jose L., Starrs, P.F., Diaz, M., Standiford, R.B., Montero, G. (Eds.), Mediterranean Oak Woodland Working Landscapes. Dehesas of Spain and Ranchlands of California. Springer New York, pp. 3–23. https://doi.org/10.1007/978-94-007-6707-2

Hussain, M.Z., Otieno, D.O., Mirzae, H., Li, Y.L., Schmidt, M.W.T., Siebke, L., Foken, T., Ribeiro, N.A., Pereira, J.S., Tenhunen, J.D., 2009. CO_2 exchange and biomass development of the herbaceous vegetation in the Portuguese montado ecosystem during spring. Agric. Ecosyst. Environ. 132, 143–152. https://doi.org/10.1016/j.agee.2009.03.008

Huyghe, C., De Vliegher, A., van Gils, B., Alain, P., 2014. Grasslands and herbivore production in Europe and effects of common policies. Editions Quae, Cedex.

Imer, D., Merbold, L., Eugster, W., Buchmann, N., 2013. Temporal and spatial variations of soil CO_2, CH_4 and N_2O fluxes at three differently managed grasslands. Biogeosciences 10, 5931–5945. https://doi.org/10.5194/bg-10-5931-2013

Iqbal, J., Castellano, M.J., Parkin, T.B., 2013. Evaluation of photoacoustic infrared spectroscopy for simultaneous measurement of N_2O and CO_2 gas concentrations

and fluxes at the soil surface. Glob. Chang. Biol. 19, 327–336. https://doi.org/10.1111/gcb.12021

Jugold, A., Althoff, F., Hurkuck, M., Greule, M., Lenhart, K., Lelieveld, J., Keppler, F., 2012. Non-microbial methane formation in oxic soils. Biogeosciences 9, 5291–5301. https://doi.org/10.5194/bg-9-5291-2012

Kahmen, A., Buchmann, N., 2007. Addressing the Functional Value of Biodiversity for Ecosystem Functioning Using Stable Isotopes, in: Terrestrial Ecology. pp. 345–359. https://doi.org/10.1016/S1936-7961(07)01022-6

Kahmen, A., Perner, J., Audorff, V., Weisser, W., Buchmann, N., 2005. Effects of plant diversity, community composition and environmental parameters on productivity in montane European grasslands. Oecologia 142, 601–615. https://doi.org/10.1007/s00442-004-1749-2

Kalcsits, L.A., Buschhaus, H.A., Guy, R.D., 2014. Nitrogen isotope discrimination as an integrated measure of nitrogen fluxes, assimilation and allocation in plants. Physiol. Plant. 151, 293–304. https://doi.org/10.1111/ppl.12167

Kardol, P., Cregger, M.A., Campany, C.E., Classen, A.T., 2010. Soil ecosystem functioning under climate change: plant species and community effects. Ecology 91, 767–781. https://doi.org/10.1890/09-0135.1

Keppler, F., Hamilton, J.T.G., Braß, M., Ro, T., 2006. Methane emissions from terrestrial plants under aerobic conditions. Nat. Publ. Gr. 439, 187–192. https://doi.org/10.1038/nature04420

Keppler, F., Hamilton, J.T.G., Mcroberts, W.C., Vigano, I., Braß, M., Röckmann, T., 2008. Methoxyl groups of plant pectin as a precursor of atmospheric methane: evidence from deuterium labelling studies. New Phytol. 178, 808–814. https://doi.org/10.1111/j.1469-8137.2008.02411.x

Kirwan, L., Connolly, J., Finn, J.A., Brophy, C., Lüscher, A., Nyfeler, D., Sebastia, M.-T.,

2009. Diversity–interaction modeling: estimating contributions of species identities and interactions to ecosystem function. Ecology 90, 2032–2038. https://doi.org/10.1890/08-1684.1

Kirwan, L., Lüscher, A., Sebastià, M.T., Finn, J.A., Collins, R.P., Porqueddu, C., Helgadottir, A., Baadshaug, O.H., Brophy, C., Coran, C., Dalmannsdóttir, S., Delgado, I., Elgersma, A., Fothergill, M., Frankow-Lindberg, B.E., Golinski, P., Grieu, P., Gustavsson, A.M., Höglind, M., Huguenin-Elie, O., Iliadis, C., Jørgensen, M., Kadziuliene, Z., Karyotis, T., Lunnan, T., Malengier, M., Maltoni, S., Meyer, V., Nyfeler, D., Nykanen-Kurki, P., Parente, J., Smit, H.J., Humm, U.T., Connolly, J., 2007. Evenness drives consistent diversity effects in intensive grassland systems across 28 European sites. J. Ecol. 95, 530–539. https://doi.org/10.1111/j.1365-2745.2007.01225.x

Kljun, N., Calanca, P., Rotach, M.W., Schmid, H.P., 2004. A simple parametrisation for flux footprint predictions. Boundary-Layer Meteorol. 112, 503–523. https://doi.org/10.1023/B:BOUN.000

Korol, R.L., Kirschbaum, M.U.F., Farquhar, G.D., Jeffreys, M., 1999. Effects of water status and soil fertility on the C-isotope signature in *Pinus radiata*. Tree Physiol. 19, 551–562. https://doi.org/10.1093/treephys/19.9.551

Kutsch, W.L., Aubinet, M., Buchmann, N., Smith, P., Osborne, B., Eugster, W., Wattenbach, M., Schrumpf, M., Schulze, E.D., Tomelleri, E., Ceschia, E., Bernhofer, C., Béziat, P., Carrara, A., Di Tommasi, P., Grunwald, T., Jones, M., Magliulo, V., Marloie, O., Moureaux, C., Olioso, A., Sanz, M.J., Saunders, M., Søgaard, H., Ziegler, W., 2010. The net biome production of full crop rotations in Europe. Agric. Ecosyst. Environ. 139, 336–345. https://doi.org/10.1016/j.agee.2010.07.016

Langford, B., Misztal, P.K., Nemitz, E., Davison, B., Helfter, C., Pugh, T.A.M., MacKenzie, A.R., Lim, S.F., Hewitt, C.N., 2010. Fluxes and concentrations of volatile organic

compounds from a South-East Asian tropical rainforest. Atmos. Chem. Phys. 10, 8391–8412. https://doi.org/10.5194/acp-10-8391-2010

Larsen, K.S., Ibrom, A., Beier, C., Jonasson, S., Michelsen, A., 2007. Ecosystem respiration depends strongly on photosynthesis in a temperate heath. Biogeochemistry 85, 201–213. https://doi.org/10.1007/s10533-007-9129-8

Lavorel, S., Garnier, E., 2002. Predicting changes in community composition and ecosystem functioning from plant traits: revisiting the Holy Grail. Funct. Ecol. 16, 545–556. https://doi.org/10.1046/j.1365-2435.2002.00664.x

Law, B.E., Falge, E., Gu, L., Baldocchi, D.D., Bakwin, P., Berbigier, P., Davis, K., Dolman, A.J., Falk, M., Fuentes, J.D., Goldstein, A., Granier, A., Grelle, A., Hollinger, D., Janssens, I.A., Jarvis, P., Jensen, N.O., Katul, G., Mahli, Y., Matteucci, G., Meyers, T., Monson, R., Munger, W., Oechel, W., Olson, R., Pilegaard, K., Paw U, K.T., Thorgeirsson, H., Valentini, R., Verma, S., Vesala, T., Wilson, K., Wofsy, S., 2002. Environmental controls over carbon dioxide and water vapor exchange of terrestrial vegetation. Agric. For. Meteorol. 113, 97–120. https://doi.org/10.1016/S0168-1923(02)00104-1

Lee, T.D., Reich, P.B., Tjoelker, M.G., 2003. Legume presence increases photosynthesis and N concentrations of co-occurring non-fixers but does not modulate their responsiveness to carbon dioxide enrichment. Oecologia 137, 22–31. https://doi.org/10.1007/s00442-003-1309-1

Legendre, P., Legendre, L.F.J., 1998. Numerical Ecology, Developments in Environmental Modelling. Elsevier Science.

Leifeld, J., Meyer, S., Budge, K., Sebastia, M.T., Zimmermann, M., Fuhrer, J., 2015. Turnover of grassland roots in mountain ecosystems revealed by their radiocarbon signature: Role of temperature and management. PLoS One 10, 1–13. https://doi.org/10.1371/journal.pone.0119184

Leitinger, G., Ruggenthaler, R., Hammerle, A., Lavorel, S., Schirpke, U., Clement, J.-C., Lamarque, P., Obojes, N., Tappeiner, U., 2015. Impact of droughts on water provision in managed alpine grasslands in two climatically different regions of the Alps. Ecohydrology 8, 1600–1613. https://doi.org/10.1002/eco.1607

Li, J., Wang, G., Zhang, R., Li, L., 2016. A negative relationship between foliar carbon isotope composition and mass-based nitrogen concentration on the eastern slope of mount gongga, China. PLoS One 11, 1–14. https://doi.org/10.1371/journal.pone.0166958

Lin, S., Iqbal, J., Hu, R., Cai, J., Shaaban, M., Chen, X., 2013. Nitrous Oxide Emissions from Yellow Brown Soil as Affected by Incorporation of Crop Residues With Different Carbon-to-Nitrogen Ratios: A Case Study in Central China. Arch. Environ. Contam. Toxicol. 65, 183–192. https://doi.org/10.1007/s00244-013-9903-7

Liu, H., Carvalhais, L.C., Crawford, M., Singh, E., Dennis, P.G., Pieterse, C.M.J., Schenk, P.M., 2017. Inner Plant Values: Diversity, Colonization and Benefits from Endophytic Bacteria. Front. Microbiol. 8, 1–17. https://doi.org/10.3389/fmicb.2017.02552

Liu, M., Gong, J.R., Pan, Y., Luo, Q.P., Zhai, Z.W., Xu, S., Yang, L.L., 2016. Effects of grass-legume mixtures on the production and photosynthetic capacity of constructed grasslands in Inner Mongolia, China. Crop Pasture Sci. 67, 1188–1198. https://doi.org/10.1071/CP16063

Lopez-Carrasco, C., Lopez-Sanchez, A., San Miguel, A., Roig, S., 2015. The effect of tree cover on the biomass and diversity of the herbaceous layer in a Mediterranean dehesa. Grass Forage Sci. 70, 639–650. https://doi.org/10.1111/gfs.12161

Luo, G.J., Kiese, R., Wolf, B., Butterbach-Bahl, K., 2013. Effects of soil temperature and moisture on methane uptakes and nitrous oxide emissions across three different ecosystem types. Biogesciences Discuss. 10, 927–965. https://doi.org/10.5194/bgd-10-927-2013

Ma, S., Baldocchi, D.D., Xu, L., Hehn, T., 2007. Inter-annual variability in carbon dioxide exchange of an oak/grass savanna and open grassland in California. Agric. For. Meteorol. 147, 157–171. https://doi.org/10.1016/j.agrformet.2007.07.008

Marañon, A., 1985. Diversidad floristica y heterogenidad ambiental en una dehesa de Sierra Morena. An Edafol. Agro- biol 44, 1183–1197.

Marañón, T., 1986. Plant species richness and canopy effect in the savanna-like “dehesa” of S.W. Spain. Ecol. Mediterr. 12, 131–141.

Marañon, T., Bartolomé, J.W., 1993. Reciprocal transplants of herbaceous communities between *Quercus agrifolia* woodland and adjacent grassland. J. Ecol. 81, 673–682. https://doi.org/10.2307/2261665

Marañón, T., Pugnaire, F.I., Callaway, R.M., 2009. Mediterranean-climate oak savannas: The interplay between abiotic environment and species interactions. Web Ecol. 9, 30–43. https://doi.org/10.5194/we-9-30-2009

Maris, S.C., Lloveras, J., Vallejo, A., Teira-Esmatges, M.R., 2018. Effect of Stover Management and Nitrogen Fertilization on N_2O and CO_2 Emissions from Irrigated Maize in a High Nitrate Mediterranean Soil. Water. Air. Soil Pollut. 229, 1–17. https://doi.org/10.1007/s11270-017-3660-6

Mendiburu, F., 2017. agricolae: Statistical Procedures for Agricultural Research. R Packag. version 1.2-8. https//CRAN.R-project.org/package=agricolae.

Merbold, L., Eugster, W., Stieger, J., Zahniser, M., Nelson, D., Buchmann, N., 2014. Greenhouse gas budget (CO_2, CH_4 and N_2O) of intensively managed grassland following restoration. Glob. Chang. Biol. 20, 1913–1928. https://doi.org/10.1111/gcb.12518

Metcalfe, D.B., Fisher, R.A., Wardle, D.A., 2011. Plant communities as drivers of soil respiration: Pathways, mechanisms, and significance for global change. Biogeosciences 8, 2047–2061. https://doi.org/10.1016/j.ausmj.2011.10.011

Milcu, A., Roscher, C., Gessler, A., Bachmann, D., Gockele, A., Guderle, M., Landais, D., Piel, C., Escape, C., Devidal, S., Ravel, O., Buchmann, N., Gleixner, G., Hildebrandt, A., Roy, J., 2014. Functional diversity of leaf nitrogen concentrations drives grassland carbon fluxes. Ecol. Lett. 17, 435–444. https://doi.org/10.1111/ele.12243

Minchin, F.R., Witty, J.F., 2005. Respiratory/Carbon Costs of Symbiotic Nitrogen Fixation in Legumes, in: Lambers, H., Ribas-Carbo, M. (Eds.), Plant Respiration. Advances in Photosynthesis and Respiration, Vol. 18. Springer, Dordrecht, pp. 195–205. https://doi.org/10.1007/1-4020-3589-6_11

Mitchell, R.M., Bakker, J.D., 2016. Grass abundance shapes trait distributions of forbs in an experimental grassland. J. Veg. Sci. 27, 557–567. https://doi.org/10.1111/jvs.12389

Moffat, A.M., 2012. A new methodology to interpret high resolution measurements of net carbon fluxes between terrestrial ecosystems and the atmosphere. Ph.D. thesis, Friedrich-Schiller-Universität, Jena, Germany, 124 pp.

Moncrieff, J., Clement, R., Finnigan, J., Meyers, T., 2004. Averaging, Detrending, and Filtering of Eddy Covariance Time Series., in: Lee, X., Massman, W., Law, B. (Eds.), Handbook of Micrometeorology. Atmospheric and Oceanographic Sciences Library, Vol 29. Springer, Dordrecht. https://doi.org/10.1007/1-4020-2265-4_2

Moncrieff, J.B., Massheder, J.M., de Bruin, H., Elbers, J., Friborg, T., Heusinkveld, B., Kabat, P., Scott, S., Soegaard, H., Verhoef, A., 1997. A system to measure surface fluxes of momentum, sensible heat, water vapour and carbon dioxide. J. Hydrol. 188–189, 589–611. https://doi.org/10.1016/S0022-1694(96)03194-0

Moody, L.B., Li, H., Burns, R.T., Xin, H., Gates, R.S., Hoff, S.J., Overhults, D.G., 2008. A quality assurance project plan for monitoring gaseous and particulate matter emissions from broiler housing. Am. Soc. Agric. Biol. Eng. 1–27.

https://doi.org/10.13031/2013.25340

Moors, E.J., Jacobs, C., Jans, W., Supit, I., Kutsch, W.L., Bernhofer, C., Béziat, P., Buchmann, N., Carrara, A., Ceschia, E., Elbers, J., Eugster, W., Kruijt, B., Loubet, B., Magliulo, E., Moureaux, C., Olioso, A., Saunders, M., Soegaard, H., 2010. Variability in carbon exchange of European croplands. Agric. Ecosyst. Environ. 139, 325–335. https://doi.org/10.1016/j.agee.2010.04.013

Moreno, G., 2008. Response of understorey forage to multiple tree effects in Iberian dehesas. Agric. Ecosyst. Environ. 123, 239–244. https://doi.org/10.1016/j.agee.2007.04.006

Moreno, G., Obrador, J.J., García, A., 2007. Impact of evergreen oaks on soil fertility and crop production in intercropped dehesas. Agric. Ecosyst. Environ. 119, 270–280. https://doi.org/10.1016/j.agee.2006.07.013

Mulder, C.P.H., Jumpponen, A., Högberg, P., 2002. How plant diversity and legumes affect nitrogen dynamics in experimental grassland communities. Community Ecol. 133, 412–421. https://doi.org/10.1007/s00442-002-1043-0

Nakano, T., Shinoda, M., 2014. Modeling gross primary production and ecosystem respiration in a semiarid grassland of Mongolia. Soil Sci. Plant Nutr. 61, 106–115. https://doi.org/10.1080/00380768.2014.966043

Ninyerola, M., Pons, X., Roure, J.M., 2000. A methodological approach of climatological modelling of air temperature and precipitation through GIS techniques. Int. J. Climatol. 20, 1823–1841. https://doi.org/10.1002/1097-0088(20001130)20:14<1823::AID-JOC566>3.0.CO;2-B

Nisbet, R.E.R., Fisher, R., Nimmo, R.H., Bendall, D.S., Crill, P.M., Gallego-Sala, A. V., Hornibrook, E.R.C., López-Juez, E., Lowry, D., Nisbet, P.B.R., Shuckburgh, E.F., Sriskantharajah, S., Howe, C.J., Nisbet, E.G., 2009. Emission of methane from plants. Proc. R. Soc. B Biol. Sci. 276, 1347–1354.

https://doi.org/10.1098/rspb.2008.1731

Niu, S., Luo, Y., Fei, S., Yuan, W., Schimel, D., Law, B.E., Ammann, C., Arain, M.A., Arneth, A., Aubinet, M., Barr, A., Beringer, J., Bernhofer, C., Black, T.A., Buchmann, N., Cescatti, A., Chen, J., Davis, K.J., Dellwik, E., Desai, A.R., Etzold, S., Francois, L., Gianelle, D., Gielen, B., Goldstein, A., Gu, L., Hanan, N., Helfter, C., Hirano, T., Hollinger, D.Y., Mike, B., Kiely, G., Kolb, T.E., Kutsch, W.L., Lafleur, P., Lawrence, D.M., Lindroth, A., Litvak, M., Loustau, D., Lund, M., Marek, M., Martin, T.A., Matteucci, G., Migliavacca, M., Montagnani, L., Moors, E., Munger, J.W., Oechel, W., Olejnik, J., U, K.T.P., Pilegaard, K., Rambal, S., Spano, D., Stoy, P., Sutton, M.A., Varlagin, A., Scott, R.L., 2012. Thermal optimality of net ecosystem exchange of carbon dioxide and underlying mechanisms. New Phytol. 194, 775–783. https://doi.org/10.1111/j.1469-8137.2012.04095.x

Niu, S., Sherry, R.A., Zhou, X., Luo, Y., 2013. Ecosystem Carbon Fluxes in Response to Warming and Clipping in a Tallgrass Prairie. Ecosystems 16, 948–961. https://doi.org/10.1007/s10021-013-9661-4

Nyfeler, D., Huguenin-Elie, O., Suter, M., Frossard, E., Connolly, J., Lüscher, A., 2009. Strong mixture effects among four species in fertilized agricultural grassland led to persistent and consistent transgressive overyielding. J. Appl. Ecol. 46, 683–691. https://doi.org/10.1111/j.1365-2664.2007.0

Nyfeler, D., Huguenin-Elie, O., Suter, M., Frossard, E., Lüscher, A., 2011. Grass-legume mixtures can yield more nitrogen than legume pure stands due to mutual stimulation of nitrogen uptake from symbiotic and non-symbiotic sources. Agric. Ecosyst. Environ. 140, 155–163. https://doi.org/10.1016/j.agee.2010.11.022

O'Mara, F.P., 2012. The role of grasslands in food security and climate change. Ann. Bot. 110, 1263–1270. https://doi.org/10.1093/aob/mcs209

Oelmann, Y., Wilcke, W., Temperton, V.M., Buchmann, N., Roscher, C., Schumacher, J.,

Schulze, E., Weisser, W.W., 2007. Soil and Plant Nitrogen Pools as Related to Plant Diversity in an Experimental Grassland. Soil Biol. Biochem. 71, 720–729. https://doi.org/10.2136/sssaj2006.0205

Oertel, C., Matschullat, J., Zurba, K., Zimmermann, F., Erasmi, S., 2016. Greenhouse gas emissions from soils — A review. Chemie der Erde 76, 327–352. https://doi.org/10.1016/j.chemer.2016.04.002

Oksanen, J., Blanchet, F.G., Friendly, M., Kindt, R., Legendre, P., McGlinn, D., Minchin, P.R., O'Hara, R.B., Simpson, G.L., Solymos, P., Stevens, M.H.H., Szoecs, E., Wagner, H., 2018. vegan: Community Ecology Package. R Packag. version 2.5-1. https//CRAN.R-project.org Packag.

Olea, L., López-Bellido, R.J., Poblaciones, M., 2005. Europe types of silvopastoral systems in the Mediterranean area: Dehesa, in: Mosquera-Losada, M.R., Rigueiro-Rodríguez, A., McAdam, J. (Eds.), Silvopastoralism and Sustainable Land Management. Proceedings of an International Congress on Silvopastoralism and Sustainable Management Held in Lugo, Spain, April 2004. pp. 30–35. https://doi.org/10.1079/9781845930011.0030

Oliveira, A.L.M., Canuto, E.L., Silva, E.E., Reis, V.M., Baldani, J.I., 2004. Survival of endophytic diazotrophic bacteria in soil under different moisture conditions. Brazilian J. Microbiol. 35, 295–299. https://doi.org/10.1590/S1517-83822004000300005

Olsvig-Whittaker, L.S., Naveh, Z., Giskin, M., Nevo, E., 1992. Microsite differentiation in a Mediterranean oak savanna. J. Veg. Sci. 3, 209–216. https://doi.org/10.2307/3235681

Orwin, K.H., Ostle, N., Wilby, A., Bardgett, R.D., 2014. Effects of species evenness and dominant species identity on multiple ecosystem functions in model grassland communities. Oecologia 174, 979–992. https://doi.org/10.1007/s00442-013-2814-5

Papale, D., 2012. Data Gap Filling, in: Aubinet, M., Vesala, T., Papale, D. (Eds.), Eddy Covariance: A Practical Guide to Measurement and Data Analysis. London and New York, pp. 159–172. https://doi.org/10.1007/978-94-007-2351-1_6

Pausch, J., Kuzyakov, Y., 2018. Carbon input by roots into the soil: Quantification of rhizodeposition from root to ecosystem scale. Glob. Chang. Biol. 24, 1–12. https://doi.org/10.1111/gcb.13850

Peel, M.C., Finlayson, B.L., McMahon, T.A., 2007. Updated world map of the Köppen-Geiger climate classification. Hydrol. Earth Syst. Sci. 11, 1633–1644. https://doi.org/10.5194/hess-11-1633-2007

Petchey, O.L., Gaston, K.J., 2006. Functional diversity: Back to basics and looking forward. Ecol. Lett. 9, 741–758. https://doi.org/10.1111/j.1461-0248.2006.00924.x

Pinheiro, J.C., Bates, D., DebRoy, S., Sarkar, D., 2015. nlme: Linear and Nonlinear Mixed Effects Models. R package version 3.1-121.

Pinheiro, J.C., Bates, D.M., 2000. Mixed-effects models in S and S-PLUS. Springer New York. https://doi.org/10.1007/b98882

Pirhofer-Walzl, K., Rasmussen, Jim, Høgh-Jensen, H., Eriksen, J., Søegaard, K., Rasmussen, Jesper, 2012. Nitrogen transfer from forage legumes to nine neighbouring plants in a multi-species grassland. Plant Soil 350, 71–84. https://doi.org/10.1007/s11104-011-0882-z

Porqueddu, C., Ates, S., Louhaichi, M., Kyriazopoulos, A.P., Moreno, G., del Pozo, A., Ovalle, C., Ewing, M.A., Nichols, P.G.H., 2016. Grasslands in “Old World” and “New World” Mediterranean-climate zones: Past trends, current status and future research priorities. Grass Forage Sci. 71, 1–35. https://doi.org/10.1111/gfs.12212

Porta Casanellas, J., López-Acevedo Reguerín, M., Rodríguez Ochoa, R., 1986. Determinación de pH y conductividad eléctrica en extractos acuosos 1/5 (p/v), in: Col·legi Oficial d’Enginyers Agrònoms de Catalunya (Ed.), Técnicas y Experimentos

En Edafología. Col·legi d'Enginyers Agrònoms de Catalunya, Universidad Politécnica de Cataluña, Escola Tècnica Superior d'Enginyers Agrònoms de Lleida.

Porter, S., Ward, R.C., Bell, H.F., 1988. The detection limit. Environ. Sci. Technol. 22, 856–861. https://doi.org/10.1021/ es00173a001

Postgate, J., 1998. Nitrogen Fixation. Cambridge University Press, Cambridge.

Praeg, N., Wagner, A.O., Illmer, P., 2017. Plant species, temperature, and bedrock affect net methane flux out of grassland and forest soils. Plant Soil 410, 193–206. https://doi.org/10.1007/s11104-016-2993-z

Pulido-Fernández, M., Schnabel, S., Lavado-Contador, J.F., Miralles Mellado, I., Ortega Pérez, R., 2013. Soil organic matter of Iberian open woodland rangelands as influenced by vegetation cover and land management. Catena 109, 13–24. https://doi.org/10.1016/j.catena.2013.05.002

Reich, P.B., Buschena, C., Tjoelker, M.G., Wrage, K., Knops, J., Tilman, D., Machado, J.L., 2003. Variation in growth rate and ecophysiology among 34 grassland and savanna species under contrasting N supply: A test of functional group differences. New Phytol. 157, 617–631. https://doi.org/10.1046/j.1469-8137.2003.00703.x

Reich, P.B., Ellsworth, D.S., Walters, M.B., 1998. Leaf Structure (Specific Leaf Area) Modulates Photosynthesis-Nitrogen relations: Evidence from within Across Species and Functional Groups. Funct. Ecol. 12, 948–958. https://doi.org/10.1046/j.1365-2435.1998.00274.x

Reich, P.B., Tjoelker, M.G., Pregitzer, K.S., Wright, I.J., Oleksyn, J., Machado, J.L., 2008. Scaling of respiration to nitrogen in leaves, stems and roots of higher land plants. Ecol. Lett. 11, 793–801. https://doi.org/10.1111/j.1461-0248.2008.01185.x

Reich, P.B., Walters, M.B., Ellsworth, D.S., 1997. From tropics to tundra: Global convergence in plant functioning. Ecology 94, 13730–13734. https://doi.org/10.1073/pnas.94.25.13730

Reichstein, M., Falge, E., Baldocchi, D., Papale, D., Aubinet, M., Berbigier, P., Bernhofer, C., Buchmann, N., Gilmanov, T., Granier, A., Grünwald, T., Havránková, K., Ilvesniemi, H., Janous, D., Knohl, A., Laurila, T., Lohila, A., Loustau, D., Matteucci, G., Meyers, T., Miglietta, F., Ourcival, J.M., Pumpanen, J., Rambal, S., Rotenberg, E., Sanz, M., Tenhunen, J., Seufert, G., Vaccari, F., Vesala, T., Yakir, D., Valentini, R., 2005. On the separation of net ecosystem exchange into assimilation and ecosystem respiration: review and improved algorithm. Glob. Chang. Biol. 11, 1424–1439. https://doi.org/10.1111/j.1365-2486.2005.001002.x

Reichstein, M., Rey, A., Freibauer, A., Tenhunen, J., Valentini, R., Banza, J., Casals, P., Cheng, Y., Grünzweig, J.M., Irvine, J., Joffre, R., Law, B.E., Loustau, D., Miglietta, F., Oechel, W., Ourcival, J.-M., Pereira, J.S., Peressotti, A., Ponti, F., Qi, Y., Rambal, S., Rayment, M., Romanya, J., Rossi, F., Tedeschi, V., Tirone, G., Xu, M., Yakir, D., 2003. Modeling temporal and large-scale spatial variability of soil respiration from soil water availability, temperature and vegetation productivity indices. Global Biogeochem. Cycles 17, 1–15. https://doi.org/10.1029/2003gb002035

Reichstein, M., Tenhunen, J.D., Roupsard, O., Ourcival, J.M., Rambal, S., Miglietta, F., Peressotti, A., Pecchiari, M., Tirone, G., Valentini, R., 2002. Severe drought effects on ecosystem CO_2 and H_2O fluxes at three Mediterranean evergreen sites: revision of current hypotheses? Glob. Chang. Biol. 8, 999–1017. https://doi.org/10.1046/j.1365-2486.2002.00530.x

Ribas, A., Llurba, R., Gouriveau, F., Altimir, N., Connolly, J., Sebastià, M.T., 2015. Plant identity and evenness affect yield and trace gas exchanges in forage mixtures. Plant Soil 391, 93–108. https://doi.org/10.1007/s11104-015-2407-7

Rice, K.J., Nagy, E.S., 2000. Oak canopy effects on the distribution patterns of two annual grasses: The role of competition and soil nutrients. Am. J. Bot. 87, 1699–1706. https://doi.org/10.2307/2656747

Robinson, D., 2001. $\delta^{15}N$ as an integrator of the nitrogen cycle. Trends Ecol. Evol. 16, 153–162. https://doi.org/10.1016/S0169-5347(00)02098-X

Roldán Ruiz, I., 1993. Estudio de la organización espacial en los pastos mediterráneos. Ph.D. thesis, Departamento de Biología Vegetal y Ecología, Universidad de Sevilla, Sevilla, Spain, 235 pp.

Rossetti, I., Bagella, S., Cappai, C., Caria, M.C., Lai, R., Roggero, P.P., Martins, P., Sousa, J.P., Querner, P., Seddaiu, G., 2015. Isolated cork oak trees affect soil properties and biodiversity in a Mediterranean wooded grassland. Agric. Ecosyst. Environ. 202, 203–216. https://doi.org/10.1016/j.agee.2015.01.008

Roumet, C., Garnier, E., Suzor, H., Salager, J.L., Roy, J., 2000. Short and long-term responses of whole-plant gas exchange to elevated CO_2 in four herbaceous species. Environ. Exp. Bot. 43, 155–169. https://doi.org/10.1016/S0098-8472(99)00055-6

Ryan, M.G., Law, B.E., 2005. Interpreting, measuring, and modeling soil respiration. Biogeochemistry 73, 3–27. https://doi.org/10.1007/s10533-004-5167-7

Sánchez, B., Medina, F., Iglesias, A., 2013. Typical farming systems and trends in crop and soil management in Europe. Madrid.

Sandau, N., Rohr, R.P., Naisbit, R.E., Fabian, Y., Bruggisser, O.T., Kehrli, P., Aebi, A., Bersier, L.F., 2014. Including community composition in biodiversity-productivity models. Methods Ecol. Evol. 5, 815–823. https://doi.org/10.1111/2041-210X.12215

Santi, C., Bogusz, D., Franche, C., 2013. Biological nitrogen fixation in non-legume plants. Ann. Bot. 111, 743–767. https://doi.org/10.1093/aob/mct048

Santruckova, H., Bird, M.I., Lloyd, J., 2000. Microbial processes and carbon-isotope fractionation in tropical and temperate grassland soils. Funct. Ecol. 14, 108–114. https://doi.org/10.1046/j.1365-2435.2000.00402.x

Schaufler, G., Kitzler, B., Schindlbacher, A., Skiba, U., Sutton, M.A., Zechmeister-

Boltenstern, S., 2010. Greenhouse gas emissions from European soils under different land use: effects of soil moisture and temperature. Eur. J. Soil Sci. 61, 683–696. https://doi.org/10.1111/j.1365-2389.2010.01277.x

Schenk, H.J., Jackson, R.B., 2002. Rooting depths, lateral root spreads and below-ground / allometries of plants in water-limited ecosystems. J. Ecol. 90, 480–494. https://doi.org/10.1046/j.1365-2745.2002.00682.x

Schultz, R., Andrews, S., O'Reilly, L., Bouchard, V., Frey, S., 2011. Plant community composition more predictive than diversity of carbon cycling in freshwater wetlands. Wetlands 31, 965–977. https://doi.org/10.1007/s13157-011-0211-6

Schulze, E.D., Luyssaert, S., Ciais, P., Freibauer, A., Janssens, I.A., Soussana, J.F., Smith, P., Grace, J., Levin, I., Thiruchittampalam, B., Heimann, M., Dolman, A.J., Valentini, R., Bousquet, P., Peylin, P., Peters, W., Rödenbeck, C., Etiope, G., Vuichard, N., Wattenbach, M., Nabuurs, G.J., Poussi, Z., Nieschulze, J., Gash, J.H., 2009. Importance of methane and nitrous oxide for Europe's terrestrial greenhouse-gas balance. Nat. Geosci. 2, 842–850. https://doi.org/10.1038/ngeo686

Schwinning, S., Parsons, A.J., 1996. Analysis of the coexistence mechanisms for grasses and legumes in grazing systems. J. Ecol. 84, 799–813.

Sebastià, M.-T., 2007. Plant guilds drive biomass response to global warming and water availability in subalpine grassland. J. Appl. Ecol. 44, 158–167. https://doi.org/10.1111/j.1365-2664.2006.01232.x

Sebastià, M.-T., Kirwan, L., Connolly, J., 2008. Strong shifts in plant diversity and vegetation composition in grassland shortly after climatic change. J. Veg. Sci. 19, 299–306. https://doi.org/10.3170/2008-8-18356

Sebastià, M.-T., Palero, N., De Bello, F., 2011. Changes in management modify agro-diversity in sainfoin swards in the Eastern Pyrenees. Agron. Sustain. Dev. 31, 533–540. https://doi.org/10.1007/s13593-011-0008-2

Seddaiu, G., Bagella, S., Pulina, A., Cappai, C., Salis, L., Rossetti, I., Lai, R., Roggero, P.P., 2018. Mediterranean cork oak wooded grasslands: synergies and trade-offs between plant diversity, pasture production and soil carbon. Agrofor. Syst. 92, 893–908. https://doi.org/10.1007/s10457-018-0225-7

Senapati, N., Chabbi, A., Faé, A., Yeluripati, J.B., Smith, P., 2016. Modelling nitrous oxide emissions from mown-grass and grain-cropping systems: Testing and sensitivity analysis of DailyDayCent using high frequency measurements. Sci. Total Environ. 572, 955–977. https://doi.org/10.1016/j.scitotenv.2016.07.226

Shaaban, M., Peng, Q., Hu, R., Lin, S., Zhao, J., 2016. Soil Nitrous oxide and Carbon dioxide emissions following incorporation of above- and below-ground biomass of green bean. Int. J. Environ. Sci. Technol. 13, 179–186. https://doi.org/10.1007/s13762-015-0843-9

Sheffer, E., Canham, C.D., Kigel, J., Perevolotsky, A., 2015. Countervailing effects on pine and oak leaf litter decomposition in human-altered Mediterranean ecosystems. Oecologia 177, 1039–1051. https://doi.org/10.1007/s00442-015-3228-3

Shvaleva, A., Costa, F., Costa, J.M., Correia, A., Anderson, M., Lobo-do-vale, R., Fangueiro, D., Bicho, C., 2014. Comparison of methane, nitrous oxide fluxes and CO_2 respiration rates from a Mediterranean cork oak ecosystem and improved pasture. Plant Soil 374, 883–898. https://doi.org/10.1007/s11104-013-1923-6

Shvaleva, A., Siljanen, H.M.P., Correia, A., Silva, F.C., Lamprecht, R.E., Lobo-do-Vale, R., Bicho, C., Fangueiro, D., Anderson, M., Pereira, J.S., Chaves, M.M., Cruz, C., Martikainen, P.J., 2015. Environmental and microbial factors influencing methane and nitrous oxide fluxes in Mediterranean cork oak woodlands: Trees make a difference. Front. Microbiol. 6, 1–11. https://doi.org/10.3389/fmicb.2015.01104

Silva, J.P., Toland, J., Jones, W., Eldridge, J., Thorpe, E., O'Hara, E., 2008. LIFE and Europe´s grasslands. Restoring a forgotten habitat. European Comission,

Luxembourg. https://doi.org/10.2779/23028

Sjögersten, S., Alewell, C., Cecillon, L., Hagedorn, F., Jandl, R., Leifeld, J., Martinsen, V., Schindlbacher, A., Sebastia, M.T., Van Miegroet, H., 2011. Mountain soils in a changing climate – vulnerability of carbon stocks and ecosystem feedbacks, in: Jandl, R., Rodeghiero, M., Olsson, M. (Eds.), Soil Carbon in Sensitive European Ecosystems: From Science to Land Management. pp. 118–148. https://doi.org/10.1002/9781119970255.ch6

Sjögersten, S., Llurba, R., Ribas, À., Yanez-Serrano, A., Sebastià, M.-T., 2012. Temperature and Moisture Controls of C Fluxes in Grazed Subalpine Grasslands. Arctic, Antarct. Alp. Res. 44, 239–246. https://doi.org/10.1657/1938-4246-44.2.239

Smit, H.J., Metzger, M.J., Ewert, F., 2008. Spatial distribution of grassland productivity and land use in Europe. Agric. Syst. 98, 208–219. https://doi.org/10.1016/j.agsy.2008.07.004

Song, L., Bao, X., Liu, X., Zhang, Y., Christie, P., Fangmeier, A., Zhang, F., 2011. Nitrogen enrichment enhances the dominance of grasses over forbs in a temperate steppe ecosystem. Biogeosciences 8, 2341–2350. https://doi.org/10.5194/bg-8-2341-2011

Soussana, J.-F., Salètes, S., Smith, P., Schils, R., Ogle, S., 2004. Greenhouse gas emissions from European grasslands.

Soussana, J.F., Allard, V., Pilegaard, K., Ambus, P., Amman, C., Campbell, C., Ceschia, E., Clifton-Brown, J., Czobel, S., Domingues, R., Flechard, C., Fuhrer, J., Hensen, A., Horvath, L., Jones, M., Kasper, G., Martin, C., Nagy, Z., Neftel, A., Raschi, A., Baronti, S., Rees, R.M., Skiba, U., Stefani, P., Manca, G., Sutton, M., Tuba, Z., Valentini, R., 2007. Full accounting of the greenhouse gas (CO_2, N_2O, CH_4) budget of nine European grassland sites. Agric. Ecosyst. Environ. 121, 121–134. https://doi.org/10.1016/j.agee.2006.12.022

Soussana, J.F., Tallec, T., Blanfort, V., 2010. Mitigating the greenhouse gas balance of

ruminant production systems through carbon sequestration in grasslands. Animal 4, 334–350. https://doi.org/10.1017/s1751731109990784

Spohn, M., 2015. Microbial respiration per unit microbial biomass depends on litter layer carbon-to-nitrogen ratio. Biogeosciences 12, 817–823. https://doi.org/10.5194/bg-12-817-2015

Stehfest, E., Bouwman, L., 2006. N_2O and NO emission from agricultural fields and soils under natural vegetation: summarizing available measurement data and modeling of global annual emissions. Nutr. Cycl. Agroecosystems 74, 207–228. https://doi.org/10.1007/s10705-006-9000-7

Symstad, A.J., 2000. A Test of the Effects of Functional Group Richness and Composition on Grassland Invasibility. Ecology 81, 99–109. https://doi.org/10.1890/0012-9658(2000)081[0099:ATOTEO]2.0.CO;2

Tang, J., Baldocchi, D.D., 2005. Spatial-temporal variation in soil respiration in an oak-grass savanna ecosystem in California and its partitioning into autotrophic and heterotrophic components. Biogeochemistry 73, 183–207. https://doi.org/10.1007/s10533-004-5889-6

Thakur, M.P., Eisenhauer, N., 2015. Plant community determines the strength of top-down control in a soil food web motif. Sci. Rep. 5, 1–6. https://doi.org/10.1038/srep09134

Thilakarathna, M.S., McElroy, M.S., Chapagain, T., Papadopoulos, Y.A., Raizada, M.N., 2016. Belowground nitrogen transfer from legumes to non-legumes under managed herbaceous cropping systems. A review. Agron. Sustain. Dev. 36, 1–16. https://doi.org/10.1007/s13593-016-0396-4

Tilman, D., 1997. Distinguishing between the effects of species diversity and species composition. Oikos 80, 185. https://doi.org/10.2307/3546532

Tilman, D., Lehman, C.L., Thomson, K.T., 1997. Plant diversity and ecosystem

productivity: Theoretical considerations. Proc. Natl. Acad. Sci. 94, 1857–1861. https://doi.org/10.1073/pnas.94.5.1857

Tirol-Padre, A., Rai, M., Gathala, M., Sharma, S., Kumar, V., Sharma, P.C., Sharma, D.K., Wassmann, R., Ladha, J., 2014. Assessing the performance of the photo-acoustic infrared gas monitor for measuring CO_2, N_2O, and CH_4 fluxes in two major cereal rotations. Glob. Chang. Biol. 20, 287–299. https://doi.org/10.1111/gcb.12347

Uribe, C., Inclán, R., Hernando, L., Román, M., Clavero, M.A., Roig, S., Van Miegroet, H., 2015. Grazing, tilling and canopy effects on carbon dioxide fluxes in a Spanish dehesa. Agroforest Syst. 89, 305–318. https://doi.org/10.1007/s10457-014-9767-5

van der Merwe, N.J., Medina, E., 1991. The canopy effect, carbon isotope ratios and foodwebs in amazonia. J. Archaeol. Sci. 18, 249–259. https://doi.org/10.1016/0305-4403(91)90064-V

Van Soest, P.J., Robertson, J.B., Lewis, B.A., 1991. Methods for Dietary Fiber, Neutral Detergent Fiber, and Nonstarch Polysaccharides in Relation to Animal Nutrition. J. Dairy Sci. 74, 3583–3597. https://doi.org/10.3168/jds.s0022-0302(91)78551-2

Venables, W.N., Ripley, B.D., 2002. Modern Applied Statistics with S, 4th ed, Fourth Edition. Springer. Springer-Verlag New York, New York. https://doi.org/10.1007/978-0-387-21706-2

Vigano, I., Weelden, H. Van, Holzinger, R., Keppler, F., Mcleod, A., 2008. Effect of UV radiation and temperature on the emission of methane from plant biomass and structural components. Biogeosciences 5, 937–947. https://doi.org/10.5194/bg-5-937-2008

Vuichard, N., Ciais, P., Viovy, N., Li, L., Ceschia, E., Wattenbach, M., Bernhofer, C., Emmel, C., Grünwald, T., Jans, W., Loubet, B., Wu, X., 2016. Simulating the net ecosystem CO_2 exchange and its components over winter wheat cultivation sites across a large climate gradient in Europe using the ORCHIDEE-STICS generic

model. Agric. Ecosyst. Environ. 226, 1–17. https://doi.org/10.1016/j.agee.2016.04.017

Walkley, A., Black, C.A., 1934. An examination of the Degtjareff method for determining soil organic matter and a proposed modification of the chromic acid titration method. Soil Sci. 37, 29–38.

Wang, B., Wu, Y., Chen, D., 2017. Stable isotopes of carbon and nitrogen help to predict the belowground communities at a regional scale. Sci. Rep. 7, 1–10. https://doi.org/10.1038/s41598-017-07517-w

Warembourg, F.R., Estelrich, H.D., 2001. Plant phenology and soil fertility effects on below-ground carbon allocation for an annual (*Bromus madritensis*) and a perennial (*Bromus erectus*) grass species. Soil Biol. Biochem. 33, 1291–1303. https://doi.org/10.1016/S0038-0717(01)00033-5

Warembourg, F.R., Roumet, C., Lafont, F., 2003. Differences in rhizosphere carbon-partitioning among plant species of different families. Plant Soil 256, 347–357. https://doi.org/10.1023/A:1026147622800

Weaver, J.E., 1958. Classification of Root Systems of Forbs of Grassland and a Consideration of Their Significance. Ecology 39, 393–401. https://doi.org/10.2307/1931749

Webb, E.K., Pearman, G.I., Leuning, R., 1980. Correction of flux measurements for density effects due to heat and water vapour transfer. Q. J. R. Meteorol. Soc. 106, 85–100. https://doi.org/10.1002/qj.49710644707

Welker, J.M., Wookey, P.A., Parsons, A.N., 1993. Leaf carbon isotope discrimination and vegetative responses of *Dryas octopetala* to temperature and water manipulations in a High Arctic polar semi-desert, Svalbard. Oecologia 95, 463–469. https://doi.org/10.1007/BF00317428

Werner, R.A., Bruch, B.A., Brand, W.A., 1999. ConFlo III - An -Interface for High Precision

d13C and d15N Analysis with an Extended Dynamic Range. Rapid Commun. Mass Spectrom. 13, 1237–1241.

Williams, D.G., Gempko, V., Fravolini, A., Leavitt, S.W., Wall, G.W., Kimball, B.A., Pinter, P.J., LaMorte, R., Ottman, M., 2001. Carbon isotope discrimination by Sorghum bicolor under CO_2 enrichment and drought. New Phytol. 150, 285–293. https://doi.org/10.1046/j.1469-8137.2001.00093.x

Wilson, J.B., Peet, R.K., Dengler, J., Meelis, P., 2012. Plant species richness: the world records. J. Veg. Sci. 23, 796–802. https://doi.org/10.1111/j.1654-1103.2012.01400.x

Wohlfahrt, G., Anderson-Dunn, M., Bahn, M., Berninger, F., Campbell, C., Carrara, A., Cescatti, A., Christensen, T., Dore, S., Friborg, T., Furger, M., Gianelle, D., Hargreaves, K., Hari, P., Haslwanter, A., Marcolla, B., Milford, C., Nagy, Z., Nemitz, E., Rogiers, N., Sanz, M.J., Siegwolf, R.T.W., Susiluoto, S., Sutton, M., Tuba, Z., Ugolini, F., Valentini, R., Zorer, R., Cernusca, A., 2008a. Biotic, Abiotic, and Management Controls on the Net Ecosystem CO_2 Exchange of European Mountain Grassland Ecosystems. Ecosystems 11, 1338–1351. https://doi.org/10.1007/s10021-008-9196-2

Wohlfahrt, G., Hammerle, A., Haslwanter, A., Bahn, M., Tappeiner, U., Cernusca, A., 2008b. Disentangling leaf area and environmental effects on the response of the net ecosystem CO_2 exchange to diffuse radiation. Geophys. Res. Lett. 35, 1–5. https://doi.org/10.1029/2008GL035090

Wolfgang, W.W., Christiane, R., Meyer, S.T., Ebeling, A., Luo, G., Allan, E., Beßler, H., Barnard, R.L., Buchmann, N., Buscot, F., Engels, C., Fischer, C., Fischer, M., Gessler, A., Gleixner, G., Halle, S., Hildebrandt, A., Hillebrand, H., de Kroon, H., Lange, M., Leimer, S., Le Roux, X., Milcu, A., Mommer, L., Niklaus, P.A., Oelmann, Y., Proulx, R., Roy, J., Scherber, C., Scherer-Lorenzen, M., Scheu, S., Tscharntke, T., Wachendorf, M., Wagg, C., Weigelt, A., Wilcke, W., Wirth, C., Schulze, E.D.,

Schmid, B., Eisenhauer, N., 2017. Biodiversity effects on ecosystem functioning in a 15-year grassland experiment: Patterns, mechanisms, and open questions. Basic Appl. Ecol. 23, 1–73. https://doi.org/10.1016/j.baae.2017.06.002

Wood, S.N., 2004. Stable and Efficient Multiple Smoothing Parameter Estimation for Generalized Additive Models. J. Am. Stat. Assoc. 99, 673–686. https://doi.org/10.1198/016214504000000980

Woodwell, G., Whittaker, R., 1968. Primary production in terrestrial ecosystems. Am. Zool. 8, 19–30.

Wu, Z., Dijkstra, P., Koch, G.W., Peñuelas, J., Hungate, B.A., 2011. Responses of terrestrial ecosystems to temperature and precipitation change: a meta-analysis of experimental manipulation. Glob. Chang. Biol. 17, 927–942. https://doi.org/10.1111/j.1365-2486.2010.02302.x

Wutzler, T., Reichstein, M., Moffat, A.M., Migliavacca, M., 2018. REddyProc: Post Processing of (Half-)Hourly Eddy-Covariance Measurements. R package version 1.1.3. https://CRAN.R-project.org/package=REddyProc. https://doi.org/10.5194/bg-3-571-2006>

Xia, J., Yuan, W., Wang, Y.P., Zhang, Q., 2017. Adaptive Carbon Allocation by Plants Enhances the Terrestrial Carbon Sink. Sci. Rep. 7, 1–11. https://doi.org/10.1038/s41598-017-03574-3

Yang, Y., Siegwolf, R.T.W., Körner, C., 2015. Species specific and environment induced variation of $\delta^{13}C$ and $\delta^{15}N$ in alpine plants. Front. Plant Sci. 6, 1–14. https://doi.org/10.3389/fpls.2015.00423

Yoneyama, T., Matsumaru, T., Usui, K., Engelaar, W.M.H.G., 2001. Discrimination of nitrogen isotopes during absorption of ammonium and nitrate at different nitrogen concentrations by rice (*Oryza sativa* L.) plants. Plant, Cell Environ. 24, 133–139. https://doi.org/10.1046/j.1365-3040.2001.00663.x

Yvon-Durocher, G., Caffrey, J.M., Cescatti, A., Dossena, M., Giorgio, P., Gasol, J.M., Montoya, M., Pumpanen, J., Staehr, P.A., Trimmer, M., Woodward, G., Allen, A.P., 2012. Reconciling the temperature dependence of respiration across timescales and ecosystem types. Nature 487, 472–476. https://doi.org/10.1038/nature11205

Zhou, J., Cai, W., Qin, Y., Lai, L., Guan, T., Zhang, X., Jiang, L., Du, H., Yang, D., Cong, Z., Zheng, Y., 2016. Alpine vegetation phenology dynamic over 16 years and its covariation with climate in a semi-arid region of China. Sci. Total Environ. 572, 119–128. https://doi.org/10.1016/j.scitotenv.2016.07.206

Zhou, X., Guo, Z., Zhang, P., Li, H., Chu, C., Li, X., Du, G., 2017. Different categories of biodiversity explain productivity variation after fertilization in a Tibetan alpine meadow community. Ecol. Evol. 7, 3464–3474. https://doi.org/10.1002/ece3.2723

Zhu, C., Ma, Y., Wu, H., Sun, T., La Pierre, K.J., Sun, Z., Yu, Q., 2016. Divergent effects of nitrogen addition on soil respiration in a semiarid grassland. Sci. Rep. 1–8. https://doi.org/10.1038/srep33541

Zimmerman, J.K., Ehleringer, J.R., 1990. Carbon isotope ratios are correlated with irradiance levels in the Panamanian orchid *Catasetum viridiflavum*. Oecologia 83, 247–249. https://doi.org/10.1007/BF00317759

Zuur, A.F., Ieno, E.N., Smith, G.M., 2007. Analysing Ecological Data. Springer New York. https://doi.org/10.1007/978-0-387-45972-1